

# Demonstration and Implementation of Thermally Passive Low-Income Housing: A Case Study in Bhuj

by

Emma Nelson

B.S., Massachusetts Institute of Technology (2015)

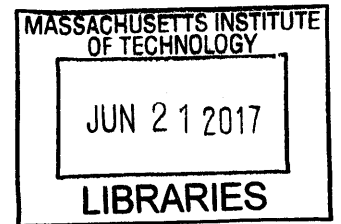
Submitted to the Department of Mechanical Engineering  
in partial fulfillment of the requirements for the degree of

Master of Science in Mechanical Engineering

at the

MASSACHUSETTS INSTITUTE OF TECHNOLOGY

June 2017



© Massachusetts Institute of Technology 2017. All rights reserved.

*^*  
**Signature redacted**

Author .....

.....  
Department of Mechanical Engineering  
May 12, 2017

**Signature redacted**

Certified by .....

.....  
Leon Glicksman  
Professor of Building Technology and Mechanical Engineering  
Thesis Supervisor

**Signature redacted**

Accepted by .....

.....  
Rohan Abeyaratne  
Chairman, Department Committee on Graduate Students



# Demonstration and Implementation of Thermally Passive Low-Income Housing: A Case Study in Bhuj

by

Emma Nelson

Submitted to the Department of Mechanical Engineering  
on May 12, 2017, in partial fulfillment of the  
requirements for the degree of  
Master of Science in Mechanical Engineering

## Abstract

In a 2004 Global Health Risks report, the World Health Organization identified insufficient protection from extreme heat as one of the primary health concerns in developing nations. The combination of a harsh environment and the lack of coping resources can lead to cardiovascular and respiratory disease and in some cases, death. Throughout May 2015, an estimated 2,500 Indian citizens lost their lives as a result of deadly heatwaves that topped 46°C. Globally, more than 7,500 deaths were caused by extreme heat the same year. Those living in resource-constrained communities without the means to construct substantial housing are the most vulnerable to these harsh weather conditions. As the developing world experiences increasing rapid urbanization, an energy gap, and frequent heatwaves due to climate change, there is a critical need for new construction techniques that can regulate indoor temperature using passive means rather than energy consuming appliances. Though some thermal passive cooling techniques have been previously researched, they have yet to be successfully implemented in resource-constrained communities.

In collaboration with the Hunnarshala Foundation, an NGO located in Bhuj, Gujarat, India, this research seeks to bridge the gap between thermal passive techniques and the application of these methods in low-income housing. This thesis presents recommendations on roof design, wall design, and fan usage based on the results from prototype field work, simulations, and the implementation of pilot homes. With an appropriate building design, measured operative temperatures in pilot homes met the ASHRAE 80% acceptability criteria for more than 60% of operating hours and remained within the IMAC 80% acceptability range 88% of operating hours in the Bhuj climate. In the context of India, the discoveries from this case study in Bhuj can be used to write building guidelines to holistically improve the thermal comfort in Indian homes as a part of India's "Housing for All" program. Beyond the context of India, the more than 300 million people living in resource-constrained regions can adopt low-cost passive thermal control techniques to build housing capable of shielding against extreme heat.

Thesis Supervisor: Leon Glicksman  
Title: Professor of Building Technology and Mechanical Engineering

## Acknowledgments

This research was sponsored by the MIT Tata Center for Technology and Design. I am deeply grateful to the Tata Center for its financial support and for establishing this unique program that encourages academic research while considering practical applications. I appreciate all the advice from my Tata mentor, Aditya Barve. This has been a truly enriching experience and a great opportunity to work within a global network to solve some of the world's greatest energy, housing, health, water, agricultural, and environmental challenges.

I would like to thank Professor Glicksman for his encouragement and guidance throughout this research. It has been a wonderful learning experience to have his mentorship.

To all the members of the Hunnarshala Foundation, I sincerely appreciate your dedication and enthusiasm in making this research possible. It has been a privilege to work with you. Thank you, Mr. Tejas Kotak, the Director of Research at Hunnarshala, for all your hospitality and invaluable support in this research endeavor. Thank you, Pradip Rangani, the Bhuj Project Manager for this research, for facilitating all the fieldwork.

Thank you to the entire MIT Building Technology Faculty and Staff for creating this rigorous and collaborative environment to pursue challenging academic research. A special thanks to Professor Ochsendorf. I am truly appreciative for your consultation on structural design. To my colleagues in the Building Technology Lab, thank you for your constructive criticism, advice, and technical expertise. I would specifically like to thank Johnathan Kongoletos. It has been wonderful collaborating on this research project. I am truly grateful for all your help throughout the challenging travels/field visits.

To my family, words could never articulate the profound gratitude I feel for your unconditional encouragement, support, and love that has allowed me to pursue opportunities including this research. Thank you for taking a chance 18 years ago and adopting/welcoming me into an extraordinary life.



# Contents

<b>1</b>	<b>Introduction</b>	<b>27</b>
1.1	Bhuj: A Case Study . . . . .	30
1.2	Government of India Housing for All Program . . . . .	31
1.3	Thermally Passive Housing Design . . . . .	33
1.3.1	Heat Avoidance . . . . .	33
1.3.2	Earth-Air Heat Exchanger . . . . .	34
1.3.3	Ventilation . . . . .	35
1.3.4	Evaporative Cooling . . . . .	35
1.3.5	Air Movement . . . . .	36
1.3.6	Thermal Mass and Insulation . . . . .	37
1.3.7	Radiant Cooling . . . . .	38
1.4	Design for Emerging markets. . . . .	39
1.5	Existing Designs and Research in Bhuj . . . . .	41
1.5.1	Next Steps . . . . .	48
1.6	Scope of Research . . . . .	50
<b>2</b>	<b>Defining Thermal Comfort and Performance Metrics</b>	<b>51</b>
2.1	Heat Stress . . . . .	52
2.2	Adaptive Thermal Comfort Standards . . . . .	55
2.3	Peak Temperatures and Phase Lags . . . . .	57
<b>3</b>	<b>Field Experiment Setup</b>	<b>59</b>
3.1	Informal Home . . . . .	59

3.2	Prototype Test Chambers . . . . .	61
3.3	Housing for All Homes . . . . .	67
<b>4</b>	<b>Performance of Existing and Proposed Roof Types</b>	<b>77</b>
4.1	Test Chamber Results and Discussion . . . . .	78
4.2	Pilot Roofs Results and Discussion . . . . .	89
4.2.1	Temperature Data . . . . .	89
4.2.2	Perception Survey Results . . . . .	97
<b>5</b>	<b>Wall Design</b>	<b>99</b>
5.1	Role of Diurnal Shifts . . . . .	99
5.2	Role of Wall Insulation . . . . .	105
5.2.1	Wall Insulation Changes on the North and South Test Chamber Walls . . . . .	105
5.2.2	Comparisons of Test Chamber with Fully Insulated and Ex- posed Walls . . . . .	106
5.3	Effects of Wall Color . . . . .	114
5.4	Recommendations for Wall Design . . . . .	120
<b>6</b>	<b>Integration</b>	<b>123</b>
6.1	Simulation Parameters . . . . .	123
6.1.1	Roof Thermal Model . . . . .	126
6.1.2	Wall Thermal Model . . . . .	130
6.1.3	Boundary Conditions . . . . .	133
6.2	Numerical Solver . . . . .	138
6.3	Comparison of Measured Data with Simulations . . . . .	140
6.4	Results . . . . .	144
6.4.1	Simulation Results: 2.4m by 2.4m by 2.4m Rooms . . . . .	144
6.4.2	Simulation Results: 5m by 5m by 2.4m Rooms . . . . .	148
6.4.3	Designs Considering Bhuj Winter Conditions . . . . .	154
6.5	Recommendations . . . . .	158



<b>7</b>	<b>Effects of Ceiling Fans on Thermal Comfort</b>	<b>159</b>
7.1	Ceiling Fans . . . . .	159
7.2	Ceiling Fan Case Study in Bhuj . . . . .	160
7.3	Methodology . . . . .	162
7.3.1	Field Experiment Parameters . . . . .	162
7.3.2	Simulation Parameters . . . . .	166
7.4	Performance Metric . . . . .	174
7.5	Results . . . . .	175
7.5.1	Field Experiments . . . . .	175
7.5.2	CFD Simulations . . . . .	180
7.6	Recommendations . . . . .	196
<b>8</b>	<b>Conclusion</b>	<b>199</b>
8.1	Thermally Passive Design Recommendations . . . . .	199
8.1.1	Roof Design . . . . .	199
8.1.2	Wall Design . . . . .	205
8.1.3	Use of Ceiling Fan . . . . .	207
8.2	Recommendations for Future Work . . . . .	209
8.2.1	Refining Thermal Autonomous Housing in Extreme Heat Cli- mates. . . . .	209
8.2.2	Housing Design Adaption for Thermal Control in Cold Climates	211
<b>A</b>	<b>Tables</b>	<b>213</b>
<b>B</b>	<b>Figures</b>	<b>219</b>



# List of Figures

1-1	Average Annual Surface Temperature Map (World Climate Maps, 2007)	28
1-2	India Absolute Maximum Temperature Map (Tom Di Liberto, 2015)	29
1-3	Bhuj 2015 Informal Settlements	31
1-4	Relationship Between Air Movement, Relative Humidity, and Upper Bound Thermal Comfort Dry Bulb Temperature (Khedari et al., 2000)	36
1-5	Qualitative Mapping of Observed Design with Climate Strategies for Case Study Buildings 1-7 (Gradillas, 2015)	42
1-6	Single-Room Dwelling with 15cm Thick Solid Concrete Masonry Unit (CMU) Walls and a Bare Asbestos Cement Corrugated Sheet Roof (Gradillas, 2015)	43
1-7	Single-Room Dwelling with 23cm Thick Uninsulated Compressed Stabilized Earth Block (CSEB) Walls and 12cm Thick RCC Slab Roof (Gradillas, 2015)	43
1-8	A Stand-Alone Two-Room Dwelling with 15cm Thick Uninsulated CMU Walls and a Single-Layer Mangalore Pattern Tile Roof (Gradillas, 2015)	43
1-9	Ceiling Temperatures for Existing Vernacular Homes, Buildings 1, 6, and 7 Adapted from <i>Analysis and Design for Thermally Autonomous Housing in Resource-Constrained Communities</i> (Gradillas, 2015)	44
1-10	Interior South Wall, Ceiling, Air Gap, and Ambient Air Temperature Sensor Locations in Five 2015 Test Chambers with Insulated Walls and Various Roof Types (Gradillas, 2015)	46

1-11 Average Temperature Deviations from Daily Outdoor Ambient Air Temperature Peaks for Two Test Chambers Fitted with a Single Layer Roof and a Double Layer Roof (Gradillas, 2015). . . . .	48
1-12 Average Temperature Deviations from Nightly Outdoor Ambient Air Temperature Minimums for Two Test Chambers Fitted with a Single Layer Roof and a Double Layer Roof (Gradillas, 2015). . . . .	49
2-1 Heat Stress Color Map of Bhuj Weather Data in 2015 . . . . .	53
2-2 Wet Bulb Globe Temperature (WBGT) Heat Stress Thresholds for Unacclimatized Individuals (NIOSH, 2017) . . . . .	54
2-3 ASHRAE, EN-15251, and IMATC Adaptive Thermal Comfort Standards and Comparison . . . . .	56
3-1 Exterior View of Informal Home (Photo Courtesy of Bradley Tran) . . . . .	60
3-2 Interior Ambient Air and Air Gap Sensor Placement in Informal Home . . . . .	60
3-3 Five 2.4m by 2.4m by 2.4m Test Chambers with 0.23 cm Thick Sandstone Walls Fitted with Different Roofs . . . . .	63
3-4 Mean Radiant Temperature Measuring Apparatus . . . . .	64
3-5 R1   Single layer Tin Roof . . . . .	64
3-6 R2   Reinforced Concrete Cement (RCC) Roof . . . . .	64
3-7 R3   Reinforced Concrete Cement (RCC) Roof with Air Gap and Thermocol Insulation . . . . .	65
3-8 R4   Double layer Tin Roof with Air Gap Radiant Barrier and Bubble Wrap Insulation . . . . .	65
3-9 R5   Double layer Tin Roof with Air Gap Radiant Barrier and Mud Roll Insulation . . . . .	65
3-10 Test Chamber Sensor Locations . . . . .	66
3-11 Cross Section and Plan View of Housing for All Homes (Image Adapted from Hunnarshala 2016) . . . . .	69
3-12 Exterior of Housing for All Homes Fitted with Pilot Roofs . . . . .	70

3-13	Roof Design and Sensor Locations in Home with a Double Layer Clay Tile, Radiant Barrier, and Mud Roll Insulated Roof (H1) Image Adapted from Hunnarshala 2016 . . . . .	71
3-14	Roof Design and Sensor Locations in home with a Double Layer Clay Tile, Radiant Barrier, and Wood Ceiling Roof (H2) Image Adapted from Hunnarshala 2016 . . . . .	72
3-15	Roof Design and Sensor Locations in Home with a Double Layer Tin, Radiant Barrier, and Wood Ceiling Roof (H3) Image Adapted from Hunnarshala 2016 . . . . .	73
3-16	Roof Design and Sensor Locations in Home with a Double Layer Tin, Radiant Barrier, and Bubble Wrap Insulation Roof (H4) Image Adapted from Hunnarshala 2016 . . . . .	74
3-17	Weather Station Placed on the Southern Border of the Housing for All Site . . . . .	75
4-1	Transient Ceiling Temperatures for Test Chambers with Roof Types R1-R5 . . . . .	79
4-2	Color Map of Temperature Differences Between Ceiling and Outdoor Ambient Air . . . . .	80
4-3	Transient Air Temperatures for Test Chamber with Roof Types R1-R5	82
4-4	Color Map of Temperature Differences Between the Indoor and Outdoor Ambient Air . . . . .	83
4-5	Transient Interior South Wall Temperatures for Test Chamber with Roof Types R1-R5 . . . . .	84
4-6	Color Map of Temperature Differences Between Interior South Wall and Outdoor Ambient Air . . . . .	85
4-7	Transient Operative Temperatures for Test Chamber with Roof Types R1-R5 . . . . .	86
4-8	Color Map of Temperature Differences Between Indoor Operative and Outdoor Ambient Air . . . . .	87

4-9	Radiant Temperatures Plotted as a Function of Ceiling Temperatures for Roofs R1-R2 . . . . .	88
4-10	Radiant Temperatures Plotted as a Function of Ceiling Temperatures for Roofs R1-R5 . . . . .	88
4-11	Test Chamber Average Interior Temperature Deviations from Daily Maximum Temperatures . . . . .	89
4-12	Transient Indoor Air Temperatures in the Housing for All and Informal Settlement Homes . . . . .	91
4-13	Transient Indoor Air Temperatures in the Housing for All Homes . . . . .	91
4-14	Transient Ceiling Temperatures in the Housing for All Homes . . . . .	92
4-15	Transient Interior South Wall Temperatures in the Housing for All Homes . . . . .	93
4-16	Transient Operative Temperatures in the Housing for All Homes . . . . .	94
4-17	Interior Transient Air, South Wall, Ceiling and Operative Temperatures for Existing Vernacular Homes . . . . .	95
4-18	Housing for All and Existing Homes: Average Interior Air, South Wall, Ceiling, and Operative Temperature Deviations from Peak Ambient Outdoor Air Temperatures . . . . .	96
4-19	Percentage of Time in which Temperatures Exceeded the IMAC and ASHRAE Upper 80% Acceptability Comfort Limits . . . . .	97
5-1	Comparison of Measured Outdoor Air Temperatures during March, a Period Characterized by 20°C Diurnal Shifts, and June, a Period Characterized by 10°C Diurnal Shifts . . . . .	101
5-2	Bhuj: Monthly Average Number of Cloudy, Sunny, and Overcast Days (Meteoblue, 2014) . . . . .	101
5-3	Comparison of Measured Relative Humidities During March, a Period Characterized by 20°C Diurnal Shifts, and June, a Period Characterized by 10°C Diurnal Shifts . . . . .	102

5-4	Comparison of Measured Night Flush Ventilated T2 Test Chamber Indoor Air Temperatures during March, a Period Characterized by 20°C Diurnal Shifts, and June, a Period Characterized by 10°C Diurnal Shifts . . . . .	102
5-5	Comparison of Measured Night Flush Ventilated T2 Test Chamber Inside South Wall Temperatures during March, a Period Characterized by 20°C Diurnal Shifts, and June, a Period Characterized by 10°C Diurnal Shifts . . . . .	103
5-6	Changes in Average Measured Indoor Air and South Wall Temperatures Between March, a Period with 20°C Diurnal Shifts, and June, a Period with 10°C Diurnal Shifts . . . . .	104
5-7	Changes in Average Peak Temperature Deviations from Outdoor Ambient Air Temperatures for Indoor Air and South Wall Temperatures Between March, a Period with 20°C Diurnal Shifts, and June, a Period with 10°C Diurnal Shifts . . . . .	104
5-8	Measured South Wall Temperatures Before and After Wall Insulation Removal . . . . .	106
5-9	Measured Operative Temperatures Before and After Wall Insulation Removal . . . . .	107
5-10	Average Interior Wall, Operative, and Air Temperature Deviations from Peak Outdoor Temperatures for Test Chambers Where Wall Insulation was Removed on June 20, 2015 . . . . .	107
5-11	Maximum Interior Temperatures as a Function of Maximum Outdoor Ambient Air Temperatures for 2015 Single Layer CGI Roof Test Chambers with Wall Insulation and 2016 Single Layer CGI Roof Test Chambers without Wall Insulation . . . . .	110
5-12	Maximum Interior Temperatures as a Function of Maximum Outdoor Ambient Air Temperatures for 2015 Test Chambers with Wall Insulation (T1, T2, T4, and T5) and 2016 Test Chambers without Wall Insulation (R2-R5) . . . . .	111

5-13	Average Interior Temperature Deviations from Daily Maximum for 2015 (Wall Insulation) and 2016 Test Chambers (No Wall Insulation)	112
5-14	Percent of Time in which Test Chamber Operative Temperatures Remain within the ASHRAE and IMAC Comfort Standards . . . . .	113
5-15	Infrared Images of Building Interior Illustrating the Effects of Exterior Wall Colors on Indoor Environments (Images Courtesy of John Kongoletos) . . . . .	115
5-16	Black Tarp Covering the South Wall of a Monitored Housing for All Home with a Multi-Layer Mangalore Tile and Mud Roll Insulated Roof	116
5-17	Transient Wall, Air, and Radiant Temperatures for Home with Black Plastic Placed on the South Wall . . . . .	116
5-18	South Wall Temperatures as a Function of Outside Temperatures . .	117
5-19	Radiant Temperatures as a Function of Outside Temperatures . . . .	118
5-20	Indoor Air Temperatures as a Function of Outside Temperatures . .	119
5-21	Average Temperatures and Precipitation for Bhuj, Gujarat, India (Meeteoblu, 2014) . . . . .	121
6-1	Geometry and Boundary Conditions for Test Chamber Control Volume	125
6-2	Single Layer Tin Roof Simulations Boundary Conditions and Geometry	128
6-3	RCC Roof Simulations Boundary Conditions and Geometry . . . . .	131
6-4	Radiant Barrier Placement Schedules for a Control Roof, Constant Radiant Barrier Roof, and Alternating Radiant Barrier Roof . . . . .	132
6-5	Boundary Conditions for Transient Wall Model . . . . .	134
6-6	Iterative Scheme for Calculating Interior Temperatures in Thermal Model	139
6-7	Comparison Between Simulated and Measured Indoor Air Temperatures for a 2.4m by 2.4m by 2.4m Test Chamber with a Single Layer CGI Roof . . . . .	141
6-8	Comparison Between Simulated and Measured Ceiling Temperatures for a 2.4m by 2.4m by 2.4m Test Chamber with a Single Layer CGI Roof	142



6-9	Comparison Between Simulated and Measured South Wall Temperatures for a 2.4m by 2.4m by 2.4m Test Chamber with a Single Layer CGI Roof . . . . .	143
6-10	March Transient Interior Air, Operative, South Wall, and Ceiling Temperatures for a Control Single Layer Tin Roof and Modifications to the Tin Sheet Roof, Wall Insulation $R = 1m^2K/W$ Wall Absorptivity = 0.75 . . . . .	146
6-11	March Average Deviation from Nightly minimums and Daily Maximums of Simulated 2.4m by 2.4m by 2.4m Test Chambers with Various CGI Roof Types, Wall Insulation Resistivities, and Exterior Wall Absorptivities . . . . .	147
6-12	March Transient Interior Air, Operative, South Wall, and Ceiling Temperatures for a Control RCC and Modifications to the RCC Sheet Roof, Wall Insulation $R = 1m^2K/W$ , Wall Absorptivity = 0.75 . . . . .	149
6-13	March Average Deviation from Nightly minimums and Daily Maximums of Simulated 2.4m by 2.4m by 2.4m Test Chambers with Various RCC Roof Types, Wall Insulation Resistivities, and Exterior Wall Absorptivities . . . . .	150
6-14	March Average Deviation from Nightly minimums and Daily Maximums of Simulated 5m by 5m by 2.4 m Test Chambers with Various CGI Roof Types, Wall Insulation Resistivities, and Exterior Wall Absorptivities . . . . .	152
6-15	March Average Deviation from Nightly minimums and Daily Maximums of Simulated 5m by 5m by 2.4 m Test Chambers with Various RCC Roof Types, Wall Insulation Resistivities, and Exterior Wall Absorptivities . . . . .	153
6-16	February Transient Interior Air, Operative, South Wall, and Ceiling Temperatures for a Control Single Layer Tin Roof and Modifications to the Single Layer Tin Roof, Wall Insulation $R = 0m^2K/W$ , Wall Absorptivity = 0.75 . . . . .	155

6-17	February Transient Interior Air, Operative, South Wall, and Ceiling Temperatures for a Control RCC Slab Roof and Modifications to the RCC Slab Roof, Wall Insulation $R = 0m^2K/W$ , Wall Absorptivity = 0.75 . . . . .	156
6-18	February Average Interior Temperature Deviations from Daily Peaks and Nightly Minimums for 5m by 5m by 2.4m Rooms with Various CGI Roof Types, Wall Insulation $R = 0m^2K/W$ , Wall Absorptivity = 0.75 . . . . .	157
6-19	February Average Interior Temperature Deviations from Daily Peaks and Nightly Minimums for 5m by 5m by 2.4m Rooms with Various RCC Roof Types, Wall Insulation $R = 0m^2K/W$ , Wall Absorptivity = 0.75 . . . . .	157
7-1	Informal Home with a Multilayer Tarpaulin, Cloth Roof and Ceiling Fan . . . . .	160
7-2	Temperature Map of the Temperature Difference Between the Outside and the Air Adjacent to the Ceiling . . . . .	161
7-3	Single Layer Corrugated CGI Roof . . . . .	163
7-4	Exterior View of Test Chamber with Single Layer Roof (Photo Cour- tesy of John Kongoletos) . . . . .	163
7-5	Double Layer Roof with Air Gap, Radiant Barrier, and Bubble Wrap Insulation . . . . .	164
7-6	Exterior View of Test Chamber with Double Layer Roof (Photo Cour- tesy of John Kongoletos) . . . . .	164
7-7	Sensor Placements for Test Chamber with a Single Layer Roof . . . .	165
7-8	Sensor Placements for Test Chamber with a Double Layer Roof . . . .	166
7-9	September 16, 2016 Transient Wall and Ceiling Temperatures for a Test Chamber with a Single Layer CGI Roof . . . . .	168
7-10	September 16, 2016 Transient Wall and Ceiling Temperatures for a Test Chamber with an RCC Roof . . . . .	169

7-11	September 16, 2016 Transient Wall and Ceiling Temperatures for a Test Chamber with a Double Layer Insulated Roof . . . . .	170
7-12	CFD Geometries for Test Chamber Simulations . . . . .	171
7-13	CFD Geometries for Single Story Housing for All Home with an RCC Roof . . . . .	172
7-14	CFD Geometries for the Housing for All Archytpе with a Peaked Roof	174
7-15	Changes in Temperature Stratification for the Test chamber with a Single Layer tin Sheet Roof . . . . .	176
7-16	Changes in Temperature Stratification for the Test Chamber with a Double Layer Insulated Roof . . . . .	177
7-17	Changes in Average Peak Temperatures as a Result of Ceiling Fan Usage . . . . .	178
7-18	Changes in Average Peak Temperatures as a Result of Ceiling Fan Usage . . . . .	178
7-19	Effects on Thermal Comfort due to Ceiling Fan Use in the Test Chamber with a Single Layer Roof . . . . .	181
7-20	Effects on Thermal Comfort due to Ceiling Fan Use in the Test Chamber with a Double Layer Roof . . . . .	182
7-21	Comparison of Simulation and Field Experiment Results for the Test Chamber with a Single Layer Roof . . . . .	183
7-22	Comparison of Simulation and Field Experiment Results for the Test Chamber with a Double Layer Roof . . . . .	184
7-23	Temperature Contours of Simulated Test Chambers without and with a Ceiling Fan . . . . .	185
7-24	Temperature Contours of Simulated Test Chambers with Various Fan Configurations . . . . .	186
7-25	Velocity Along a Horizontal Line Placed 1.5 m Above the Floor in a Test Chamber with a Single Layer Tin Sheet . . . . .	187
7-26	Comparison of the Velocity Profiles Along a Vertical Line in the Center of the Room for a Test Chamber with a Single Layer Tin Sheet . . .	187

7-27 Comparison of the Velocity Profiles Along a Vertical line 0.5 m from the Upright Fan for a Test Chamber with a Single Layer Tin Sheet . . . 188

7-28 Temperatures Along a Vertical Line in the Center of the Simulated Test Chamber with a Single Layer Tin Roof . . . . . 189

7-29 Temperatures Along a Vertical Line in the Center of the Simulated Test Chamber with a Double Layer Insulated Roof . . . . . 189

7-30 Temperature Contours of Simulated RCC Roof Housing for All Archetype with Different Fan Configurations . . . . . 190

7-31 Velocity Along a Horizontal Line Placed 1.5 m Above the Floor in a Room with an RCC Roof . . . . . 191

7-32 Temperatures Along a Vertical Line in the Center of the Simulated Housing for All home with an RCC Roof . . . . . 191

7-33 Calculated PMV Values for CFD Simulations of Test Chambers and Homes with RCC Roofs . . . . . 192

7-34 Temperature Contours of Simulated Housing for All homes with Peaked Roofs with Various Fan Configurations . . . . . 194

7-35 Average Room Temperatures as a Function of Ceiling Fan Placement 195

7-36 Velocity Profile Along a Vertical Line from the Floor to the Roof Peak 195

7-37 PMV Values for Simulated Housing for All Archetypes with Peaked Roofs . . . . . 196

8-1 Percentage of the Data Collection Period (June 17, 2016 to December 30, 2016) in which 2016 Test Chamber Operative Temperatures Exceeded IMAC and ASHRAE 80% Acceptability Limits . . . . . 202

B-1 Comparison Between Indoor Air Temperatures in Simulated Test Chambers with Full Scale Prototype Test Chambers with Roof Types R2-R5 220

B-2 Comparison Between Interior Ceiling Temperatures in Simulated Test Chambers with Full Scale Prototype Test Chambers with Roof Types R2-R5 . . . . . 221

B-3 Comparison Between Interior South Wall Temperatures in Simulated  
Test Chambers with Full Scale Prototype Test Chambers with Roof  
Types R2-R5 . . . . . 222



# List of Tables

1.1	MoHUPA Income Group Definition and Affordability Criteria . . . . .	32
2.1	Universal Thermal Comfort Index categorizations of thermal stress .	52
2.2	OSHA: Permissible Heat Exposure Limit Value . . . . .	53
2.3	ASHRAE, EN-15251, and IMATC Comfort Standards and Criteria .	55
3.1	Thermal Conductivities of Various Insulation Materials . . . . .	61
5.1	2015 and 2016 Test Chamber Comparisons . . . . .	108
6.1	Independent Variables and Input Parameters in Thermal Simulations	124
6.2	Thermal Properties of the RCC Roof . . . . .	130
6.3	Thermal Properties of Simulated Walls . . . . .	133
7.1	Boundary Conditions for a Room with a Single Layer Roof . . . . .	167
7.2	Boundary Conditions for a Room with an RCC Roof . . . . .	168
7.3	Boundary Conditions for a Room with a Double Layer Insulated Roof	169
7.4	Summary of Simulation Cases . . . . .	173
8.1	Performance Rankings of Test Chamber Roof Types Based Operative Temperatures Peak Deviations . . . . .	201
8.2	Performance Rankings of Housing for All Homes Based Operative Tem- peratures Peak Deviations . . . . .	203
8.3	Cost of Various Roof Types . . . . .	204

8.4	Performance Rankings of Wall Treatments Based on Simulated Operative Temperature Deviations from Outdoor Ambient Temperature Peaks . . . . .	207
8.5	Home with a Well Insulated Roof: Performance Rankings of Fan Location and Usage Based on PMV Values . . . . .	208
8.6	Home with a Single Layer Tin Sheet: Performance Rankings of Fan Location and Usage Based on PMV Values Assuming a 90%RH . . .	209
8.7	Performance Rankings of Simulated CGI Roof Types Based Operative Temperatures Peak Deviations . . . . .	210
A.1	Inputs for Calculating PMV of Field Experiment Test Chambers at 50%RH . . . . .	214
A.2	Inputs for Calculating PMV of Field Experiment Test Chambers at 90%RH . . . . .	214
A.3	Inputs for Calculating PMV of Simulated Single Layer Roof Test Chambers at 50%RH . . . . .	214
A.4	Inputs for Calculating PMV of Simulated Single Layer Roof Test Chambers at 90%RH . . . . .	215
A.5	Inputs for Calculating PMV of Simulated Double Layer Roof Test Chambers at 50%RH . . . . .	215
A.6	Inputs for Calculating PMV of Simulated Double Layer Roof Test Chambers at 90%RH . . . . .	215
A.7	Inputs for Calculating PMV of Simulated RCC Roof Room at 50%RH	216
A.8	Inputs for Calculating PMV of Simulated RCC Roof Room at 90%RH	216
A.9	Inputs for Calculating PMV of Simulated Housing for All Room with Single Layer Peaked Roof at 50%RH . . . . .	216
A.10	Inputs for Calculating PMV of Simulated Housing for All Room with Single Layer Peaked Roof at 90%RH . . . . .	217
A.11	Inputs for Calculating PMV of Simulated Housing for All Room with Double Layer Peaked Roof at 50%RH . . . . .	217



A.12 Inputs for Calculating PMV of Simulated Housing for All Room with  
Double Layer Peaked Roof at 90%RH . . . . . 217



# Chapter 1

## Introduction

In May 2015, an estimated 2,500 Indian citizens lost their lives as a result of a deadly heatwave (the Centre for Research on the Epidemiology of Disasters (CRED), 2015; Bob Kopp, 2015; Buzan and Huber, 2015). Unfortunately, adverse health effects due to inadequate protection against extreme heat occur globally and is among one of the top major health concerns identified by the World Health Organization (World Health Organization, 2010). The combination of a harsh environment and the lack of coping resources can lead to cardiovascular and respiratory disease and in some cases, death (World Health Organization, 2010). For regions that experience high temperatures, there is an increase of 11% mortality when the temperature rises above 40°C (Vijesh Vasanth Joshi, 2015). With global climate change and average air temperatures projected to rise 1-3°C within the 21st century (Lori Perkins, 2014; Jackson, 2017), there emerges a need to design housing capable of providing protection in extreme heatwaves. The negative effects of these frequent heatwaves will be predominantly felt in the hot/arid desert and tropic regions where most of the developing nations are located, as shown in Figure 1-1.

Citizens of these regions facing major economic and material constraints are disproportionately affected by the extreme heatwaves as many, due to lack of resources, tend to live in housing that provides little to no protection against extreme heat (World Health Organization, 2010). According to a 2011 census, in India alone, an estimated 10 million impoverished households earning less than 100,000Rs ( \$1600)

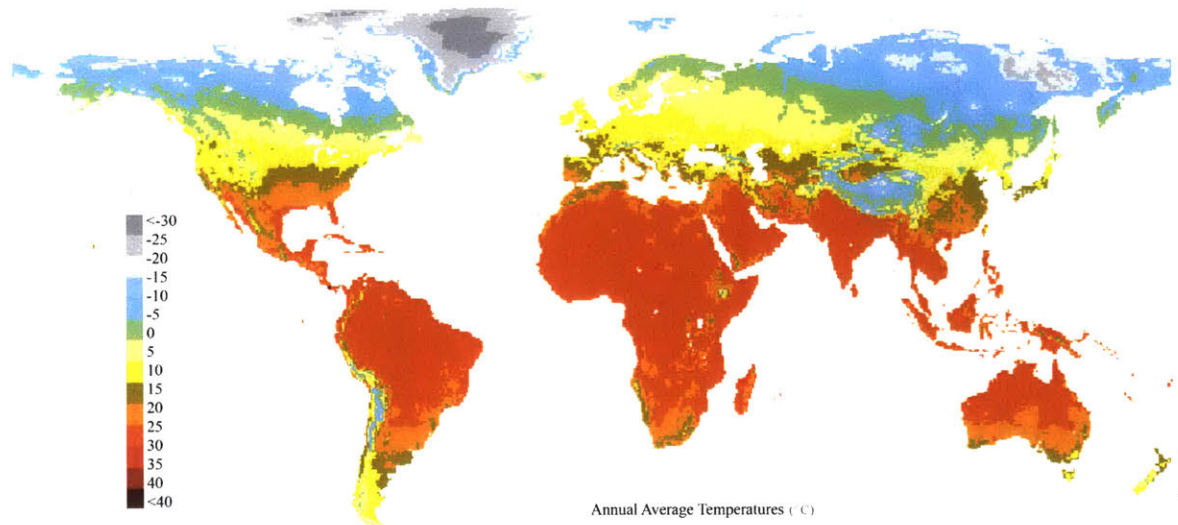


Figure 1-1: Average Annual Surface Temperature Map (World Climate Maps, 2007)

per household per year, (Census Population Data, 2015; Maps of India, 2012; C. Rangarajan et al., 2015) reside in climates considered hot and dry as shown in Figure 1-2.. An estimated 1.25 million of these households would be considered slum households (Indian Agricultural Statistics Institute Research, 2011; Government of India Ministry of Housing and Urban Poverty Alleviation National Buildings Organization, 2013) where a slum is defined as one or a group of individuals living under the same roof in an urban area, lacking in one or more of the following five amenities

1. "Durable housing (a permanent structure providing protection from extreme climatic conditions)" (Nolan, 2015).
2. "Sufficient living area (no more than three people sharing a room)" (Nolan, 2015).
3. "Access to improved water (water that is sufficient, affordable, and can be obtained without extreme effort)" (Nolan, 2015).
4. "Access to improved sanitation facilities (a private toilet, or a public one shared with a reasonable number of people)" (Nolan, 2015).
5. "Secure tenure (de facto or de jure secure tenure status and protection against forced eviction)" (Nolan, 2015).

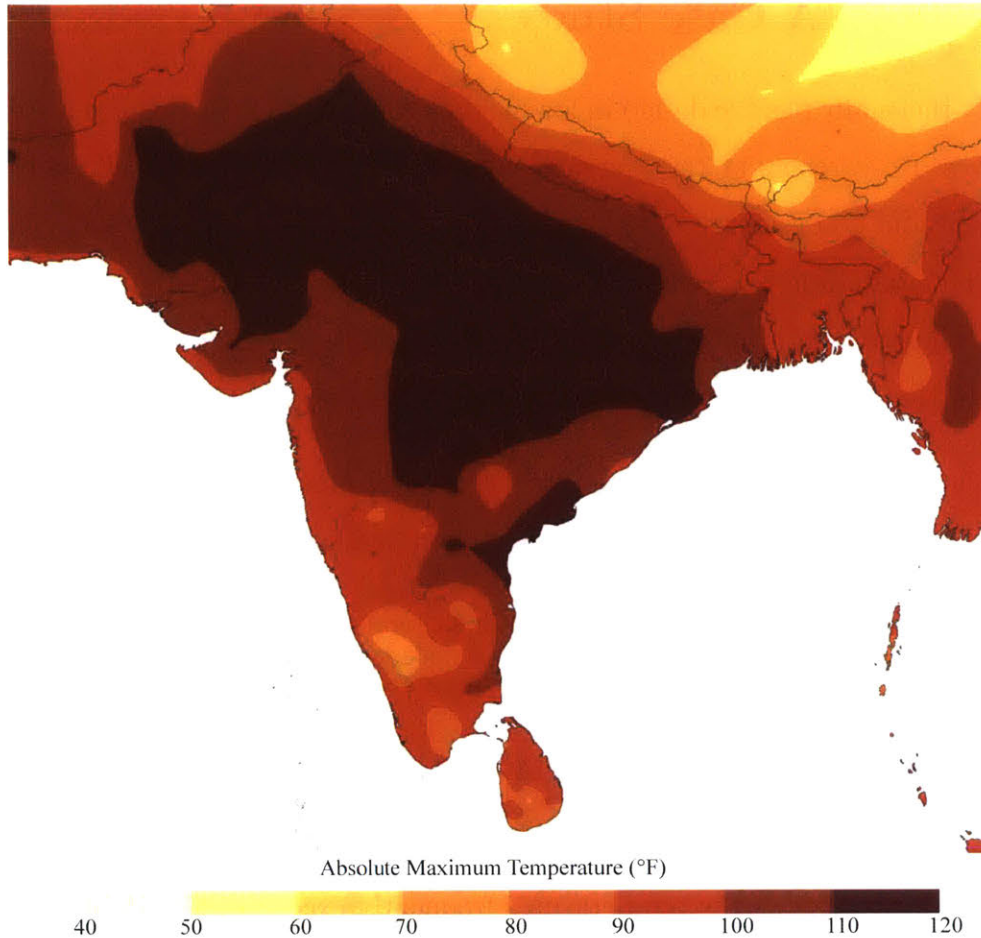


Figure 1-2: India Absolute Maximum Temperature Map (Tom Di Liberto, 2015)

Given the aforementioned economic and climate challenges, the following research focuses on demonstrating and optimizing thermally passive housing design as a means to improve interior conditions in resource-constrained regions. Using passive thermal controls mitigates energy costs and allows housing solutions to be more accessible even for citizens who do not have a stable connection to electricity. The results and discoveries of this research can be applied to improve housing for not just the impoverished population in India, but also for those in other parts of the world who experience similar socioeconomic and climate challenges and those of a higher income brackets looking to conserve energy.

## 1.1 Bhuj: A Case Study

To study thermally passive design in low-income communities that experience extreme heatwaves, Researchers at the Massachusetts Institute of Technology have been collaborating and co-designing with a non-government organization (NGO), The Hunnarshala Foundation, located in Bhuj, Gujarat, India. The case study city, Bhuj, exhibits climate conditions associated with hot, arid regions as well as frequent heatwaves. In the context of India, an extreme heat weather condition is declared when

- Temperatures exceed "normal daily historical maximum temperature (30 year average) by 5°C given those averages are less than 40°C" (Azhar et al., 2014)
- Temperatures exceed "normal daily historical maximum temperature (30 year average) by 4°C given those averages are greater than 40°C" (Azhar et al., 2014)
- "Actual maximum temperature [exceeds] 45°C" (Azhar et al., 2014)

Based on this definition, throughout May to September, Bhuj is very susceptible to dangerous heatwaves as the temperatures frequently exceed 45°C (Gradillas, 2015).

In addition to facing extreme climate challenges, similar to the rest of India, many residents of Bhuj face major economic and resource constraints; an estimated 33% of the population live in slums (Hunnarshala Foundation, 2016; Gradillas, 2015; Government of India Ministry of Housing and Urban Poverty Alleviation National Buildings Organization, 2013) as defined by the United Nations State of the World's Cities report. Bhuj is located near the epicenter of a 2001 earthquake which left hundreds of thousands homeless (Emily Buchanan and Bhasker, 2011). Since the earthquake, there have been efforts to rebuild the city. Today, as a part of a national housing program, the *Slum Free Bhuj Project* sets goals to improve the housing situations of impoverished families.

Currently, the low-income homes in Bhuj do not provide proper means to protect against extreme heat. Based on observation during site visits, residents often use corrugated asbestos concrete sheets, corrugated tin sheets, plastic sheets, cloth, and thin thatch for roofing materials. Uninsulated sandstone bricks, concrete, rock, and

stabilized earth bricks are used for the walls as shown in Figure 1-3. Residents may use ceiling fans as a low-cost means to provide some relief from the extreme heat. Only 6-9% of Indian households own air conditioners as many cannot afford a unit (Barry and Davenport, 2016).



Figure 1-3: Bhuj 2015 Informal Settlements

## 1.2 Government of India Housing for All Program

The *Slum Free Bhuj* project falls under a national housing initiative in India. In response to the housing challenges facing India, the Ministry of Housing and Urban Poverty Alleviation (MoHUPA) has enacted a program "Housing for All" to provide housing for 20 million slum households by 2022. This program includes a technology submission to incorporate innovative technologies and materials, design green buildings using natural resources, and incorporate earthquake/disaster resistant technologies and designs (Ministry of Housing and Urban Poverty Alleviation, 2007). In alignment with this mission to provide affordable, durable, protective housing, MIT and the Hunnarshala Foundation, are currently collaborating to holistically improve design, construction, and integration of housing to address the issue of thermal comfort and reduce heat-related health risks. The proposed designs stress achieving thermal comfort through passive means as a way of reducing energy costs in resource-constrained locations where most citizens cannot afford the luxury of air conditioning. For households that can afford air conditioning, achieving thermal comfort through

passive means can help reduce energy costs and the urban heat island effect. In the context of India, these new building designs and guidelines are meant to serve the Economically Weak Sections (EWS), Low Income Group (LIG), and the Middle Income Group (MIG) as defined by MoHUPA. Table 1.1 shows MoHUPA’s definitions of various socioeconomic groups. MoHUPA asserts that affordable housing should not exceed four times a family’s gross annual income (Deepak Parkh et al., 2008; The Hindu Business Line, 2012; Anshul Dhamija, 2009)

Table 1.1: MoHUPA Income Group Definition and Affordability Criteria

Income Group	Annual Income (Rs)	Affordable Living Area per Household Given Income( $m^2$ )
EWG	100,000Rs	28-46
LIG	100,000-200,000	46-55
MIG	300,000-1,000,000	55-110

MIT and Hunnarshala seek to apply thermally passive/low-energy housing design that fits within the resource, economic, and social constraints of many low-income communities.

Beyond the context of India, the results and designs from this research will be used to write improved building guidelines that can be applied in other regions that face similar climate and economic challenges. Approximately 1 billion of the world’s population live in slums (United Nations, 2016). Of the 1 billion slum dwellers, an estimated 300 million live in Sub-Saharan Africa (World Health Organization, 2009) in addition to the 10 million households that live in the extreme heat regions of India (Indian Agricultural Statistics Institute Research, 2011; Government of India Ministry of Housing and Urban Poverty Alleviation National Buildings Organization, 2013; Census Population Data, 2015). According to the United Nations, "The livelihoods of more than 1 billion people in some 100 countries are threatened by desertification. Nearly 1 billion of the poorest and most marginalized people will be the most severely affected by desertification" (United Nations, 2010; National Geographic Society, 2017). With global climate change, this vulnerable population will



need housing that can protect from forecasted heatwaves. Furthermore, residents in more stable economic situations stand to benefit from thermally passive housing. The International Energy Agency estimates, "in hot climates, the energy savings potential from reduced energy needs for cooling are estimated at between 10% and 40%" (International Energy Agency, 2013).

## 1.3 Thermally Passive Housing Design

Thermal comfort through passive means or low energy means has been well researched and tested. In order to achieve thermal autonomy, "the percent of occupied time over a year where a thermal zone meets or exceeds a given set of thermal criteria through passive means only" (Brendon Levitt et al., 2013), early research first looked to ancient vernacular architecture as a way to achieve thermal autonomy and reduce energy consumption (Gradillas, 2015). Through this study, researchers compiled qualitative data linking building characteristics and ambient conditions (B. Rudofsky, 1964; A. Rapoport, 1969). *The Manual of Tropical Housing and Building* builds on previous Design with Climate research to suggest practicing night flush ventilation with proper thermal mass, heat avoidance, and evaporative cooling as the main methods for passive thermal cooling (Koenigsberger, O. H., 1974). To quantitatively analyze the effectiveness of these methods, researchers conducted field experiments and simulations, studying heat avoidance, use of earth air tunnels, ventilation, evaporative cooling, air movement, proper insulation combined with thermal mass, and radiant cooling. The following sections review past research on thermal autonomy or low energy thermal controls and assess the application of these methods in India.

### 1.3.1 Heat Avoidance

Heat avoidance attempts to achieve thermal comfort by reducing the heat absorption from the sun. Many structures do this by shading areas from direct sunlight and incorporating radiant barriers. Examples of ways to reduce exposure to the sun include vegetation shading, constructing houses with common walls, window shade,

and building orientation. Additionally, visible and shortwave reflective coatings, such as white paint and white tiles, can be used to reduce the amount of incoming solar heat flux. In practice, the incorporation of white tiles in roof design can lower indoor air temperatures, by as much as "5.1°C...[when] compared to a regular room without any [roof] treatment" (Nahar et al., 2003). The method of heat avoidance is often combined with other passive cooling techniques such as proper ventilation and building materials. Current communities in Bhuj practice this method of heat avoidance by building communities with shared walls, thereby reducing solar gains on exterior walls. However, heat avoidance methods have yet to be applied to roofs in Bhuj.

### **1.3.2 Earth-Air Heat Exchanger**

The earth-air heat exchanger takes advantage of the earth's cool temperatures. One of the earliest applications of this method can be seen in ancient Iranian architecture (Bisoniya et al., 2013). Atmospheric air is blown through a tunnel or tube underground. By the time, the air reaches the house, the ground has already cooled the air below ambient temperatures. Earth air tubes have been installed in some buildings in Belgium, Switzerland, Germany, France, and India (Santamouris and Kolokotsa, 2013). In the France case study, "It is reported that the used exchanger improves considerably comfort conditions during summer, while it keeps the indoor temperature of the house below 27°C without the use of air conditioning systems" (Santamouris and Kolokotsa, 2013). Another experiment done in Western India showed earth-air heat exchangers "gives cooling in the range of 8.0-12.7°C for the flow velocities of 2-5m/s (Bisoniya et al., 2013). Though the earth-air heat exchangers show potential, they also have many design challenges such as optimizing size and ensuring cleanliness of the tube, making this method more difficult and expensive to implement. This method of cooling also requires the necessary ground space which, in the context of Bhuj, is not available. In addition, due to the hot arid climate conditions in Bhuj, the ground does not act as an effective heat sink at shallow depths.

### 1.3.3 Ventilation

Successful ventilation in hot arid climates flushes out hot air during the night, bringing in the cooler night air. The literature studies focus on operation schedules and optimizing natural buoyancy-driven ventilation. In hot arid regions, it is best to take advantage of the cool night temperatures to flush out the room's warm air and cool the thermally massive components of the building. Windows and wall openings should be placed at heights and locations to encourage the rising hot air to evacuate the room. "Most of the studies conclude that the use of night ventilation in free floating buildings may decrease the next day peak indoor temperature [by] up to 3°C" (Santamouris and Kolokotsa, 2013).

### 1.3.4 Evaporative Cooling

Evaporative cooling occurs when air moves "over a wetted surface, [causing] some of the water to evaporate. This evaporation results in a reduced temperature" (Santamouris and Kolokotsa, 2013). Proposed methods range from water atomizers, thin film waterfalls, and evaporative roofs to porous materials. Simulations and optimization of some of these evaporation methods show a temperature decrease of up to 8°C (Santamouris and Kolokotsa, 2013). The evaporative roof was tested with prototype chambers in hot-arid Rajasthan, India. Soaked gunny bags were placed on top of the roof for evaporative cooling. The room's ambient temperature decreased due to the heat transfer from the air required to evaporate the moisture in the soaked gunny bags. On average, the temperature of the 1.28m by 6.1m by 1.10m test chamber with the evaporative cooling roof was 13.2°C cooler than the control test chamber with an untreated RCC slab roof (Nahar et al., 2003). When this temperature decrease is extrapolated for a regular building, a fall in temperature of about 5°C can be expected. This method, however, required 50L/m<sup>2</sup> of water per day (Gradillas, 2015; Nahar et al., 2003) as well as the arduous work of constantly preparing and replacing evaporative roof covers. Consequently, this method does not fit in the context of affordable thermally autonomous housing in arid regions.

### 1.3.5 Air Movement

The correlation between air movement and perceived thermal comfort has been well studied. Air movement helps enhance the human body's ability to release heat through evaporative cooling and convective heat transfer. In a study done in the "hot dry climates of Northern India and Iraq," researchers showed that "the presence of air movement can be equivalent to a reduction in temperature of as much as 4°C" (Nicol, 2004). Figure 1-4 shows results from a study done in Thailand, where the lines drawn in the figure represent frontiers of equal comfort levels. This study helps illustrate that increasing air velocities, such as those imparted by a fan, help to increase the Dry Bulb Temperature, temperature measurements shielded from radiation and moisture, at which occupants are comfortable.

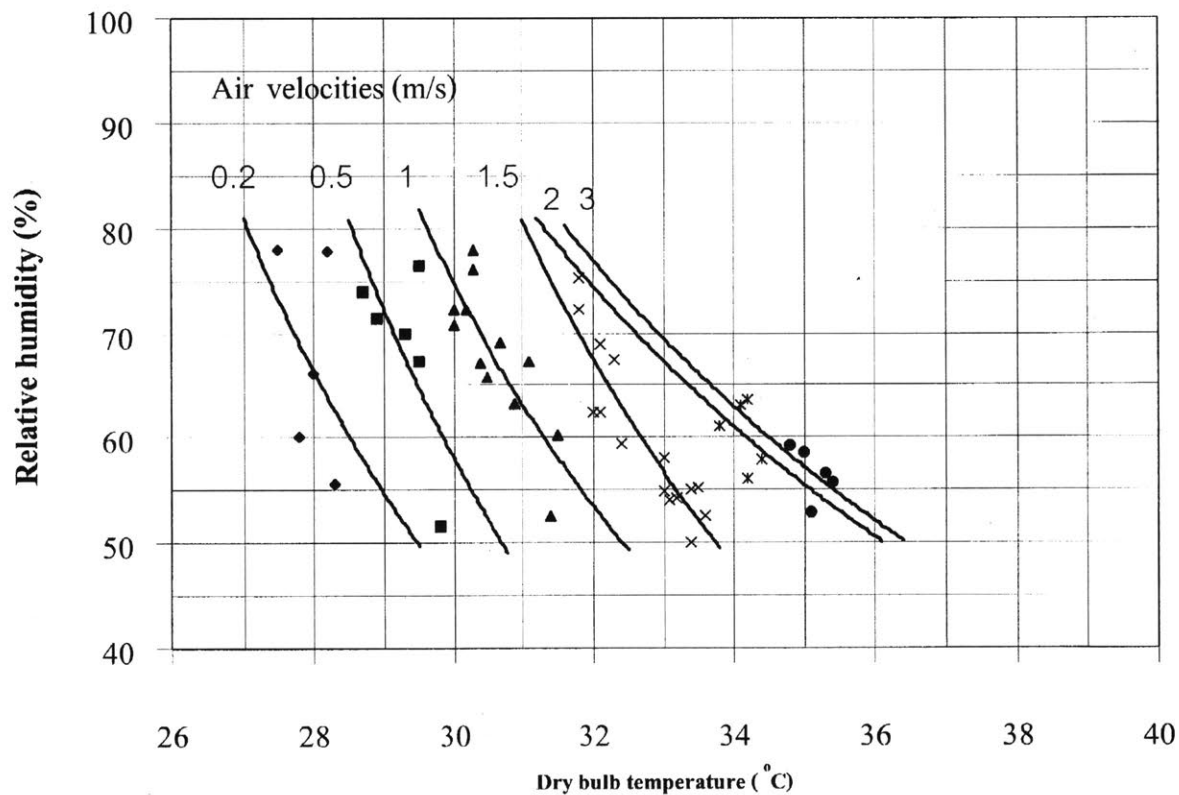


Figure 1-4: Relationship Between Air Movement, Relative Humidity, and Upper Bound Thermal Comfort Dry Bulb Temperature (Khedari et al., 2000)

As air velocities rise, humans are comfortable at higher temperatures. However, air movement effects become less pronounced with increased humidity (Khedari et al.,

2000) as the air has a finite capacity for holding moisture. Other case studies such as those in Pakistan (Nicol, 2004) draw similar conclusions.

Studies have also examined the air movement acceptability limits at given operative temperatures and humidity levels (Candido et al., 2010), and researchers conclude that ceiling fan use can improve thermal comfort (Mallick, 1996; Ho et al., 2009; Arens, Edward et al., 2009; Schiavon and Melikov, 2008). Studies in Australia go so far to conclude that in "low to middle-income housing, features such as ceiling fans...are an integral part of [housing] design" due to their low-cost (Soebarto and Bennetts, 2014).

The prior research, however, does not explore the possibility that air movement from a ceiling fan can increase ambient indoor temperatures. Many informal settlements found in resource-constrained communities use tin sheet roofs that easily become greater than 10°C warmer than the ambient outdoor temperatures. To mitigate risks that come with extreme heat, residents use ceiling fans as a low energy means to improve thermal comfort. Existing studies conclude that air movement positively correlates with thermal comfort because it enhances the body's natural way of releasing heat through evaporative cooling and convection. However, in the context of many developing world homes, this approach may be sub optimal. As the ceiling transfers heat to the air directly underneath the ceiling, the ceiling fan circulates this hot air throughout the living space and increases the temperature at lower levels of the room surrounding the occupants.

### **1.3.6 Thermal Mass and Insulation**

Often, the use of insulation and thermal mass are combined to achieve thermal comfort. Insulation keeps the desired indoor temperature cooler by reducing heat transfer from the inside environment to the outside environment. Thermal mass acts as a way to dampen temperature amplitudes and delay external heat stresses. For example, in the desert region, a house's thermal mass can "store" the cool night temperatures and keep the house cool during the day. Previous experiments by Pearlmutter and Meir in Israel's Negev desert have shown that proper wall design can improve thermal

comfort (Pearlmutter and Meir, 1995). Givoni confirms these findings by conducting experiments with various test chambers in which wall construction was the independent variable. The results showed temperature amplitudes could drop from 66% of the outside swing temperature to about 33% of the outdoor swing temperature (Givoni, 2011). Another study in Morocco, showed, with proper thermal mass and insulation, "the discomfort hours based on an acceptable thermal comfort zone of 16°C-28°C [were] reduced by 62%" (Mastouri et al., 2017).

### 1.3.7 Radiant Cooling

Radiant cooling releases heat from the building envelope through longwave radiation heat transfer to the sky. Given minimal cloud coverage and low humidity, the sky temperatures can often be 20-30°C cooler than outdoor ambient temperatures (Balcomb, 1992). Though longwave radiation cooling occurs constantly, "the radiant balance is negative only during the night" (Givoni, 1991) due to solar heat gains during the day counteracting longwave radiation cooling. Several roof concepts incorporating radiation cooling have been developed. One "concept of radiant cooling is ...a heavy and highly conductive roof [such as a concrete slab] exposed to the sky during the night" (Givoni, 1991). The concrete "stores" the night coolness for part of the day. Though this roof is effective at cooling during the night, it offers little protection from solar heat gains during the day.

Another roof concept, "The Skytherm" by Harold Hay, follows the same thermodynamic principle as the thermally massive highly conductive roof. This roof consists of a steel panel as the highly conductive component and water bags underneath as the thermally massive component. Removable insulation panels are used to protect from solar heat gains during the day (Hay, 1978). Unfortunately, "the conventional horizontally rolling (insulation) panels have...been expensive and mechanically unreliable" (Clack and Cook, 1989). Alternatively, rather than modifying roofs to harness longwave radiation cooling for passive thermal controls, residents can place a ceiling fan under the ceiling of a radiantly cooled roof to mix the cold air directly beneath the ceiling throughout the room. Experiments have shown that this method can

decrease ambient temperatures by 3-5°C on cloudless nights (Givoni, 1991). This method however, still does not address the issue of solar heat gains during the day.

Researchers are now developing and testing surface treatments that have low absorptivity in the visible and shortwave spectrum emitted by the sun, but high emissivity in the longwave spectrum. This reduces the net heat gains during the day while allowing for nocturnal radiant cooling (Zhai et al., 2017). "However, converting a standard roof that's in good condition into a cool roof can be expensive" (Department of Energy, 2017) and out of the budget of those in resource-constrained communities. Painting a surface white is a more economic way of reducing the positive radiant heat flux throughout the day. However, the coating becomes less effective once dirt covers the white surface

## 1.4 Design for Emerging markets.

Though many solutions exist for achieving thermal comfort through low energy or passive means, those solutions have not been successfully implemented in resource-constrained emerging markets. Dissemination of technology and new ideas in resource-constrained regions presents a challenge for many innovators. Oftentimes, the technology designed for customers in wealthy countries are introduced into emerging markets with simple modifications. However, "what works for the rich won't automatically receive wide acceptance in emerging markets" (Govindarajan et al., 2013).

Design for development requires

- Extensive research on available resources, the supply-chain, and user needs in a specific region.
- Meeting the affordability criteria.
- Social acceptance.

The understanding of available materials in the case of designing housing for the developing world is especially important. In a research project on wall construction

in Gujarat, India, Porst found that many bricks used in India did not meet specified strength standards set by the Indian masonry code. Consequently, new models needed to be made for assessing seismic performances (Christopher Porst, 2015). Similarly, when engineering thermally passive controlled homes, initial research on material inventory and behavior must be conducted.

Many housing construction materials commonly used in countries like the US might not be readily available in emerging markets or outside the affordability range of many residents. As a result, researchers have examined the reuse of available byproducts from manufacturing or agricultural processes for the purpose building construction. This encompasses using recycled materials for insulation as a way to reduce construction material cost and to start practicing more sustainable methods. Some examples of this research include a Portuguese research group that found similar thermal conductivities between mineral wool and insulation fabricated from textile waste (Briga-Sa et al., 2013). In Vilnius Gediminas Technical University and Oak Ridge National Laboratories, studies have found insulation constructed from straw to have conductivities as low as 0.04 W/mK (Vejeliene, 2012; Tav Commins and Jeff Christian, 1998). Other experiments used sunflower stalks as insulation (Binici et al., 2014).

Outside academia, companies, and projects, such as Green Roof, ModRoof, and Resilient Modular Systems [RMS], have begun reusing recycled materials such as Tetra Paks, coconut fibers, and reused plastic for roof construction (ReMaterials, 2017; Tetra Pak et al., 2014; Mendoza, 2014; WE DESIGNS LLC, 2014). This method of using recycled and available materials has also been applied in India. Section 1.5 describes initial research in using material ubiquitous and indigenous to India

In addition to being cognizant of the local economy and available resources, the designed housing solution must fit within the social constraints of the region (Rogers, 2003). This involves understanding the socioeconomic aspirations of the end users as well as proper identification of early adopters. "How potential adopters view a change agent affects their willingness to adopt new ideas" (Rogers, 2003). In this Bhuj case study, users aesthetic tastes are considered and input from respected community



leaders is incorporated into the design. Subsequent demonstration and testing of the design illustrate the advantages of the proposed concepts.

## 1.5 Existing Designs and Research in Bhuj

Initial work on passive cooling methods using locally available and recycled materials has been conducted in Bhuj. Madeline Gradillas collected temperature data on existing homes to establish a baseline of existing designs and their thermal comfort performance (Gradillas, 2015). Onset HOBO® Four Channel Analogue External Temp/RH Data Loggers (U23-00) were placed to measure wall, ceiling, and ambient air temperatures in 30-minute increments in seven buildings. The monitored buildings included those found in low-income communities and those found in middle-income and wealthier communities. Building performance and design characteristics are summarized in Figure 1-6, where Buildings 1-7 are ranked by level of effectiveness, y-axis and frequency, x-axis.

Figure 1-6, Figure 1-7 and Figure 1-8 show three of the seven monitored homes. Building 1 (Figure 1-6) is a single-room dwelling with 15cm thick solid concrete masonry unit (CMU) walls and a bare asbestos cement corrugated sheet roof. Building 6 (Figure 1-7) is a single-room dwelling with 23cm thick uninsulated compressed stabilized earth block (CSEB) walls and 12cm thick reinforced cement concrete (RCC) slab roof. Building 7 (Figure 1-8) is a stand-alone two-room dwelling with 15cm thick uninsulated CMU walls and a single-layer Mangalore Pattern tile roof.

Temperature data from existing occupied buildings showed the need for improved roof design. During the data collection period, the outdoor temperature peaked at 40°C. However, ceiling temperatures of the low-income homes reached up to 50°C. Oftentimes, these dwellings do not incorporate passive cooling design methods such as reflective coatings to reduce solar heat flux, radiant barriers, insulation, and ventilation. Thus, the exposed roofs are not protected from the intense solar radiation. Figure 1-9 shows the ceiling temperatures for Building 1, a single-room dwelling with 15cm thick solid CMU walls and a bare asbestos cement corrugated sheet roof, Build-

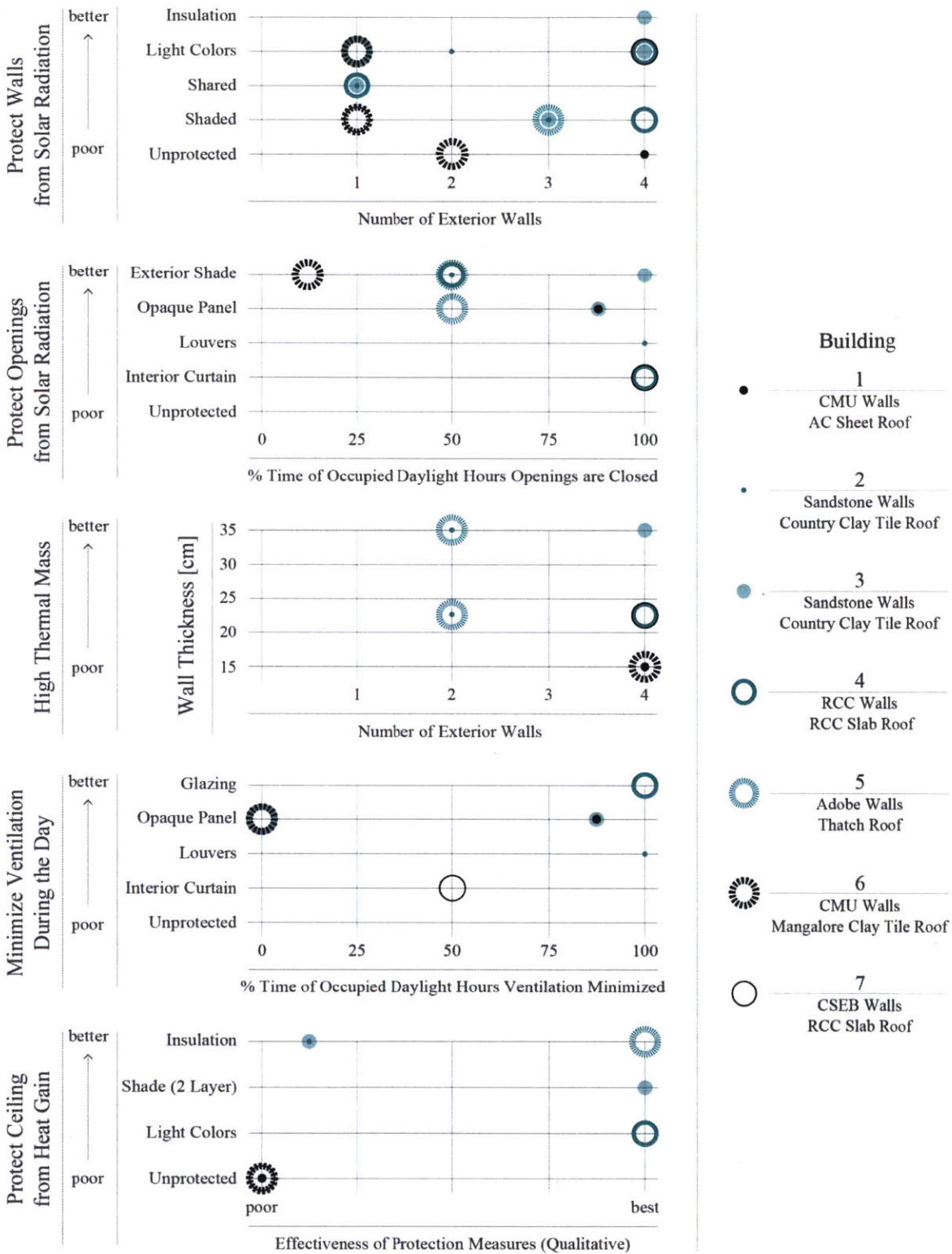


Figure 1-5: Qualitative Mapping of Observed Design with Climate Strategies for Case Study Buildings 1-7 (Gradillas, 2015)



Figure 1-6: Single-Room Dwelling with 15cm Thick Solid Concrete Masonry Unit (CMU) Walls and a Bare Asbestos Cement Corrugated Sheet Roof (Gradillas, 2015)



Figure 1-7: Single-Room Dwelling with 23cm Thick Uninsulated Compressed Stabilized Earth Block (CSEB) Walls and 12cm Thick RCC Slab Roof (Gradillas, 2015)



Figure 1-8: A Stand-Alone Two-Room Dwelling with 15cm Thick Uninsulated CMU Walls and a Single-Layer Mangalore Pattern Tile Roof (Gradillas, 2015)

ing 6, a single-room dwelling with 23cm thick uninsulated compressed stabilized earth block (CSEB) walls and 12cm thick RCC slab roof, and Building 7, a stand-alone two-room dwelling with 15cm thick uninsulated CMU walls and a single-layer Mangalore Pattern tile roof.

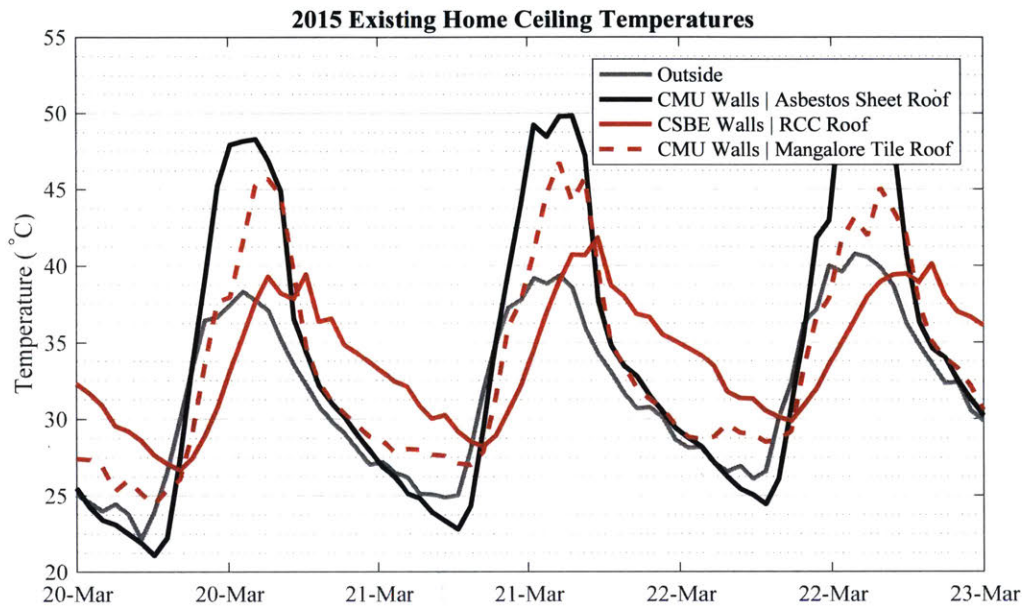


Figure 1-9: Ceiling Temperatures for Existing Vernacular Homes, Buildings 1, 6, and 7 Adapted from *Analysis and Design for Thermally Autonomous Housing in Resource-Constrained Communities* (Gradillas, 2015)

Following the assessment of vernacular architecture, various roof types with differing thermal resistances, solar radiation absorptivities, geometries, and ventilation schedules were modeled and tested in 2.4m by 2.4m by 2.4m prototype test chambers. Five test chambers, each constructed with identical 23cm thick sandstone walls insulated with a 15cm thick layer of straw, were fitted with the following roof types:

- T1 | A Mangalore clay tile roof. This roof is an experimental control, representing traditional building methods found in Bhuj. The Mangalore clay tile configuration allows ventilation through the gaps between the tiles (Vijesh Vasanth Joshi, 2015).
- T2 | A double layer roof structure with insulation composed of recycled shredded plastic as the bottom layer and traditional Mangalore tiles as the top layer. A

7.5cm air gap between the two layers allows hot air to ventilate out to the ambient environment. This roof tests design modifications implemented to improve thermal comfort.

- T3 | A corrugated 0.5mm tin sheet roof. This roof is an experimental control, representing traditional building methods found in Bhuj.
- T4 | A double layer roof structure with insulation composed of recycled shredded plastic as the bottom layer, and corrugated tin sheet as the top layer. A 7.5cm air gap between the two layers allows hot air to ventilate. This roof tests design modifications implemented to improve thermal comfort.
- T5 | A double layer roof structure with a corrugated tin sheet as the bottom layer and a corrugated tin sheet with aluminum foil (a radiant barrier) adhered to the air gap face as the top layer. A 7.5cm air gap between the two layers allows for ventilation. This roof tests design modifications implemented to improve thermal comfort.

Onset HOBO® Pro v2 sensors were placed to measure the interior south wall, ceiling, roof air gap (if applicable), and ambient temperatures in 30-minute increments. The geometry of the test chamber, the various roof types tested, and the sensor locations are shown in Figure 1-10. Throughout the data collection period, the following ventilation schedules were practiced to study the effects of occupant ventilation habits:

- No Ventilation: Jan 31 - Feb 14, 2015 All openings are covered by solid panels 24 hours a day.
- Constant Ventilation: Feb 15 - Mar 3, 2015 All openings remain unobstructed 24 hours a day.
- Night Flush Ventilation: Mar 4 - Mar 23, 2015 All openings are unobstructed from 7 pm to 7 am.

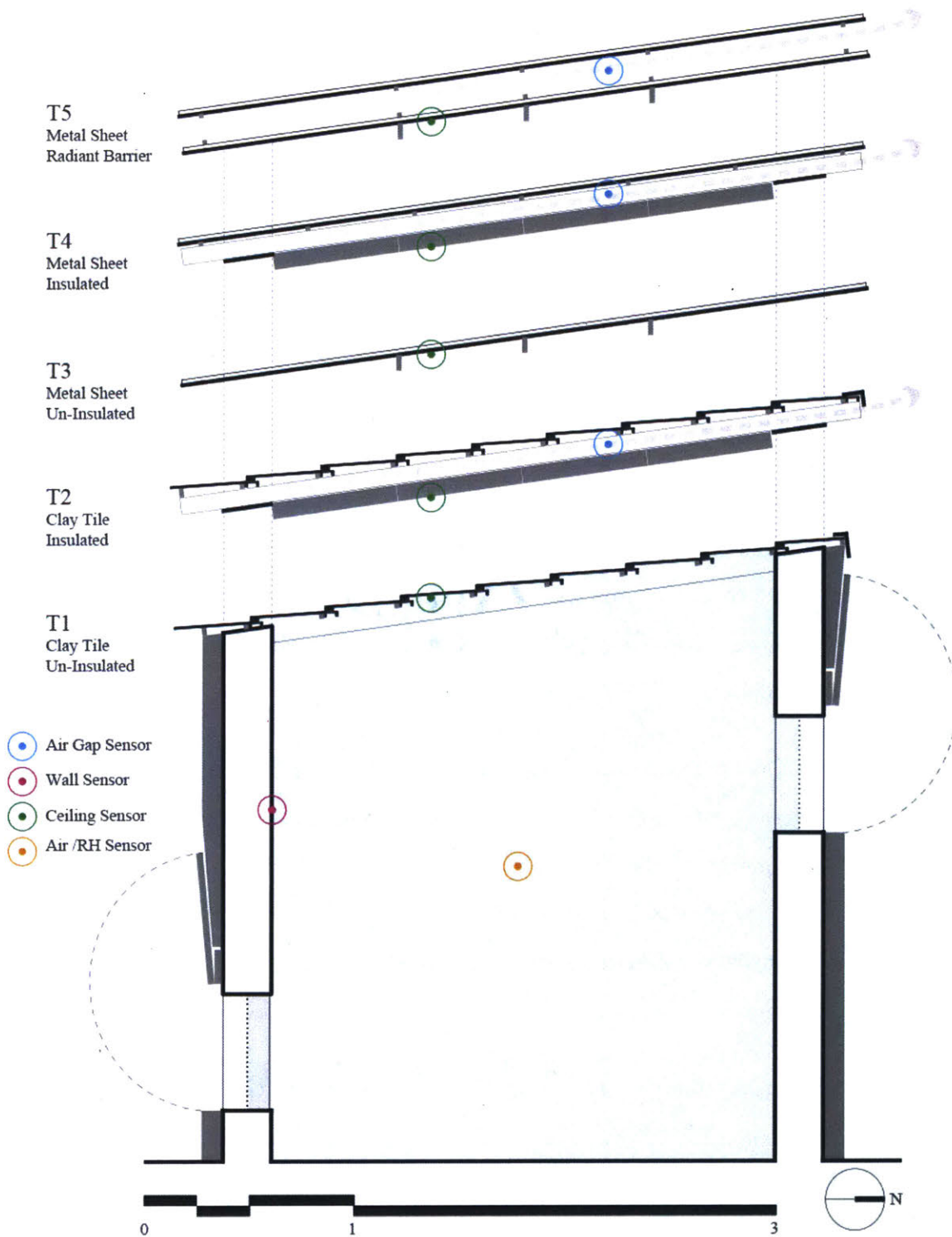


Figure 1-10: Interior South Wall, Ceiling, Air Gap, and Ambient Air Temperature Sensor Locations in Five 2015 Test Chambers with Insulated Walls and Various Roof Types (Gradillas, 2015)

The uninsulated clay tile roof (T1) and the uninsulated metal sheet roof (T3) represent current common roof construction practices in Bhuj. The other roof types incorporate various passive cooling methods to improve thermal comfort. Air gaps were implemented in the double layer tin roofs (T2, T4, and T5) to allow for ventilation between the two roof layers. The air between the two roof layers does not interact with the interior of the test chamber. Insulation was added to the clay tile and tin insulated roofs (T2 and T4) to reduce heat transfer with the external environment. A radiant barrier was placed on the double layer metal sheet roof (T5) to reduce radiant heat transfer.

Prototype chamber field work conducted in 2015 illustrated the influence of roof design and proper ventilation (Gradillas, 2015). For roof design, a performance comparison was done between roof T3, the single layer metal sheet roof that is common among low-income homes, and roof T4, the double-layer insulated metal sheet roof. The double layer allows for roof ventilation and an air gap insulation. During the hottest part of the day, operative temperatures in the chamber with roof T4 were at least 2°C cooler than in the test chamber with roof T3. Thermal comfort was further improved in the test chamber with roof T4 by practicing night flush ventilation. The experimental results of these two test chambers with different roofs are shown in Figure 1-11

These test results led to new low-cost, multi-layered passive roof assembly designs which, coupled with night flush ventilation, showed improvements in thermal comfort. "Interior conditions [were able to] approach ASHRAE and EN-15251 Adaptive Thermal Comfort standards through most of the operating hours" (Gradillas, 2015). In terms of average temperature deviation from the daily maximum outdoor air temperature, the combination of a double-layer tin roof with night flush ventilation decreased operative temperatures by 4°C when compared to a single-layer tin roof with constant ventilation.

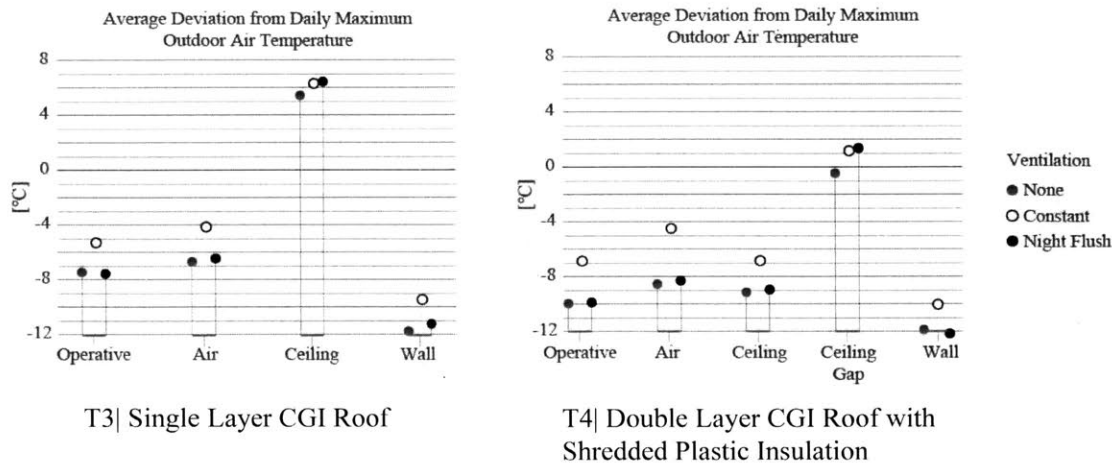


Figure 1-11: Average Temperature Deviations from Daily Outdoor Ambient Air Temperature Peaks for Two Test Chambers Fitted with a Single Layer Roof and a Double Layer Roof (Gradillas, 2015).

### 1.5.1 Next Steps

Though these initial findings made great contributions in the beginning phase of designing thermally autonomous low-income housing, there remain gaps for improvement. One caveat of the proposed ventilated double layer roof design is that the home interior can no longer feel the effects of a nighttime radiantly cooled roof which can be 10°C cooler than the outside ambient air. During the night, the bottom layer of the proposed ventilated roof blocks the heat transfer from the radiantly cooled surfaced to the building interior. The phenomenon can be observed when comparing the test chambers average temperature deviations from nighttime minimums. The single layer roof (T3) allows for more cooling effects than the double layer roof (T4). Operative nighttime temperature deviations temperatures for T3 are almost 3°C cooler than operative temperatures for T4 due to the exposure of the radiantly cooled roof to the interior of the building as shown in Figure 1-12.

The ideal roof would incorporate the radiant cooling effects of a single layer roof during the night with the protection from solar heat gains of a double layer ventilated roof. Questions still remain on how to optimize the performance of the multilayer



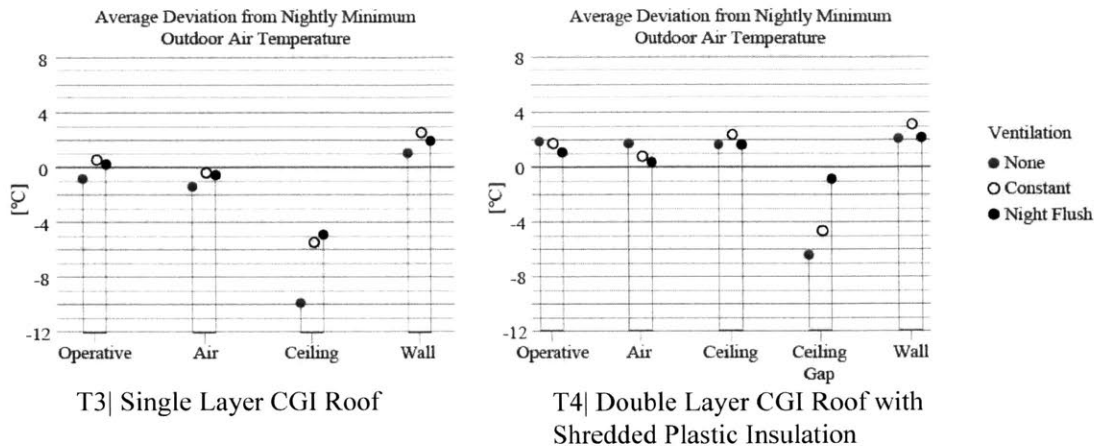


Figure 1-12: Average Temperature Deviations from Nightly Outdoor Ambient Air Temperature Minimums for Two Test Chambers Fitted with a Single Layer Roof and a Double Layer Roof (Gradillas, 2015).

roof structure to allow the benefits of nighttime radiant cooling while protecting from daytime solar heat gains.

In addition to roof elements, "to reach full thermal autonomy by low-cost, passive means, wall treatments must be closely examined in future work" (Gradillas, 2015). Further studies need to quantify how wall insulation affects indoor temperatures and how do the buildings perform given the use of ceiling fans. In addition, Research on materials for housing construction must be more thoroughly investigated for achieving affordability and the successful implementation of these designs. Continuation of this research will examine the effects of varying materials, seek to address questions on wall design; thermal properties, and geometries; fan usage; and improve roof performance.

With the successful demonstration of these passive cooling techniques, this research will look into how to disseminate and implement these building methods by considering the affordability standards written by MoHUPA, past successful methods in design for development, and comprehensive assessments of the soft needs of the residents.

## 1.6 Scope of Research

The following report presents the findings from a collaboration between the MIT and the Hunnarshala Foundation. Through field experiments, simulations, and community surveys, this research seeks to

- Bridge the gap between existing thermal passive cooling methods and design for development in impoverished regions.
- Present an optimal roof design for residents in resource-constrained regions located in hot and arid/humid climates.
- Assess comfort of ceiling fan usage with current poorly insulated roof types and proposed roof types.
- Assess how wall designs and treatment affect thermal comfort.
- Make recommendations for housing design.
- Outline future work.

The thesis is structured as follows: Chapter 2 defines thermal comfort standards against which each design will be assessed. Chapter 3 describes the experimental methodologies, equipment, and test chambers used to design and test various thermally passive designs. Chapter 4 discusses existing and proposed roof types in Bhuj. Chapter 5 illustrates the importance of wall protection on thermal comfort. Chapter 6 gives recommendations on the integration of proposed roof and wall designs. Chapter 7 assesses how the residents' use of ceiling fans with certain roof types might affect comfort. Chapter 8 then summarizes the results and findings of this research.

## Chapter 2

# Defining Thermal Comfort and Performance Metrics

To assess the success of various building and design methods, several standards and metrics have been developed. This chapter discusses the definitions of heat stress, thermal comfort, and healthy temperature levels for mitigating heat-related health risks.

According to Brake, Bates, and Epstein, the human body maintains an internal temperature of 37°C to 38°C, in standard healthy conditions. Core temperatures exceeding 38°C results in heat stress (Brake and Bates, 2002; Epstein and Moran, 2006). Though there is general universal agreement on the definition of "normal" core body temperatures, the causes of core temperature increases vary across human beings depending on age, physical health, and a body's individual reaction to environmental conditions. Consequently, there currently exists no global metric for defining extreme heat or thermal comfort in interior spaces. To account for this, multiple performance metrics looking at different health and comfort aspects in various environments are used throughout this thesis to gain a more inclusive sense of how proposed building designs will affect comfort.

## 2.1 Heat Stress

Before defining thermal comfort in the interior environment, it is important to define heat stress and the climatic or environmental conditions that can increase the risk of heat stress. Individuals exposed to or working in extremely hot environments risk heat stress and experience symptoms including "heat stroke, heat exhaustion, heat cramps, or heat rashes...and dizziness" (The National Institute for Occupational Safety and Health (NIOSH), 2016; Seth H. Holmes, 2016). For public health services, "a non-occupational hygiene index", the Universal Thermal Climate Index (UTCI), was developed "to assess heat stress in the outdoor thermal environment" (Blazejczyk et al., 2012). According to the UTCI, temperatures above 32° constitute as "Strong Heat Stress" as shown in Table 2.1.

Table 2.1: Universal Thermal Comfort Index categorizations of thermal stress

<b>UTCI Range (°C)</b>	<b>Stress Category</b>
Above +46	Extreme Heat Stress
+38 to +46	Very Strong Heat Stress
+32 to +38	Strong Heat Stress
+26 to +32	Moderate heat Stress
+9 to +26	No Thermal Stress
+9 to 0	Slight Cold Stress
0 to -13	Moderate Cold Stress
-13 to -27	Strong Cold Stress
-27 to -40	Very Strong Cold Stress
Below -40	Extreme Cold Stress

Adopting the UTCI's metric for defining outdoor environmental heat stress, residents in Bhuj are susceptible to some level of heat stress heat stress during 73% of the year as shown in Figure 2-1

If exposed to extreme heat environments, one should not exert an excessive amount of energy. Overexertion can lead adverse health effects. The US Department of Labor Occupational Safety and Health Administration outlines heat disorders and health effects (Occupational Safety and Health Administration, 2017) . Heat fatigue can lead to dampened mental performance, heat strokes, medical emergencies, and in

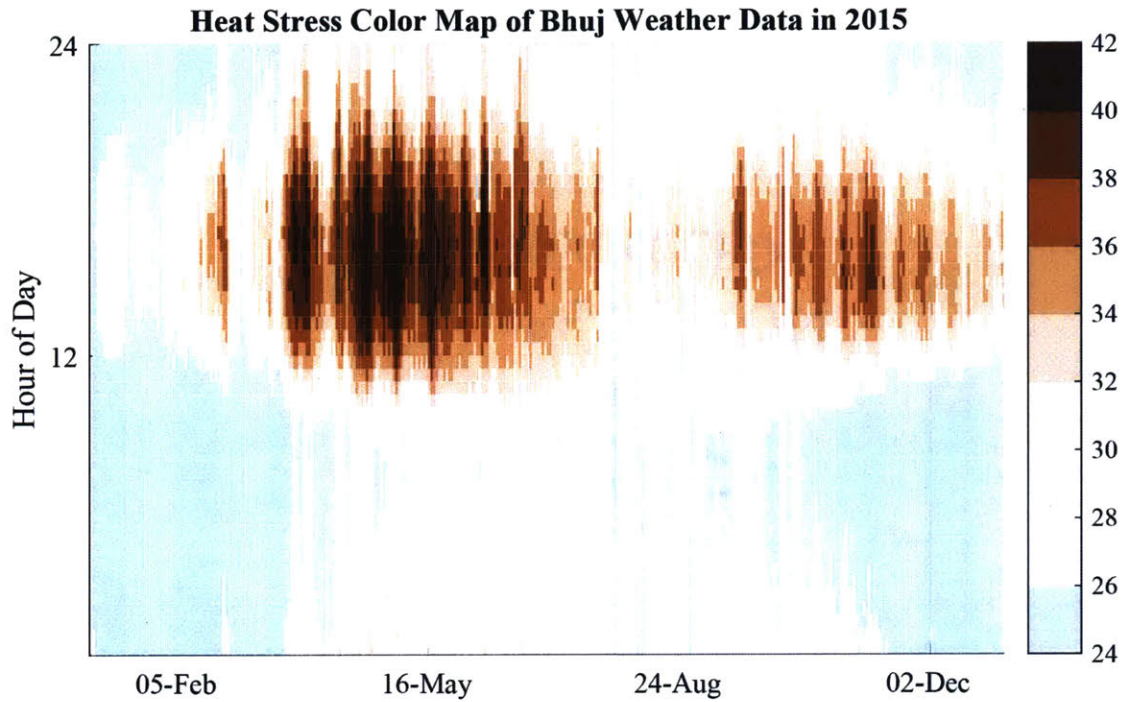


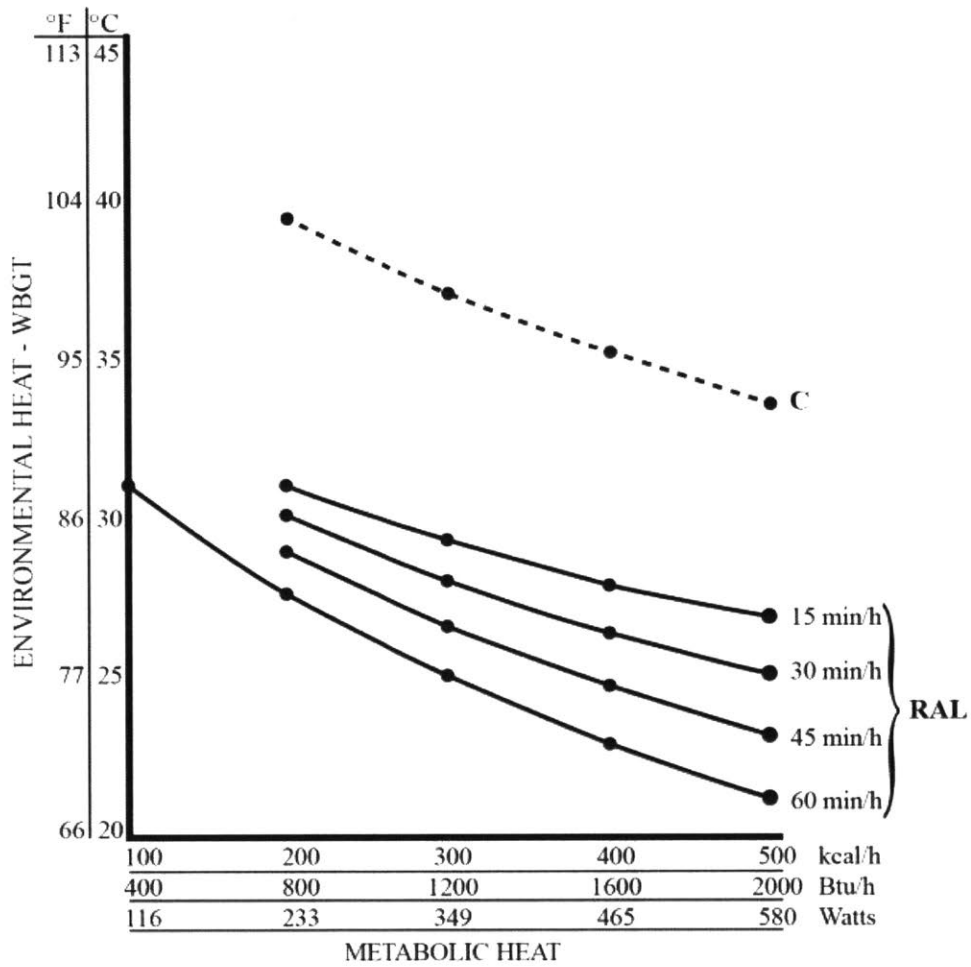
Figure 2-1: Heat Stress Color Map of Bhuj Weather Data in 2015

some extreme cases, death. To minimize these risks, Table 2.2 shows the ideal work to rest ratio in various ambient temperatures based on OSHA’s technical manual.

Table 2.2: OSHA: Permissible Heat Exposure Limit Value

	Work Load (WGBT)		
	Light	Moderate	Heavy
100% Work	30°C	26.7°C	25°C
75% Work, 25% Rest	30.6°C	28°C	25.9°C
50% Work, 50% Rest	31.4°C	29.4°C	27.9°C
25% Work, 50% Rest	32.2°C	31.1°C	30°C

Similar to OSHA, The National Institute of Occupational Health and Safety (NIOSH) has also defined thresholds for working given the Wet Bulb Globe Temperature (WBGT), "a measure of the heat stress in direct sunlight, which takes into account: temperature, humidity, wind speed, sun angle and cloud cover (solar radiation)" (US Department of Commerce and NOAA, 2017), as shown in Figure 2-2



C = Ceiling Limit  
 RAL = Recommended Alert Limit  
 \*For "standard worker" of 70 kg (154 lbs) body weight and 1.8 m<sup>2</sup> (19.4 ft<sup>2</sup>) body surface

Figure 2-2: Wet Bulb Globe Temperature (WBGT) Heat Stress Thresholds for Un-acclimatized Individuals (NIOSH, 2017)

Given extreme exterior heat conditions, it is important that a built environment can protect indoor residents from uncontrollable environmental factors.

## 2.2 Adaptive Thermal Comfort Standards

For determining thermal comfort in indoor environments, organizations such as the American Society of Heating, Refrigeration, and Air-Conditioning Engineers (ASHRAE) (ASHRAE, 2013), EN 15251 European Indoor Environmental Criteria (M. Wilson and Nicol J. F., 2010), and CEPT University’s Centre for Advanced Research in Building Science and Energy (CARBSE) have written standards for adaptive thermal comfort models (ASHRAE, 2013; M. Wilson and Nicol J. F., 2010; Manu et al., 2016). These criteria are summarized in Table 2.3.

Table 2.3: ASHRAE, EN-15251, and IMATC Comfort Standards and Criteria

<i>Standard</i>	<i>Standard Criteria</i>
ASHRAE	Upper 80% Acceptability Limit ( $^{\circ}$ ) = $0.31T_{amb} + 21.3^{\circ}C$ Lower 80% Acceptability Limit ( $^{\circ}$ ) = $0.31T_{amb} + 14.3^{\circ}C$
EN 15251	Upper III Acceptability Limit ( $^{\circ}$ ) = $0.33T_{amb} + 22.8^{\circ}C$ Lower III Acceptability Limit ( $^{\circ}$ ) = $0.33T_{amb} + 14.8^{\circ}C$
IMATC	Upper 80% Acceptability Limit ( $^{\circ}$ ) = $0.54T_{amb} + 16.93^{\circ}C$ Lower 80% Acceptability Limit ( $^{\circ}$ ) = $0.54T_{amb} + 8.83^{\circ}C$
$T_{amb}$ ,	Average temperature over a 30 day period

The adaptive models assume, given changes in average outdoor temperatures, the human body will react by adjusting to these changes, shifting their ranges of comfort (ASHRAE and Fanger, 2017). The CARBSE developed the Indian Model for Adaptive (Thermal) Comfort IMATC to better assess the comfort of residents in India as compared to the ASHRAE-55 and European EN-15251 adaptive model. This model incorporates the results from several survey campaigns across India, including the hot-dry regions of Gujarat, to determine the 80% acceptability limit, where "more than 80% of occupants find thermally acceptable". Figure 2-3 shows a comparison of the ASHRAE-55, EN-15251, and IMATC comfort models.

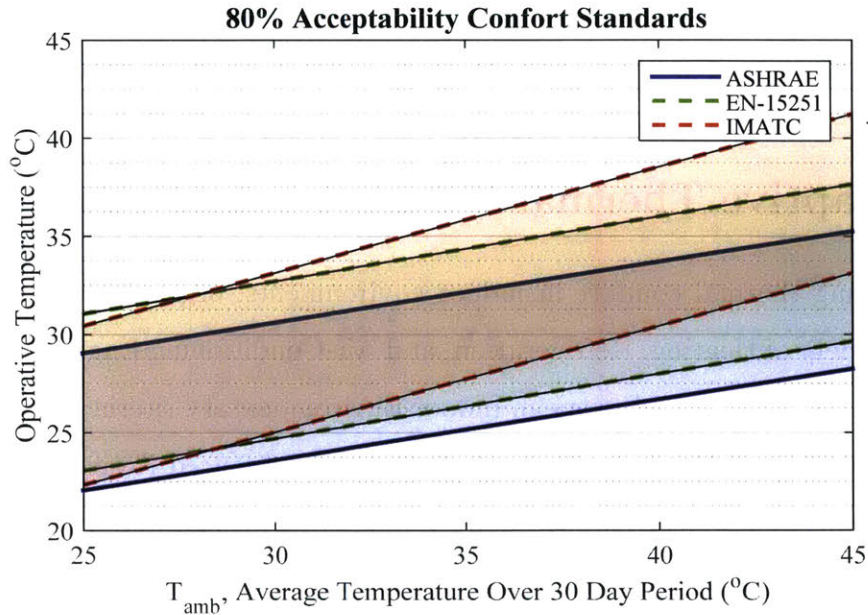


Figure 2-3: ASHRAE, EN-15251, and IMATC Adaptive Thermal Comfort Standards and Comparison

The IMATC model "shows Indians are more adaptive than the prevailing ASHRAE and EN-15251 models would suggest" (Manu et al., 2016). However, the current the IMATC model does not consider air movement or humidity in their thermal comfort model.

ASHRAE-55 Thermal Comfort Environment Conditions Standards were used to determine thermal comfort while considering air movement, humidity, and temperatures (ASHRAE, 2013). The CBE Thermal Comfort Tool, developed by the Center for the Built Environment, University of California-Berkeley, calculates comfort levels, where comfort levels are measured in Predicted Mean Vote (PMV) and Predicted Percent of Dissatisfied (PPD), based on the ASHRAE-55 standards (Hoyt Tyler et al., 2013). The scale of PMV values created by Fanger ranges from -3 to +3, where -3 is too cold and +3 is too hot. The PPD estimated percentage of people uncomfortable based on PMV values. (P.O. Fanger, 1970). The AHSRAE and Fanger models, however, have limitations when defining comfort in the context of Indian buildings as some residents in India may adapt differently to warmer ambient temperatures. Estimated observations on comfort will consider assessments using both the ASHRAE



and IMATC comfort models.

## 2.3 Peak Temperatures and Phase Lags

Other performance metrics used to quantitatively compare the performance of each building design with respect to outdoor environmental conditions are Temperature Deviation from Daily Maximum ( $\Delta T_{peak}$ ), Temperature Deviation from Nightly Minimum ( $\Delta T_{min}$ ) (Gradillas, 2015), and phase shifts( $\phi_{lag}$ ).

The Temperature Deviations from Daily Maximums examine the temperatures for a given temperature vector,  $T_i$ , (i.e. ceiling, wall, or air temperatures) at peak outdoor ambient temperature,  $T_{OAT}$ , conditions. These differences for n number of days are then averaged across a given time domain of n days as written in equation 2.3

$$\Delta T_{peak} = \frac{\sum_{i=1}^n T_i (time(max(T_{i,OAT})) - max(T_i))}{n} \quad (2.1)$$

The Temperature Deviation from Nightly Minimum are calculated by examining the temperatures for a given temperature vector during outdoor minimum temperature conditions. These differences for n number of days are averaged across a given time domain as written in equation 2.3

$$\Delta T_{min} = \frac{\sum_{i=1}^n T_i (time(min(T_{i,OAT})) - min(T_i))}{n} \quad (2.2)$$

If  $\Delta T_{peak}$  or  $\Delta T_{min}$  is positive, the given temperature vector  $T_i$  is, on average, greater than outside temperatures. If the value negative, then the given temperature vector is, on average, cooler than outside temperatures.

Phase lag is calculated by taking the difference between the time when a given temperature vector peaks and when the outdoor temperature peaks. These differences are averaged across a given time domain as written in equation 2.3

$$\phi_{lag} = \frac{\sum_{i=1}^n (time(max(T_{i,OAT})) - time(max T_i))}{n} \quad (2.3)$$

This metric determines the delays in the effects of external heat stresses on the indoor environment.

# Chapter 3

## Field Experiment Setup

Building methods to improve comfort and mitigate health risks were demonstrated and implemented in five model test chambers each with different roof types and four newly occupied homes built under the Housing for All program. This chapter describes the experimental setups used to compare different thermally passive wall and roof designs in both experimental test chambers and newly built occupied homes.

### 3.1 Informal Home

Prior to the *Slum Free Bhuj* project under the national "Housing for All" program described in Section 1.2, some program beneficiary households resided in informal settlements characterized as tent-like structures. Temperature sensors were placed in one of the informal settlements to create a baseline for comparing the thermal comfort of new designs. The monitored informal settlement, shown in Figure 3-1, used two tarp layers and an inner cloth layer as the roof. The walls consisted of 0.20m thick stone of 1m height. Metal sheet and tarp were then used to fill gaps between the wall and roof in the roof gable. Two temperature probes were connected to a HOBO UX120 4-Channel Analog Data Logger (UX120-006M) to measure the air gap and indoor ambient air temperatures as illustrated in Figure 3-2.

The air gap and interior air temperature were measured from January 27, 2016 to December 31, 2016 at 5-minute increments.



Figure 3-1: Exterior View of Informal Home (Photo Courtesy of Bradley Tran)



Figure 3-2: Interior Ambient Air and Air Gap Sensor Placement in Informal Home

## 3.2 Prototype Test Chambers

Five 2.4m by 2.4m by 2.4m test chamber structures with 0.23m thick sandstone walls, shown in Figure 3-3, were constructed to study the temperature and thermal comfort effects of different roof types and ceiling fans. In these experiments, the test chambers did not have wall insulation to compare the effects of uninsulated walls on thermal comfort with previous test chamber configurations which had wall insulation as described in Section 1.5. Each test chamber was fitted with a different roof construction using locally sourced materials shown in Figure 3-3.

It is important to note that the possible materials for the housing in Bhuj was constrained by the available resources. Therefore, in parallel with analytical work, a survey of possible materials (recycled or manufactured) was conducted. During this survey, the thermal properties of recycled materials used for insulation were measured with HFM 436/3 Lambda Heat Flow Meter. The resulting conductivities are listed in Table 3.1. These materials were implemented in prototype roofs. The five roof types

Table 3.1: Thermal Conductivities of Various Insulation Materials

Material	Conductivity (W/mK)
Aluminum Bubble Wrap (4mm)	0.037
Aluminum Bubble Wrap (6mm)	0.039
Aluminum Bubble Wrap (8mm)	0.047
Thermocol	0.053
Mud Roll	0.117

are listed below:

- (R1) A single layer white painted exterior 0.5mm thick corrugated galvanized iron (CGI) sheet that is commonly found in informal settlements as shown in Figure 3-5.
- (R2) A single Layer white painted exterior, 0.11m thick reinforced cement concrete (RCC) slab that is commonly chosen by families with the means to build a more substantial roof as shown in Figure 3-6.

- (R3) A multi-layer roof composed of a white painted exterior and aluminum foil coated interior, 0.11m thick RCC slab. Thermocol (Styrofoam) insulation was placed 15cm below the slab to insulate the roof as well as provide an air gap for ventilation as shown in Figure 3-7
- (R4) A multi-layer roof composed of a white painted exterior, aluminum foil coated interior CGI sheet as the top layer. A layer of bubble wrap, covered with aluminum on both sides, was placed 15cm below the CGI sheet to insulated the roof as well as provide an air gap for ventilation as shown in Figure 3-8
- (R5) A multi-layer roof composed of a white painted exterior, aluminum foil coated interior CGI sheet as the top layer. Mud and straw rolls was placed 15cm below the CGI sheet to insulate the roof as well as provide an air gap for ventilation as shown in Figure 3-9

The single layer CGI sheet roof and RCC slab roof represent roofing commonly used by residents in Bhuj. The multi-layer roofs are modifications on the existing roof types. With better insulation and a geometry that allows hot air directly adjacent to the upper layer tin sheet or RCC slab to ventilate through the air gap, the indoor environment should be better protected from the extreme outdoor temperatures and solar heat gains.

Onset HOBO® Pro v2 sensors were placed to measure the interior south wall, ceiling, roof air gap (if applicable), and stratified ambient temperatures at 1.75m and 0.75m from the floor in 30-minute synchronized increments as shown in Figure 3-10. The mean radiant temperature was measured using a black painted 15.24cm (6inch) diameter copper sphere as shown in Figure 3-4. A HOBO® Pro v2 sensor was then placed in the center of the sphere.

The outside ambient temperatures and relative humidities were measured using an Onset HOBO® U23 Pro v2 (U23-00) data logger. The logger was placed in a shaded area to protect from solar radiation. An Onset Silicon Pyranometer (S-LIBM003) connected to a HOBO Micro Station Data Logger (H21-002) measured solar heat flux. The solar radiance sensor was placed such that no trees or other obstructions



2.4m Cubed Test Chambers with 23cm Thick Sandstone Walls and Ventilation Windows



Tin Roof (R1)



RCC Roof (R2)



RCC Roof + Thermocol Insulation + Ventilated Air Gap (R3)

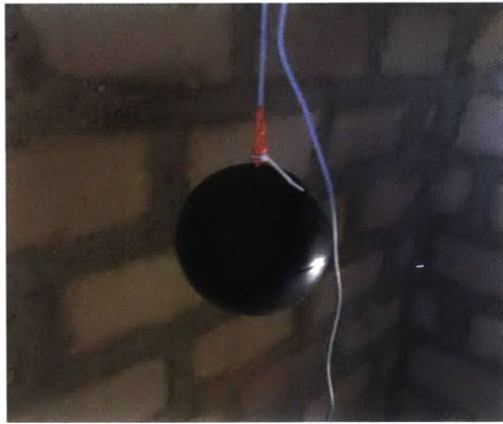


Tin Roof + Ventilated Air Gap + Bubble Wrap Insulation (R4)



Tin Roof + Ventilated Air Gap + Mud Roll Insulation (R5)

Figure 3-3: Five 2.4m by 2.4m by 2.4m Test Chambers with 0.23 cm Thick Sandstone Walls Fitted with Different Roofs



Radiant Temperature Measured at Center of Chamber



HOB0 Pro v2 Sensor Placed Inside 15.24cm Diameter Black Painted Copper Sphere

Figure 3-4: Mean Radiant Temperature Measuring Apparatus

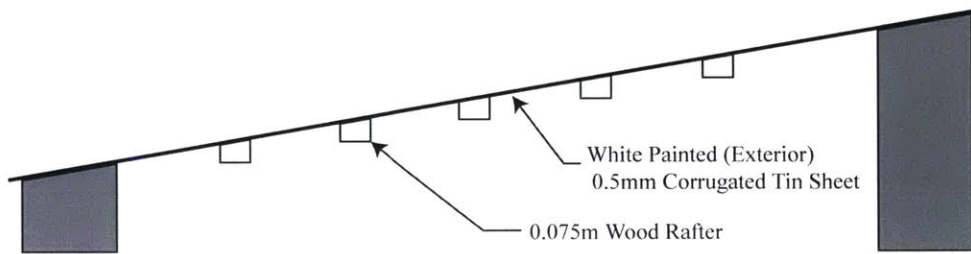


Figure 3-5: R1 | Single layer Tin Roof

could invalidate the data.

The test chamber interior temperatures and outdoor climate conditions were monitored from June 17, 2016 to December 31, 2016 to include both extreme heat and temperate conditions.

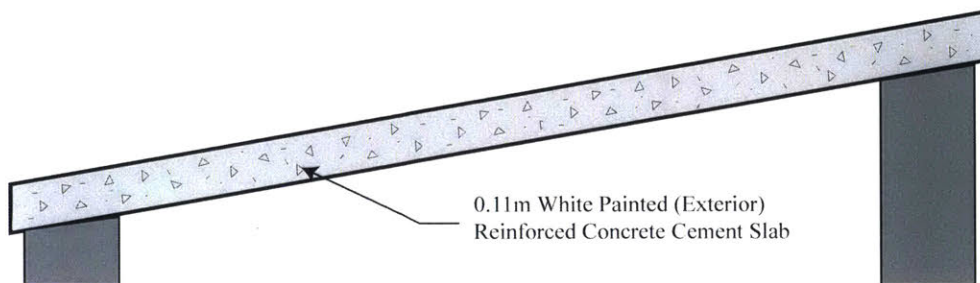


Figure 3-6: R2 | Reinforced Concrete Cement (RCC) Roof



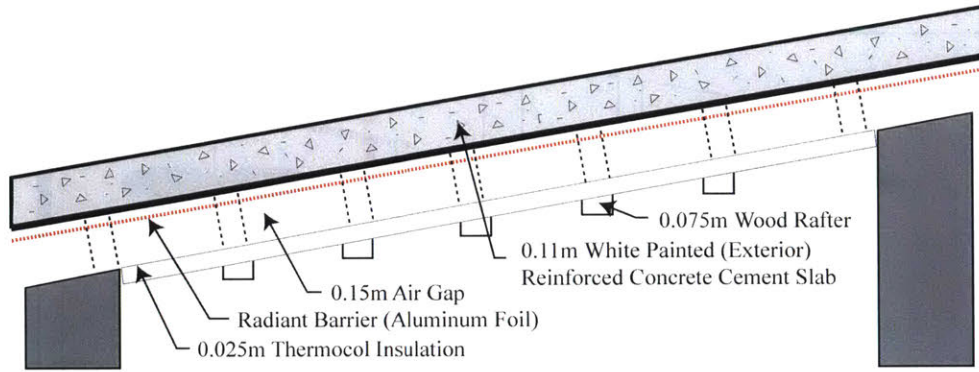


Figure 3-7: R3 | Reinforced Concrete Cement (RCC) Roof with Air Gap and Thermocol Insulation

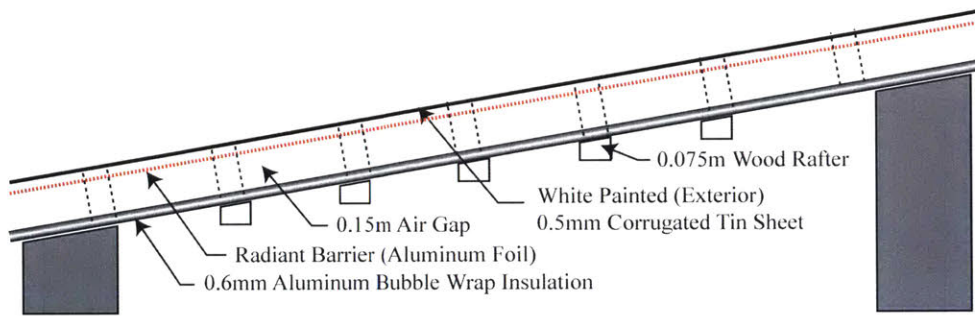


Figure 3-8: R4 | Double layer Tin Roof with Air Gap Radiant Barrier and Bubble Wrap Insulation

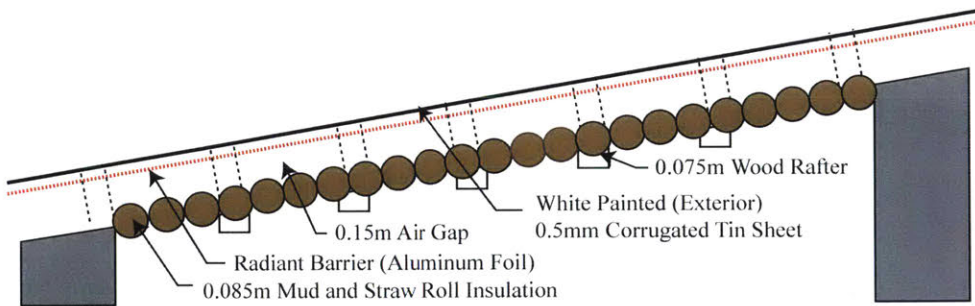
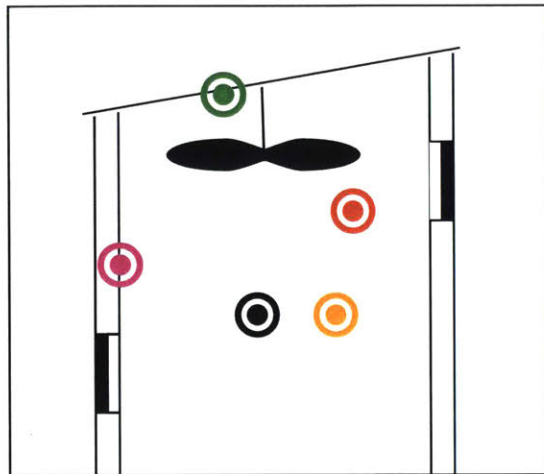
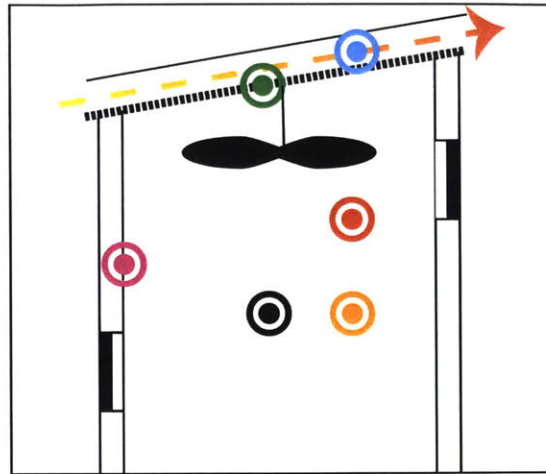


Figure 3-9: R5 | Double layer Tin Roof with Air Gap Radiant Barrier and Mud Roll Insulation

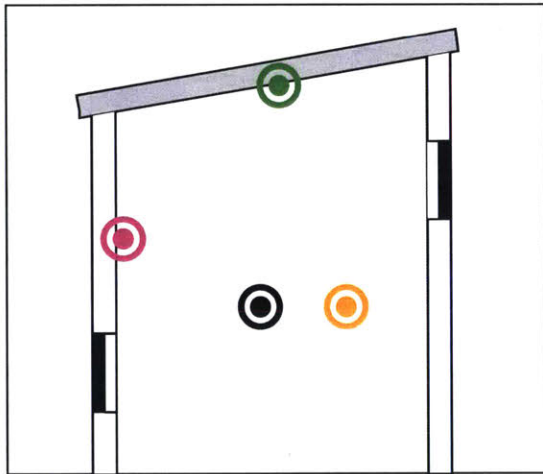
Throughout the test chamber data collection period, night flush ventilation was practiced in which windows were closed from 7:00am to 7:00pm and opened from 7:00pm to 7:00am.



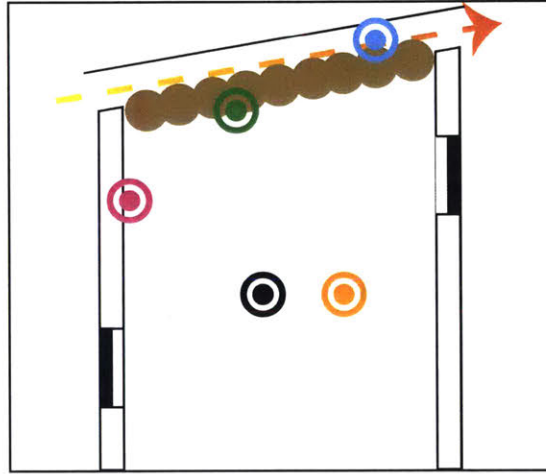
R1 | Single Layer CGI Roof With Ceiling Fan



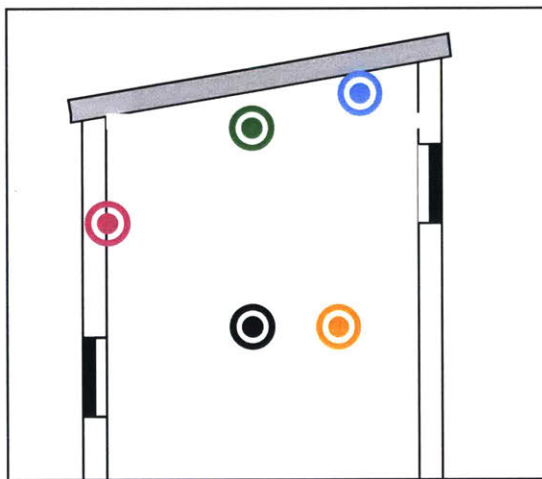
R4 | Double Layer Bubble Wrap Insulated CGI Roof With Air Gap and Ceiling Fan



R2 | Single Layer White Painted RCC Roof



R5 | Double Layer Mud Roll Insulated CGI Roof With Air Gap



R3 | White Painted RCC Roof with Air Gap and Thermocol Insulation







-  Air Temperature at 0.75m Above the Floor
-  Inside Wall Temperature
-  Inside Ceiling Temperature
-  Mean Radiant Temperature at Center of Room
-  Roof Air Gap Temperature (If Applicable)
-  Air Temperature at 1.75m Above the Floor (Test Chambers with Ceiling Fans)

Figure 3-10: Test Chamber Sensor Locations

### 3.3 Housing for All Homes

In addition to testing thermally passive roof designs and wall treatments in prototype test chambers, new building designs were also tested and implemented in four newly built Housing for All homes located at Ramdevnagar. Each home consists of a courtyard, a first floor, and an upper floor as shown in Figure 3-11 and Figure 3-12. The four households opted to build multi-layer peaked roof designs as recommended based on results from field experiments within prototype test chambers. Each house was fitted with a different roof construction as listed below:

- (H1) A multi-layer roof composed of traditional Mangalore tiles as the top layer. Directly underneath the Mangalore tiles, a layer of aluminum foil coated cardboard acts as a radiant barrier. Mud and straw rolls are placed 15cm below the slab to insulate the roof as well as provide an air gap for ventilation as shown in Figure 3-13.
- (H2) A multi-layer roof composed of traditional Mangalore tiles as the top layer. Directly underneath the Mangalore tiles, a layer of aluminum coated foil cardboard acts as a radiant barrier. A wooden ceiling at least 15cm offset from the tiles allows for a ventilated air gap as shown in Figure 3-14
- (H3) A multi-layer roof composed of a white painted exterior, aluminum foil coated interior CGI sheet as the top layer. A ridge vent at the peak of the roof allows hot air to ventilate via buoyancy effects. A wooden ceiling offset 15cm from the tin sheet allows for ventilated air gap as shown in Figure 3-15
- (H4) A multi-layer roof composed of a white painted exterior, aluminum foil coated interior CGI sheet as the top layer. A ridge vent at the peak of the roof allows hot air to ventilate via buoyancy effects. A layer of bubble wrap, covered with aluminum on both sides, is placed 15cm below the slab to insulated the roof as well as provide an air gap. Tin sheets are placed below the bubble wrap as a fire safety measure as shown in Figure 3-16

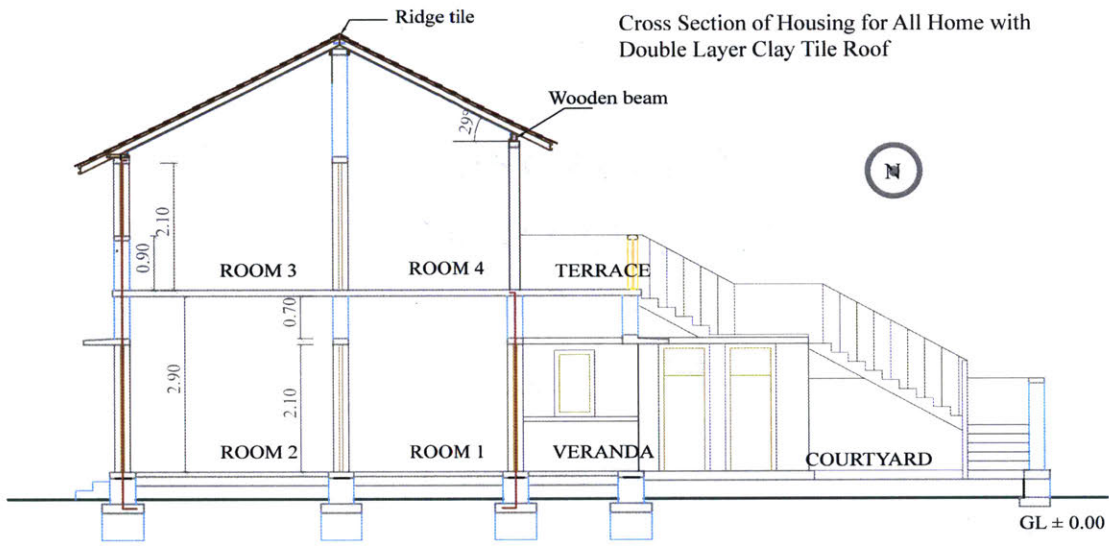
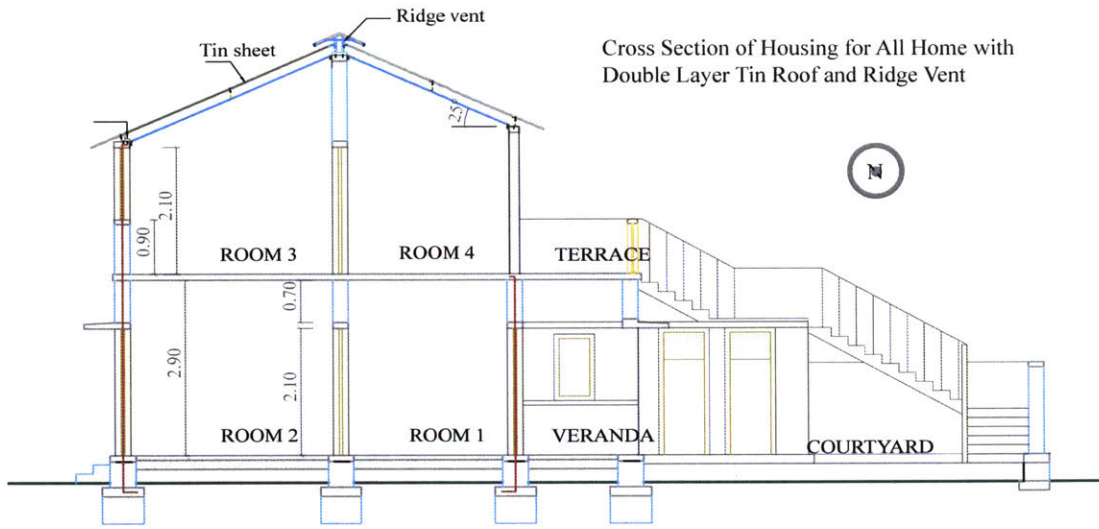
HOBO® UX120 4-Channel Analog Data Logger (UX120-006M) with four temperature probes were placed in each home to measure interior south wall, ceiling, air, and radiant temperatures in 30-minute synchronized increments as shown in Figures 3-13, 3-14, 3-15, and 3-16. As done in the test chamber field experiments described in Section 3.2, the mean radiant temperature was measured using a black painted 15.24cm (6inch) diameter copper sphere with a temperature probe placed centrally inside.

To measure exterior conditions, a weather station was constructed on the southern perimeter of the Housing for All site as shown in Figure 3-17. The following sensors were connected to a HOBO USB Micro Station Data Logger:

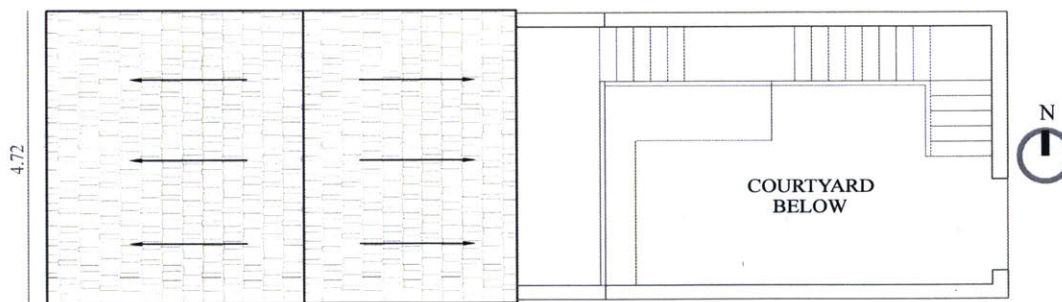
- Onset S-WSB-M003 Wind Speed Smart Sensor to measure wind speed
- Onset S-WDA-M003 Wind Direction Smart Sensor to measure wind direction
- Onset Solar Radiation (Silicon Pyranometer) Smart Sensor that was installed with a Light Sensor Level to measure solar heat flux
- Onset 12-Bit Temperature/Relative Humidity Smart Sensor to measure outdoor ambient temperatures and relative humidities. A HOBO M-RSA Mounted Solar Radiation Shield was used to reduce the effects of solar radiation in temperature monitoring.

Outdoor environmental conditions were measured at 30 minute increments synchronized with the interior temperatures sensors in the four homes.

Throughout the roof construction process, social perception surveys were conducted to understand homeowners and the communities opinions of these pilot roofs. The results from the data collection and survey are discussed in Chapter 4 and 5



Plan View of Housing for All Home



Units in Meters (m)

Figure 3-11: Cross Section and Plan View of Housing for All Homes (Image Adapted from Hunnarshala 2016)



H4 | Exterior of Home with Tin Sheet Roof and Wood Ceiling



H1 | Exterior of Home with Clay Tile and Mud Roll Roof



Housing for All Homes Construction

Figure 3-12: Exterior of Housing for All Homes Fitted with Pilot Roofs

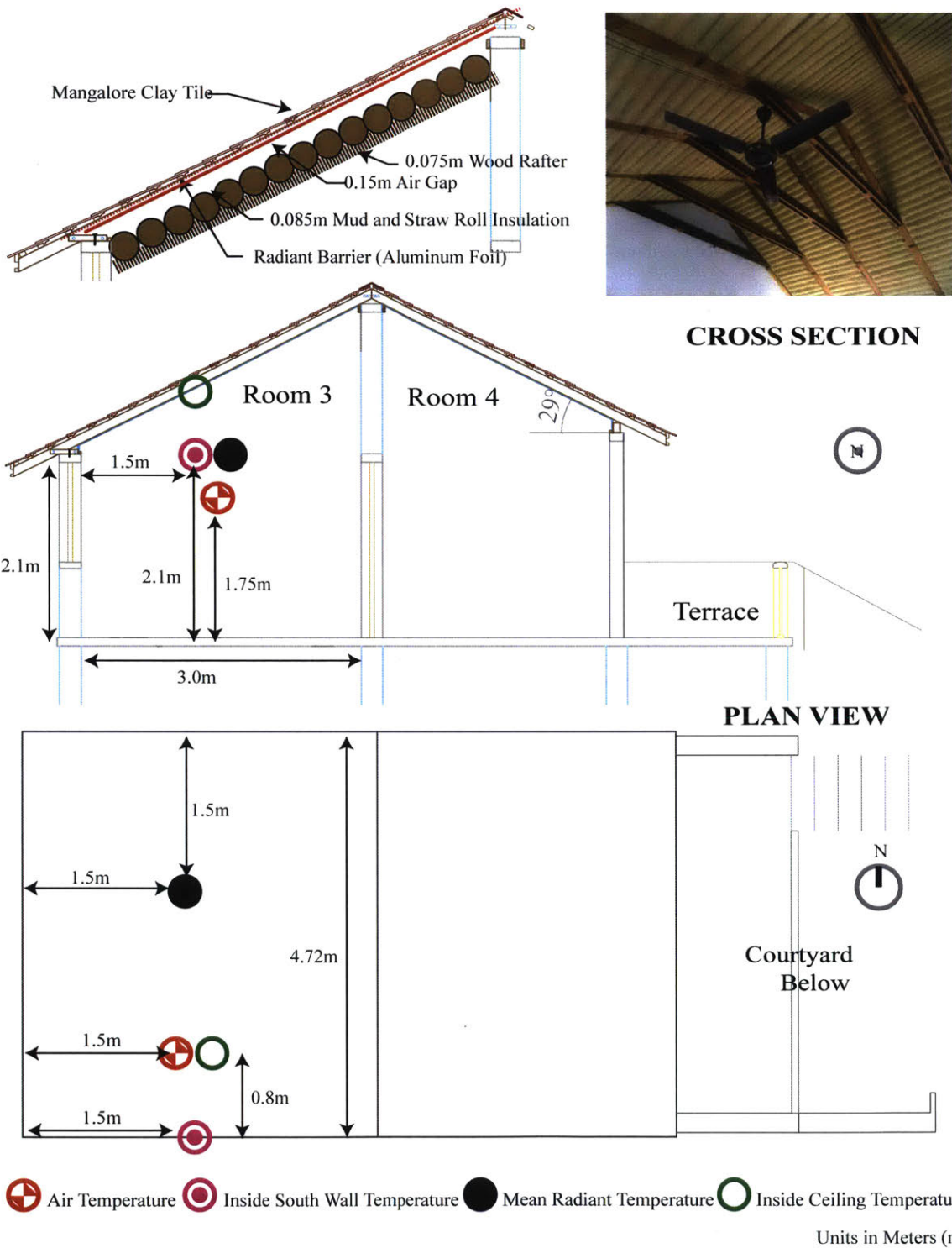


Figure 3-13: Roof Design and Sensor Locations in Home with a Double Layer Clay Tile, Radiant Barrier, and Mud Roll Insulated Roof (H1) Image Adapted from Hunnarshala 2016

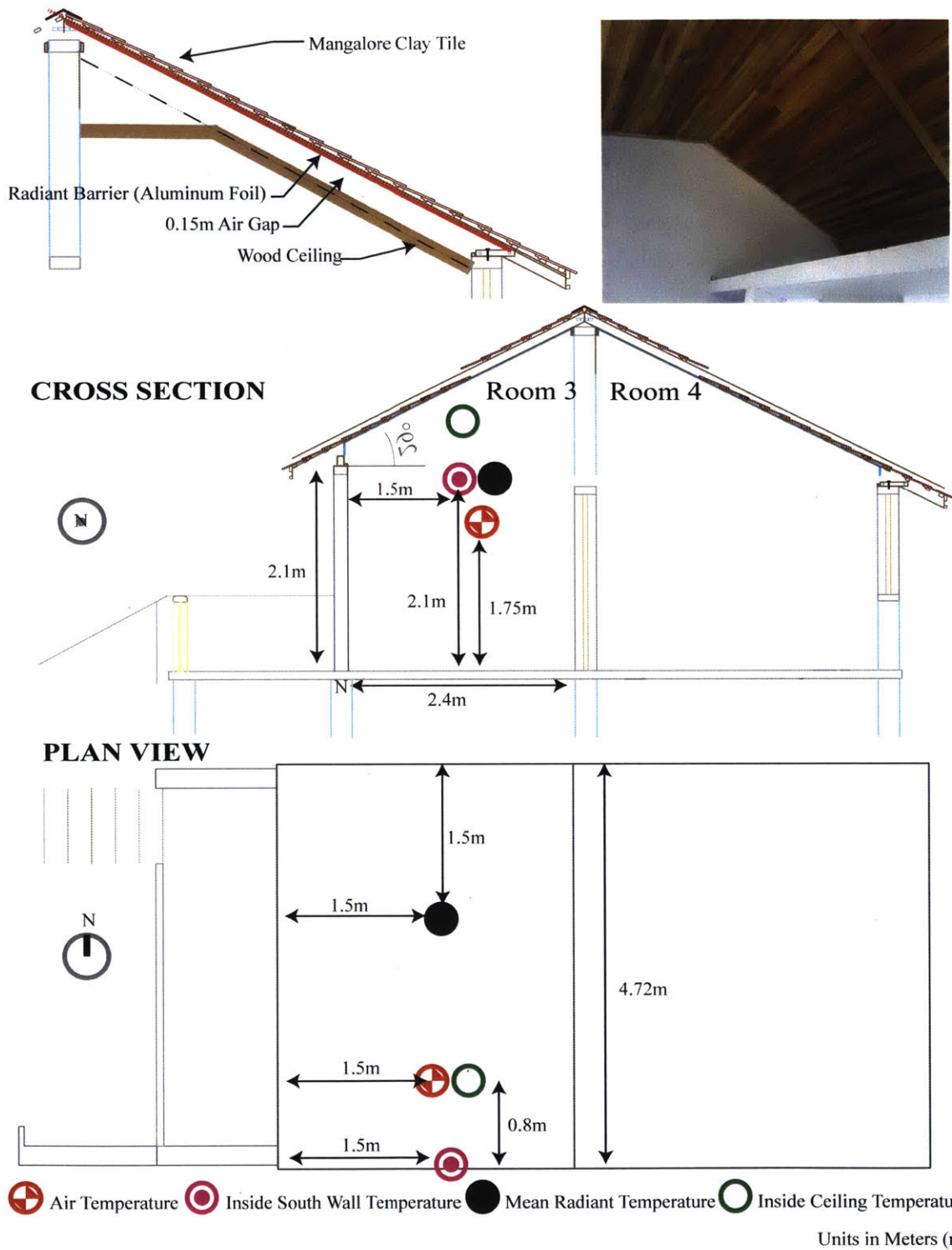
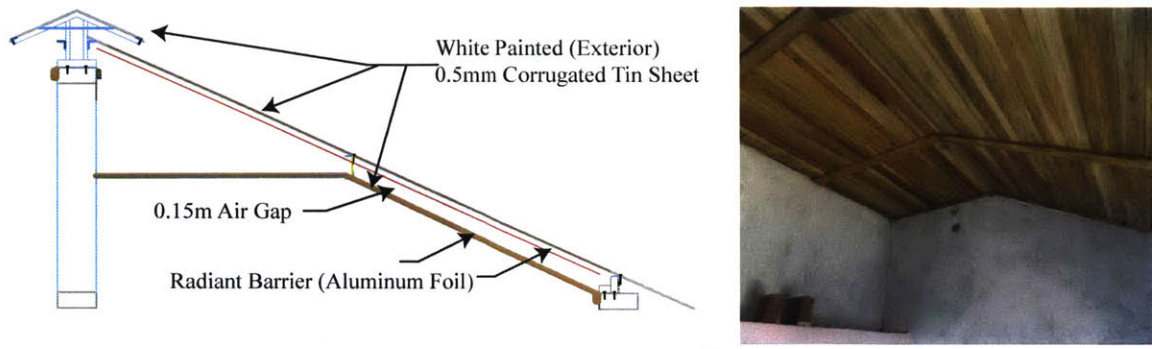
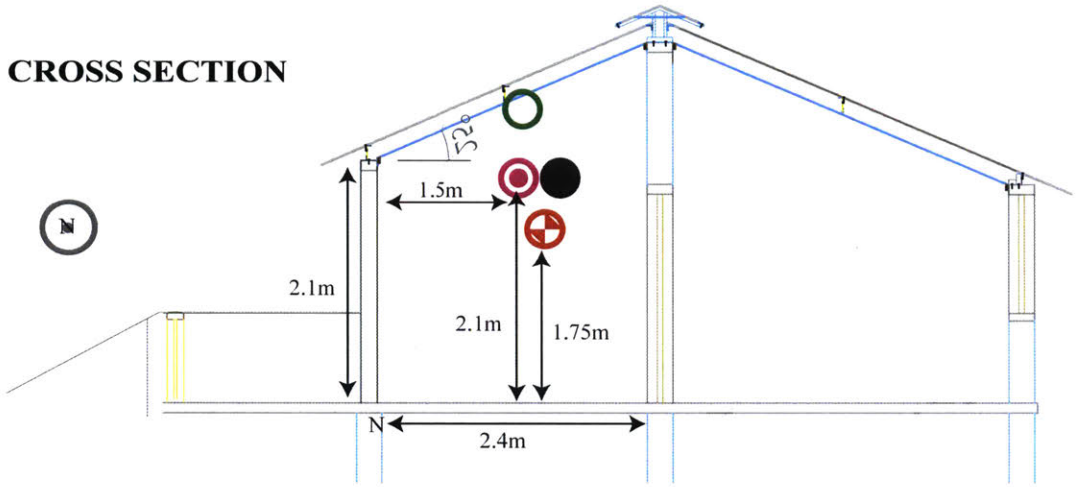


Figure 3-14: Roof Design and Sensor Locations in home with a Double Layer Clay Tile, Radiant Barrier, and Wood Ceiling Roof (H2) Image Adapted from Hunnarshala 2016

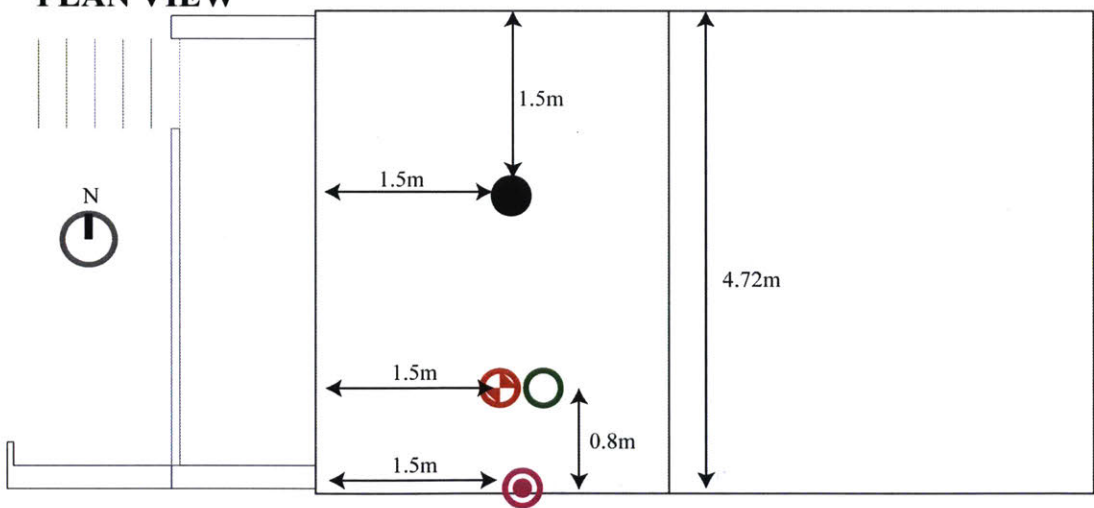





**CROSS SECTION**



**PLAN VIEW**



 Air Temperature 
  Inside South Wall Temperature 
  Mean Radiant Temperature 
  Inside Ceiling Temperature

Units in Meters (m)

Figure 3-15: Roof Design and Sensor Locations in Home with a Double Layer Tin, Radiant Barrier, and Wood Ceiling Roof (H3) Image Adapted from Hunnarshala 2016

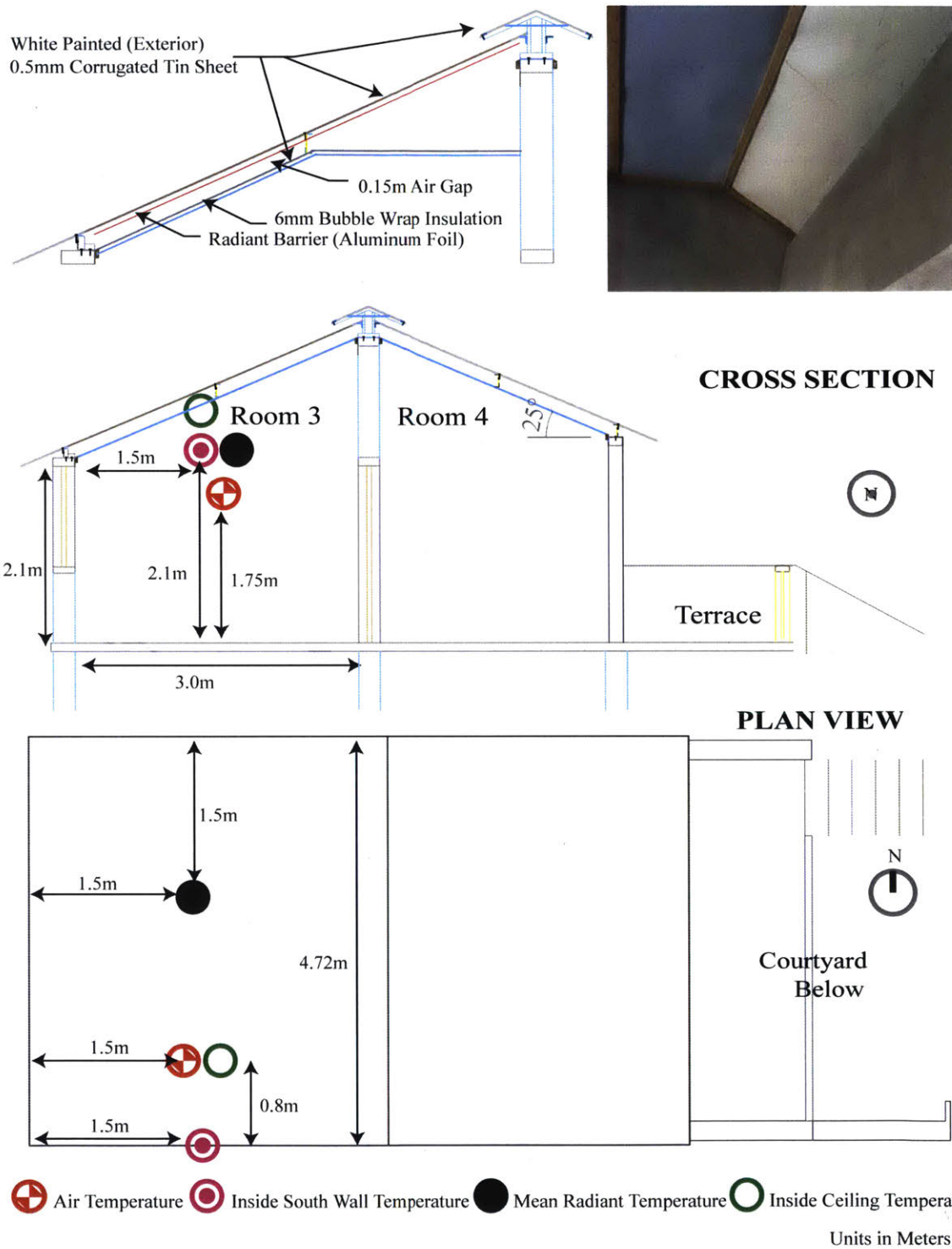


Figure 3-16: Roof Design and Sensor Locations in Home with a Double Layer Tin, Radiant Barrier, and Bubble Wrap Insulation Roof (H4) Image Adapted from Hunnarshala 2016

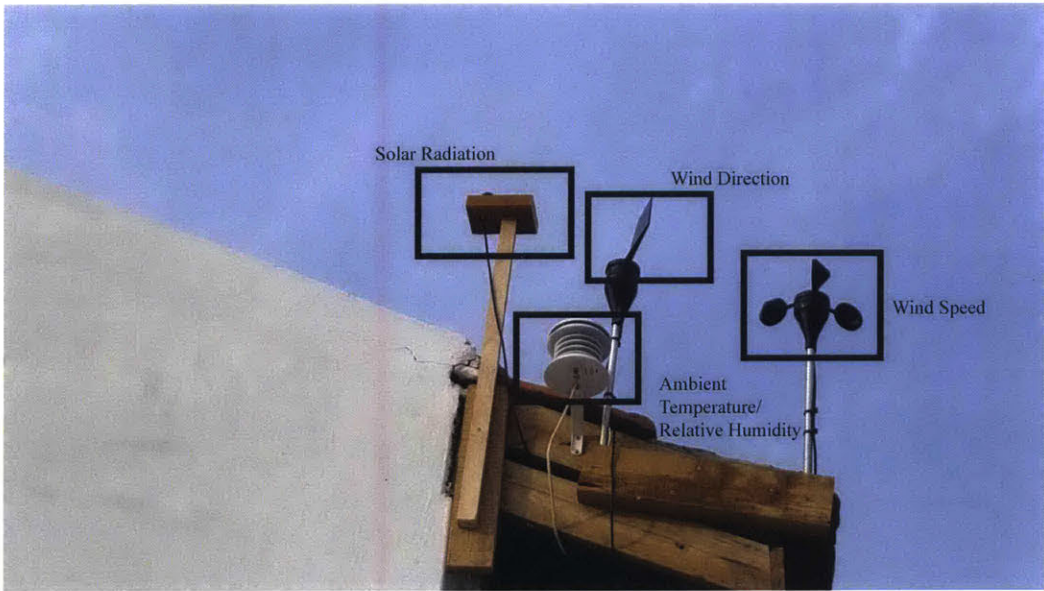


Figure 3-17: Weather Station Placed on the Southern Border of the Housing for All Site



# Chapter 4

## Performance of Existing and Proposed Roof Types

Worldwide, over 800 million urban slum dwellers "lack safe, adequate roofing" (United Nations, 2016; ReMaterials, 2017). Due to resource constraints, residents frequently use corrugated asbestos cement or tin sheets as roofing material. Often, rain leaks through and ambient sounds disturb the residents. Besides the discomfort of these roofs, they also pose major health threats. Asbestos cement sheets contain toxic carcinogenic chemicals. Both types of corrugated roofing provide little to no protection for the residents from solar heat gains. Consequently, indoor temperatures can often exceed outdoor ambient temperatures, especially with the use of a ceiling fan that mixes the hot air directly adjacent to the uninsulated ceiling (see Chapter 7 for more discussion). In Bhuj, roofs are the least thermally protected component in a home and account for approximately 25% of the housing costs (Rupesh Hurmade and Tejas Kotak, 2016). This chapter discusses the results and intra-chamber comparisons of the five prototype test chambers described in Section 3.2. The test chamber data then informs designs for full-scale homes. This chapter also examines roof performance in four pilot homes described in Section 3.3. The performance of these pilot homes are then compared with the performances of existing vernacular homes described in Section 1.5 and a monitored informal home described in Section 3.1

## 4.1 Test Chamber Results and Discussion

As described in Section 3.2, the team constructed five 2.4m by 2.4m by 2.4m test chambers with exposed sandstone walls. Night flush ventilation was practiced in all the test chambers. The five roof types installed on these test chambers include a single layer tin sheet (R1), an RCC slab (R2), a ventilated RCC slab with thermocol insulation (R3), a ventilated tin roof with bubble wrap insulation (R4), and a ventilated tin roof with mud roll insulation (R5). Roof types R1 and R2 represent control roofs, ubiquitous existing roof types in Bhuj and other similar resource-constrained regions. Roof types R3-R5 represent modifications of these indigenous roof types.

Figure 4-1 shows transient ceiling temperatures of the test chambers with various roof types. The control roofs, a single layer tin sheet and an RCC slab, exceed outdoor peak temperatures daily. On July 24th, the single layer tin roof ceiling temperatures exceed the outdoor peak temperature by 10°C. Ceiling temperatures for the RCC roof can exceed outdoor exterior temperatures by 5°C. The addition of a ventilated air gap and insulation can lower ceiling temperatures to be less than the outdoor ambient air temperatures.

The difference between the ceiling temperatures and the outside temperatures are illustrated through a temperature map for the period of July 17, 2016 to December 31, 2016 shown figure 4-2. Of the five prototype roofs in this testing period, the single layer tin roof (R1) reaches the hottest temperatures during the day. The CGI sheet's lower thermal mass and high conductivities do little to protect against solar heat gains. The installation of a ventilated air gap and an insulation layer reduces peak ceiling temperatures by greater than 10°C. The ceiling with the bubble wrap insulation (R4) stays cooler in the evenings and early mornings than the ceiling with the mud roll insulation (R5). Unlike the mud roll insulation, the bubble wrap has a negligible amount of thermal mass to "store" heat or nighttime coolness. Heat capacitance properties of the mud roll insulated roof allow the ceiling temperatures to stay cooler during the outdoor ambient air temperature peaks in the early afternoon. Though the modified tin sheet roofs reduce peak outdoor air temperatures, the single

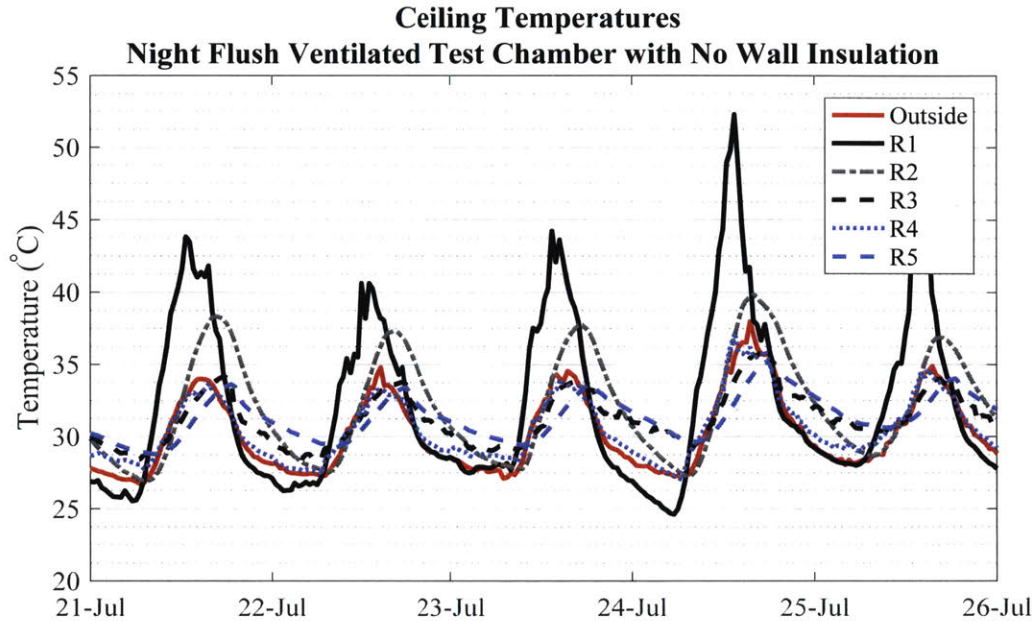


Figure 4-1: Transient Ceiling Temperatures for Test Chambers with Roof Types R1-R5

layer CGI roof without insulation (R1) is the most effective roof for radiant cooling. During the night, when net radiant heat transfer is negative, the ceiling can be 10°C cooler than then exterior temperatures.

Ceiling temperatures of the RCC roof (R3) do not exceed outdoor ambient air temperatures during noon. However, approximately four hours after noon, ceiling temperatures can exceed outdoor air temperatures by greater than 5°C. The thermal mass properties of the RCC roof delay the effects of the solar heat gains to a later part of the day, ultimately still not properly protecting the building interior from extreme exterior heat stresses. Adding ventilation and insulation to the control RCC roof (R4) lowers the peak ceiling temperatures. However, similar to the effects of modifications on a single layer tin sheet roof, the addition of insulation and a ventilated air gap insulates against some of the early morning radiant cooling effects of the RCC roof.

In the 2016 test chambers, indoor ambient air temperatures often exceed outdoor ambient temperatures as shown in Figure 4-3, a plot of the transient temperatures and Figure 4-4, a color map of the temperature temperatures differences between the

Night Flush Ventilated Test Chamber with No Wall Insulation:  
Difference Between Ceiling and Outdoor Air Temperatures

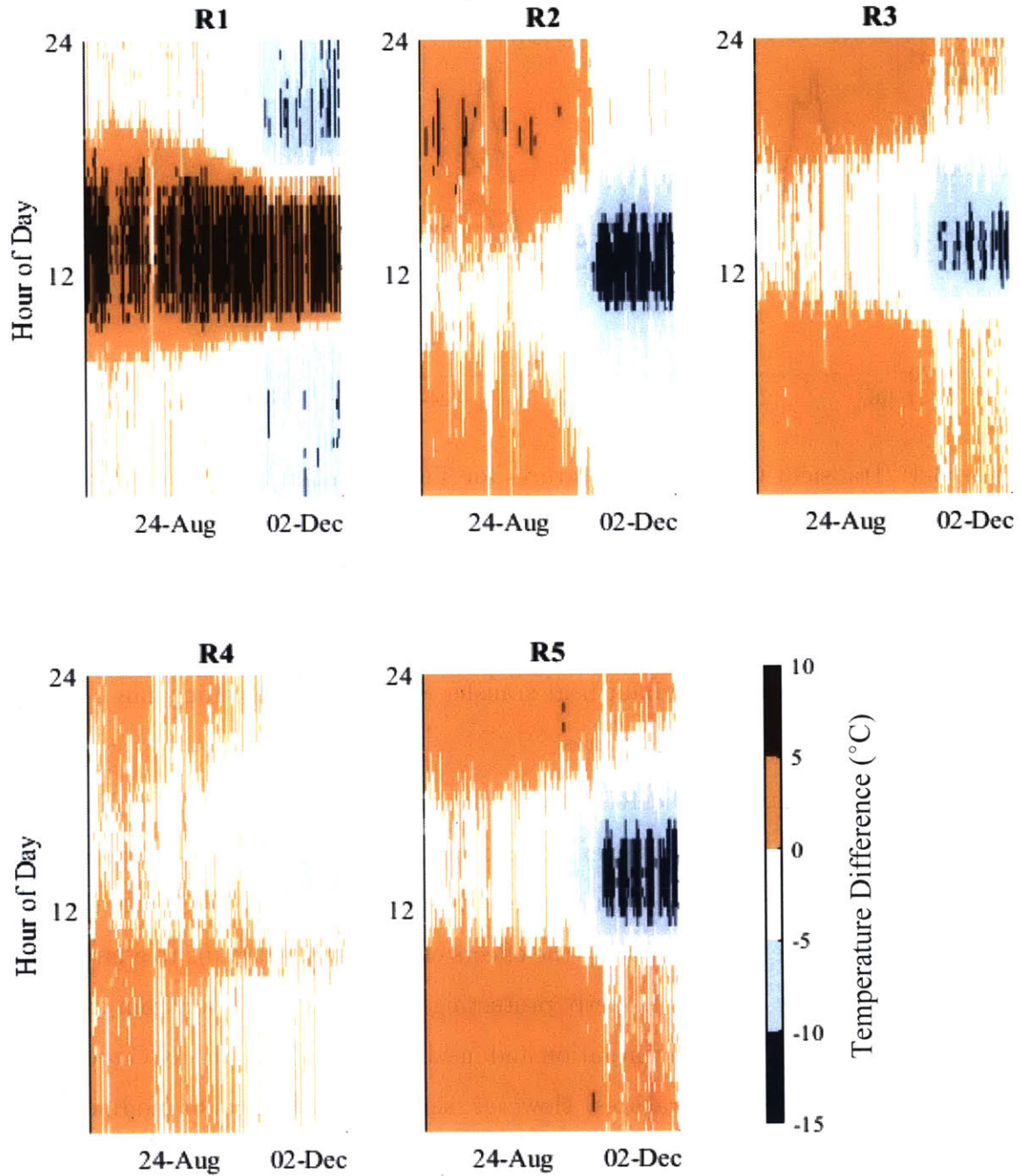


Figure 4-2: Color Map of Temperature Differences Between Ceiling and Outdoor Ambient Air



interior and exterior environment. Given these test chambers' walls lack of protection from solar heat gains and wall to roof ratios of 4:1, indoor air temperatures are highly correlated with wall temperatures. Wall transient temperatures and color maps are shown in Figure 4-5 and Figure 4-6. Chapter 5 discusses in detail how wall design affects indoor temperatures. Though wall protection highly influences indoor ambient air and interior wall temperatures, measured interior temperatures illustrate some differences in air and south wall temperature due to roof design. Test chambers with the control roof types, the single layer tin sheet and the RCC slab reach warmer mid-day indoor air temperatures as shown in Figure 4-4. Test chambers with roofs constructed from thermally massive materials such as RCC (R2 and R3) or mud roll (R5), experience evening hours in which indoor air temperatures exceed outdoor temperatures by at least 5°C during summer months near the humid monsoon season (June-August). Following November, when nighttime temperatures decrease and lower humidity levels allows for more effective radiant cooling, the thermally massive roofs can "store" night coolness to keep mid day temperatures cooler.

The effects of radiant cooling appears most prominent in the test chamber with the single layer CGI roof where ceiling temperatures can be 10°C cooler than the outdoor ambient temperatures from late evening to early morning. Transient interior air temperatures in Figure 4-3 show that the test chamber with the single layer CGI roof is the coolest of all the test chambers during periods when the net radiant heat transfer is negative. This test chamber can be 1-2°C cooler than the other test chambers with roofs composed an insulated air gap that dampens the effects of radiant cooling. The cooler nighttime ambient air in the test chamber with a single layer CGI roof correlates with cooler nighttime interior south wall temperatures. The colder surface temperatures contribute to more comfortable operative temperatures in an extreme heat environment.

Operative temperatures, used in adaptive thermal comfort metrics, consider the radiant heat flux from surrounding interior building surfaces as well as the effects of convective heat transfer from the ambient indoor air. During the daytime, though the single layer test chamber's ceiling temperatures exceed all other test chamber ceiling

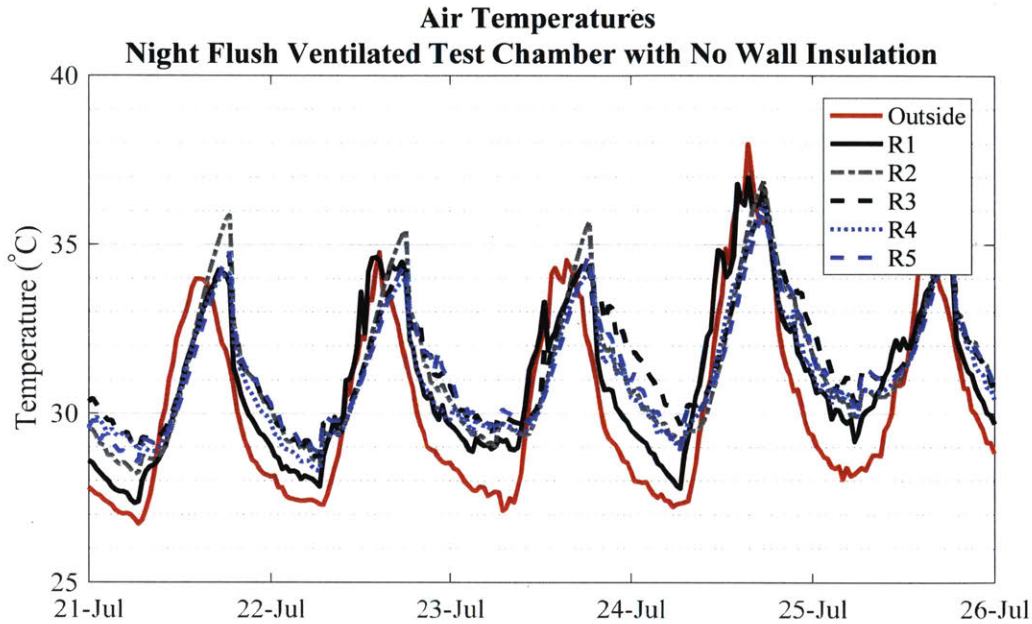


Figure 4-3: Transient Air Temperatures for Test Chamber with Roof Types R1-R5

temperatures, the test chamber with the RCC roof reaches the highest operative temperatures of all the test chambers as illustrated in Figure 4-7 and Figure 4-8. Radiant temperatures were plotted as a function of ceiling temperatures for the single layer tin sheet and the RCC test chamber to determine the cause of this discrepancy between operative and ceiling temperatures. Figure 4-9 shows that ceiling temperatures have a greater influence on radiant temperatures in the test chamber with the RCC roof.

RCC radiant temperatures can exceed  $40^{\circ}\text{C}$  while RCC ceiling temperatures do not exceed  $45^{\circ}\text{C}$ . Despite single layer tin sheet ceiling temperatures often exceeding  $45^{\circ}\text{C}$ , the radiant temperatures do not exceed  $40^{\circ}\text{C}$ . Best fit lines to plots of radiant temperatures as a function of ceiling temperatures as shown in Figure 4-10, illustrate that compared to test chambers with roofs R2-5, the ceiling temperatures of test chamber with roof R1 causes little impact on the radiant temperatures.

The emissivity of the tin roof, measured by Surface Optics Corporation SOC 400T, is 0.09. Thus, there is very little infrared heat transfer between the CGI roof and the rest of the interior. The radiation coming off of the CGI roof is primarily reflected radiation from the walls. Due to the low emissivity of the ceiling, wall

Night Flush Ventilated Test Chamber with No Wall Insulation:  
Difference Between Indoor Air and Outdoor Air Temperatures

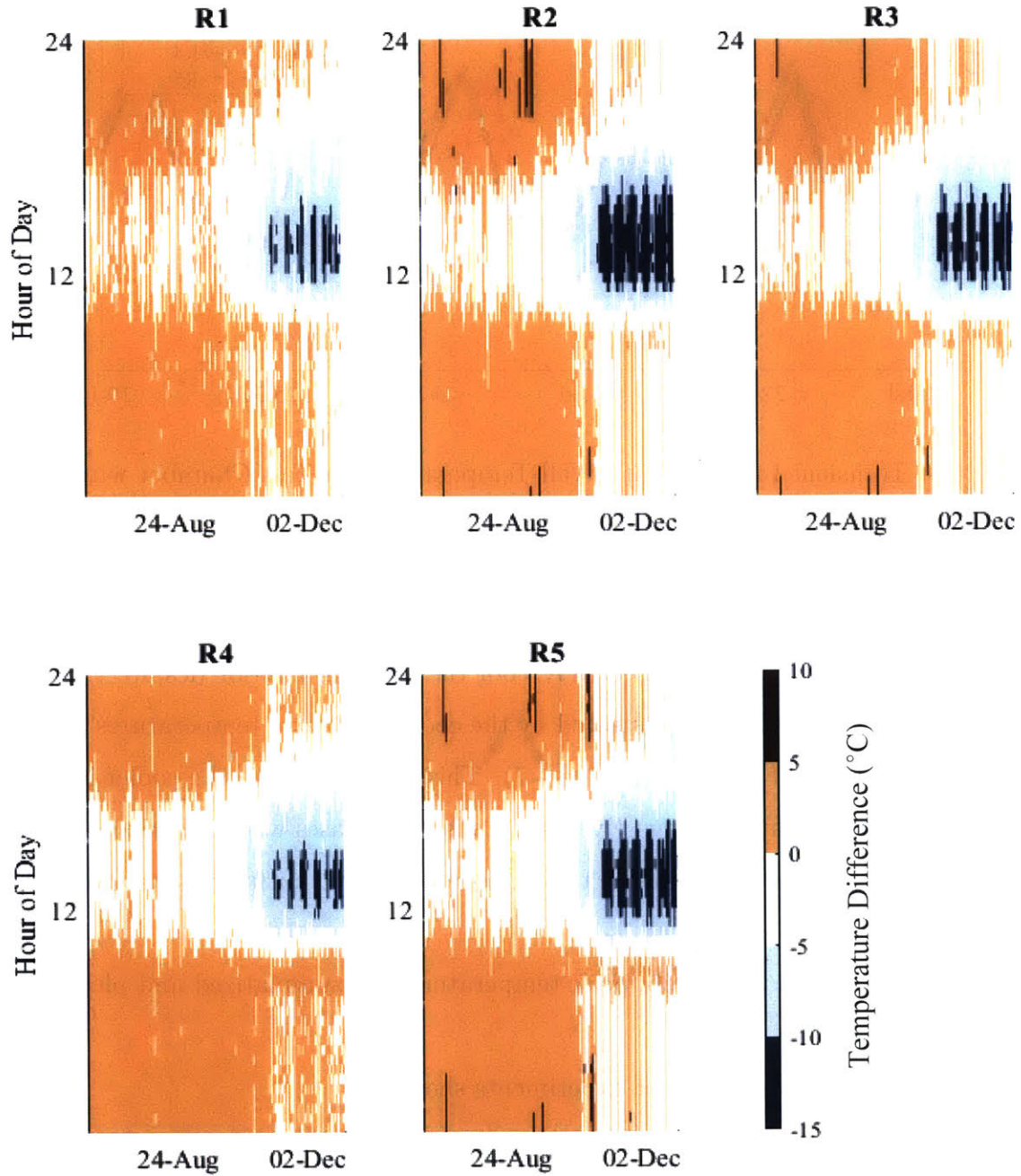


Figure 4-4: Color Map of Temperature Differences Between the Indoor and Outdoor Ambient Air

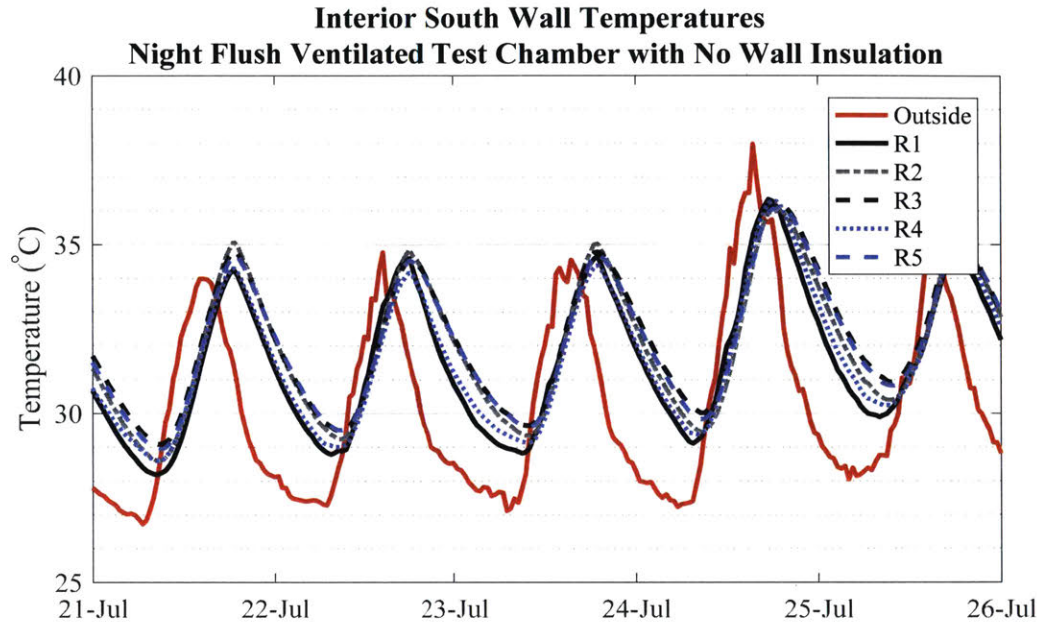


Figure 4-5: Transient Interior South Wall Temperatures for Test Chamber with Roof Types R1-R5

temperatures dominantly affect radiant temperatures. During the nighttime, the single layer CGI roof can still effectively cool the building interior despite the roof having a low emissivity as demonstrated by the cooler operative temperatures for the test chamber with roof type R1 (Figure 4-7). This is likely due to the cooler interior air and wall temperatures. Convective heat transfer increases when a horizontal cold horizontal surface is facing down due to the more dense cold air falling away from the cold surface.

Average deviations from daily peak temperatures are summarized and plotted in Figure 4-11

The results from test chamber experiments show

- Thermally massive roofs tend to decrease thermal comfort compared to a light weight double layer insulated tin roof during summer months where the roof surface experiences the most solar gains.
- During months following monsoon season, lower humidity levels and less cloudy skies allow thermally massive roofs to "store" cold nighttime temperatures and

Night Flush Ventilated Test Chamber with No Wall Insulation:  
Difference Between Interior South Wall and Outdoor Ambient Air  
Temperatures

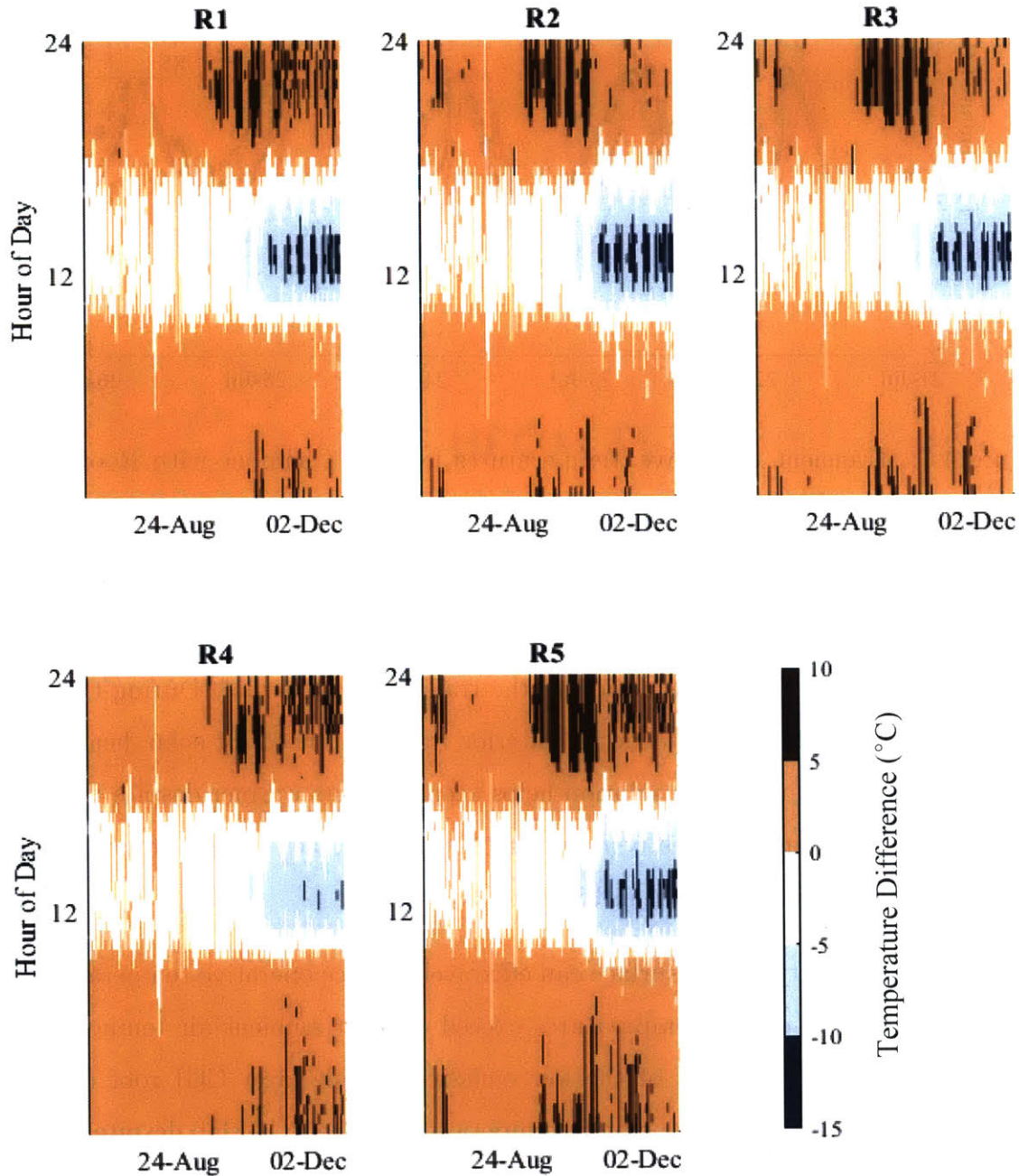


Figure 4-6: Color Map of Temperature Differences Between Interior South Wall and Outdoor Ambient Air

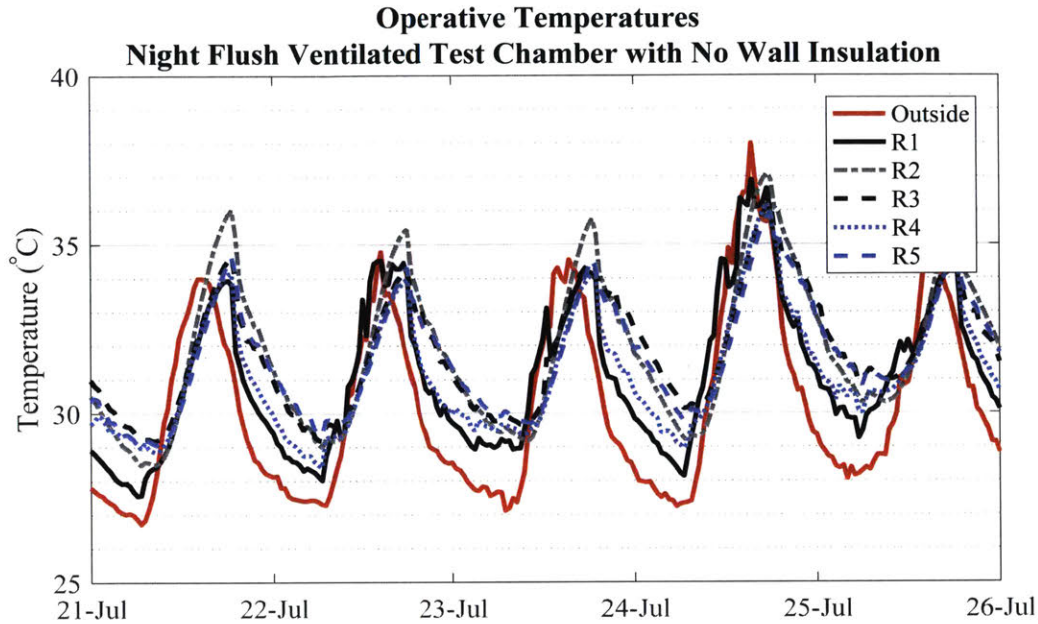


Figure 4-7: Transient Operative Temperatures for Test Chamber with Roof Types R1-R5

improve daytime comfort.

- It is necessary to add insulation to the traditional RCC roof. During the summer, the insulation protects the interior from the effects of solar heat gains. During the winter, the insulation helps keep residents warmer despite the RCC slab ceiling temperatures being more than 10°C cooler than outdoor ambient air temperatures as shown in Figure 4-2.
- A low emissivity ceiling surface can effectively reduce operative temperatures in a room where ceiling temperatures exceed outdoor ambient air temperatures. Operative temperatures of the low emissivity single layer CGI roof (R1) remained cooler than the operative temperatures of the RCC slab despite average peak ceiling temperatures of ceiling R1 exceeding that of ceiling R2. To improve the thermal comfort conditions in a room with an RCC roof, a radiant barrier should be added to the RCC roof.

Night Flush Ventilated Test Chamber with No Wall Insulation:  
Difference Between Indoor Operative and Outdoor Ambient Air  
Temperatures

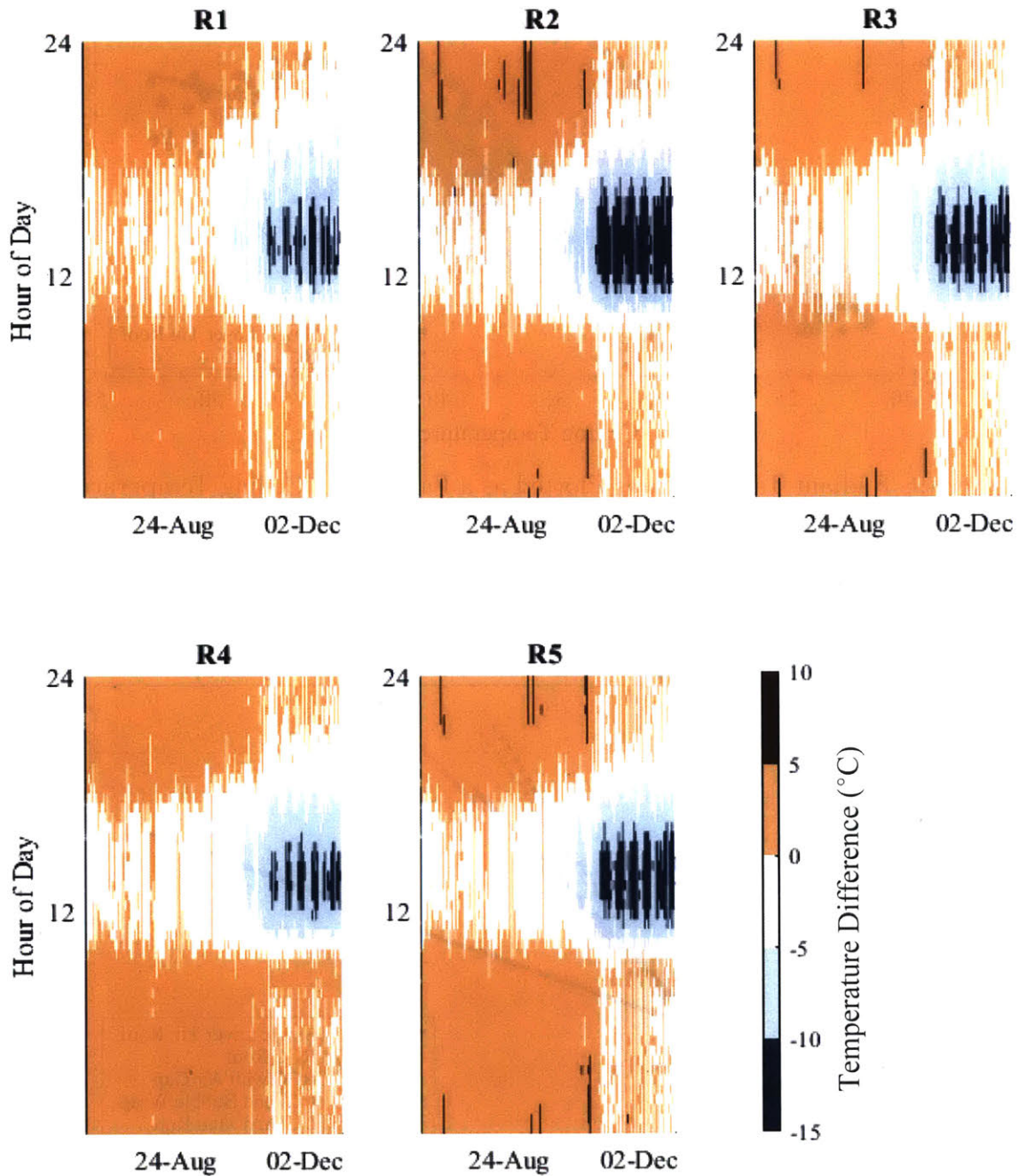


Figure 4-8: Color Map of Temperature Differences Between Indoor Operative and Outdoor Ambient Air

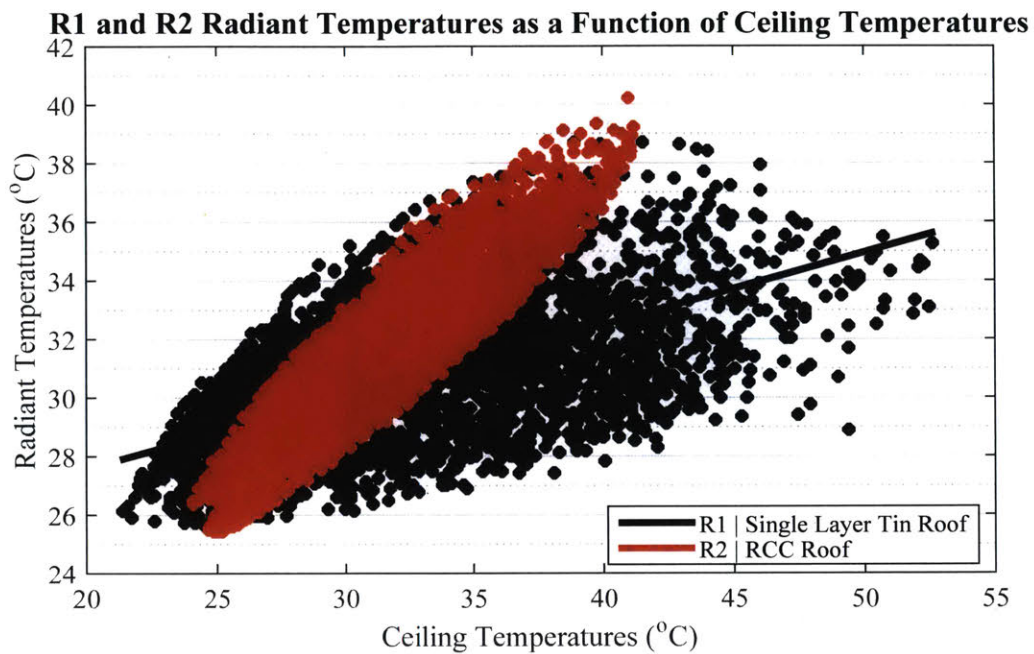


Figure 4-9: Radiant Temperatures Plotted as a Function of Ceiling Temperatures for Roofs R1-R2

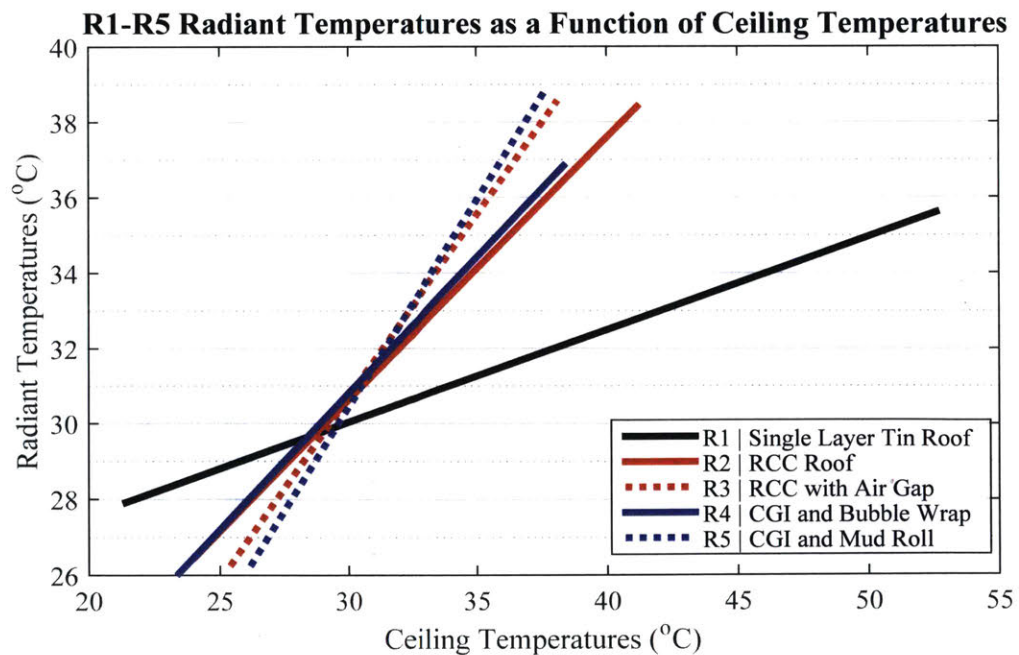


Figure 4-10: Radiant Temperatures Plotted as a Function of Ceiling Temperatures for Roofs R1-R5



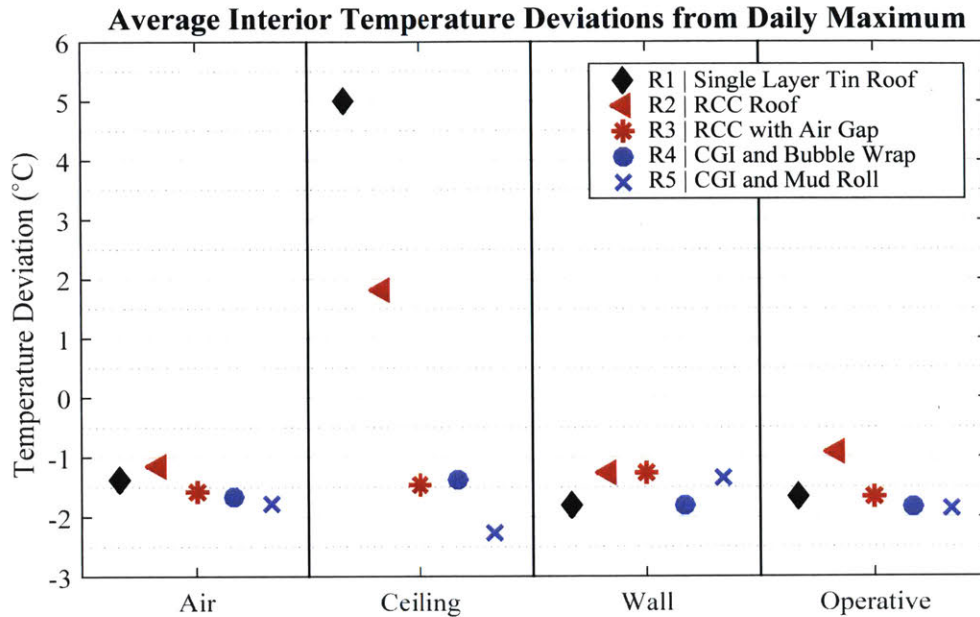


Figure 4-11: Test Chamber Average Interior Temperature Deviations from Daily Maximum Temperatures

## 4.2 Pilot Roofs Results and Discussion

### 4.2.1 Temperature Data

Results from the test chambers with prototype roof designs informed the design and implementation of pilot roofs in four Housing for All homes. The roof types include

- H1 | A Mangalore Pattern Clay Tile Upper Surface and Mud Roll Insulated Ceiling
- H2 | A Mangalore Pattern Clay Tile Upper Surface and Wood Ceiling
- H3 | A White Painted Exterior Tin Sheet Upper Surface with a Wood Ceiling
- H4 | A White Painted Exterior Tin Sheet Upper Surface and Bubble Wrap Insulated Ceiling with a Thin Metal Sheet for a Fire Safety Barrier

Each roof incorporated an air gap to ventilate hot air as well as a radiant barrier to reduce heat transfer from the upper surface to the ceiling. Refer to Section 3.3 for details on temperature monitoring, housing layout, and roof construction.

The Housing for All homes were compared with existing homes monitored in 2015 as described in Section 1.5 and an informal home as described in Section 3.1. One existing home is constructed from concrete masonry unit (CMU) and an asbestos sheet roof. The other home is constructed from compressed stabilized brick earth (CSBE) walls and an RCC Roof. The third existing home is composed of bare CMU walls and Mangalore pattern tile roof. The informal home consists of stone walls and a cloth tarp roof.

Figure 4-12 shows the indoor ambient air transient temperatures of the monitored Housing for All homes and the informal settlement during March 2017. Through observations from site visits, the team deduced that residents did not follow a formal ventilation schedule. Oftentimes, a window or a door is left constantly open. During this period, temperatures of the informal home closely follow the ambient outdoor air temperatures. Some days, the air temperature in the informal home exceeds outdoor ambient air temperatures. The average temperature deviation from the daily maximum is 0.9°C. Daytime temperatures in the Housing for All home do not exceed the outdoor air temperatures as shown in Figure 4-13.

Average indoor air temperature deviations from the daily maximum for the home with the tile mud roll ceiling is 7.41°C. For the home with the tin and bubble wrap roof, the average interior air temperature deviated the least from outdoor ambient air temperatures. However, peak air temperature still remained significantly cooler than in the informal home by 2.47°C. During the peak outdoor temperatures of the day, home H1 air temperatures were, on average, 4.94°C cooler than home H4.

The relative air temperatures differences among the Housing for All homes with the pilot roofs match the relative ceiling temperature differences in these homes. Ceiling temperatures in the home H4, the tin and bubble wrap, exceed those of houses H1-H3 as shown in Figure 4-14. This can be due to the steel framing of the roof where thermal bridging effects are more likely to occur uniquely to home H4, while homes H1-H3 are constructed with a lower conductivity wooden frame.

In homes H2 and H3, though both have a wooden ceiling as the bottom layer, the average peak ceiling temperatures for the tin and wood roof (H3) exceed average

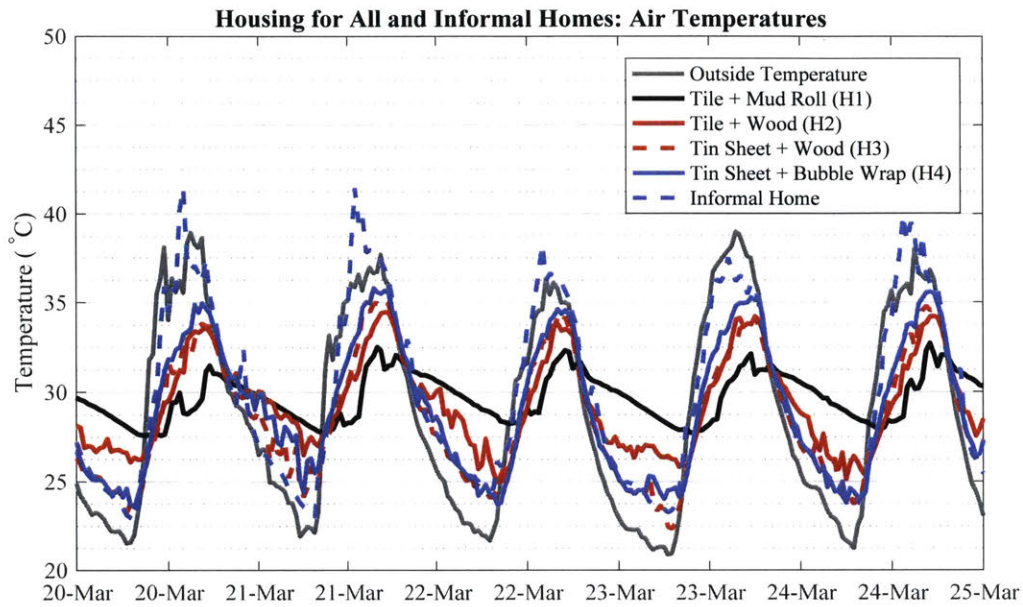


Figure 4-12: Transient Indoor Air Temperatures in the Housing for All and Informal Settlement Homes

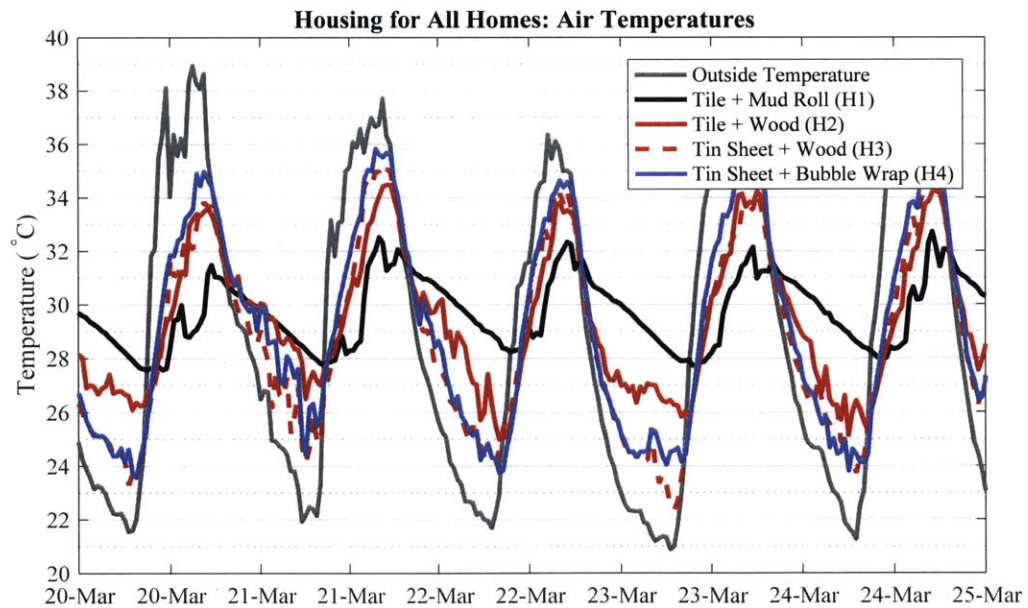


Figure 4-13: Transient Indoor Air Temperatures in the Housing for All Homes

ceiling temperatures for the tile and wood roof (H2) by  $2.88^{\circ}\text{C}$ . The warmer temperatures of the upper layer tin likely increases the ceiling temperatures when compared to the upper layer Mangalore pattern clay tile temperatures. The clay tile with the mud roll roof outperforms the other roofs in keeping the ceiling temperatures cooler. The average ceiling temperature deviation from the daily maximum for home H1 is  $6.14^{\circ}\text{C}$  which is  $1.85^{\circ}\text{C}$  cooler than home H2 average ceiling temperature deviations.

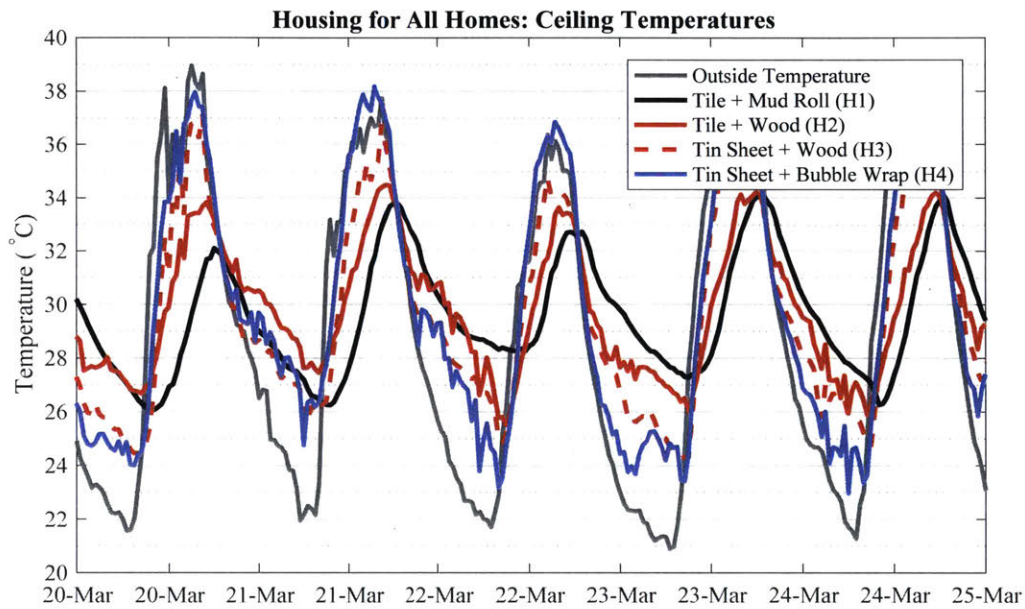


Figure 4-14: Transient Ceiling Temperatures in the Housing for All Homes

The cooler ceiling and interior air temperatures in home H1 correlate with cooler interior wall temperatures. Radiant heat transfer from the ceiling affects wall temperatures given wall and ceiling surfaces with high emissivity in the infrared region. Lower ceiling temperatures contribute to lower interior wall temperatures due to radiation heat transfer between the ceiling and wall surfaces. Figure 4-15 illustrates transient interior south wall temperatures in the four Housing for All Homes with pilot roofs. The average measured peak interior south wall temperatures in home H3, a home with peak ceiling temperatures  $5^{\circ}\text{C}$  degrees warmer than that of home H1, are  $>3^{\circ}\text{C}$  warmer than wall temperatures for home H1. The warmer wall temperatures are likely caused by radiation heat transfer from the ceiling to the wall. In

the analysis of wall temperatures, it is important to note that the walls of home H4 remain unfinished without any exterior white paint. The estimated absorptivity in the visible spectrum of the white paint is 0.25 where as the estimated absorptivity of the unfinished wall is 0.70. The walls of homes H1-H3 are finished with a white limewashed exterior. Consequently, interior south wall temperatures of home H4 exceed wall temperatures of home H1 by at least 4°C. More discussion on wall color and thermal comfort follow in Chapter 5

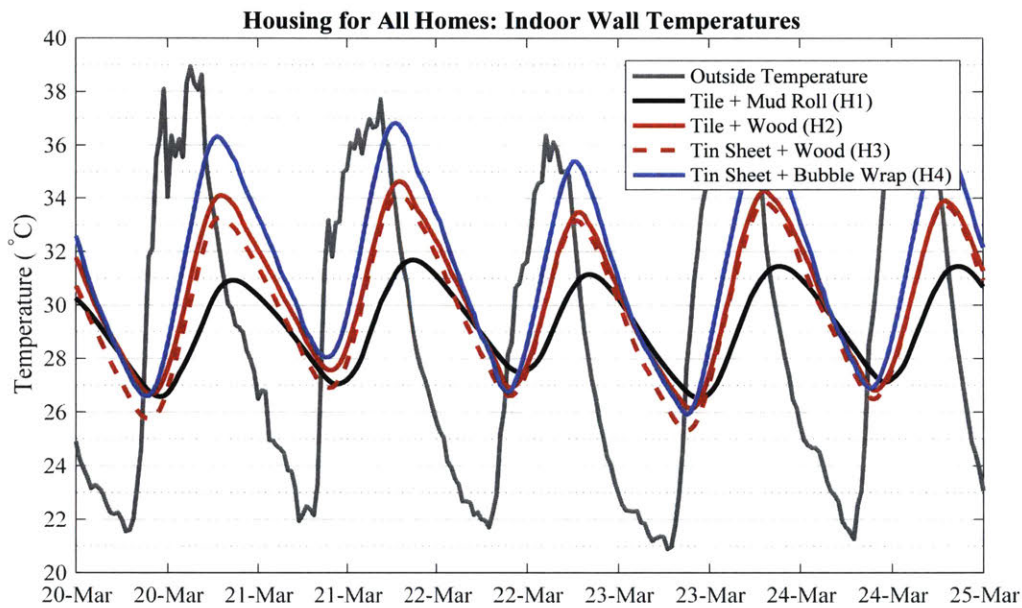


Figure 4-15: Transient Interior South Wall Temperatures in the Housing for All Homes

Figure 4-16 shows transient operative temperatures in the homes with pilot roofs. Similar to the intra-home comparisons of the air, ceiling, and interior wall temperatures, the clay tile and mud roll roof peaks remain the coolest. The average operative peak temperature deviations for the clay tile mud roll roof is 7.73°C below outdoor ambient temperatures while average peak temperature deviations for homes H2-H4 range from 4.15°C to 5.24°C cooler than outdoor ambient temperatures.

The Housing for All homes with the four modified roofs provide improvements in comfort when compared to the existing homes monitored in 2015. Figure 4-17 shows transient interior air, wall, ceiling, and operative temperatures for the existing

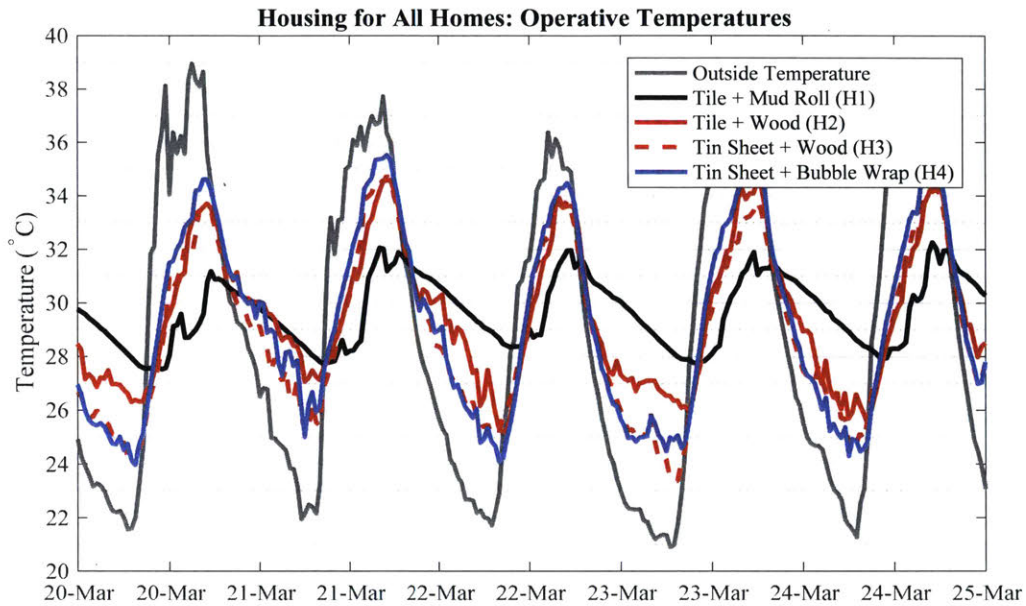
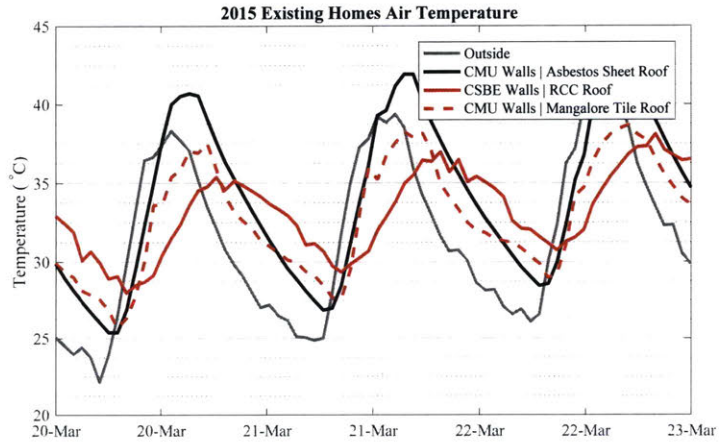


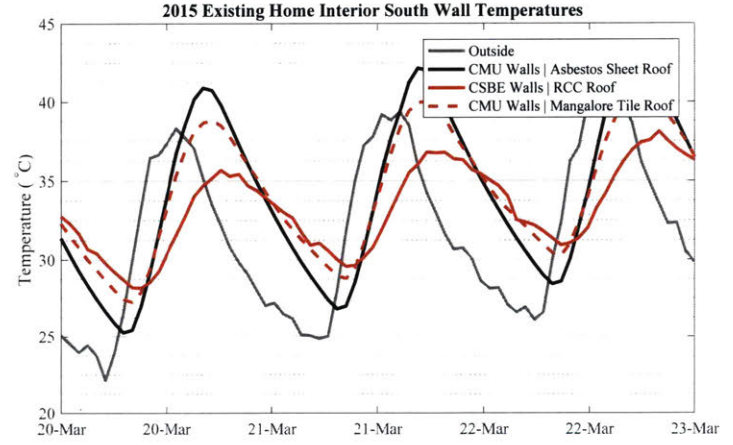
Figure 4-16: Transient Operative Temperatures in the Housing for All Homes

vernacular homes monitored in 2015. The interior transient temperatures often exceed outdoor ambient temperatures. Average peak temperature deviations were calculated and shown in Figure 4-18 from both the Housing for All homes and existing homes. The average peak deviation air temperature of the coolest Housing for All home is 3°C cooler than the average peak deviation air temperature of the coolest existing home. In the Housing for All homes, none of the average peak ceiling temperatures exceed outdoor air temperatures. However, all of the average peak ceiling temperatures of the existing homes exceed the peak outdoor ambient air temperature. Peak deviation operative temperatures are greater than 3°C cooler in the Housing for All homes than in the existing homes. These results highlight the importance of roof designs in homes as the pilot homes with insulated roofs outperformed existing homes with no roof insulation.

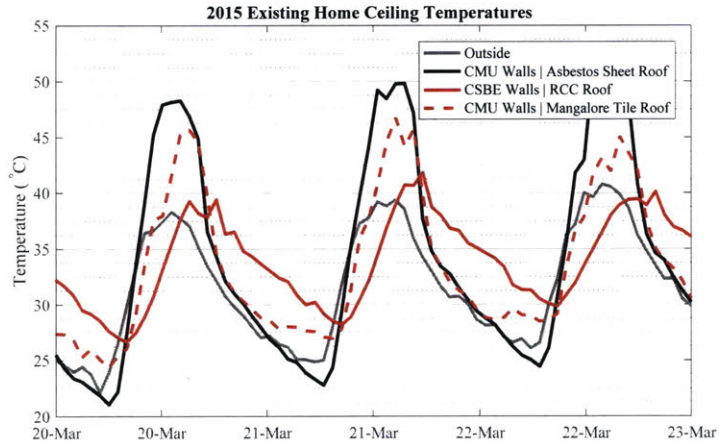
The measured data from the pilot and existing homes was used to rate each home's comfort based on ASHRAE and IMAC comfort standards. When comparing the 2016 pilot homes and the existing homes, the lower operative temperatures in the 2016 pilot homes lead to more time during the data collection period in which the



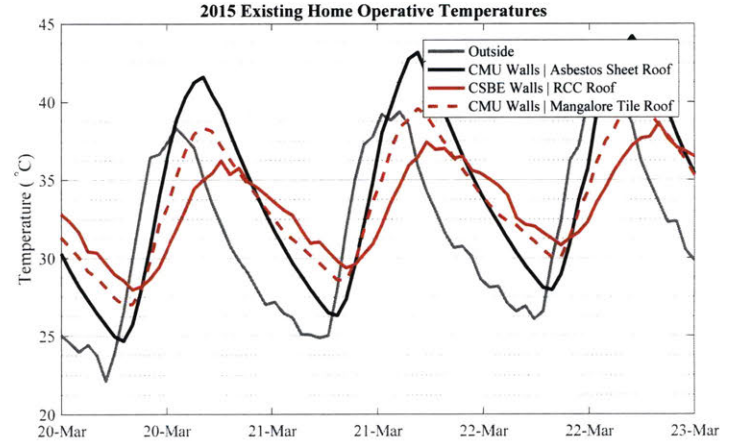
(a) Interior Air Temperature



(b) Interior South Wall Temperature



(c) Ceiling Temperatures



(d) Operative Temperatures

Figure 4-17: Interior Transient Air, South Wall, Ceiling and Operative Temperatures for Existing Vernacular Homes

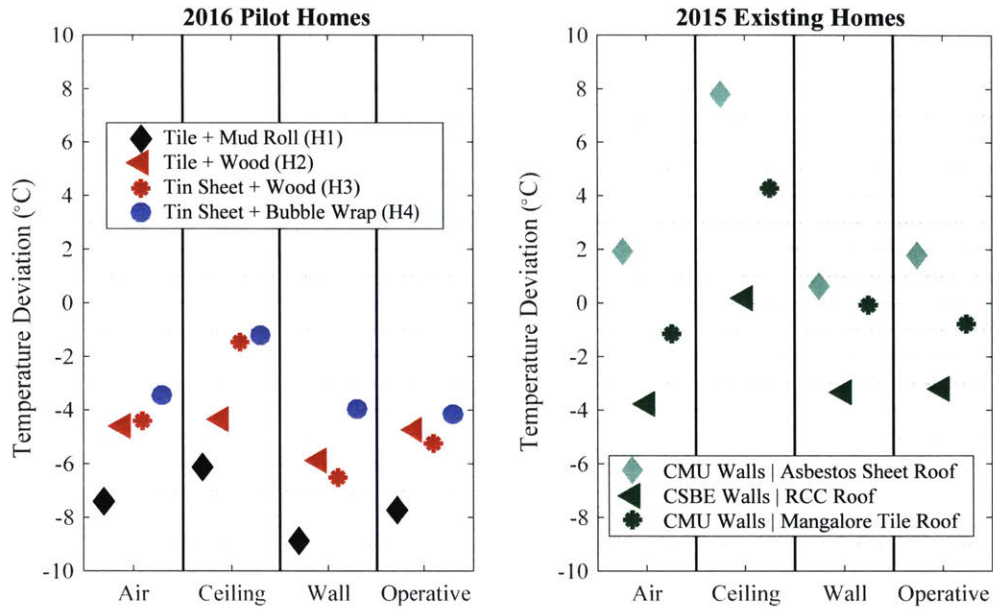


Figure 4-18: Housing for All and Existing Homes: Average Interior Air, South Wall, Ceiling, and Operative Temperature Deviations from Peak Ambient Outdoor Air Temperatures

operative temperature remained within the IMAC and ASHRAE 80% acceptability limits. Using the IMAC model, the Housing for All homes stayed within acceptable comfort ranges for at least 80% of the data collection period where as the best performing existing home stayed within acceptable comfort ranges for only 75% of the data collection period. Similarly, using the ASHRAE standard, the percent of time in which operative temperatures remained within comfort limits is greater than 60% in the Housing for All homes with pilot roofs. The existing homes remained within ASHRAE comfort limits <60% of the data collection period.

Of the Housing for All homes with the pilot roofs, comfort calculations based on the IMAC standards indicate the home with clay tile and mud roll insulation roof is the most comfortable, remaining within the 80% acceptability limit for 88.5% of the time.



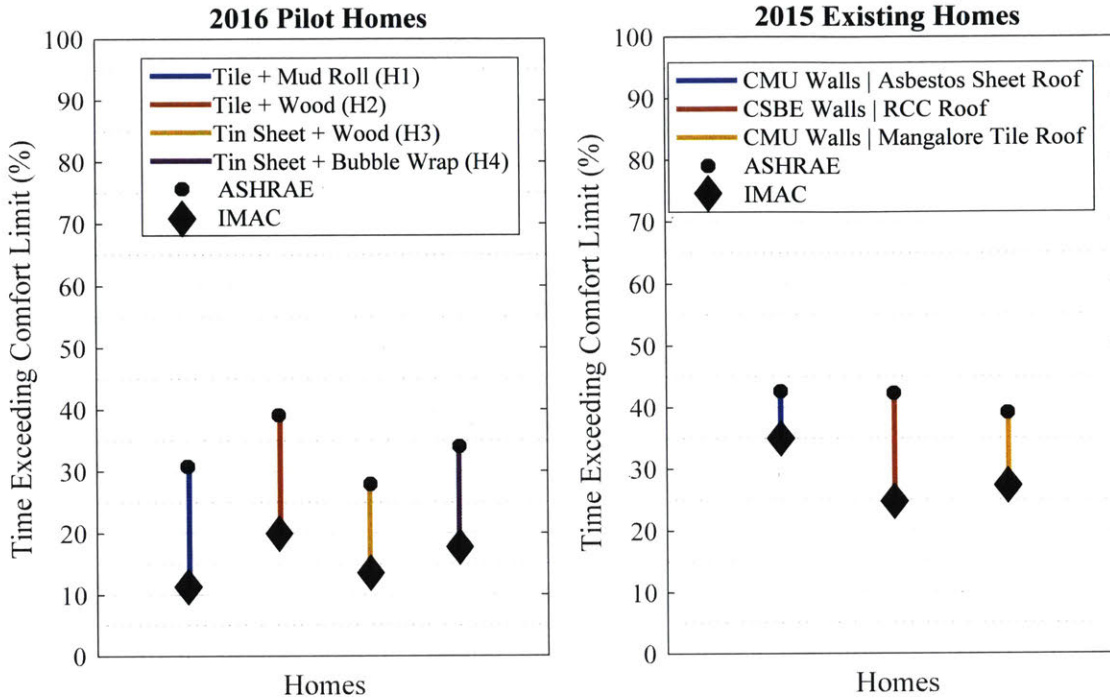


Figure 4-19: Percentage of Time in which Temperatures Exceeded the IMAC and ASHRAE Upper 80% Acceptability Comfort Limits

### 4.2.2 Perception Survey Results

During a site visit in January 2017, the team performed an informal perception survey to gauge residents' opinions and thoughts on their new homes. The questions asked included

- What do you think about your new home?
- How do you stay warm in the winter and cool in the summer?
- What do you think about the roof?
- What would you change about your home if you could rebuild it?
- What does the community think of the different roofs?
- Do you notice a temperature difference between the homes?
- Where were you living previously?

- Do you miss anything from your previous home?
- Which roofing style do you prefer?

From an informal conversation with residents, the community agreed on some aesthetic standards for the exterior portion of the roof. Occupants and neighbors indicated they preferred the sloping tile roof aligned with traditional architectural style over the sloping tin roof. However aesthetic tastes for the interior differed. Some stated they prefer a wood ceiling for their ideal roof.

The family inhabiting the home with a clay tile and mud roll roof stated they wouldn't change their roof for aesthetic reasons and thermal comfort reasons. They stated they could feel the temperature difference between their home and that of their neighbors. With the mud roll ceiling, they homeowners thought that their home would stay cooler in hot weather. However, this temperature sensation was not universally felt.

## **Recommendations**

Considering both the perception survey and the collected data, the clay tile and mud roll roof emerges as the most viable roof type. This roof meets the aesthetic and social requirements of the residents. Though all the Housing for All homes performed well thermally with 80% of measured operative temperatures remaining within the IMAC 80% acceptability range, the clay tile roof remained within the IMAC comfort range for 88.5% of the time. On average, the interior air, south wall, ceiling and operative temperature were all at least 6°C cooler than exterior temperatures during the hottest part of the day, 3°C cooler than existing homes.

# Chapter 5

## Wall Design

To achieve thermal autonomous housing design, walls must be properly designed with climate considerations. This chapter discusses results from field experiments described in Section 1.5, 3.2, and 3.3. These results illuminate the role of thermal mass in climates with diurnal shifts characteristic of desert-like regions such as Bhuj. Furthermore, the experimental results demonstrate how wall insulation and color influence thermal comfort.

### 5.1 Role of Diurnal Shifts

As discussed in Section 1.3.6, one of the methods for passive thermal control designs in buildings relies on the proper combination of thermal mass, insulation, and ventilation. The thermally massive building components can retain or "store" the cold night temperatures and keep the indoor environment cooler throughout the day. This method, however, works best when the climate is characterized by large diurnal temperature shifts. Through the monitoring of prototype test chambers in 2015 (see Section 1.5 for more details) researchers can examine the role of diurnal shifts on the effectiveness of thermal mass by comparing periods of smaller diurnal temperature shifts with periods of larger diurnal temperature shifts. In Bhuj, during the early half of the year, from February to March, the difference between the nightly minimum and the daily peak temperatures ("diurnal shift") can exceed 20°C. In the months leading

up to the monsoon season and afterward (May to October) the diurnal temperature shift decreases from 20°C to 10°C. The seasonal changes and outdoor ambient temperature patterns are illustrated in Figure 5-1 where ten days of outdoor ambient temperature data from the month of March and June 2015 are plotted. The mean temperatures of these two time periods differ by 0.63°C. However, standard deviation of the outside temperatures differ by 2.29°C. These changes in the temperature amplitudes are likely due to the increase in humidity and cloud coverage from March to June. As shown in Figure 5-3, the average humidity increases by more than 30 percentage points from the March data collection period to the June data collection period. Additionally, the average number of partly cloudy and overcast days increases by ten days from March to June as shown in Figure 5-2.

These increases in humidity and cloud coverage can lead to a decrease in longwave radiant cooling. As a result, during periods with higher humidity levels and more cloud coverage, thermally massive building components cannot release enough heat during the nighttime to effectively provide some cooling during the daytime. In the March period shown in Figure 5-1, average daily minimum temperatures are 4.6°C cooler than average daily minimum temperatures in June.

Though average peak temperatures for the March period exceed peak temperatures for the June period by 3.9°C, indoor ambient temperatures in the test chamber with the insulated clay tile roof and 15cm thick straw bale insulated walls (T2) are 3.3°C cooler in March. Night flush ventilation was practiced in both periods characterized by 20°C diurnal shifts and 10°C diurnal shifts. See Section 1.5 for more detail on test chamber experimental apparatus and data collection. Figure 5-4 compares transient night flush ventilated test chamber indoor ambient air temperatures over an 11 day period during March, where the climate is characterized by a mean 35% relative humidity and 20°C diurnal shifts, with temperatures during June, where the climate is characterized by a mean 65% relative humidity and 10°C diurnal shifts.

Similar to indoor ambient temperatures, the average interior south wall temperatures increase from 29.04°C to 32.41°C from March to June. Figure 5-5 compares the transient night flush ventilated test chamber wall temperatures over an 11 day

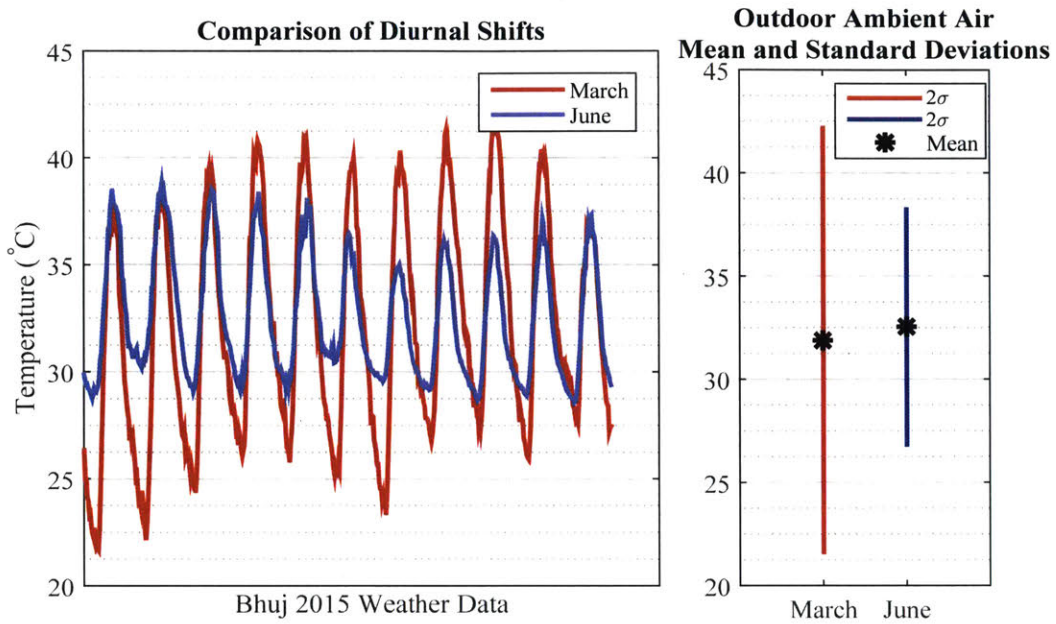


Figure 5-1: Comparison of Measured Outdoor Air Temperatures during March, a Period Characterized by 20°C Diurnal Shifts, and June, a Period Characterized by 10°C Diurnal Shifts

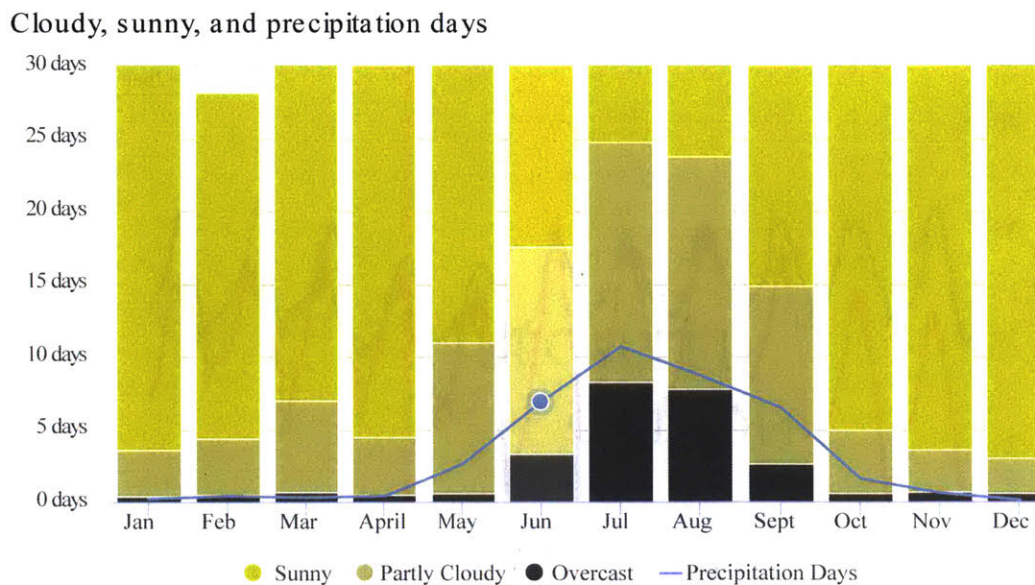


Figure 5-2: Bhuj: Monthly Average Number of Cloudy, Sunny, and Overcast Days (Meteoblue, 2014)

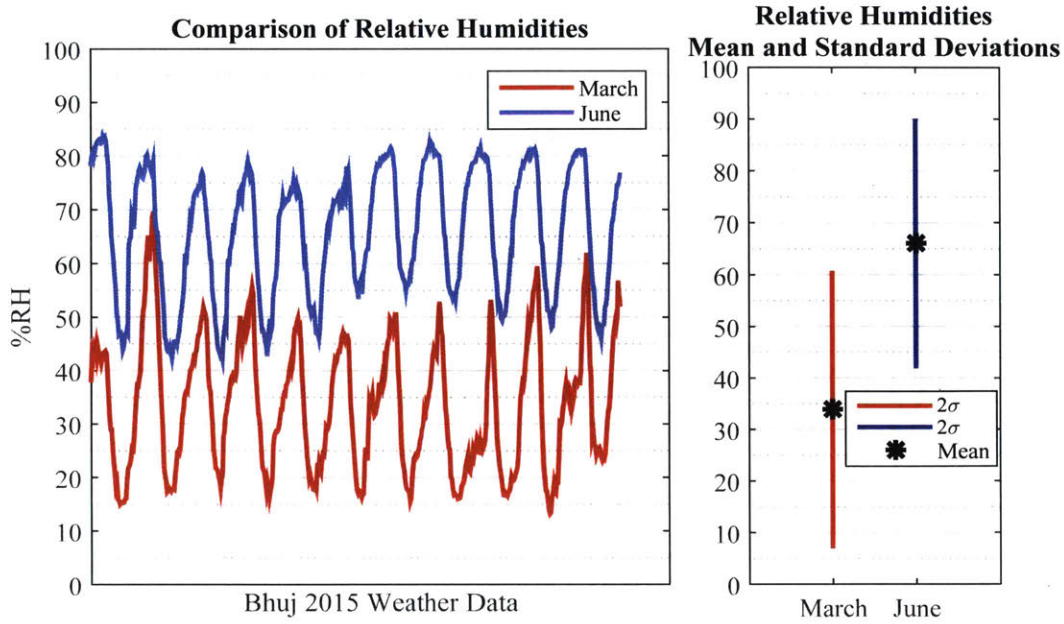


Figure 5-3: Comparison of Measured Relative Humidities During March, a Period Characterized by 20°C Diurnal Shifts, and June, a Period Characterized by 10°C Diurnal Shifts

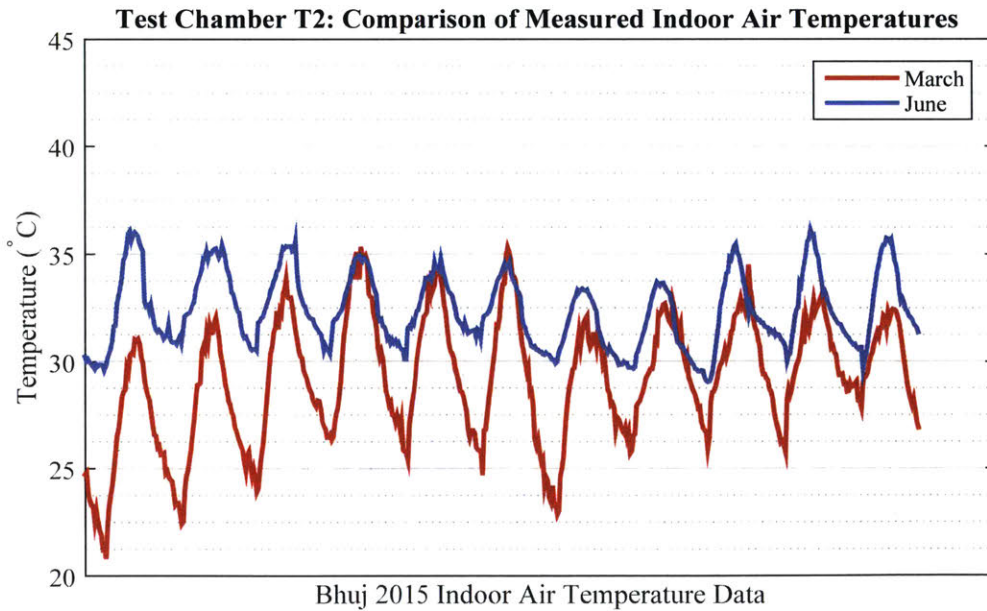


Figure 5-4: Comparison of Measured Night Flush Ventilated T2 Test Chamber Indoor Air Temperatures during March, a Period Characterized by 20°C Diurnal Shifts, and June, a Period Characterized by 10°C Diurnal Shifts

period during the period in March with larger diurnal temperature shifts and June with smaller diurnal temperature shifts.

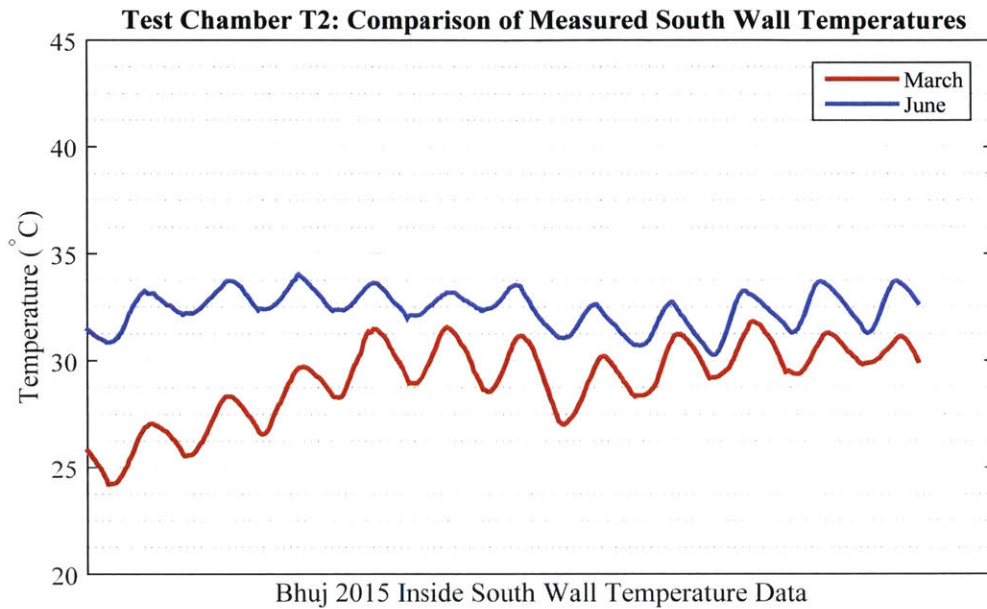


Figure 5-5: Comparison of Measured Night Flush Ventilated T2 Test Chamber Inside South Wall Temperatures during March, a Period Characterized by 20°C Diurnal Shifts, and June, a Period Characterized by 10°C Diurnal Shifts

Though the average outdoor air temperature between these two periods increases by less than 1°C, the average indoor air temperatures and inner wall temperatures all increase by more than 3°C as shown in Figure 5-6. Average interior temperature deviations from the outside peak temperatures *increase* in periods with larger diurnal shifts as shown in Figure 5-7, a plot of average inside south wall and air temperature deviations.

Utilization of thermally massive building components combined with night flush ventilation works best in regions with large diurnal shifts and low humidity. For most of the year, excluding monsoon season, Bhuj’s climate conditions are ideal for the passive thermal control method of thermal mass combined with night flush ventilation.

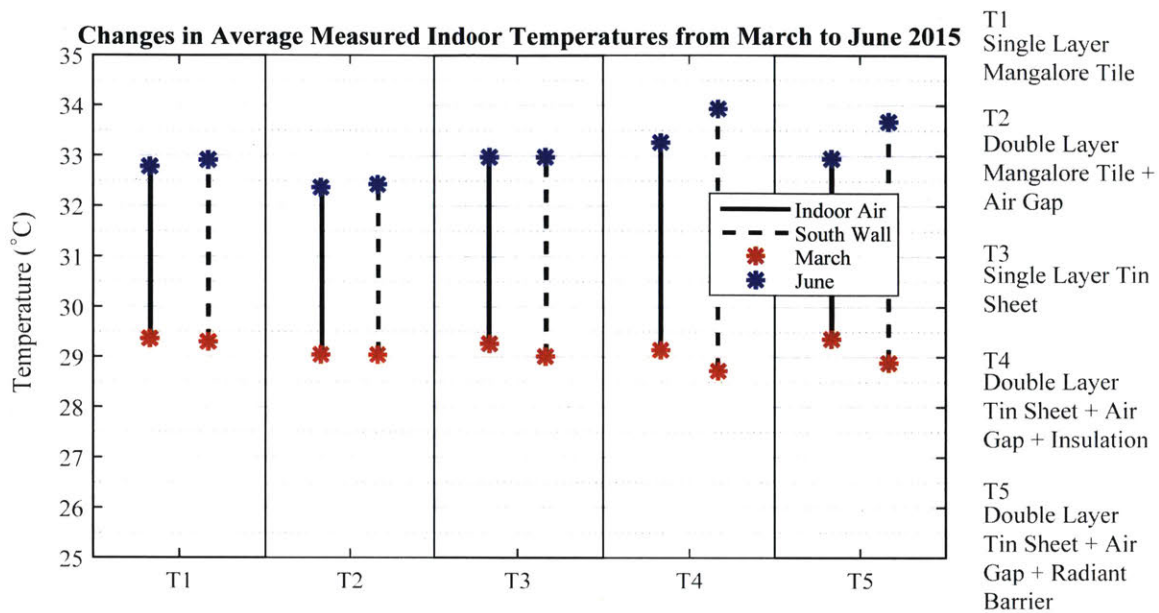


Figure 5-6: Changes in Average Measured Indoor Air and South Wall Temperatures Between March, a Period with 20°C Diurnal Shifts, and June, a Period with 10°C Diurnal Shifts

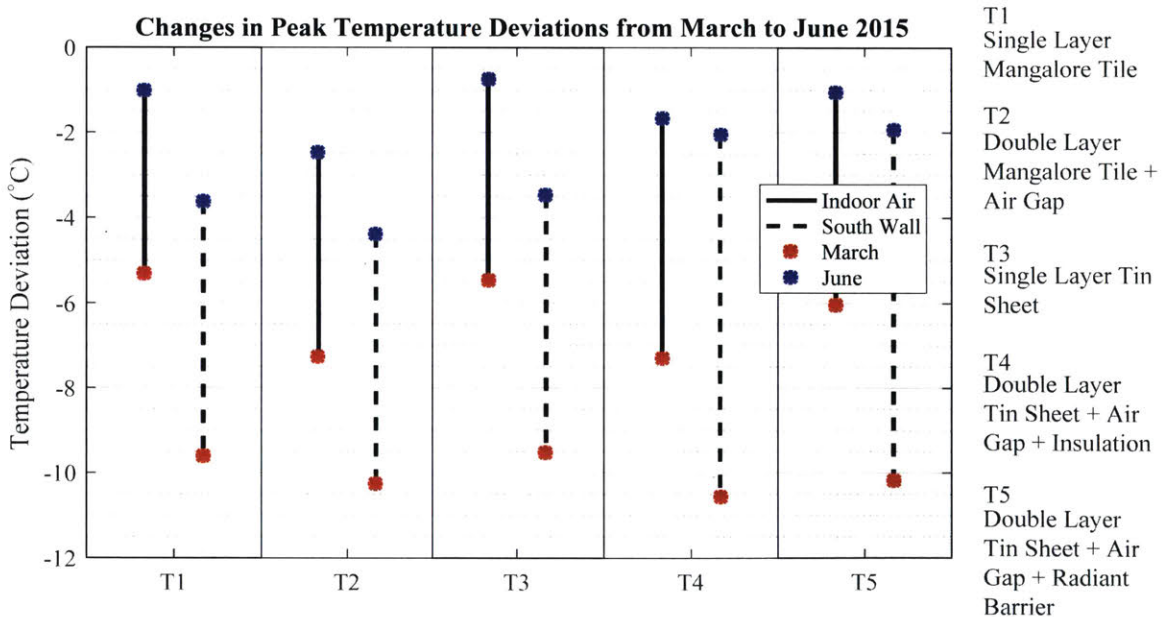


Figure 5-7: Changes in Average Peak Temperature Deviations from Outdoor Ambient Air Temperatures for Indoor Air and South Wall Temperatures Between March, a Period with 20°C Diurnal Shifts, and June, a Period with 10°C Diurnal Shifts



## 5.2 Role of Wall Insulation

Section 5.1 concludes that thermally massive structures work best in dry desert-like regions that experience diurnal shifts greater than  $10^{\circ}\text{C}$  and clear night skies. Although thermal mass is effective at delaying the effects of external heat stresses, highly conductive thermal mass materials do not substantially reduce heat flux. A majority of the thermally massive wall construction materials found in Bhuj act as poor thermal insulators, with conductivity values ranging from  $1\text{W}/\text{m}^2\text{K}$  to  $3\text{W}/\text{m}^2\text{K}$ . Consequently, wall insulation plays a key role in dampening the solar heat gain effects and ambient temperature heat stresses. As described in Section 1.3.6, the low thermal conductivity reduces the heat transfer from exposed exterior wall surfaces to the interior wall surfaces. Partial removal of wall insulation in 2015 and comparisons between 2015 field experiments, where all the test chambers walls were protected with a 15cm external layer of straw insulation, and 2016 field experiments, where all the test chamber walls were exposed, reveal and quantify the crucial importance of wall protection for passive thermal comfort.

### 5.2.1 Wall Insulation Changes on the North and South Test Chamber Walls

On June 20, 2015, insulation was removed from the north and south walls of two test chambers (one with a double layer insulated air gap roof, the other a double layer radiant barrier air gap roof). This test chamber reconfiguration caused immediate changes in wall temperatures as shown in Figure 5-8, a transient graph of measured interior south wall temperatures. The increase in south wall temperatures led to an increase in operative temperatures as shown in Figure 5-9. Calculated average interior wall and operative temperature deviations from peak outdoor temperatures illustrate that the removal of wall insulation decreases the relative difference between the interior temperatures and exterior ambient air temperatures. For the test chamber with the double layer roof with an air gap and radiant barrier (T4), average wall temperatures increased during peak outside temperature conditions by  $2.2^{\circ}\text{C}$ . Aver-

average operative temperatures during the warmest part of the day increased by  $0.95^{\circ}\text{C}$  following wall insulation removal as shown in Figure 5-10. Average air temperature during peak exterior conditions increased by  $0.27^{\circ}\text{C}$ . In the twenty days chosen for analysis (ten days before insulation removal, ten days after insulation removal), the average peak outdoor ambient air temperature was  $37.66^{\circ}\text{C}$  before insulation removal. Following insulation removal, the average peak outdoor ambient temperature decreased by a negligible  $0.3^{\circ}\text{C}$ . Average peak solar heat flux differed by  $19.4\text{W}/\text{m}^2$  across the insulation-on and insulation-off periods.

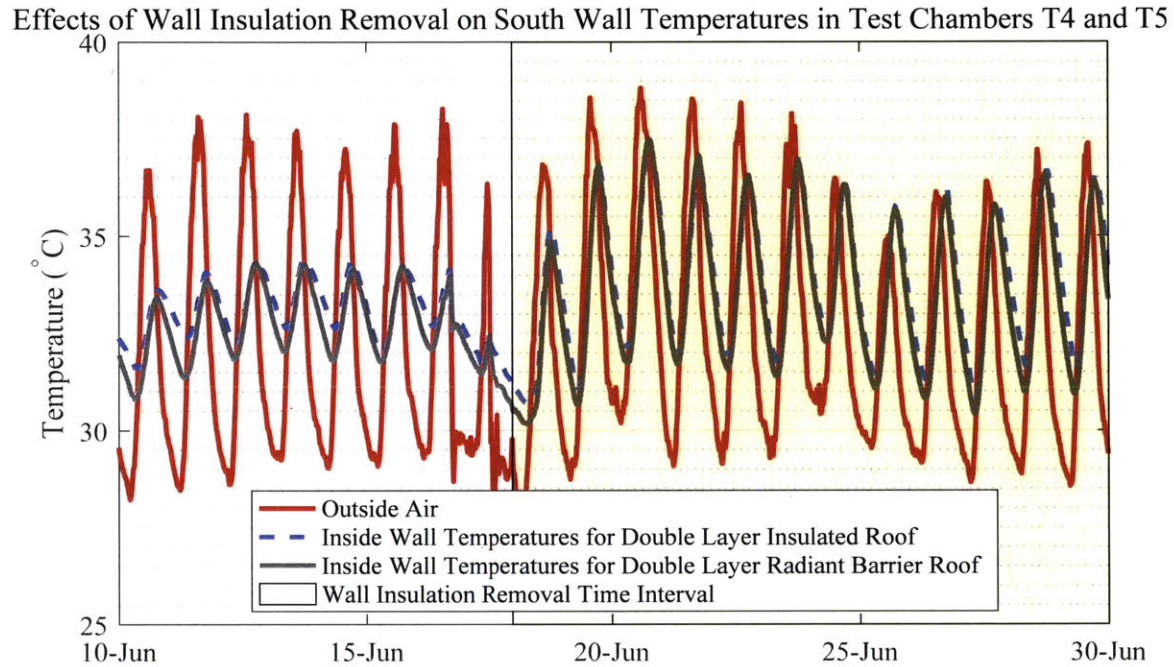


Figure 5-8: Measured South Wall Temperatures Before and After Wall Insulation Removal

### 5.2.2 Comparisons of Test Chamber with Fully Insulated and Exposed Walls

These aforementioned temperature changes due to partial insulation removal understate the negative effects of uninsulated walls on thermal comfort. In the above analysis comparing conditions before and after partial insulation removal, insulation still

**Effects of Wall Insulation Removal on Operative Temperatures in Test Chambers T4 and T5**

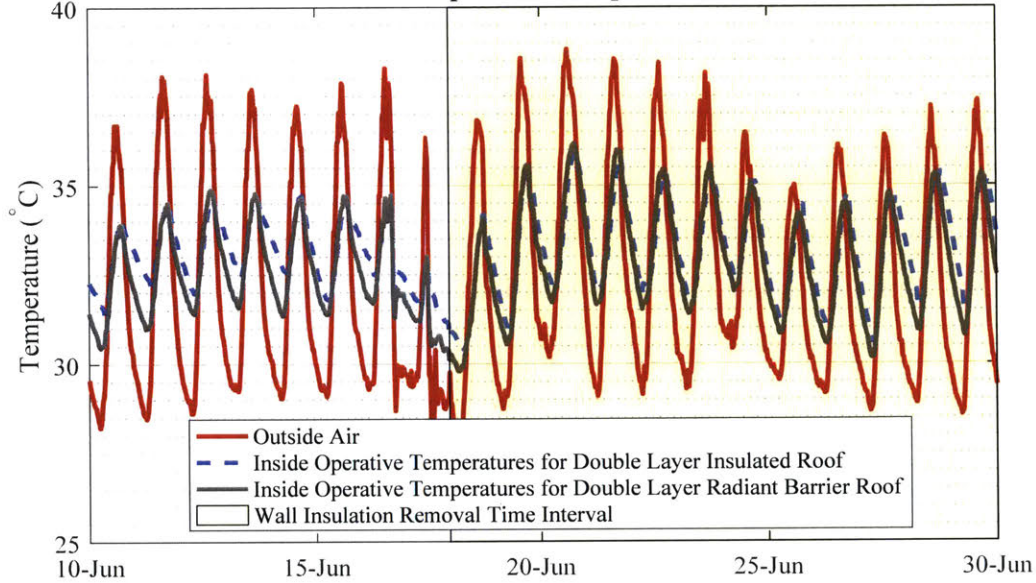


Figure 5-9: Measured Operative Temperatures Before and After Wall Insulation Removal

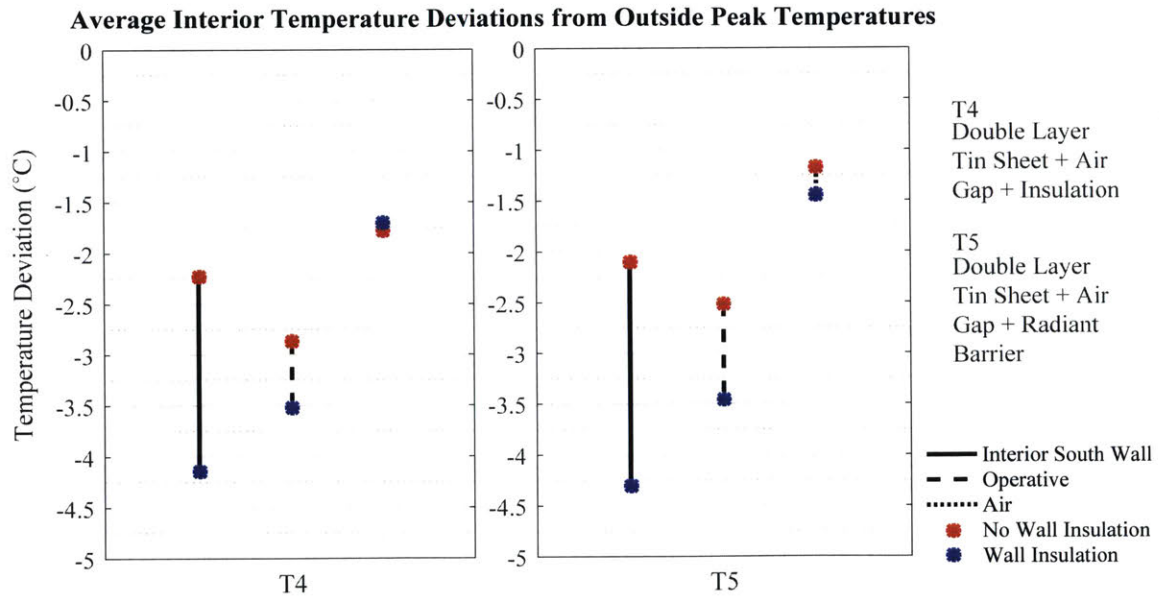


Figure 5-10: Average Interior Wall, Operative, and Air Temperature Deviations from Peak Outdoor Temperatures for Test Chambers Where Wall Insulation was Removed on June 20, 2015

covered the east and west walls to provide wall protection. Additionally, ventilation schedules changed concurrently with the insulation removal from constant ventilation during the insulated wall period to night flush ventilation during the post-insulation-removal period. Constant ventilation during the period with wall insulation leads to sub-optimal interior thermal comfort conditions due to air infiltration during peak exterior conditions. A comparison between test chamber field experiments in 2015 and 2016 further illuminates the effects of wall insulation. During the 2015 field tests, a 15cm thick layer of straw with white burlap protected the exterior all four sandstone walls. In 2016, all sandstone walls remained exposed and unprotected against the elements. Test chambers with similar roof constructions were compared to study the effects of wall insulation as shown in Table 5.1. The ventilation schedules remained the same, night flush ventilation, across the 2015 and 2016 field experiments.

Table 5.1: 2015 and 2016 Test Chamber Comparisons

2015		2016
T1   Single Layer Clay Tile 15cm Thick Straw Exterior Wall Insulation Covered with White Burlap	→	R2   Single Layer RCC Roof Exposed Brick Sandstone Walls
T2   Double Layer Insulated Clay Tile 15cm Thick Straw Exterior Wall Insulation Covered with White Burlap	→	R3   Double Layer Insulated RCC Roof Exposed Brick Sandstone Walls
T3   Single Layer CGI 15cm Thick Straw Exterior Wall Insulation Covered with White Burlap	→	R1   Single Layer CGI Exposed Brick Sandstone Walls
T4   Double Layer CGI with Plastic Insulation 15cm Thick Straw Exterior Wall Insulation Covered with White Burlap	→	R5   Double Layer CGI with Mud Roll Insulation Exposed Brick Sandstone Walls
T5   Double Layer CGI with Radiant Barrier 15cm Thick Straw Exterior Wall Insulation Covered with White Burlap	→	R 4   Double Layer CGI with Bubble Wrap Insulation Exposed Brick Sandstone Walls

When comparing the test chambers with a single layer CGI sheet roof, wall insulation proves to have a significant impact on indoor ambient air, wall, operative and

ceiling temperatures. Figure 5-11 shows daily maximum interior temperatures plotted as a function of daily maximum exterior temperatures. Best-fit lines illustrate the relationship between the outdoor ambient air temperatures and indoor temperatures. On average, the addition of a 15cm layer of straw insulation to the exterior walls of the test chamber with a single layer CGI roof reduced wall temperatures by greater than 6°C. This led to a 2-3°C decrease in average maximum indoor temperatures and a 4-5°C in average maximum operative temperatures. Average maximum ceiling temperatures also decreased by 1-2°C. Similar patterns of average maximum interior temperature decreases can be found when comparing other test chambers with similar roof types as shown in Figure 5-12. The average maximum interior south wall, indoor air, and operative temperatures for 2015 (insulated test chamber walls) are all less than those of 2016 (uninsulated test chamber walls).

Calculated average interior temperature deviation from outdoor daily maximum temperatures confirm the wall insulation's impact on protecting the indoor built environment from external factors. Figure 5-10 shows average indoor air, south wall, operative, and ceiling temperature deviations from peak outdoor ambient temperatures. With insulated walls, air temperatures decreased by 1-3°C, wall temperatures decreased by approximately 6°C, and operative temperatures decrease by 3-5°C relative to outdoor temperatures.

The temperature decreases led to substantial improvements in thermal comfort as defined by both the ASHRAE and India Model for Adaptive Comfort (IMAC) 80% Acceptability thresholds. A smaller percentage of the operative temperatures in the 2015 data collection period, where test chamber walls were insulated, exceeded the upper 80% acceptability limit thresholds. According to the ASHRAE adaptive comfort standard, insulated test chambers' operative temperatures were within comfort 80% or more of the time, 20 percentage points greater than test chambers with no insulation. Using the IMAC standard, insulated test chambers' operative temperatures were within comfort 95% or more of the time, 10 percentage points greater than test chambers with no insulation as shown in Figure 5-14.

Wall insulation proves to be an effective means to protect thermally massive walls

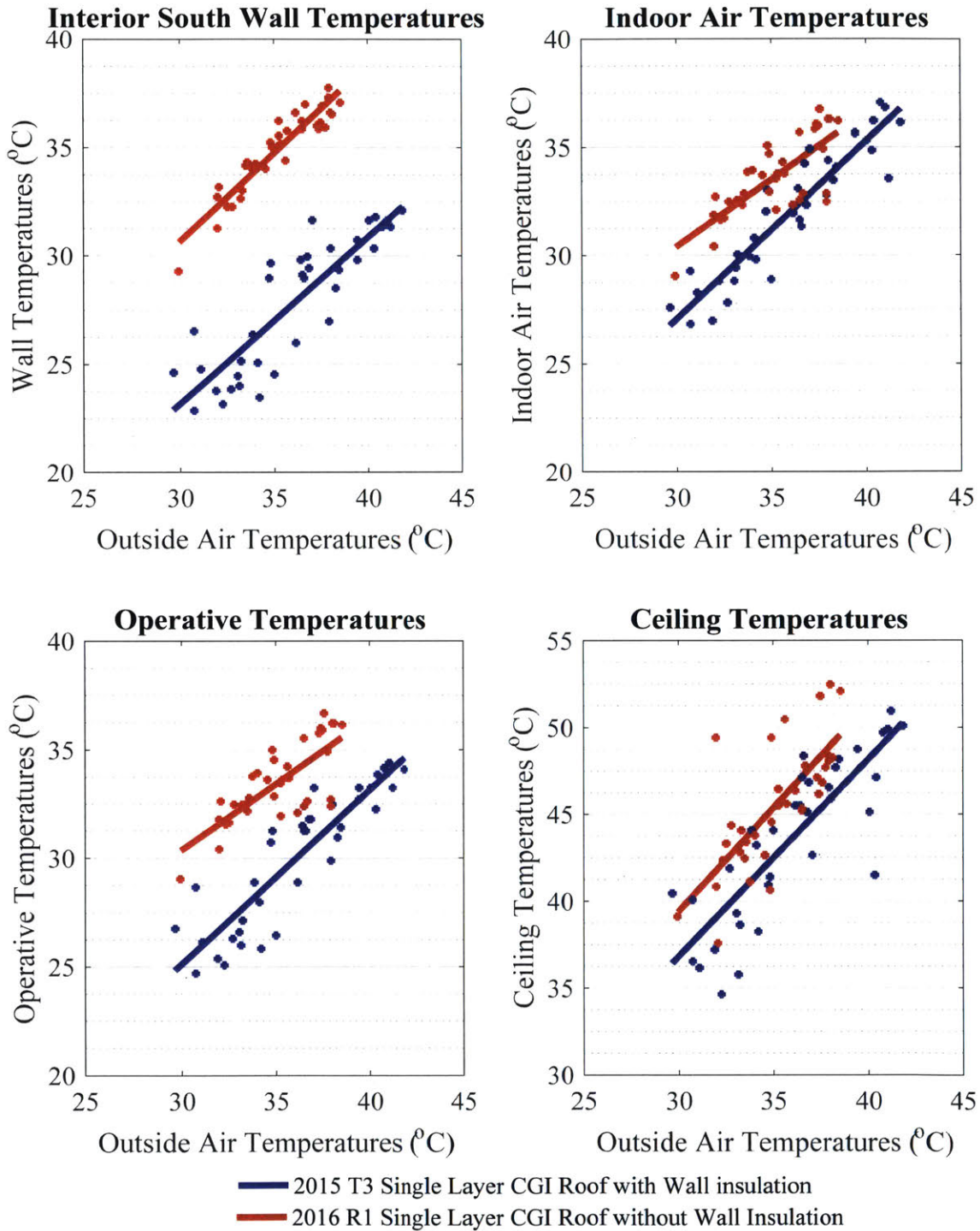


Figure 5-11: Maximum Interior Temperatures as a Function of Maximum Outdoor Ambient Air Temperatures for 2015 Single Layer CGI Roof Test Chambers with Wall Insulation and 2016 Single Layer CGI Roof Test Chambers without Wall Insulation

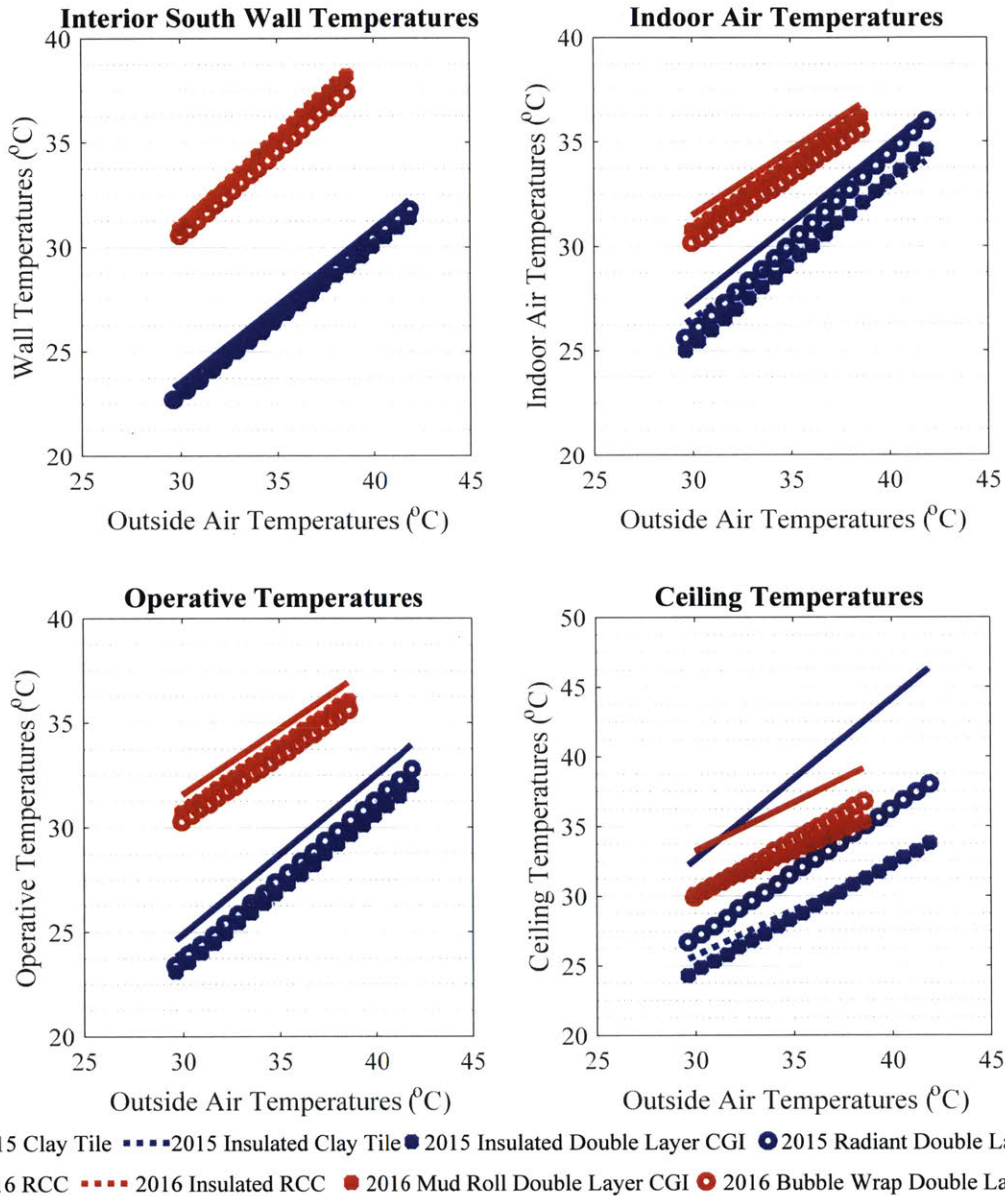


Figure 5-12: Maximum Interior Temperatures as a Function of Maximum Outdoor Ambient Air Temperatures for 2015 Test Chambers with Wall Insulation (T1, T2, T4, and T5) and 2016 Test Chambers without Wall Insulation (R2-R5)

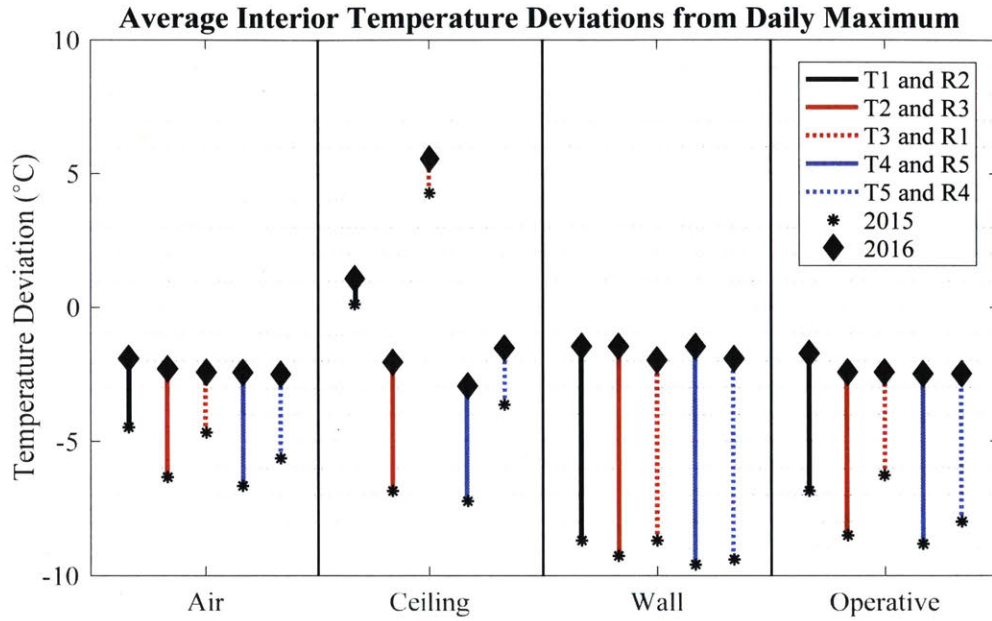
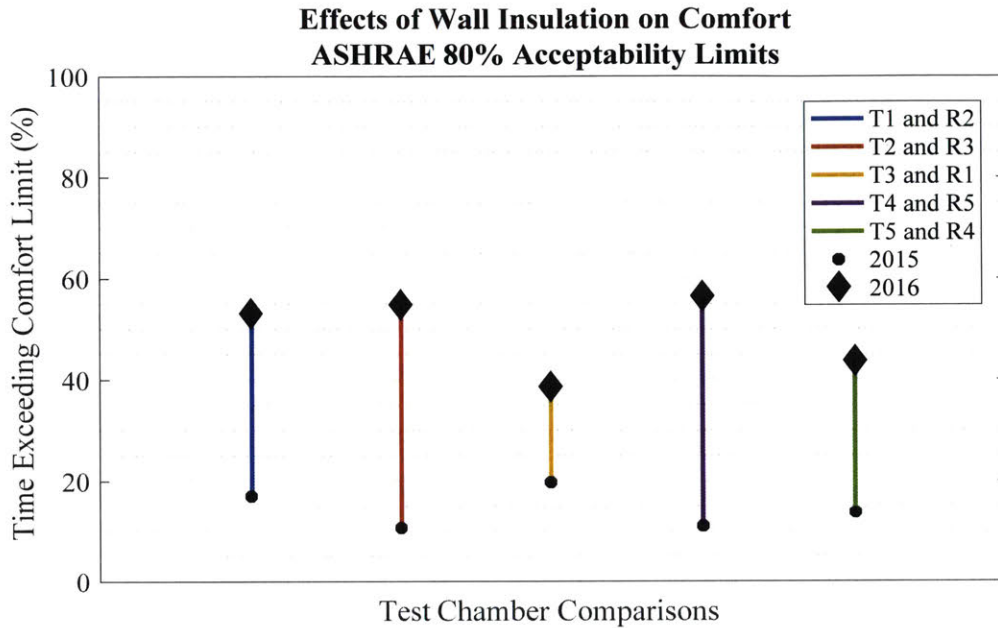


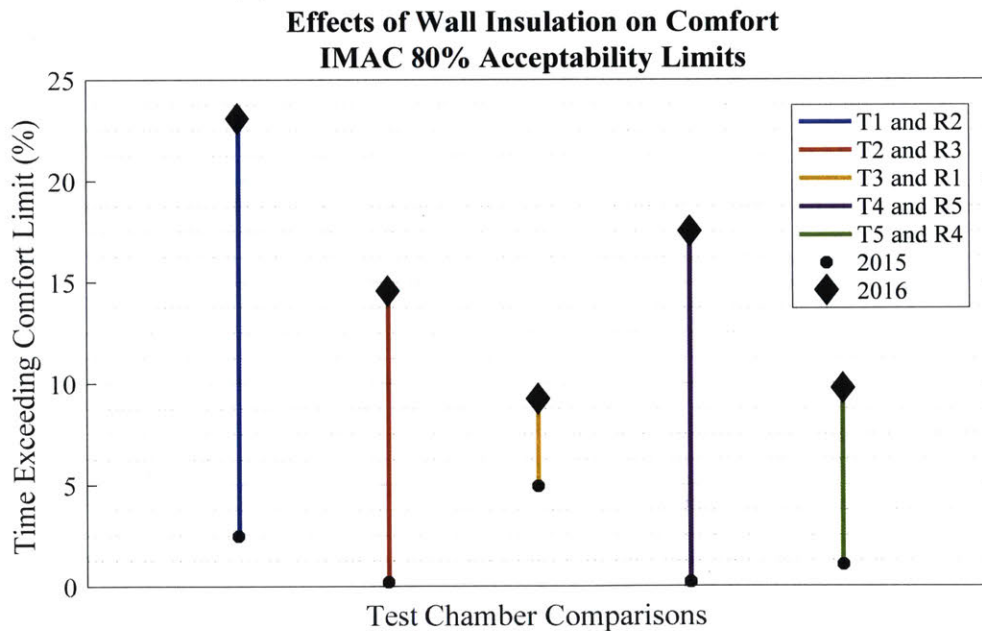
Figure 5-13: Average Interior Temperature Deviations from Daily Maximum for 2015 (Wall Insulation) and 2016 Test Chambers (No Wall Insulation)

from solar heat gains.





(a) Comfort Defined by ASHRAE Standards



(b) Comfort Defined by IMAC Standards

Figure 5-14: Percent of Time in which Test Chamber Operative Temperatures Remain within the ASHRAE and IMAC Comfort Standards

## 5.3 Effects of Wall Color

Heat avoidance through shading or reflective surfaces has been tested and proven as a viable technique for protecting against solar heat gains. Section 1.3.1 and 1.3.7 elaborate on how light colors plays a role in protecting the building from solar heat gains. In the context of Bhuj, some residents understand the importance of color finishes and choose to paint exposed walls white to reflect the visible spectrum of incident solar energy. Exterior wall treatments and their effects can be seen in Figure 5-15, infrared images of a Housing for All home (H3) interior. Infrared temperature measurements reveal that the interior south wall temperatures is 2°C warmer in the regions corresponding to the dark brown striped regions on the wall exterior.

To further investigate the impact of wall color on indoor thermal comfort, the team placed a black plastic sheet on the south side of the monitored Housing for All home with multi-layer Mangalore tile and Mud Rull Roof (H1) described in Section 3.3. The black plastic sheet fell flush against the unpatterned light blue south wall from January 23, 2017 17:30 to January 27, 18:00 (Figure 5-16).

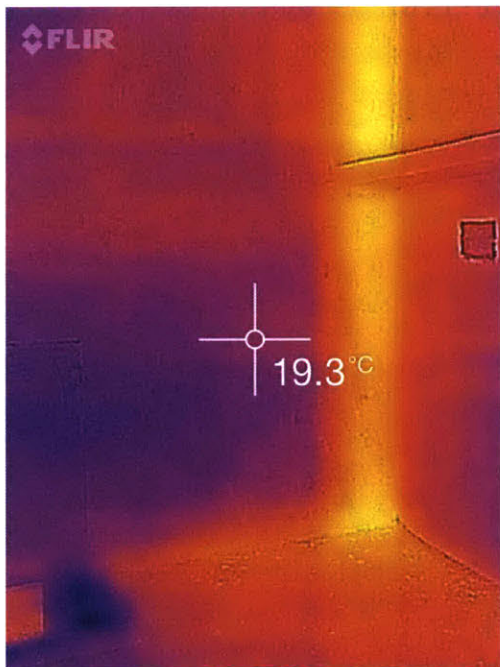
During this time temperature data on inner south wall, radiant, air, and ceiling temperatures were collected at 30-minute synchronized increments as detailed in Section 3.3. Results from the black plastic test show that wall color affects the building envelope temperatures. The addition of a black plastic sheet covering the south wall in the home with the mud roll roof caused south wall temperatures to increase as shown in Figure 5-17.

When the south wall temperatures were plotted as a function of outside air temperatures, an increase of over 4°C was observed in the south wall temperatures during the daytime as well as during the nighttime as shown in Figure 5-18.

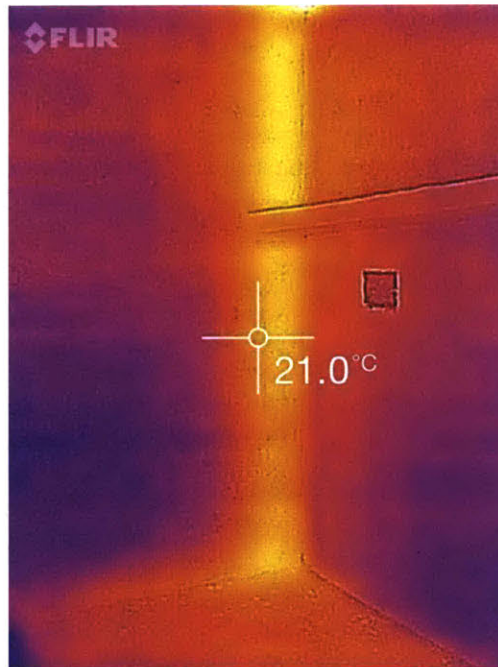
When radiant temperatures are plotted as a function of outside air temperatures, an average of a 2°C temperature increase occurred during both the day and night as shown in Figure 5-19. When indoor air temperatures are plotted as a function of outside air temperatures, an average of a 2°C increase can be seen during the day and night as shown in Figure 5-20. In the context of hot desert climates similar to



Exterior of Housing for All Home with a Double Layer Tin Roof and Wood Ceiling



IR Readings on Interior Wall



IR Readings on Interior Wall

Figure 5-15: Infrared Images of Building Interior Illustrating the Effects of Exterior Wall Colors on Indoor Environments (Images Courtesy of John Kongoletos)



Figure 5-16: Black Tarp Covering the South Wall of a Monitored Housing for All Home with a Multi-Layer Mangalore Tile and Mud Roll Insulated Roof

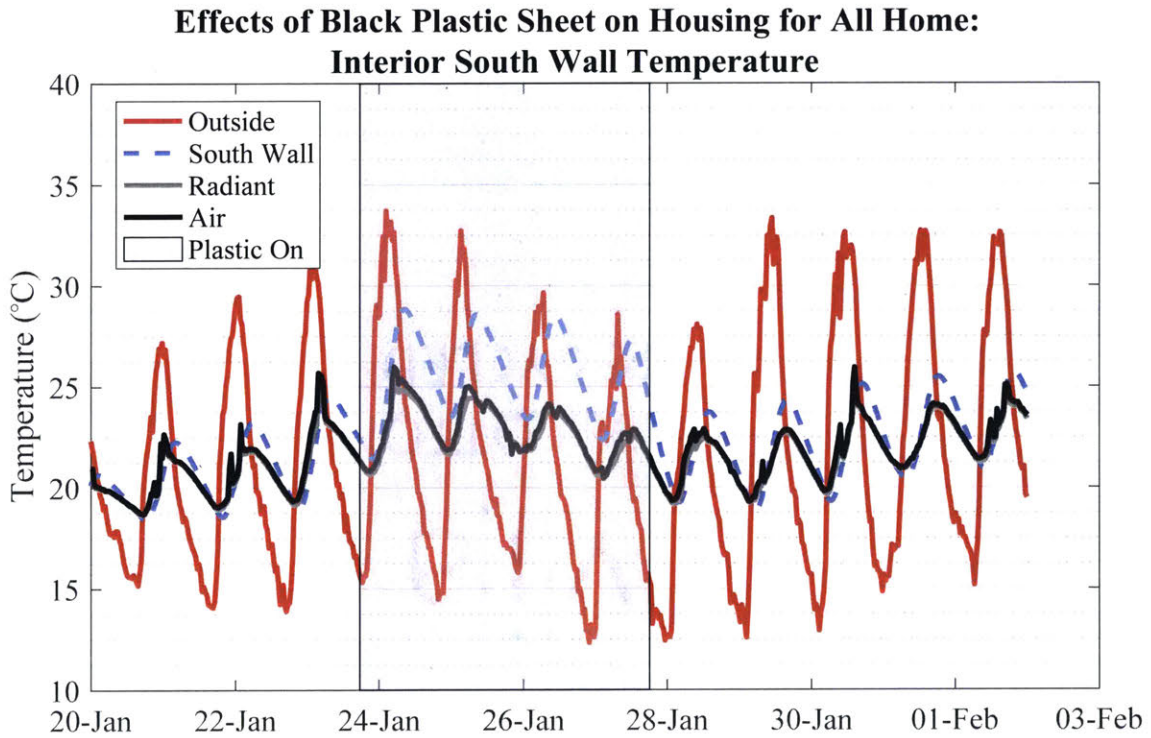
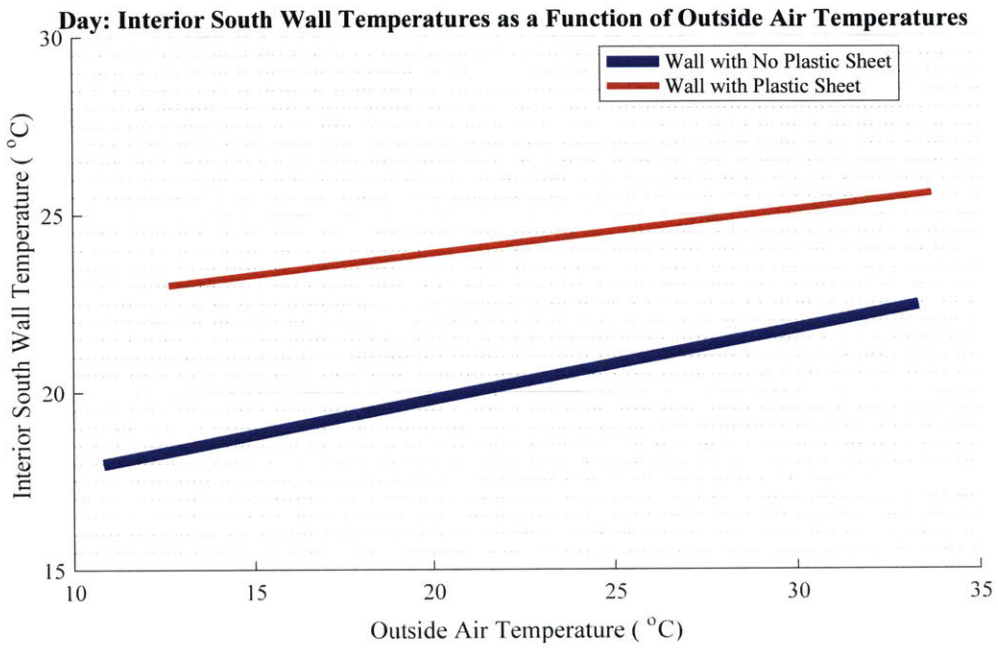
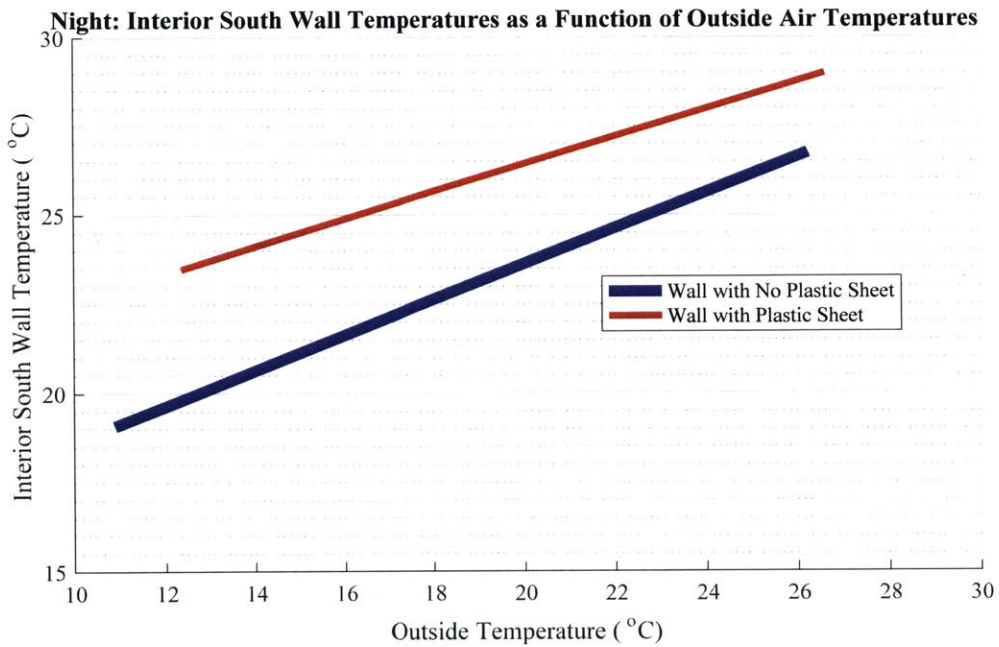


Figure 5-17: Transient Wall, Air, and Radiant Temperatures for Home with Black Plastic Placed on the South Wall

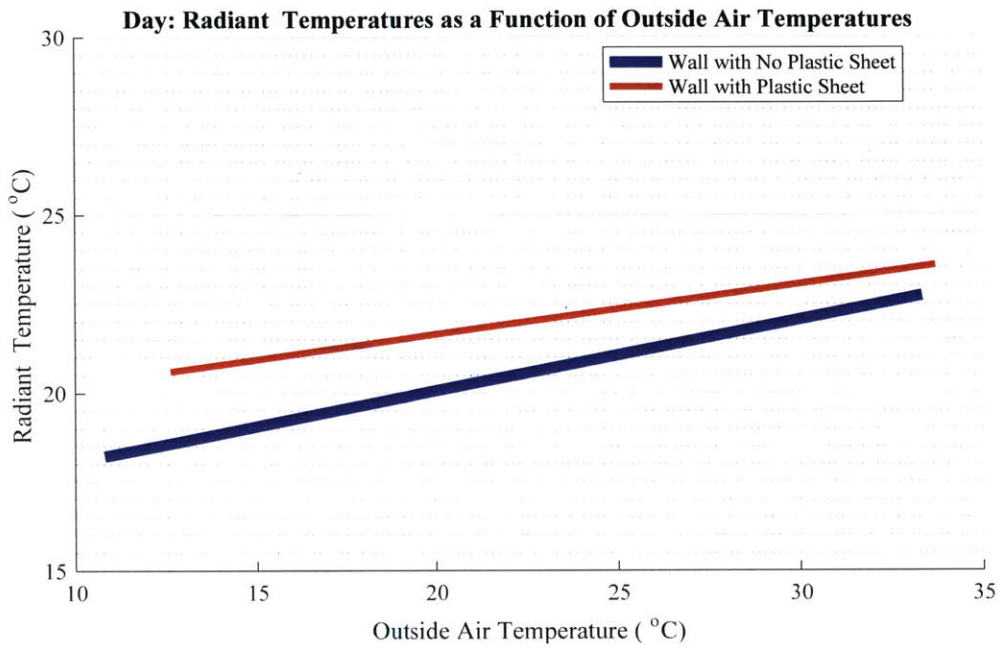


(a) Daytime South Wall Temperatures

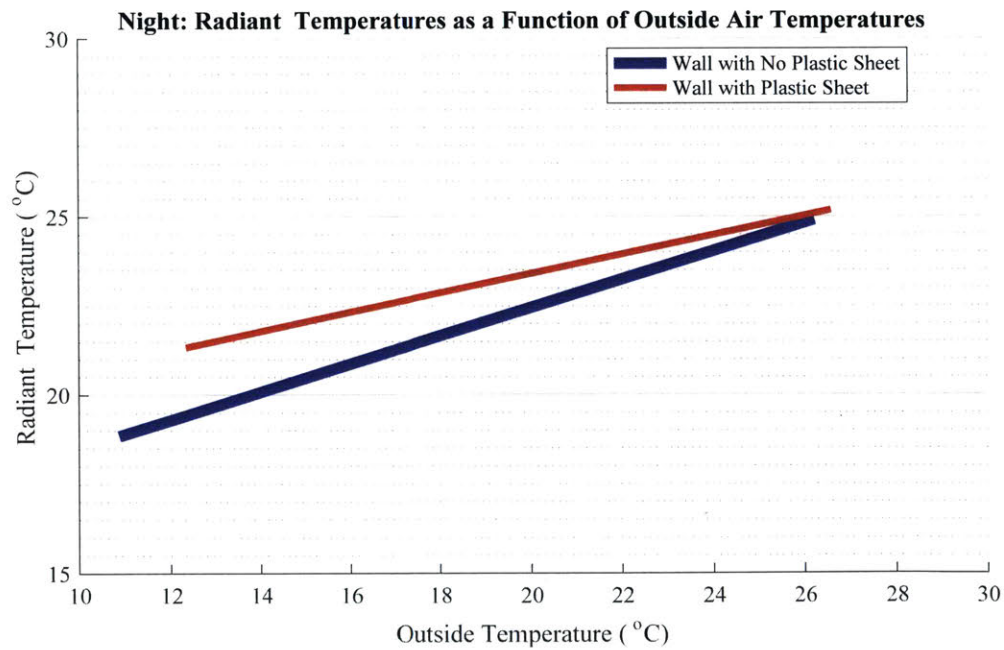


(b) Nighttime South Wall Temperatures

Figure 5-18: South Wall Temperatures as a Function of Outside Temperatures

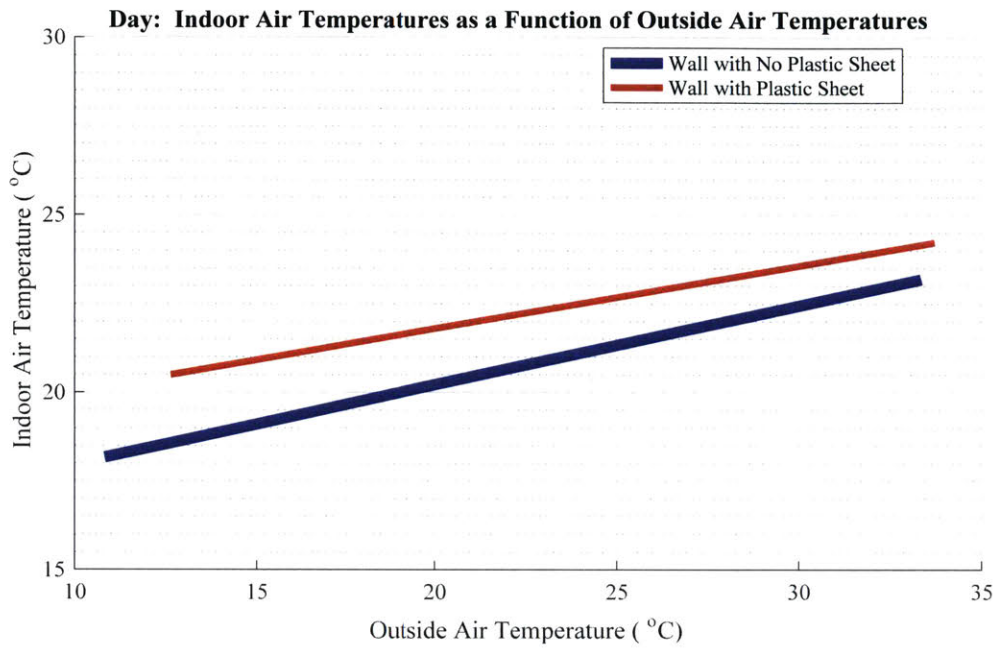


(a) Daytime Radiant Temperatures

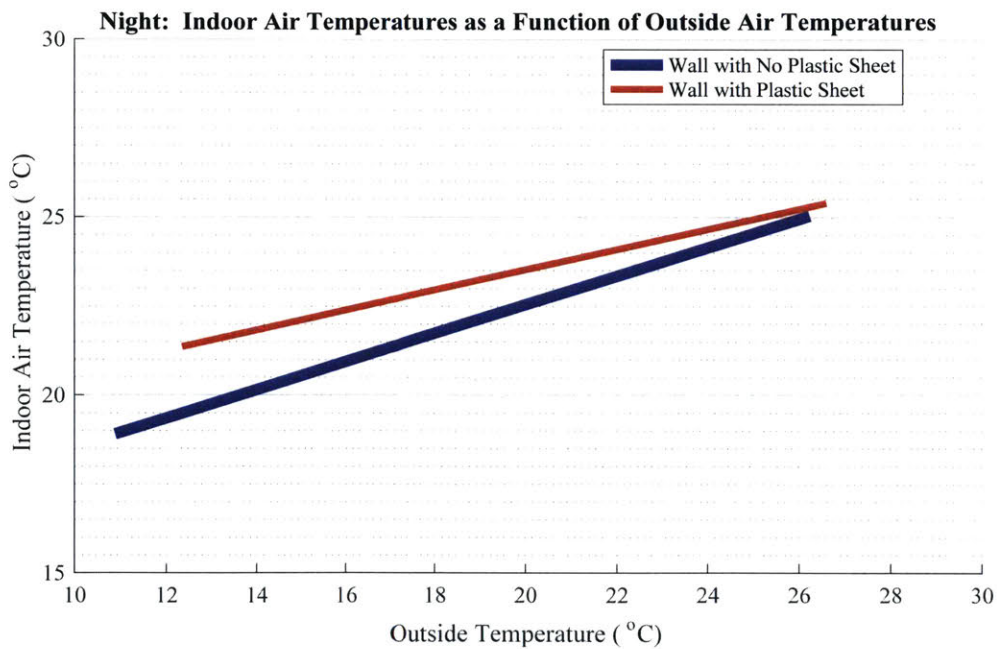


(b) Nighttime Radiant Temperatures

Figure 5-19: Radiant Temperatures as a Function of Outside Temperatures



(a) Daytime Indoor Air Temperatures



(b) Nighttime Indoor Air Temperatures

Figure 5-20: Indoor Air Temperatures as a Function of Outside Temperatures

Bhuj, walls exteriors should be coated with a light color to reflect the visible spectrum (approximately 40% of solar radiation).

## 5.4 Recommendations for Wall Design

Experimental results from test chamber and Housing for All homes indicate that regardless of roof types, wall protection is necessary for achieving thermal autonomy in Bhuj. The wall protection reduces the negative effects of solar heat gains and dampens external heat strains, allowing the thermally massive walls to retain coolness from night conditions.

### Thermal Mass

The combination thermal mass and insulation play an integral role in the thermal performance of the built environment given optimal climate conditions. This passive cooling method works most efficiently where climates are characterized by large diurnal temperature shifts, low humidity levels, and minimum cloud coverage. In the context of Bhuj, a thermally massive wall will work best in the months of October to April as shown in Figure 5-21. Though peak temperatures are greater in pre-monsoon season and average temperatures comparable, peak temperatures in test chambers during pre-monsoon season were 3°C lower in the March than in June 2015.

The use of thermal mass as a passive cooling technique is recommended for dry regions with at least 10°C diurnal shifts and humidity levels below 50%RH.

### Wall Insulation

The use of wall insulation can lead to a 1°C decrease in maximum air temperatures and a 3°C decrease in maximum operative temperatures. In buildings with a well designed thermally passive roof, the average maximum air temperature can decrease by as much as 3°C. Maximum interior south wall, air, and operative temperatures can decrease by 5°C.



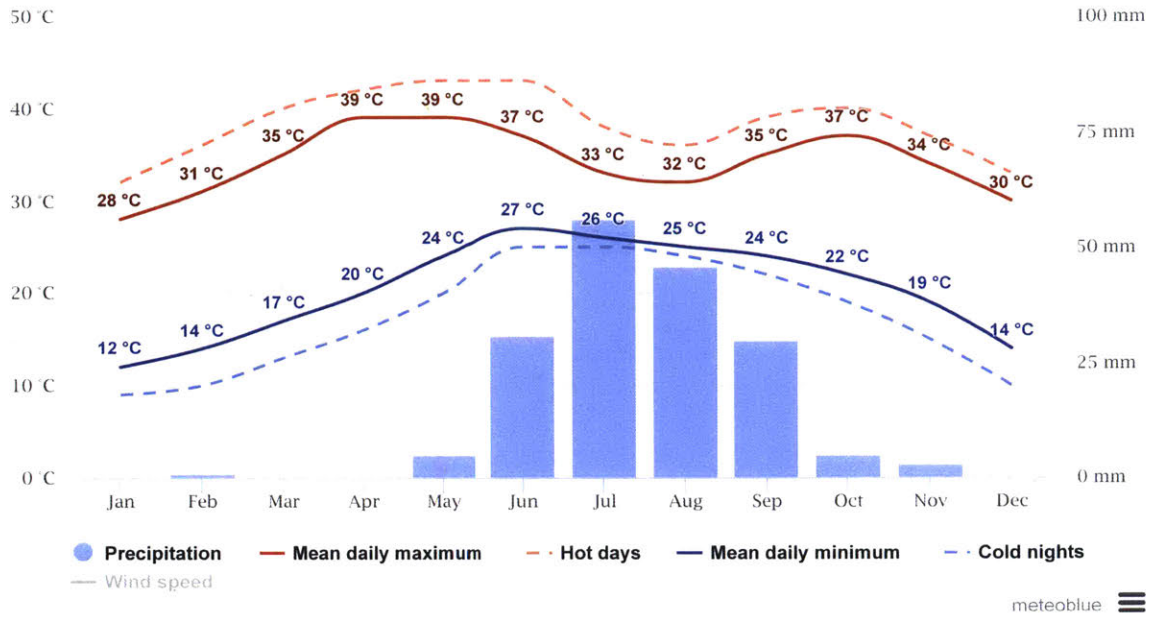


Figure 5-21: Average Temperatures and Precipitation for Bhuj, Gujarat, India (Meteoblue, 2014)

### Exterior Wall Color

Depending on climate conditions, different wall treatments are preferable. In places with climates characterized as hot/arid or hot/humid, it is recommended to paint walls white as this lowers daytime wall temperatures by more than 4°C when compared to a dark colored wall. The decrease in wall temperature leads to a 2°C decrease in radiant and indoor temperatures. However, for colder regions, dark colored walls are advisable for warmer the building envelope.



# Chapter 6

## Integration

Chapter 4 and 5 discusses recommendations for roof and wall design individually based on results from field experiments. This chapter discusses the integration of various roof and wall designs based on simulated results. Section 6.1 describes the boundary conditions, geometry, and assumptions in building the thermal model. The accuracy of these models was determined by comparing simulation results to measured data results. Following the comparison of the model with measured results, a variety of roof and wall design combination were simulated to determine several different constructions that could achieve thermal comfort in hot arid climates similar to Bhuj

### 6.1 Simulation Parameters

Three main components were examined in the test chamber building simulations: wall construction, roof construction, and room size. Properties of these components, such as wall insulation resistivity, were varied to examine their effects on the indoor temperature of the house given the extreme heat climate conditions. Table 6.1 shows the various components and their independent variables. These simulations were used to see what, if any, component most affects thermal comfort as well as what material(s) and geometry are best for housing construction.

A control volume analysis was used to determine the interior ambient air temperatures as shown in Figure 6-1. Boundary conditions include heat flux from the

Table 6.1: Independent Variables and Input Parameters in Thermal Simulations

Roof	Roof Type	RCC Insulated
		RCC Radiant Barrier + Air Gap
		RCC Alternating Radiant Barrer + Air Gap
		Single Layer Tin Sheet
		Single Layer Tin Roof + Radiant Barrier
		Double Layer Tin Roof + Air Gap + Radiant Barrier
		Single Layer Tin Roof + Alternating Radiant Barrier
	Double Layer Tin Roof + Alternating Radiant Barrier + Air Gap	
External Absorptivity	Untreated $\alpha = 0.5$	
	White Paint $\alpha = 0.2$	
Wall	R-Value ( $m^2K/W$ )	R = 0
		R = 0.25
		R = 1
	External Absorptivity	Untreated, $\alpha = 0.75$
White Paint $\alpha = 0.2$		
Room	Floor Area	2.4m by 2.4m
		3m by 3m

walls, heat flux from the ground, heat flux from the roof, and mass exchange with the outdoor environment (air infiltration/ventilation). Equation 6.1 describes the energy balance of this control volume given the assumed heat fluxes.

$$\begin{aligned}
 \rho_{air}c_{v,air}V_{room}\frac{dT_{in}}{dt} = & h_{conv}A_{ceiling}(T_{ceiling} - T_{in}) + \\
 & h_{conv}A_{wall}(T_{wall,west} - T_{in}) + h_{conv}A_{wall}(T_{wall,east} - T_{in}) + \\
 & h_{conv}A_{wall}(T_{wall,south} - T_{in}) + h_{conv}A_{wall}(T_{wall,north} - T_{in}) + \\
 & h_{conv}A_{floor}(T_{floor} - T_{in}) + \dot{m}_{air}c_{p,air}(T_{out} - T_{in}) \quad (6.1)
 \end{aligned}$$

where  $\rho_{air}$ ,  $c_{p,air}$ ,  $c_{v,air}$ , and  $\dot{m}_{air}$  represent the density, specific heat, and mass flow rate of air.  $V_{room}$  is the volume of air in the control volume room. The floor area, ceiling area, and wall area are denoted by  $A_{floor}$ ,  $A_{ceiling}$ , and  $A_{wall}$  respectively. The  $h_{conv}$  signifies the convection heat transfer coefficient. Floor, ceiling, wall, outdoor

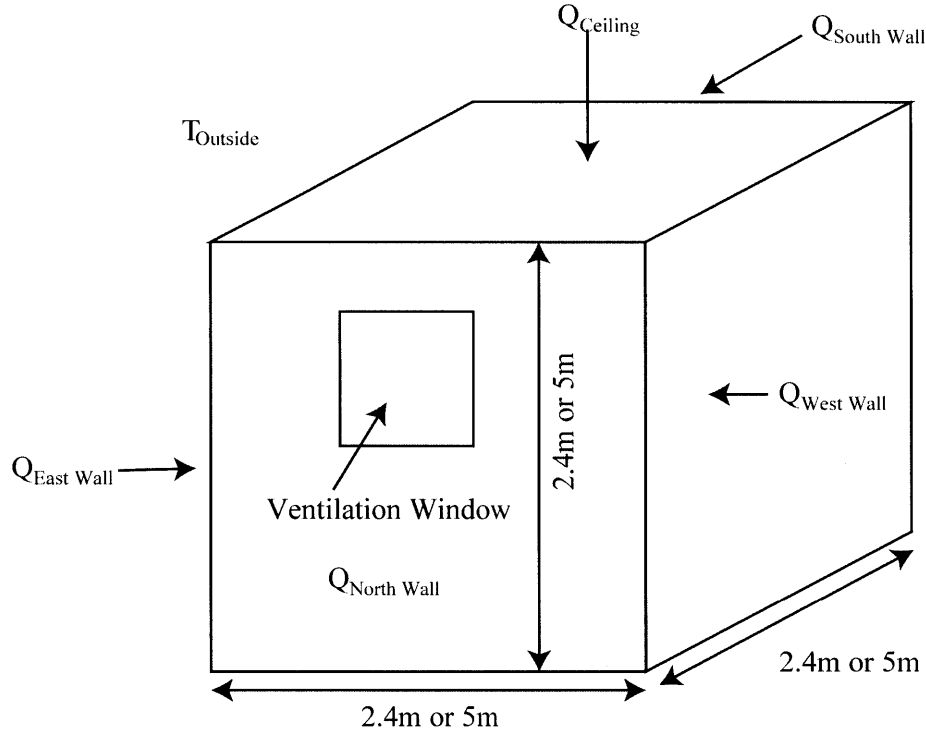


Figure 6-1: Geometry and Boundary Conditions for Test Chamber Control Volume

air, and indoor air temperatures are written as  $T_{floor}$ ,  $T_{ceiling}$ ,  $T_{wall}$ ,  $T_{out}$ , and  $T_{in}$  respectively.

Due to the air's low heat capacitance, a steady state analysis on the air can be used. In addition, based on data collected in site visits, it is reasonable to assume  $T_{ceiling}$  temperatures equal  $T_{wall}$ . Accepting these assumptions, the energy balance simplifies to

$$\begin{aligned}
 0 = & h_{conv}A_{ceiling}(T_{ceiling} - T_{in}) + 2h_{conv}A_{wall}(T_{wall,west} - T_{in}) + \\
 & h_{conv}A_{wall}(T_{wall,east} - T_{in}) + h_{conv}A_{wall}(T_{wall,south} - T_{in}) + \\
 & h_{conv}A_{wall}(T_{wall,north} - T_{in}) + \dot{m}_{air}c_{p,air}(T_{out} - T_{in}) \quad (6.2)
 \end{aligned}$$

In all the simulation cases, night flush ventilation was assumed with an air change rate of 6 roomfuls per hour (ACH) during the night, and 1 roomful per hour (ACH) during the day. The walls and roofs were modeled as one-dimensional structures. The following Sections 6.1.1 and 6.1.2 describe the thermal model used to predict

roof and wall temperatures. Equation 6.1 was solved simultaneously with the thermal models for the roof (Section 6.1.1) and walls (Section 6.1.2). Section 6.2 describes the numerical scheme used to calculate interior wall, ceiling, and air temperatures.

### 6.1.1 Roof Thermal Model

The simulations examined nine different roof types that were either painted white on the exterior or left untreated. Two of these nine roof types, the single layer corrugated galvanized iron (CGI) or tin sheet and the reinforced cement concrete roofs (RCC), represent common roof types used in Bhuj. Other roof types incorporate thermally passive design modifications into the control roof types.

#### Low Thermal Mass Tin Sheet Roofs

The following alterations were applied to the tin roof.

- **Constant Radiant Barrier:** A radiant barrier was installed flush against the ceiling exposed to the interior of the building. This is meant to reduce radiation heat transfer. The radiant barrier remains fixed through the day.
- **Constant Radiant Barrier with Ventilated Air Gap:** A radiant barrier, with low emissivity surfaces on both sides, was installed 10cm below the ceiling exposed to the interior of the building to create a buoyancy driven ventilated air gap. This is meant to reduce radiation heat transfer and add an insulation layer between the ceiling and room. The radiant barrier remains fixed through the day.
- **Alternating Radiant Barrier:** A radiant barrier was installed flush against the ceiling exposed to the interior of the building. This is meant to reduce radiation heat transfer. The radiant barrier remains fixed through the day. During the night, when the net radiant heat transfer from the roof is negative, the radiant barrier is removed. This allows the radiantly cooled roof with a high infrared emissivity to cool the indoor environment.

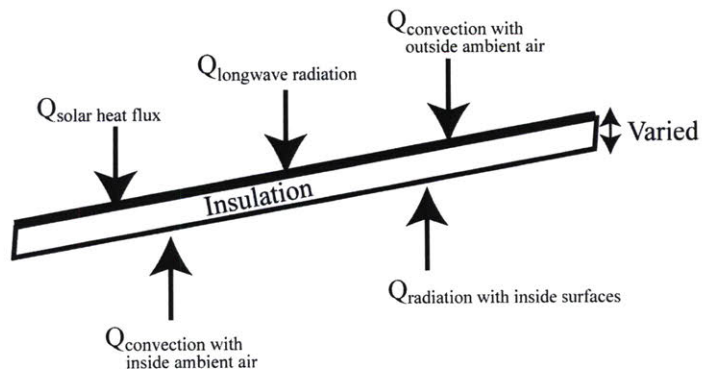
- **Alternating Radiant Barrier with Ventilated Air Gap:** A radiant barrier, with low emissivity surfaces on both sides, was installed 10cm below the ceiling exposed to the interior of the building to create a buoyancy driven ventilated air gap. This is meant to reduce radiation heat transfer and add an insulation layer between the roof and room. The radiant barrier remains fixed throughout the day. During the night, when the net radiant heat transfer from the roof is negative, the radiant barrier is removed. This allows the high infrared emissivity roof to cool the indoor environment.

Schedules of the radiant barrier installation are shown Figure 6-4. The air gaps of roofs with a constant air gap are ventilated continuously. In roofs with alternating air gap systems, the air gaps are only ventilated during the daytime. When modeling the ventilated air gaps, it is assumed that the air between the two roof layers are an average of the upper layer roof temperature and the outdoor ambient temperature

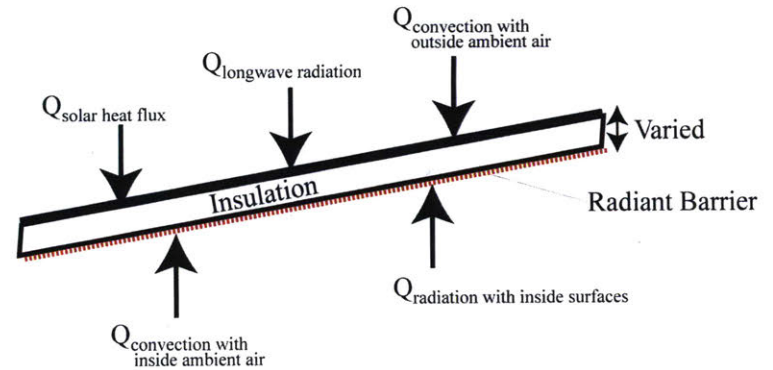
The CGI sheets found in Bhuj are approximately 0.5mm thick. Due to the tin sheets' low thermal mass properties, ceiling temperatures for the control CGI roof and modified CGI roofs were predicted with a steady state analysis.

$$0 = Q_{solar} + Q_{radiation, longwave} + Q_{convection, outside} + Q_{radiation, inside} + Q_{convection, inside} \quad (6.3)$$

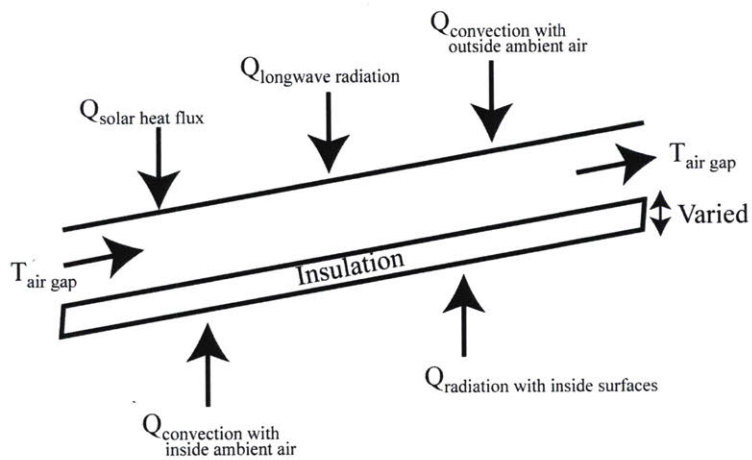
The boundary conditions on the exterior portion of the roof include longwave radiation to the sky ( $Q_{radiation, longwave}$ ), solar heat flux ( $Q_{solar}$ ), and convection with the ambient air ( $Q_{convection, outside}$ ). The boundary conditions on the interior portion of the roof include radiant heat transfer with the walls and floor ( $Q_{radiation, inside}$ ) and convection heat transfer with the indoor air ( $Q_{convection, inside}$ ). Figure 6-2 shows the assumed geometries and boundary conditions for the control tin sheet roof and modified tin sheet roofs. The ventilated air gaps were modeled assuming each layer experiences convective heat transfer with the air gap temperatures (an average of the upper layer roof temperature and outdoor air temperature) within the air gap and radiation heat transfer across the two layers.



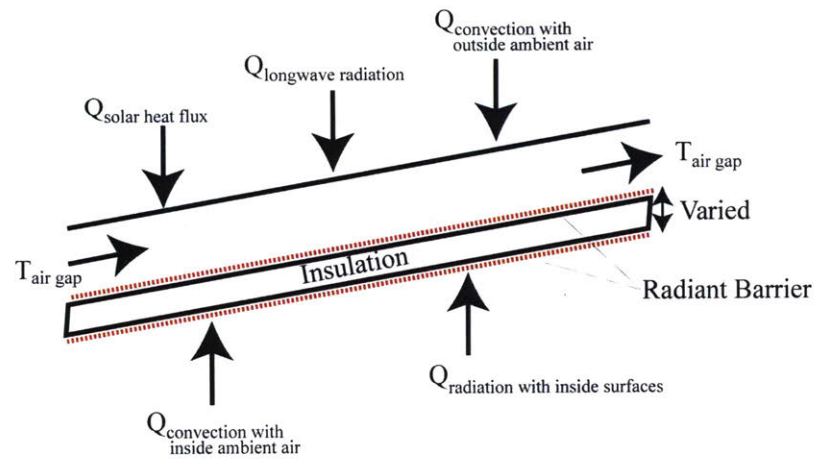
(a) Single Layer Tin Sheet, No Radiant Barrier



(b) Single Layer Tin Sheet, Radiant Barrier



(c) Double Layer Tin Sheet with Air Gap, No Radiant Barrier



(d) Double Layer Tin Sheet with Air Gap, Radiant Barrier

Figure 6-2: Single Layer Tin Roof Simulations Boundary Conditions and Geometry



## High Thermal Mass RCC Roof

The following alterations were applied to the tin roof.

- **Constant Ventilated Air Gap:** A buoyancy driven ventilated air gap was built under the RCC roof. The air gap remains fixed through the day.
- **Constant Radiant Barrier with Ventilated Air Gap:** A radiant barrier was installed 10cm below the ceiling exposed to the interior of the building. This is meant to reduce radiation heat transfer and add a buoyancy driven ventilated air gap layer between the roof and room. The radiant barrier remains fixed through the day.
- **Alternating Radiant Barrier with Ventilated Air Gap:** A radiant barrier, with low emissivity surfaces on both sides, was installed 10cm below the ceiling exposed to the interior of the building. This is meant to reduce radiation heat transfer and add a buoyancy driven ventilated air gap layer between the roof and room. The radiant barrier remains fixed throughout the day. During the night, when the net radiant heat transfer from the roof is negative, the radiant barrier is removed. This allows the radiantly cooled roof to cool the indoor environment.

Schedules of the radiant barrier installation are shown Figure 6-4. The air gaps of roofs with a constant air gap are ventilated continuously. In roofs with alternating air gap systems, the air gaps are only ventilated during the daytime. When modeling the ventilated air gaps, it is assumed that the air between the two roof layers are an average of the upper layer roof temperature and the outdoor ambient temperature

Given the thermal mass properties of an RCC slab, the RCC roofs were modeled using a transient heat transfer analysis described by equation 6.4.

$$\frac{dT_{rcc}}{dt} = \alpha \frac{d^2T_{rcc}}{dx^2} \quad (6.4)$$

In this analysis, the RCC roofs are assumed to be 11cm thick as measured in field

Table 6.2: Thermal Properties of the RCC Roof

Property	Value
Thermal Conductivity, $k$ ( $W/mK$ )	0.9
Heat Capacitance, $c_p$ ( $J/kgK$ )	900
Density, $\rho$ ( $kg/m^3$ )	1300
Emissivity, Upper layer Surface, $\epsilon$	0.98
Absorptivity, Exterior Surface, $\alpha$	0.5

visits. The following RCC thermal properties listed in Table 6.2 were used for calculations.

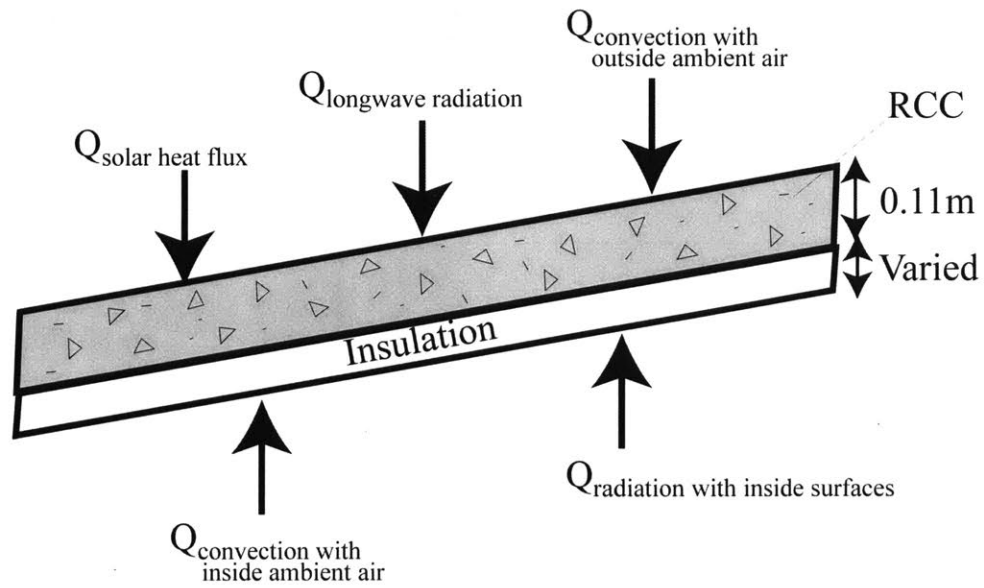
The boundary conditions on the exterior portion of the roof include longwave radiation to the sky, solar heat flux, and convection with the ambient air. The boundary conditions on the interior portion of the roof include radiation heat transfer with the walls and floor and convection heat transfer with the indoor air. Figure 6-3 shows the assumed geometries and boundary conditions for the control RCC slab roof and modified RCC slab roofs.

The thermal model employed a modified MATLAB function, `pdex1pde.m`, to solve the Fourier Heat Transfer equation, equation 6.4, using an implicit scheme (MathWorks, 2017). The RCC roof was discretized to 30 segments solved every 30 minutes. The ventilated air gaps were modeled assuming each layer experiences convective heat transfer with the air gap temperatures (an average of the upper layer roof temperature and the outdoor ambient temperature) within the air gap and radiation heat transfer across the two layers.

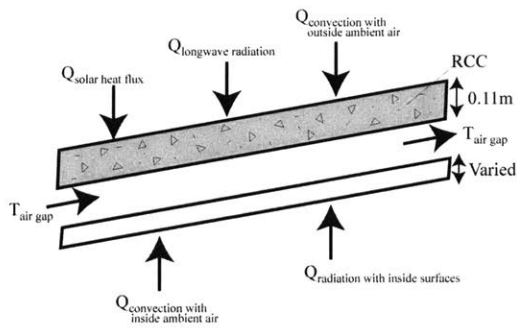
### 6.1.2 Wall Thermal Model

Simulated thermal models studied how exterior wall color and insulation alter thermal comfort. The walls were modeled as a finite thermally massive one-dimensional slab as shown in equation 6.5

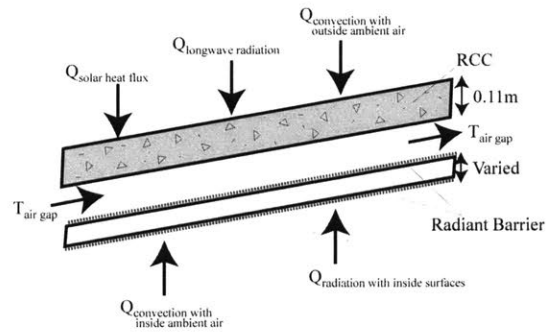
$$\frac{dT_{wall}}{dt} = \alpha \frac{d^2T_{wall}}{dx^2} \quad (6.5)$$



(a) RCC Slab, Radiant Barrier



(b) RCC Slab with Air Gap, No Radiant Barrier



(c) RCC Slab with Air Gap, Radiant Barrier

Figure 6-3: RCC Roof Simulations Boundary Conditions and Geometry

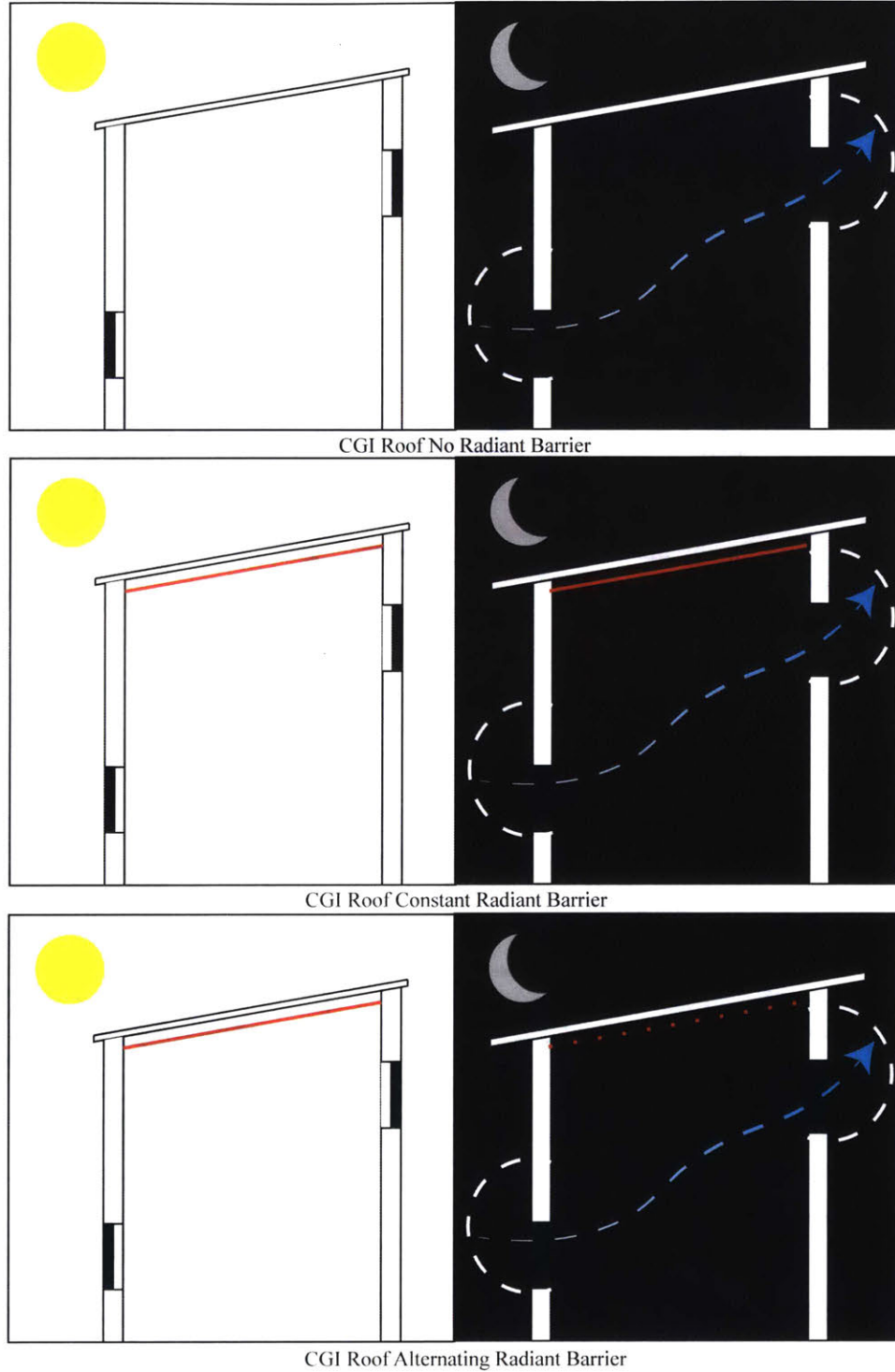


Figure 6-4: Radiant Barrier Placement Schedules for a Control Roof, Constant Radiant Barrier Roof, and Alternating Radiant Barrier Roof

Table 6.3: Thermal Properties of Simulated Walls

Property	Value
Thermal Conductivity, $k$ ( $W/mK$ )	1.93
Heat Capacitance, $c_p$ ( $J/kgK$ )	712
Density, $\rho$ ( $kg/m^3$ )	2200
Emissivity, Exterior and Interior Surface $\epsilon$	0.98
Absorptivity, Exterior Surface $\alpha$	0.75

Observations from field work indicated many residents use sandstone, limestone, or other thermally massive materials for wall structural material. In this model, the estimated wall properties are shown in Table 6.3.

The boundary conditions for the exterior facing wall surface of the test chamber include solar heat flux, long wave radiation to the sky, and convective heat transfer to the outdoor ambient air. Boundary conditions for the surface of the wall facing the interior of the test chamber include radiant heat transfer to the ceiling and convective heat transfer with the indoor ambient air. Figure 6-5 shows the wall geometries and the assumed boundary conditions. A modified MATLAB function, `pdex1pde.m`, was used to solve the Fourier Heat Transfer equation, equation 6.5, (MathWorks, 2017). The 23cm thick sandstone wall was discretized to 30 segments solved every 30 minutes.

### 6.1.3 Boundary Conditions

#### Exterior Boundary Conditions

The boundary conditions for surfaces facing the outdoor environment include solar heat flux, longwave radiation to the sky, and convection with the ambient air.

##### *Solar Heat Flux*

Measured solar heat flux using the ONSET Silicon Pyranometer (S-LIBM003) was directly inputted as the boundary condition for the roof thermal models. The solar heat flux sensor measured incident solar radiation on a horizontal surface, such as a roof. To obtain estimates for solar heat flux on vertical surfaces facing the north,

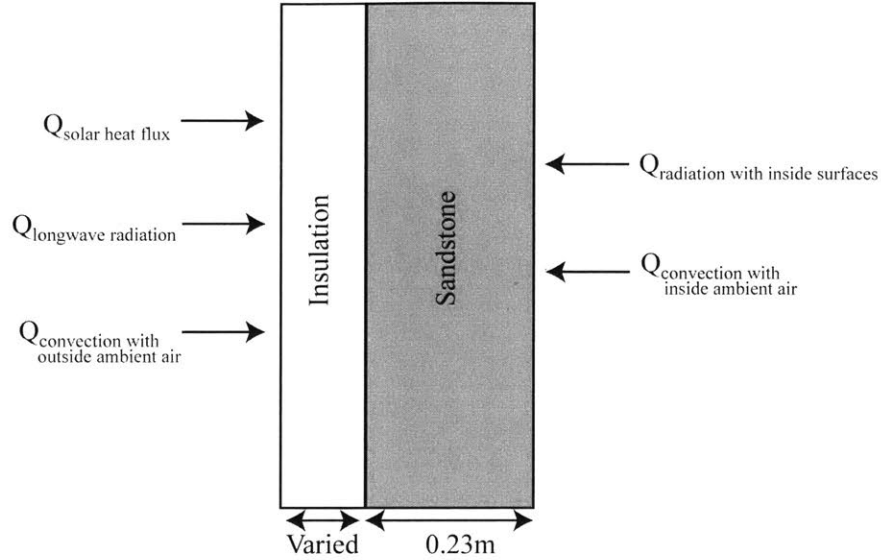


Figure 6-5: Boundary Conditions for Transient Wall Model

south, east, and west, ratios of solar incidences on horizontal surfaces to vertical surfaces were calculated using ASHRAE incident solar heat flux data for 24°N Latitude (American Society of Heating, Refrigerating and Air-Conditioning Engineers, 2005), close to Bhuj located at 23.2420°N. These ratios were used to calculate the incident wall solar heat flux based on the direct normal radiation measurements

#### *Longwave Radiant Heat Flux*

Radiation heat transfer to the sky is calculated using the equation 6.7

$$q_{\text{building,sky}} = \sigma \epsilon F_{\text{building,sky}} (T_{\text{building}}^4 - T_{\text{sky}}^4) \quad (6.6)$$

where  $q_{\text{building,sky}}$  is the longwave radiation to the sky,  $\sigma$  is the Stefan-Boltzmann constant,  $\epsilon$  is the emissivity of the building surface assumed to be a blackbody ( $\epsilon = 1$ ),  $F_{\text{building,sky}}$  is the view factor from the building to the sky,  $T_{\text{building}}$  is the building surface temperature, and  $T_{\text{sky}}$  is the sky temperature. For computational purposes, the above nonlinear equation 6.7 can be simplified to

$$q_{\text{building,sky}} = h_{\text{rad}} F_{\text{building,sky}} (T_{\text{building}} - T_{\text{sky}}) \quad (6.7)$$

Where the view factor to the sky,  $F_{building,sky}$ , is approximated as 1 for the roof and 0.5 for the walls. This approximation is an upper bound for the heat transfer from the building to the sky (Glicksman and Lienhard, 2016). The radiant heat transfer coefficient,  $h_{rad}$ , is approximated as

$$h_{rad} = 4\sigma\epsilon T_{mean}^3 \quad (6.8)$$

The sky temperature was calculated using the following equation 6.1.3 describe in Balcomb's *Longwave Radiation on the Outside of Buildings* (Balcomb, 1992).

$$\epsilon_{sky} = 0.711 + 0.56 \left( \frac{T_{dew}}{100} \right) + 0.73 \left( \frac{T_{dew}}{100} \right)^2 \quad (6.9)$$

where temperature is in °C.

$$T_{sky} = \epsilon_{sky}^{0.25} \times T_{ambient} \quad (6.10)$$

where temperature is in  $K$ . The dew temperature,  $T_{dew}$  can be estimated using the following correlation between relative humidity levels,  $RH$ , and outdoor ambient dry bulb temperatures,  $T_{db}$  found in the *Bulletin of the American Meteorological Society* (Lawrence, 2005)

$$T_{dew} = T_{db} - \frac{100 - RH}{5} \quad (6.11)$$

where temperature is in °C. This approximates the sky temperatures as 15-25°C below ambient sky temperatures depending on humidity levels and assuming clear skies.

#### *Convective Heat Transfer*

The convective heat flux between the building surface and the environment is governed by the following equation

$$q_{conv} = h_{conv}(T_{surface} - T_{ambient}) \quad (6.12)$$

where  $q_{conv}$  is the heat flux via convection,  $T_{surface}$  is the surface temperature, and  $T_{ambient}$  is the ambient air temperature surrounding the surface. Correlations found in

*A Survey of Wind Convection Coefficient Correlations for Building Envelope Energy Systems' Modeling* (Palyvos, 2008), were used to calculate the heat transfer coefficient between the building surface and the outdoor ambient environment.

$$h_{conv} = 7.13V_w^{0.78} + 5.35e^{-0.6V_w} \quad (6.13)$$

where  $V_w$  is the wind velocity. Assuming daytime wind speeds of 7m/s and nighttime wind speeds of 5m/s, the following external convection heat transfer coefficients were used.

$$\begin{aligned} h_{night} &= 25.3 \frac{W}{m^2K} \\ h_{day} &= 32.2 \frac{W}{m^2K} \end{aligned} \quad (6.14)$$

All walls and ceilings are assumed to have the same exterior convection heat transfer boundary condition.

### **Interior Boundary Conditions**

The internal boundary conditions consist of heat flux across interior building surfaces via radiant heat transfer and convection heat transfer with the ambient indoor air.

#### *Radiation Heat Transfer*

The radiant heat transfer between the wall and the ceiling depends on the view factor between these two elements and surface temperatures as written in the following equation

$$q_{wall,ceiling} = 4\sigma\epsilon F_{wall,ceiling} \left( \frac{T_{wall} + T_{ceiling}}{2} \right)^3 (T_{wall} - T_{ceiling}) \quad (6.15)$$

where the view factor,  $F_{wall,ceiling}$ , can be estimated as 0.2 (Glicksman and Lienhard, 2016) and  $q_{wall,ceiling}$  is the radiation heat transfer between the wall and ceiling. The  $\epsilon$  represents the building interior surface infrared emissivities. If the surface is a wall, it is assumed to be a black body with  $\epsilon = 1$ . Ceiling surface emissivities depend on roof type. If the roof consists of a radiant barrier,  $\epsilon = 0.1$ . Otherwise, the roof is



assumed to be a black body with  $\epsilon = 1$ .

In these simulations, it is assumed that floor temperatures are equal to the south wall temperatures. The resulting radiant heat transfer coefficient between the wall and the ceiling is on the order of  $1.5W/m^2K$ .

### *Convective Heat Transfer*

Internal heat transfer coefficients were calculated using natural convection Nusselt correlations found in literature. In the case of the ceiling, separate Nusselt correlations were utilized depending on whether the ceiling temperatures exceeded indoor ambient temperatures (M. Fishenden and O. A. Saunders, 1950).

If the ceiling temperature is cooler than ambient temperatures, the Nusselt correlation for a cold horizontal plate facing down is used

$$\begin{aligned} Nu &= 0.54Ra^{\frac{1}{4}}, \text{ for } Ra < 2 \times 10^7 \\ Nu &= 0.14Ra^{\frac{1}{3}}, \text{ for } Ra > 2 \times 10^7 \end{aligned} \tag{6.16}$$

where the characteristic dimension for calculating the Rayleigh number ( $Ra$ ) is the width of the ceiling. If ceiling temperatures exceeded ambient air temperatures the following correlation (M. Fishenden and O. A. Saunders, 1950) is used

$$Nu = 0.25Ra^{\frac{1}{5}} \tag{6.17}$$

Using these correlations, the convection heat transfer coefficient when ceiling temperatures exceed indoor ambient temperature is approximately  $0.15W/m^2K$ . The convection heat transfer coefficient increases to approximately  $1.5W/m^2K$  when ambient indoor air temperatures exceed ceiling temperatures.

The below Nusselt correlations for vertical surfaces, where used to measure con-

vection from the walls. (S. W. Churchill and H. H. S. Chu, 1975)

$$\begin{aligned}
 Nu &= 0.825 + \frac{0.387^{\frac{1}{6}}}{1 + \frac{0.492^{\frac{9}{16}}}{Pr^{\frac{8}{27}}}}, \text{ for } Ra < 10^9 \\
 Nu &= 0.68 + \frac{0.670^{\frac{1}{4}}}{1 + \frac{0.492^{\frac{9}{16}}}{Pr^{\frac{4}{9}}}}, \text{ for } Ra > 10^9
 \end{aligned}
 \tag{6.18}$$

where the characteristic dimension for calculating the Rayleigh number ( $Ra$ ) is the height of the wall. Throughout the day, the calculated wall heat transfer coefficient is approximately  $1.2W/m^2K$ . All walls are assumed to have the same interior radiation and convection heat transfer boundary conditions.

## 6.2 Numerical Solver

An iterative scheme was employed to solve for transient ceiling, wall, air temperatures, and operative temperatures. For the first iteration, the numerical solver uses measured transient indoor air, wall, and ceiling temperature as an initial guess to calculate convective and radiation heat transfer coefficients. These calculated coefficients are then used to solve for new transient wall and ceiling temperatures, given assumed ceiling, wall, and interior air temperature. The scheme then calculates the maximum difference between the previous iteration of wall, ceiling, and air temperature with the most recently calculated wall ceiling and air temperatures. If the maximum difference is less than  $0.5^\circ C$  the iterations terminate. Otherwise, iterations continue with the updated wall, ceiling, and air temperatures to calculate the next iteration's heat transfer coefficients and interior temperatures. Iterations continue until the solution converges. On average, the temperatures converge within five iterations. Figure 6-6 shows the iterative scheme used to calculate interior air, wall, and ceiling temperatures.

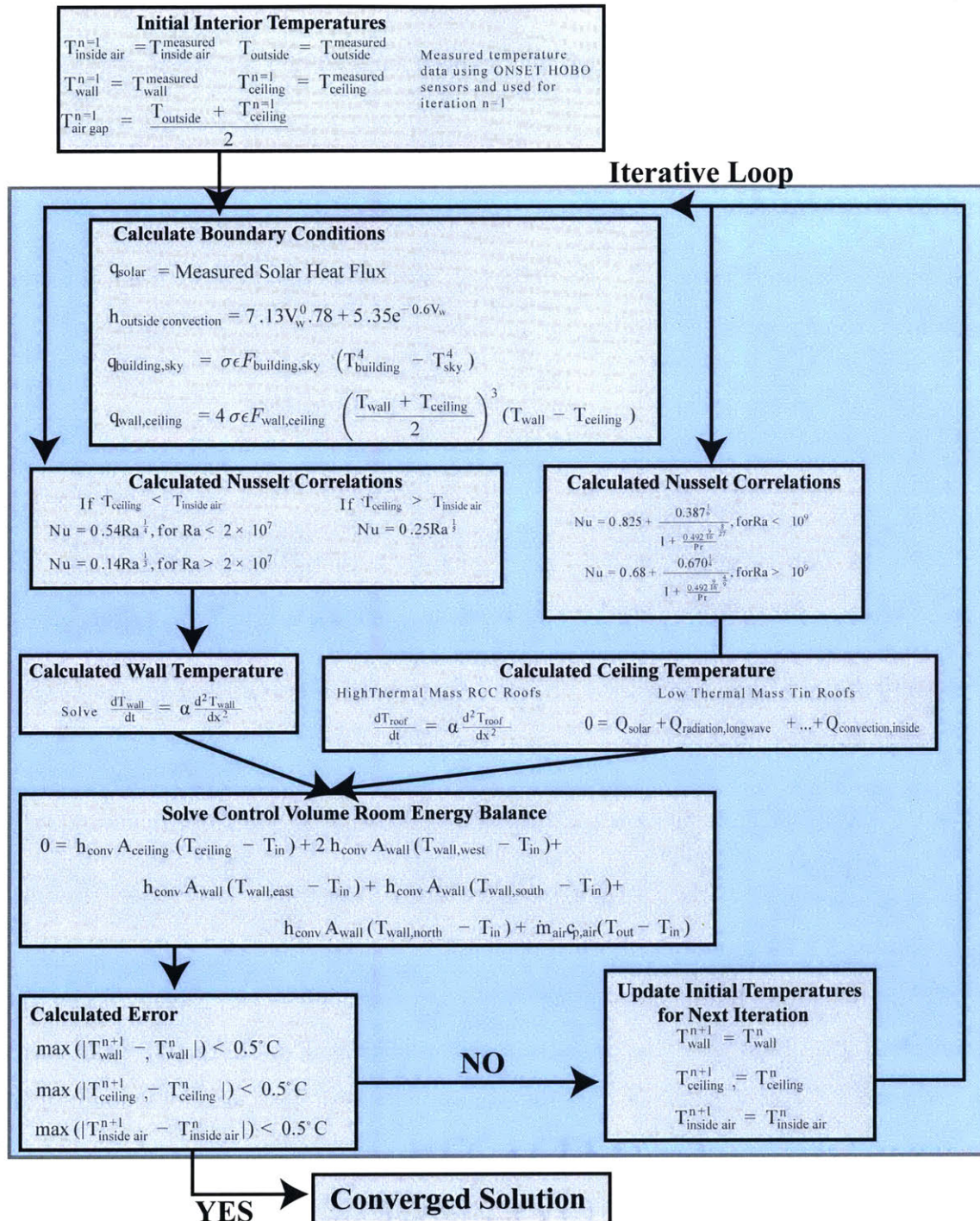


Figure 6-6: Iterative Scheme for Calculating Interior Temperatures in Thermal Model

## 6.3 Comparison of Measured Data with Simulations

The simulated results for several 2.4m by 2.4m test chambers were compared to measured data in the 2015 and 2016 field experiments to determine the accuracy of the thermal model.

### Indoor Ambient Air

Thermal Models were created for the following 2016 test chambers with unprotected walls for the purpose of calibrating the models.

- R1 | A Test Chamber with a Single Layer Tin Sheet Roof
- R2 | A Test Chamber with a 11cm Thick RCC Slab Roof
- R3 | A Test Chamber with a 11cm Thick RCC Slab, Ventilated Air Gap, and Thermocol Insulation (Styrofoam) Roof
- R4 | A Test Chamber with a Double Layer Ventilated Tin Roof Insulated with Aluminized Bubble Wrap
- R5 | A Test Chamber with a Double Layer Ventilated Tin Roof Insulated with Mud Rolls

See Chapter 3.2 for more details on test chamber construction.

Figure 6-7 shows indoor air temperature comparisons between the simulated and monitored 2016 2.4m by 2.4m by 2.4m test chamber with unprotected walls and a single layer CGI roof (R1). In all the simulated cases, it is assumed night flush ventilation was practiced.

In this comparison, the average peak air temperatures for the simulated and measured results disagree by 0.79°C. The average minimum indoor air temperatures of the thermal model and field experiment differ by 0.35°C. Comparison of results from four different simulations and the 2016 field experiments are illustrated in Figure B-1 found in Appendix B. In all these simulated cases, the maximum disagreement

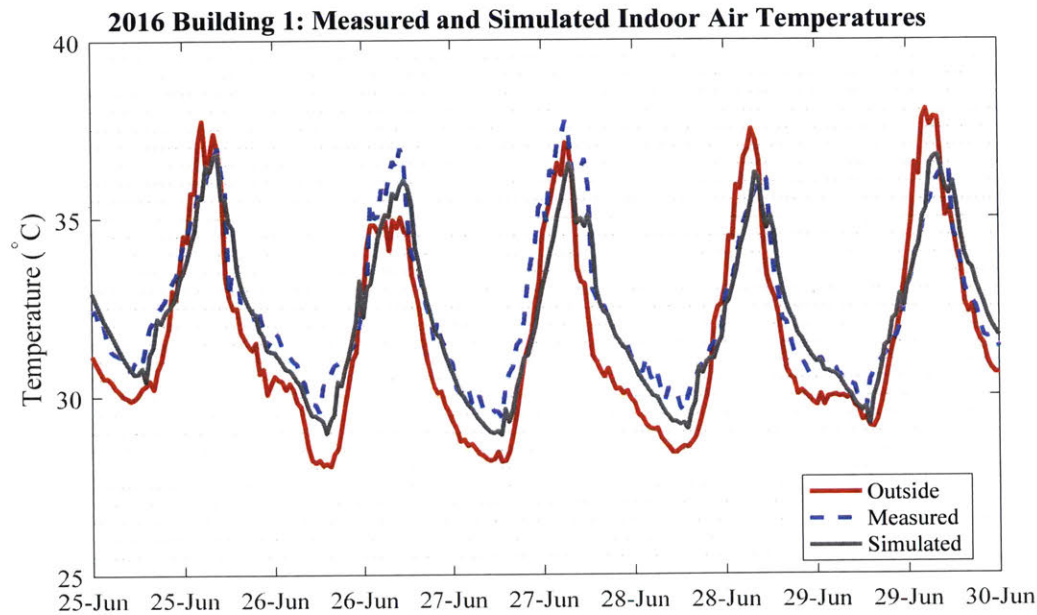


Figure 6-7: Comparison Between Simulated and Measured Indoor Air Temperatures for a 2.4m by 2.4m by 2.4m Test Chamber with a Single Layer CGI Roof

on average peak indoor ambient air temperatures was  $0.79^{\circ}\text{C}$ , and the maximum disagreement on average minimum interior air temperatures was  $0.54^{\circ}\text{C}$ .

## Ceiling

The following thermal models were simulated and compared with measured data from 2015 and 2015 field experiments.

- R1 | A Test Chamber with a Single Layer Tin Sheet Roof
- R2 | A Test Chamber with a 11cm Thick RCC Slab Roof
- R3 | A Test Chamber with a 11cm Thick RCC Slab, Ventilated Air Gap, and Thermocol Insulation (Styrofoam) Roof
- R4 | A Test chamber with a Double Layer Ventilated Tin Roof Insulated with Bubble Wrap ( $R = 0.5\text{m}^2\text{K}/\text{W}$ )

- T5 | A Test Chamber with a Double Layer Ventilated Tin Roof with a Radiant Barrier (see Section 1.5 for more detail)

Figure 6-8 shows ceiling temperature comparisons between a simulated and the 2016 constructed 2.4m by 2.4m by 2.4m test chamber with unprotected walls and a single layer CGI roof.

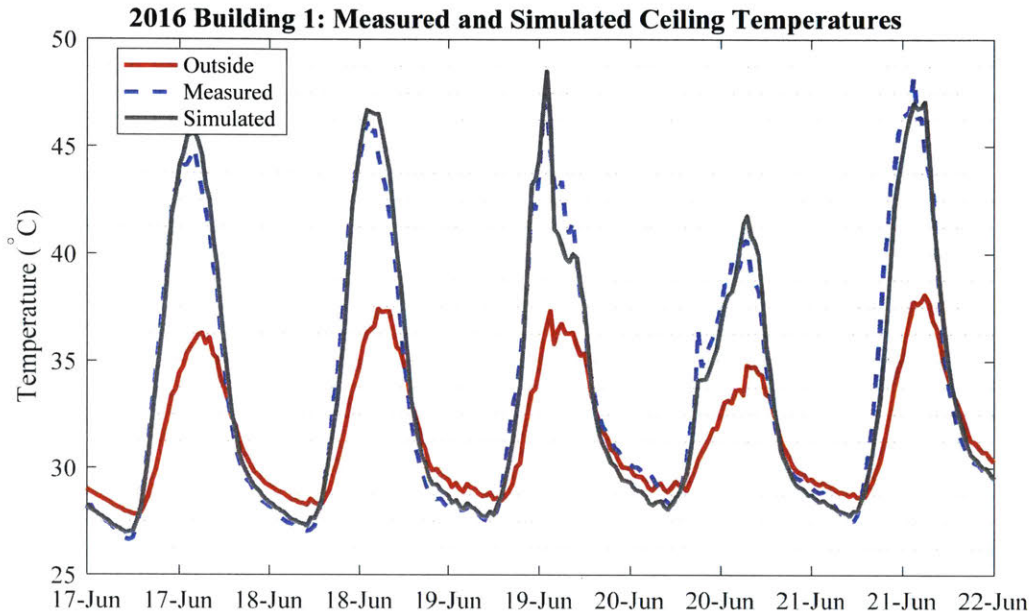


Figure 6-8: Comparison Between Simulated and Measured Ceiling Temperatures for a 2.4m by 2.4m by 2.4m Test Chamber with a Single Layer CGI Roof

In this comparison, the average peak ceiling temperatures for the simulated and measured results disagree by 1.70°C. The simulations predicted greater peak ceiling temperatures. The predicted solar absorptivity of 0.5 could be greater than the actual value for the tin roof causing predicted ceiling temperatures to be higher than measured. The average minimum ceiling temperatures of the thermal model and field experiment differ by 0.38°C representing good agreement between the model and the measured data. Comparison of results from four different simulations and the 2016 field experiments are illustrated in Figure B-3 found in Appendix B.

In all these simulated cases, the maximum disagreement between measured and simulated average peak ceiling temperatures was 1.70°C. However the average dis-

agreement in peak ceiling temperatures was  $0.5^{\circ}\text{C}$ . The maximum disagreement in average minimum ceiling temperatures was  $0.57^{\circ}\text{C}$ .

## Wall

Simulated interior south wall temperatures were compared the R1-R5 test chambers built and monitored in 2016. The exterior walls of these test chambers do not have insulation or any color coating. Figure 6-9 shows south wall temperature comparisons between a simulated 2.4m by 2.4m by 2.4m test chamber with unprotected walls and a single layer CGI roof with the 2016 single layer CGI roof test chamber (R1).

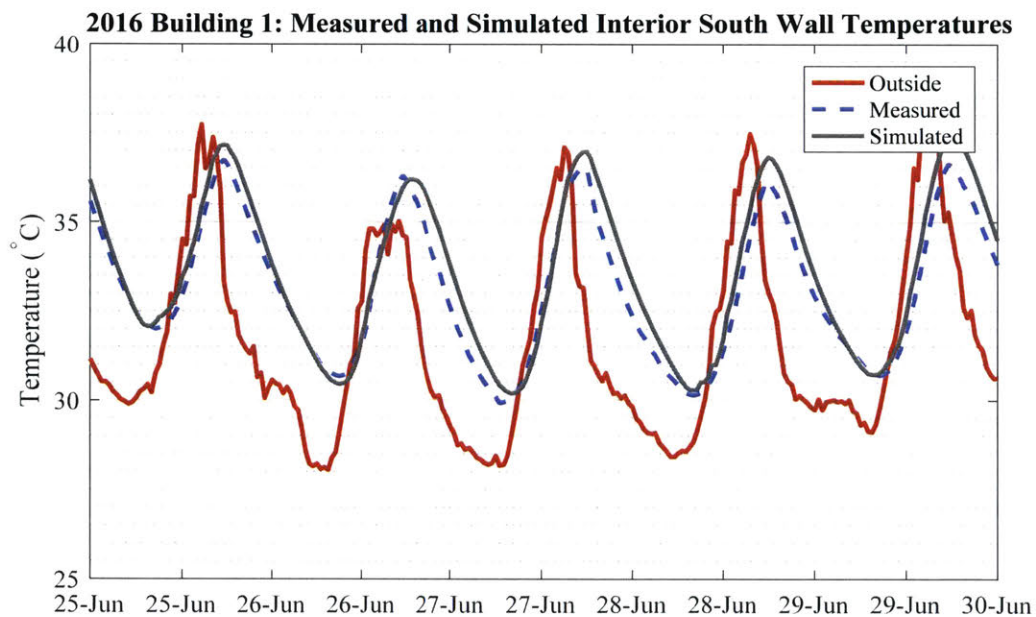


Figure 6-9: Comparison Between Simulated and Measured South Wall Temperatures for a 2.4m by 2.4m by 2.4m Test Chamber with a Single Layer CGI Roof

In this comparison, the average peak interior south wall temperatures for the simulated and measured results disagree by  $0.05^{\circ}\text{C}$ . The average minimum temperatures between the thermal model and field experiment differ by  $0.19^{\circ}\text{C}$  indicating general agreement between the simulation and measured results. Comparison of results from four different simulations and the 2016 field experiments are illustrated in Figure B-3 found in Appendix B. Considering all these simulated cases, the max-

imum disagreement on average peak interior south wall temperatures was 0.66°C, and the maximum disagreement on average minimum interior south wall temperatures was 0.46°C, demonstrating the thermal model can predict interior south wall temperatures within 1°C accuracy.

## 6.4 Results

Following the comparison of the thermal model with measured experimental results, various building designs, shown in Table 6.1, were simulated. The simulations examined the effects of roof types and wall treatments for a 2.4m by 2.4m by 2.4m room and a 5m by 5m by 2.4m room. The subsequent analysis of results led to recommendations for optimizing the integration of wall and roof design (Section 6.5).

### 6.4.1 Simulation Results: 2.4m by 2.4m by 2.4m Rooms

Simulations with the room size set to 2.4m by 2.4m and room height set to 2.4m predict wall and roof design effects in rooms with a greater wall to ceiling ratio. In these simulations, the wall to ceiling ratios are 4:1.

#### Simulated Test Chambers with CGI Roofs

Figure 6-10 shows the interior transient air, operative, south wall, and ceiling temperatures for a test chamber with  $R = 1m^2K/W$  insulated walls and various tin sheet roof geometries. Results of these simulation runs indicate the alternating radiant barrier roof outperforms the single layer tin roof and other simulated modifications on the control CGI roof. The implementation of an alternating radiant barrier with buoyancy driven ventilated open to the exterior environment lowers peak indoor ambient air temperatures by 3°C when compared to the control roof, a single layer tin sheet.

The added air gap insulation and alternating radiant barrier decrease single tin sheet ceiling temperatures by 15°C. This leads to a 6°C decrease in operative temperatures. Roof systems with constant radiant barriers and air gaps still provide



some level of protection from solar heat gains through the roof. Peak indoor ambient air temperatures are 2°C cooler in rooms with a constant radiant air gap roof than rooms with a single layer tin sheet. Based on these simulated results, a radiant barrier should be placed on the ceiling exposed to the room interior. Though this may increase ceiling temperatures, operative temperatures can decrease by 4°C with this modification. However, if occupants use ceiling fans, it will be more important to keep ceiling temperatures cooler as the ceiling fan can mix the hot air directly adjacent to the ceiling to lower sections of the room near the occupants. More explanation can be found in Chapter 7.

Regardless of the roof type, the success of a thermal autonomous design requires proper wall protection. As shown in Figure 6-11, the addition of exterior wall insulation with  $R = 0.25m^2K/W$  resistivity can decrease peak air temperatures by at least 1°C and peak operative temperatures by at least 2°C for all tin sheet roof types. Alternatively, painting the walls white can decrease peak indoor ambient air temperatures by at least 1°C as illustrated in Figure 6-11. With white painted exterior walls, peak operative temperatures can decrease by as much as 2°C in a modified tin roof test chamber.

Furthermore, wall protection is necessary for optimizing the positive effects of a thermally passive roof design. Given a test chamber with no wall protection, the alternating radiant barrier system can decrease average peak operative temperatures by approximately 3°C when compared with the control single layer CGI roof. However, this improvement in operative temperatures can increase to 6°C with a  $R = 1m^2K/W$  exterior wall insulation (no white paint) and 4°C with white paint (no wall insulation) on the exterior surface.

### **Simulated Test Chambers with RCC Roofs**

Modifications on the RCC roof did not significantly impact the interior temperatures when compared to the impact of modifications on the tin roof. Though the RCC ceiling temperatures exceeded outdoor ambient temperatures, the maximum ceiling temperatures for the RCC roof were, on average, greater than 6°C cooler than peak

**Transient Temperatures for Simulated 2.4m Square CGI Roof Test Chambers**  
**Wall Insulation  $R = 1\text{m}^2\text{K/W}$ , Wall Absorptivity = 0.75**

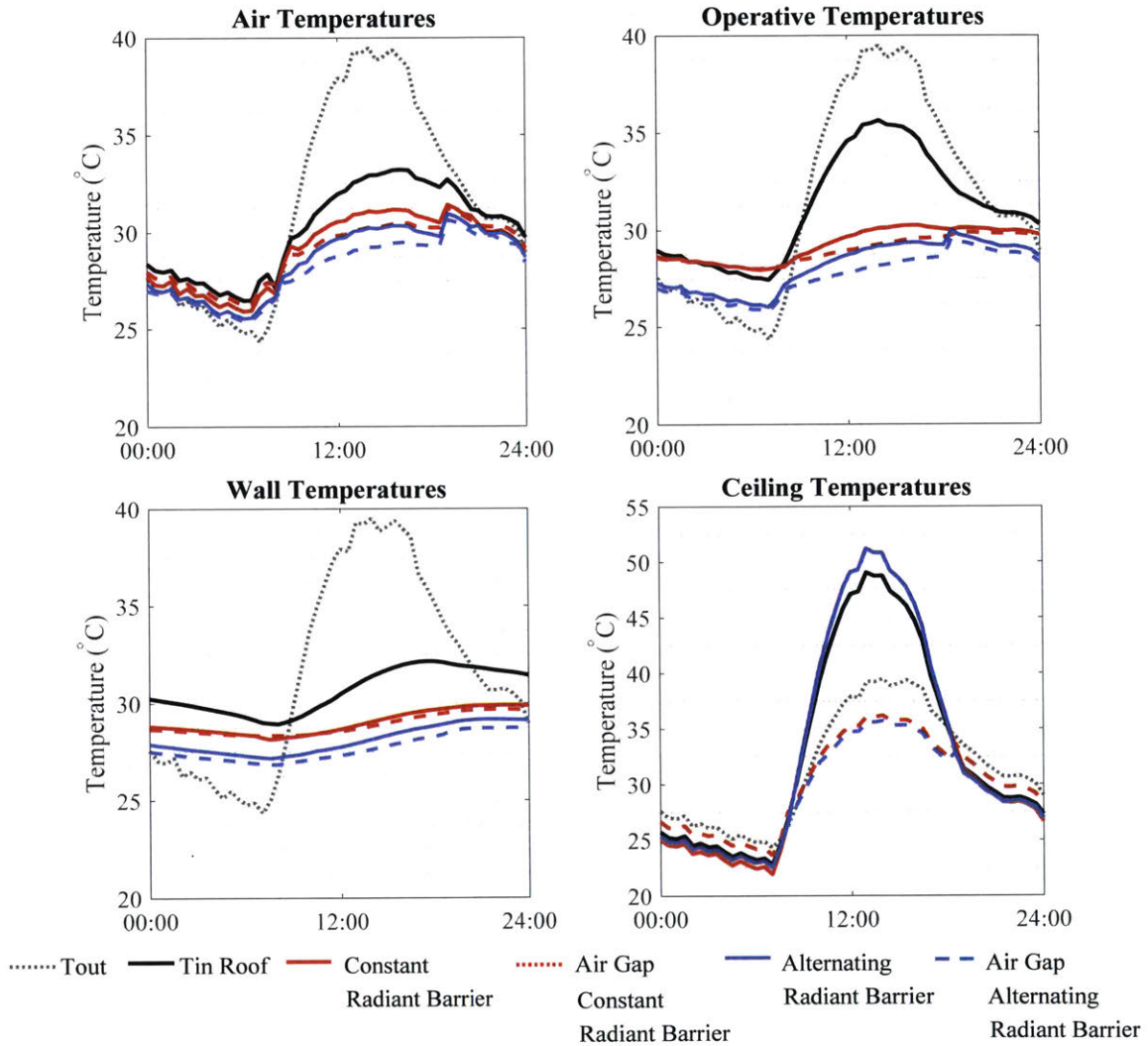
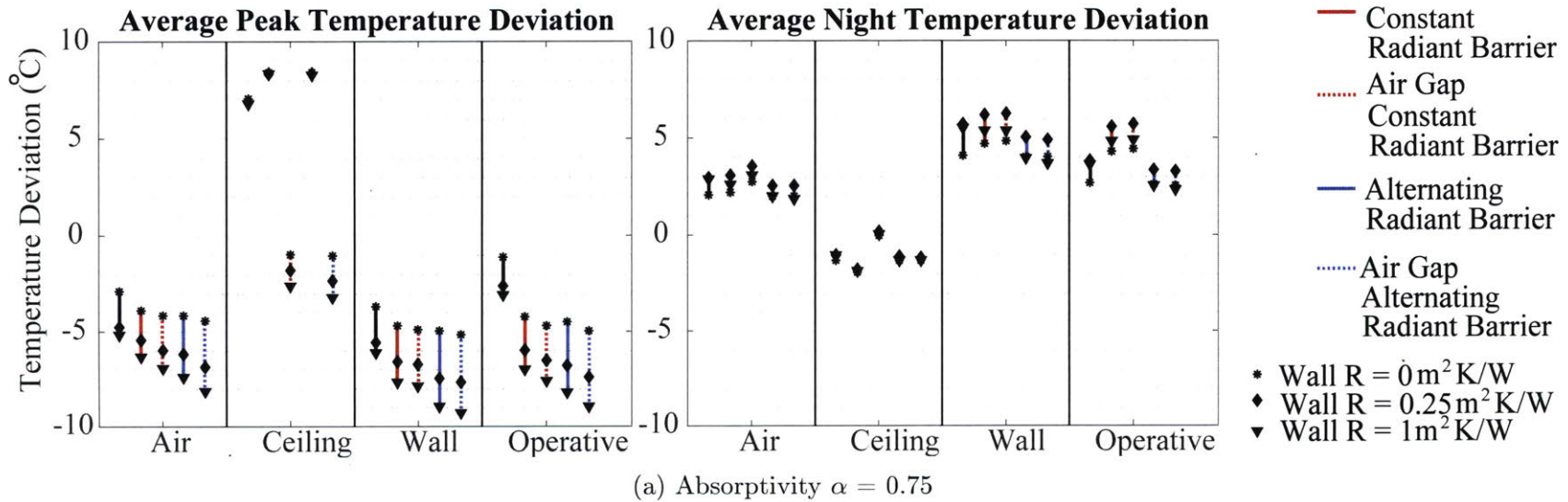


Figure 6-10: March Transient Interior Air, Operative, South Wall, and Ceiling Temperatures for a Control Single Layer Tin Roof and Modifications to the Tin Sheet Roof, Wall Insulation  $R = 1\text{m}^2\text{K/W}$  Wall Absorptivity = 0.75

Effects of Wall Insulation on Simulated 2.4m Square Test Chambers with Various CGI Roof Types



Effects of Wall Absorptivities on Simulated 2.4m Square Test Chambers with Various CGI Roof Types

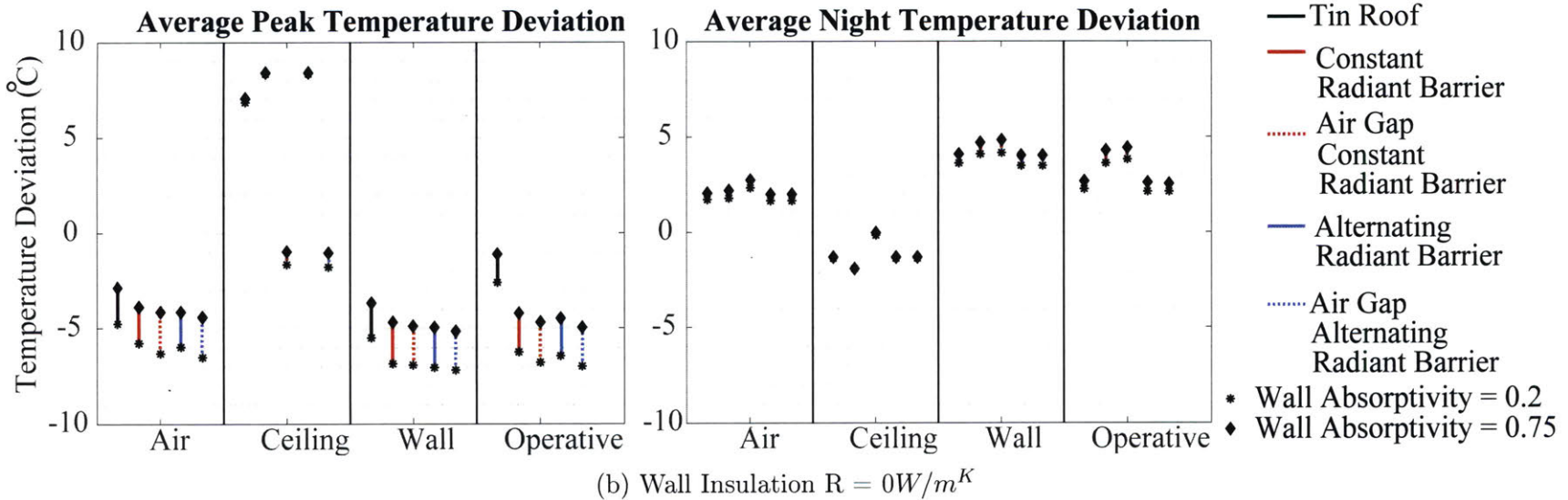


Figure 6-11: March Average Deviation from Nightly minimums and Daily Maximums of Simulated 2.4m by 2.4m by 2.4m Test Chambers with Various CGI Roof Types, Wall Insulation Resistivities, and Exterior Wall Absorptivities

CGI ceiling temperatures. Figure 6-12 shows the interior transient air, operative, south wall, and ceiling temperatures for test chamber with  $R = 1\text{ m}^2\text{K}/\text{W}$  insulated walls and various RCC roof geometries. All modifications (constant radiant barrier, constant radiant barrier with a ventilated air gap, alternating radiant barrier with a ventilated air gap) on the traditional RCC roof led to similar changes in interior air, south wall, and operative temperatures when compared to the untreated RCC slab. These modified RCC roof designs led to a  $1^\circ\text{C}$  decrease in peak air temperatures,  $1^\circ\text{C}$  decrease in peak interior south wall temperatures, and a  $1^\circ\text{C}$  decrease in peak operative temperatures. Based on these simulated results, an air gap or another type of ceiling insulation improves thermal comfort in a room with an RCC roof. Simulations indicate alternating radiant barrier systems do not dramatically improve thermal comfort when compared to constant air gap and radiant barrier systems.

As discussed earlier in Section 6.4.1, the success of a thermal autonomous design requires proper wall protection regardless of roof types. As shown in Figure 6-13, the addition of wall insulation with  $R = 0.25\text{ m}^2\text{K}/\text{W}$  resistivity can decrease peak air temperatures by at least  $1^\circ\text{C}$  and peak operative temperatures by at least  $1^\circ\text{C}$  for all tin sheet roof types. Alternatively, painting walls white can decrease peak indoor ambient air temperatures by at least  $1^\circ\text{C}$  as illustrated in Figure 6-13. With white painted exterior walls, peak operative temperatures can decrease by as much as  $2^\circ\text{C}$  in a modified tin roof test chamber. In the case of 2.4m by 2.4m by 2.4m rooms with RCC roofs, wall treatment predominantly affects thermal comfort and leads to greater decreases in interior air, operative, and wall temperatures.

#### **6.4.2 Simulation Results: 5m by 5m by 2.4m Rooms**

Simulations with the room size set to 5m by 5m predict wall and roof design effects in rooms with a greater wall to ceiling ratio. In these simulations the wall to ceiling ratio is nearly 2:1, instead of the 4:1 found in the test chambers.

**Transient Temperatures for Simulated 2.4m Square RCC Roof Test Chambers**  
**Wall Insulation  $R = 1\text{m}^2\text{K/W}$ , Wall Absorptivity = 0.75**

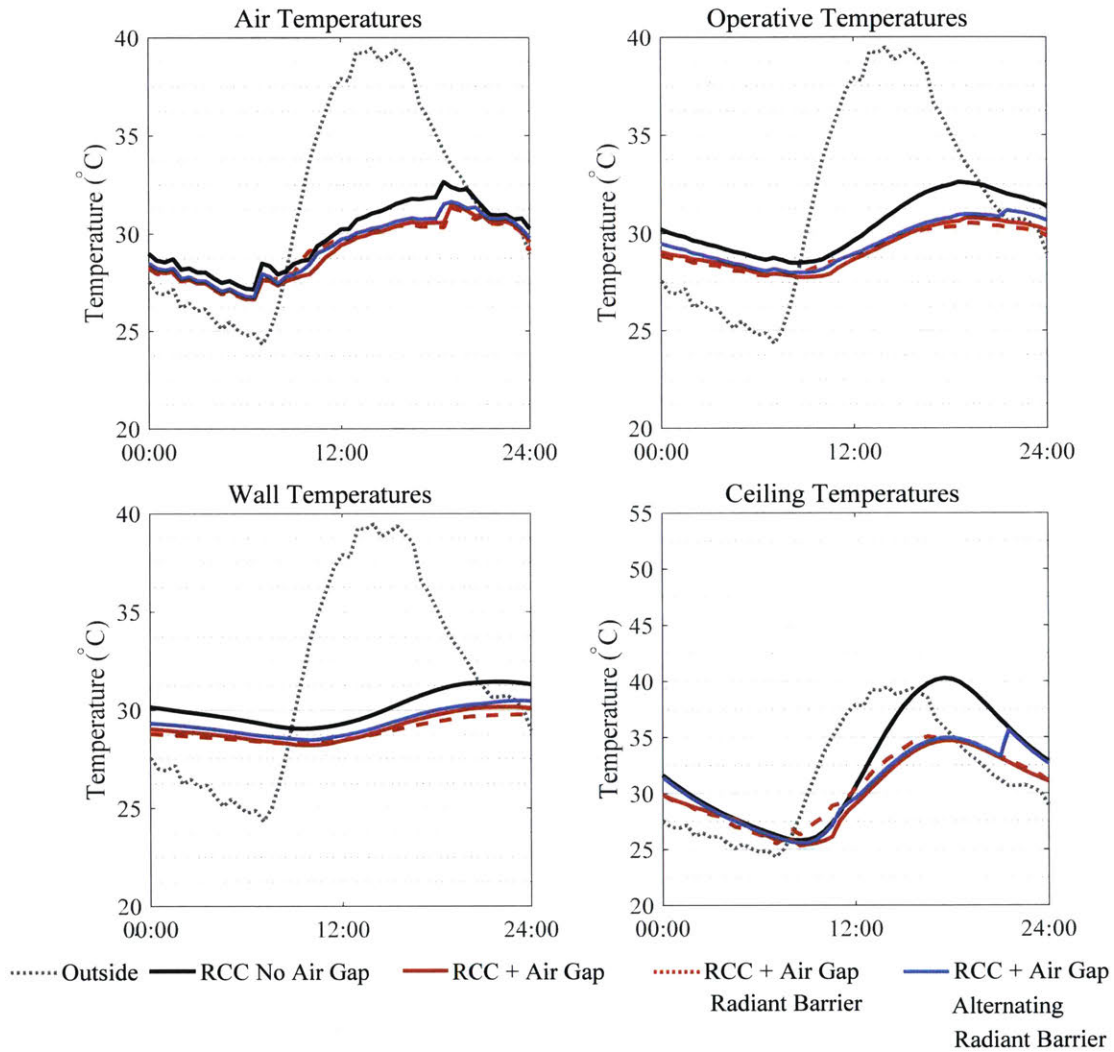
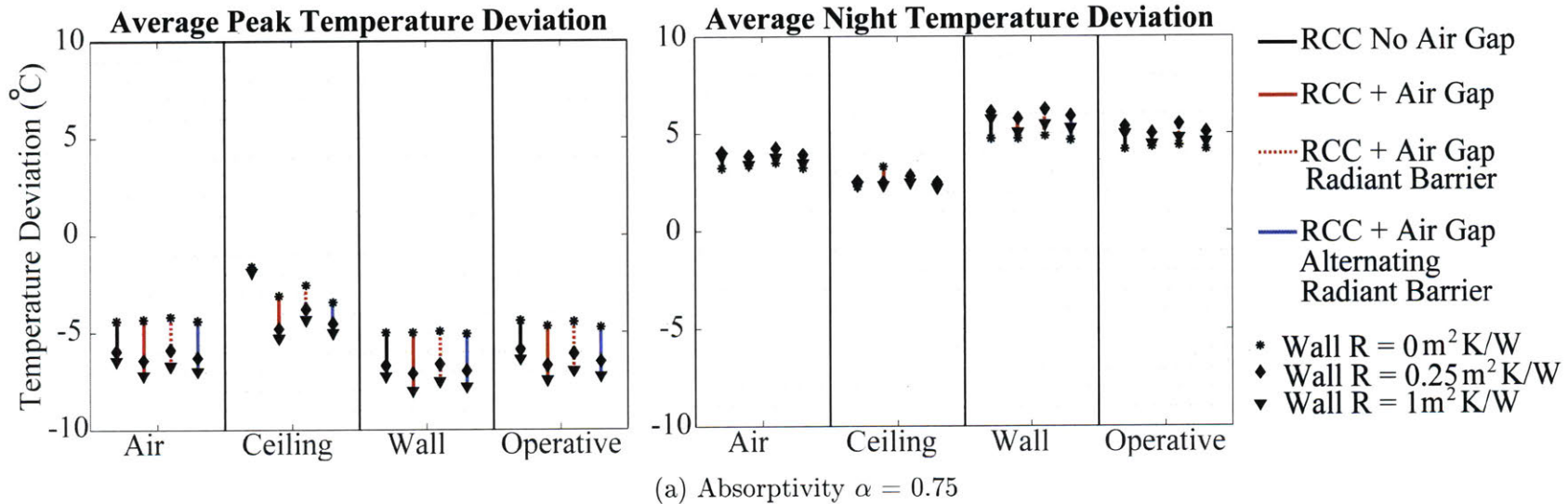


Figure 6-12: March Transient Interior Air, Operative, South Wall, and Ceiling Temperatures for a Control RCC and Modifications to the RCC Sheet Roof, Wall Insulation  $R = 1\text{m}^2\text{K/W}$ , Wall Absorptivity = 0.75

**Effects of Wall Insulation on Simulated 2.4m Square Test Chambers with Various RCC Roof Types**



**Effects of Wall Absorptivities on Simulated 2.4m Square Test Chambers with Various RCC Roof Types**

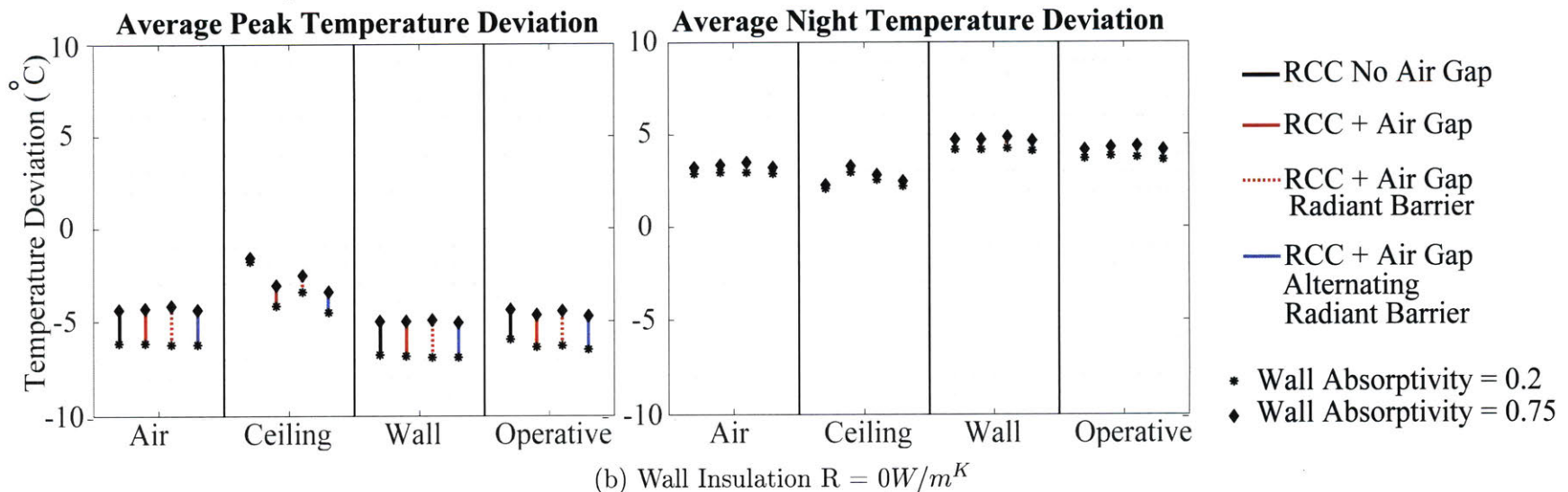


Figure 6-13: March Average Deviation from Nightly minimums and Daily Maximums of Simulated 2.4m by 2.4m by 2.4m Test Chambers with Various RCC Roof Types, Wall Insulation Resistivities, and Exterior Wall Absorptivities

## Simulated Test Chambers with CGI Roofs

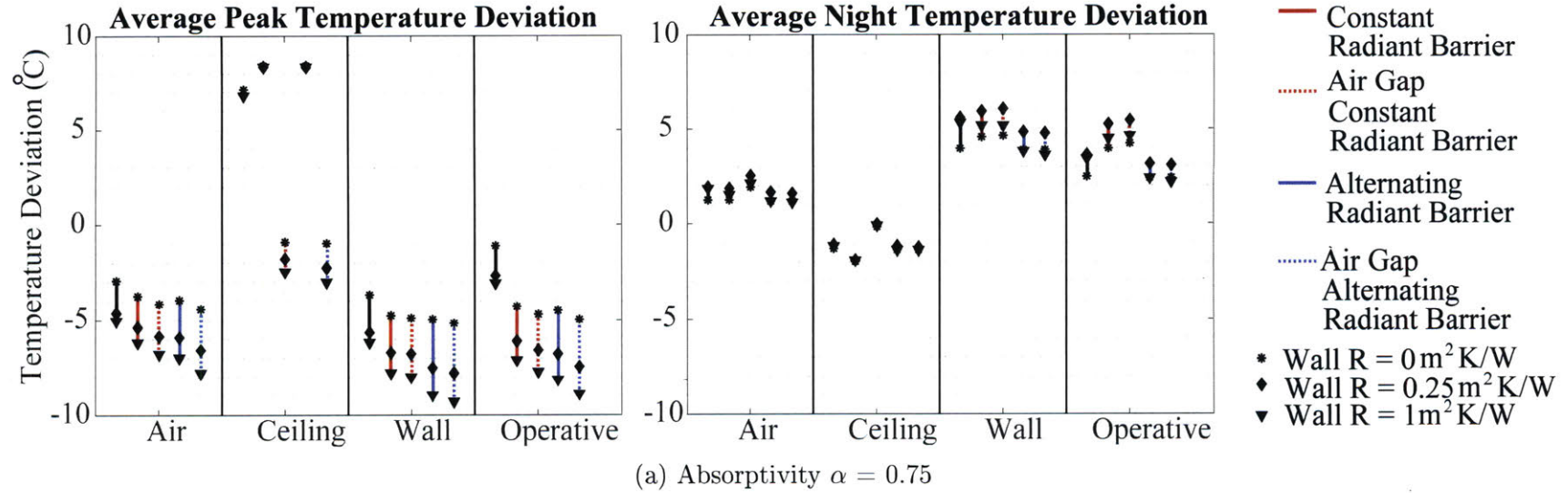
Despite a different wall-to-roof ratio, the success of a thermal autonomous design continues to require proper wall protection regardless of the roof type. As shown in Figure 6-14, the addition of wall insulation with  $R = 0.25m^2K/W$  resistivity can decrease peak air temperatures by at least  $1^\circ\text{C}$  and peak operative temperatures by at least  $1^\circ\text{C}$  for all tin sheet roof types. Alternatively, painting walls white can decrease peak indoor ambient air temperatures by at least  $1^\circ\text{C}$  as illustrated in Figure 6-14. With white painted exterior walls, peak operative temperatures can decrease by as much as  $2^\circ\text{C}$  in a modified tin roof test chamber.

Additionally, the positive effects of passive roof design is maximized in simulated rooms with wall protection. Given a test chamber with no wall protection, the alternating radiant barrier system can decrease average peak operative temperatures by approximately  $3^\circ\text{C}$  when compared with the control single layer CGI roof. However this improvement in operative temperatures can increase to  $4^\circ\text{C}$  with exterior white paint (uninsulated) and  $6^\circ\text{C}$  with  $R = 1m^2K/W$  exterior wall insulation (no white paint).

## Simulated Test Chambers with RCC Roofs

Figure 6-15 shows that  $R = 0.25m^2K/W$  wall insulation in rooms with RCC roofs can decrease peak air temperatures by at least  $1^\circ\text{C}$  and peak operative temperatures by at least  $1^\circ\text{C}$  for all RCC roof types. Alternatively, painting wall exteriors white can decrease peak indoor ambient air temperatures by at least  $1^\circ\text{C}$  as illustrated in Figure 6-15. With white painted exterior walls, peak operative temperatures can decrease by as much as  $2^\circ\text{C}$  in a test chamber with a modified RCC roof. In the case of 5m by 5m by 2.4m rooms with RCC roofs, wall treatment predominantly affects thermal comfort and can lead to an even greater decrease in interior air, operative, and wall temperatures.

**Effects of Wall Insulation on Simulated 5m Square Test Chambers with Various CGI Roof Types**



**Effects of Wall Absorptivities on Simulated 5m Square Test Chambers with Various CGI Roof Types**

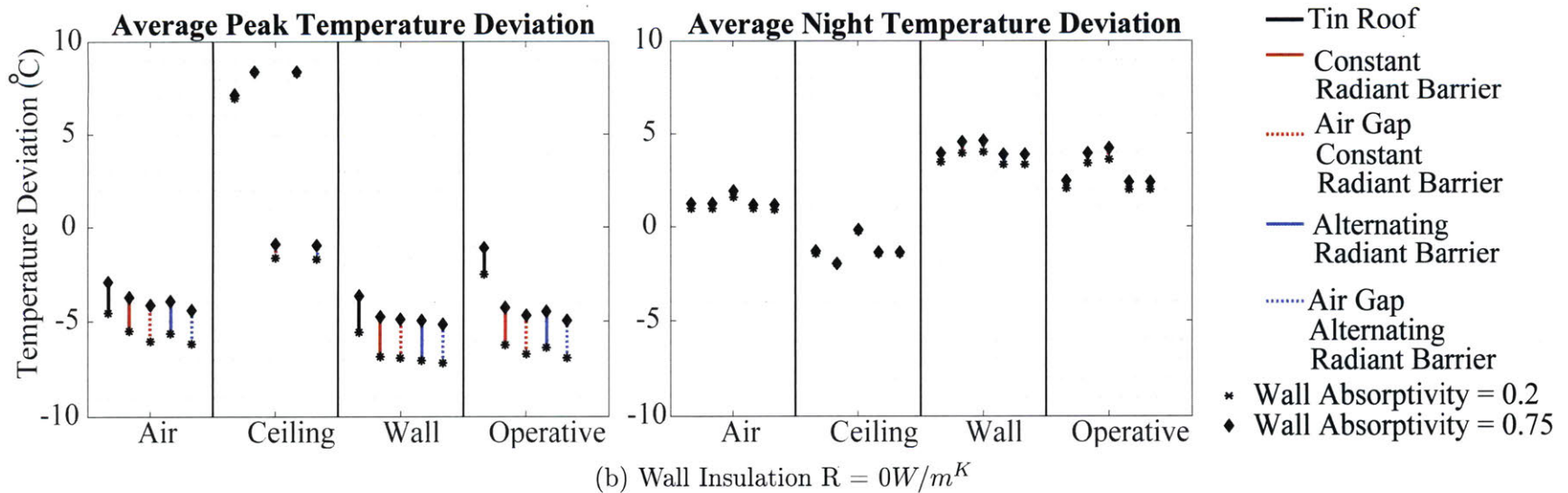
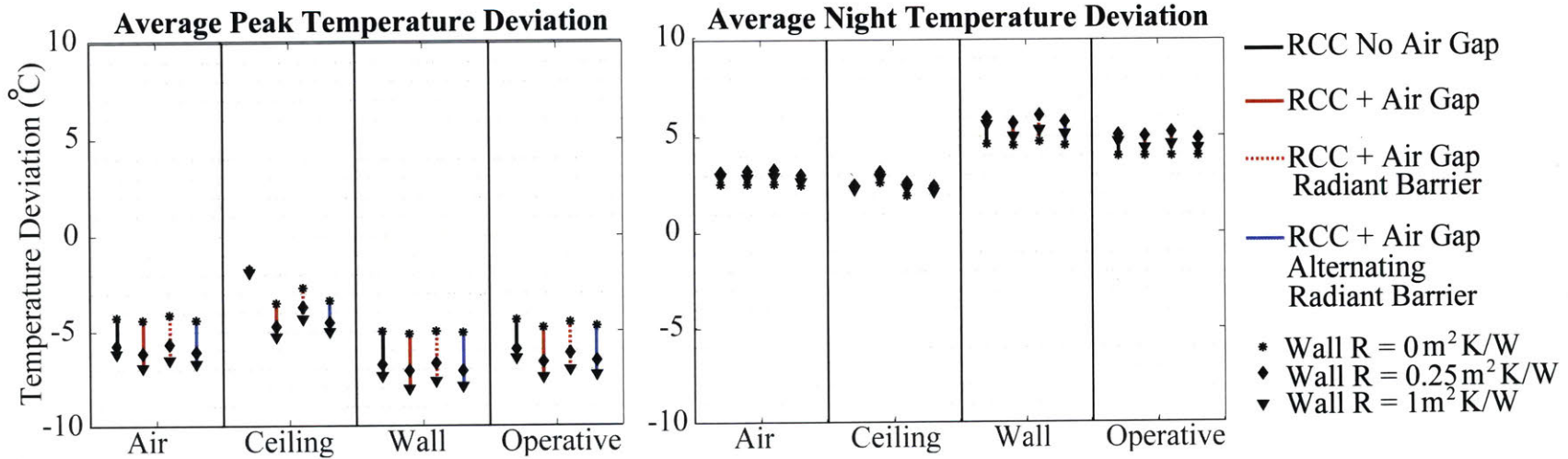


Figure 6-14: March Average Deviation from Nightly minimums and Daily Maximums of Simulated 5m by 5m by 2.4 m Test Chambers with Various CGI Roof Types, Wall Insulation Resistivities, and Exterior Wall Absorptivities

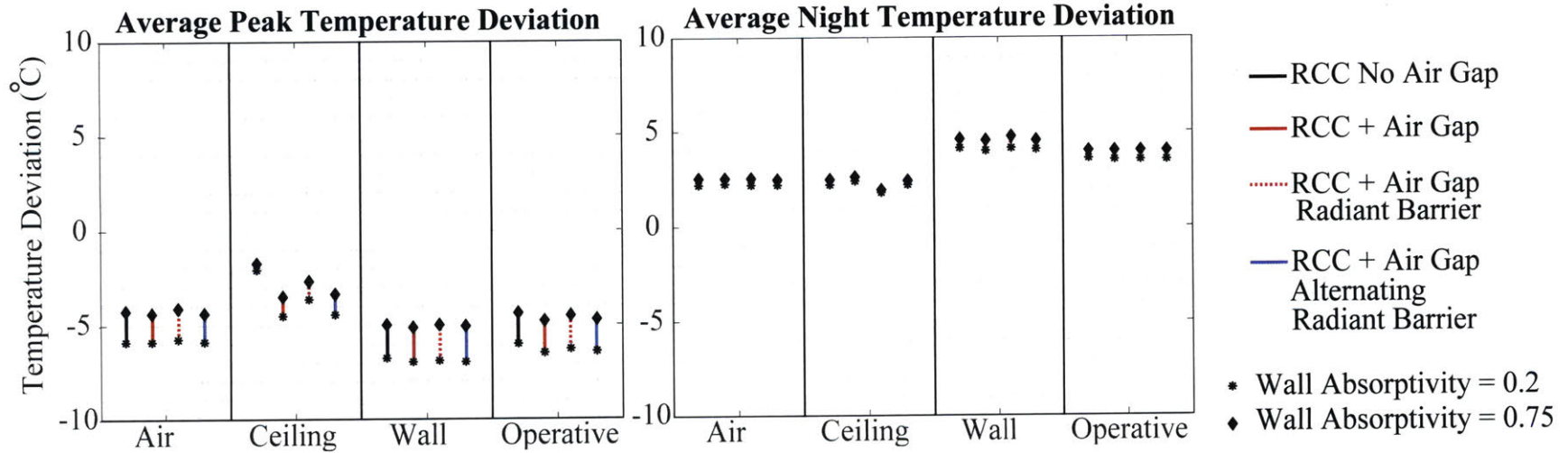


**Effects of Wall Insulation on Simulated 5m Square Test Chambers with Various RCC Roof Types**



(a) Absorptivity  $\alpha = 0.75$

**Effects of Wall Absorptivities on Simulated 5m Square Test Chambers with Various RCC Roof Types**



(b) Wall Insulation  $R = 0 \text{ W/m}^K$

Figure 6-15: March Average Deviation from Nightly minimums and Daily Maximums of Simulated 5m by 5m by 2.4 m Test Chambers with Various RCC Roof Types, Wall Insulation Resistivities, and Exterior Wall Absorptivities

### 6.4.3 Designs Considering Bhuj Winter Conditions

Though temperatures on most days throughout the year in Bhuj exceed the Universal Thermal Climate Index's definition of heat stress, residents still need some measure of passive heating during the winter. From conversations during field visits, residents have stated, during some winter nights, where temperatures drop below 20°C, the indoor temperatures can be uncomfortably cold. Simulations were run assuming Bhuj February exterior climate conditions to determine optimal thermal passive designs given winter conditions. In the February simulations, test chambers dimensions are 5m by 5m by 2.4m height with uninsulated ( $R = 0m^2K/W$ ) and unpainted walls (exterior absorptivity = 0.75). No ventilation is practiced and the air change rate is assumed to be a constant 1 roomful per hour. Based on results from simulations, it is recommended to place an air gap or low emissivity surface during the night. Figure 6-17 and 6-16 show transient indoor air, south wall, ceiling, and operative temperatures during February for a rooms with RCC based roof and CGI based roofs.

Low emissivity ceiling surfaces help keep operative temperatures at least 1°C warmer during the night in a 5m by 5m room with a tin sheet roof. In rooms with an RCC slab roof, a low emissivity surface with an air gap can raise minimum operative temperatures by 1°C. Average interior temperature deviations from daily maximums and nightly minimums are shown in Figures 6-18 and 6-19. Given a test chamber with a CGI roof, the constant radiant barrier roof types increase operative temperatures during the night by >1°C and indoor air temperatures by 0.9°C. In the RCC Roof, a low emissivity surface can help keep operative temperatures warmer at night as shown in Figure 6-17, where the minimum operative temperature for a RCC roof with air gap and radiant barrier is 1°C warmer than an RCC roof with no air gap or radiant barrier. However, in other hours of the night, the operative temperatures are warmer with the control RCC roof. This is due to the RCC roof storing the solar heat gains from the day and slowly releasing the heat throughout the night. Due to the phase lag of the RCC roof, it is recommended to place a radiant barrier 2.5 hours after minimum nightly temperatures to improve night time operative temperatures.

**Transient Temperatures for Simulated 5m Square CGI Roof Test Chambers:  
Wall Insulation  $R = 0m^2K/W$ , Wall Absorptivity = 0.75**

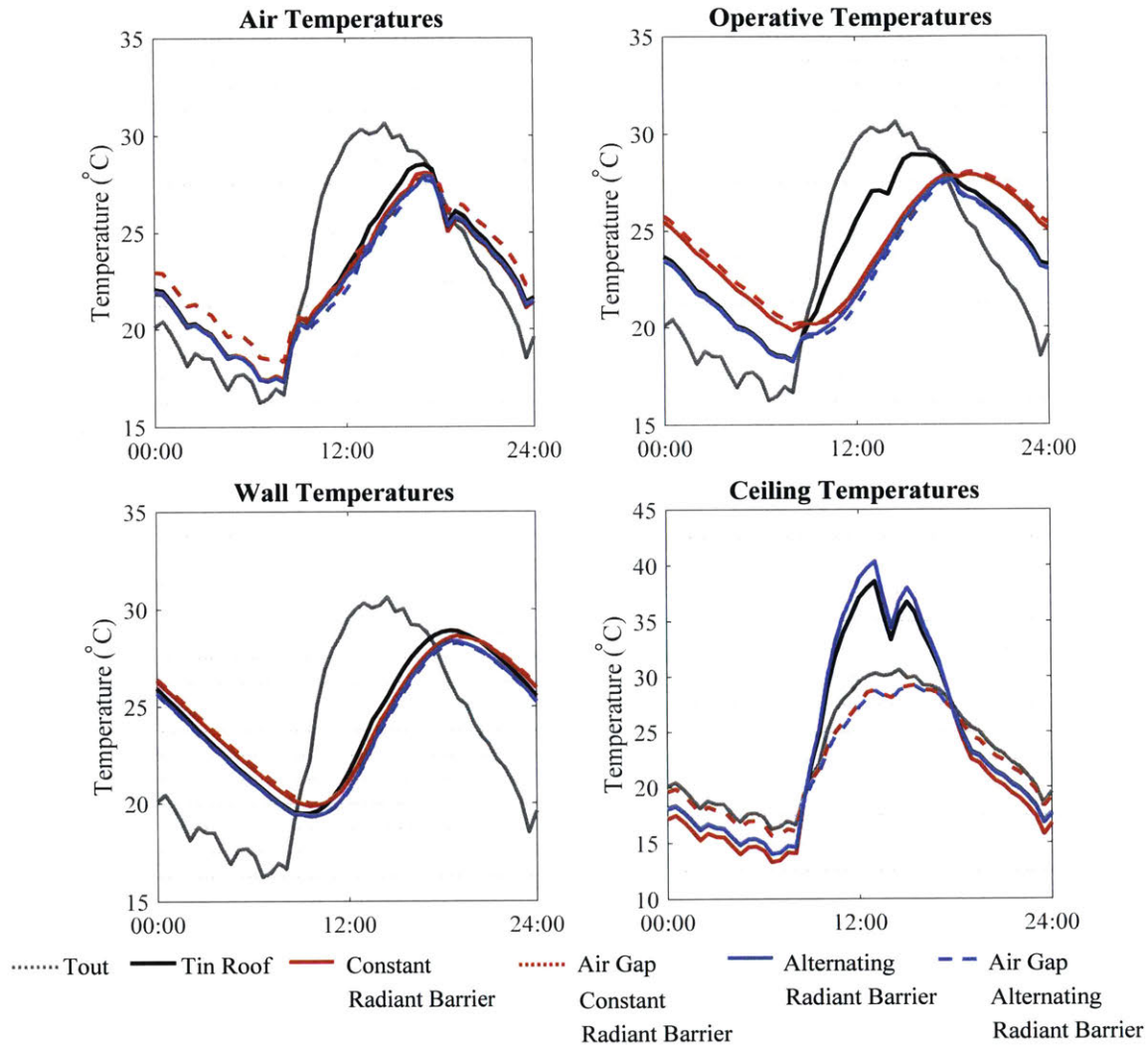


Figure 6-16: February Transient Interior Air, Operative, South Wall, and Ceiling Temperatures for a Control Single Layer Tin Roof and Modifications to the Single Layer Tin Roof, Wall Insulation  $R = 0m^2K/W$ , Wall Absorptivity = 0.75

**Transient Temperatures for Simulated 5m Square RCC Roof Test Chambers**  
**Wall Insulation  $R = 1\text{m}^2\text{K/W}$ , Wall Absorptivity = 0.75**

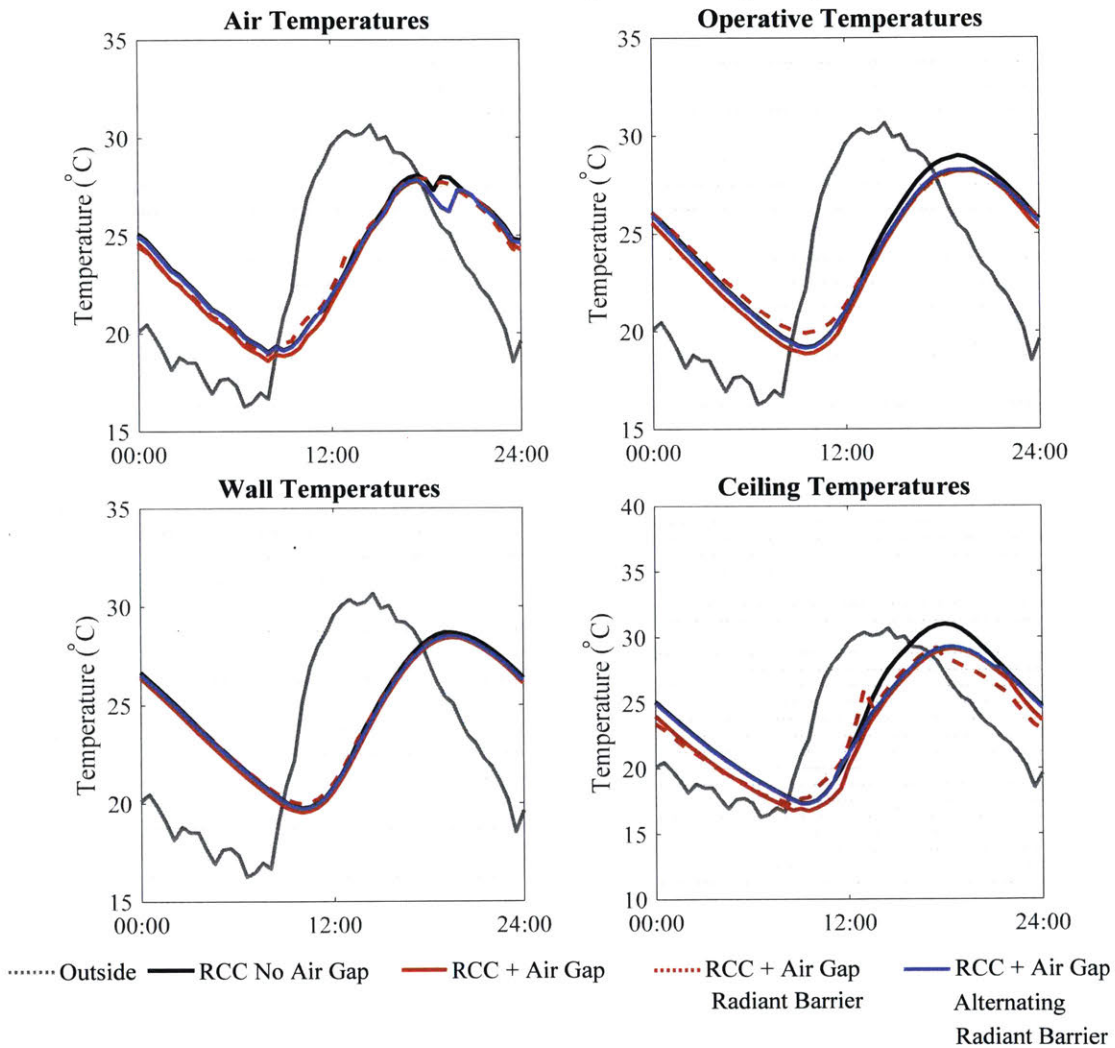


Figure 6-17: February Transient Interior Air, Operative, South Wall, and Ceiling Temperatures for a Control RCC Slab Roof and Modifications to the RCC Slab Roof, Wall Insulation  $R = 0\text{m}^2\text{K/W}$ , Wall Absorptivity = 0.75

**5m Square Test Chamber, Tin Roof, Wall Insulation  $R = 0m^2K/W$ , Wall Absorptivity = 0.75**  
**February Average Daily Peak and Nightly Minimum Temperature Deviation**

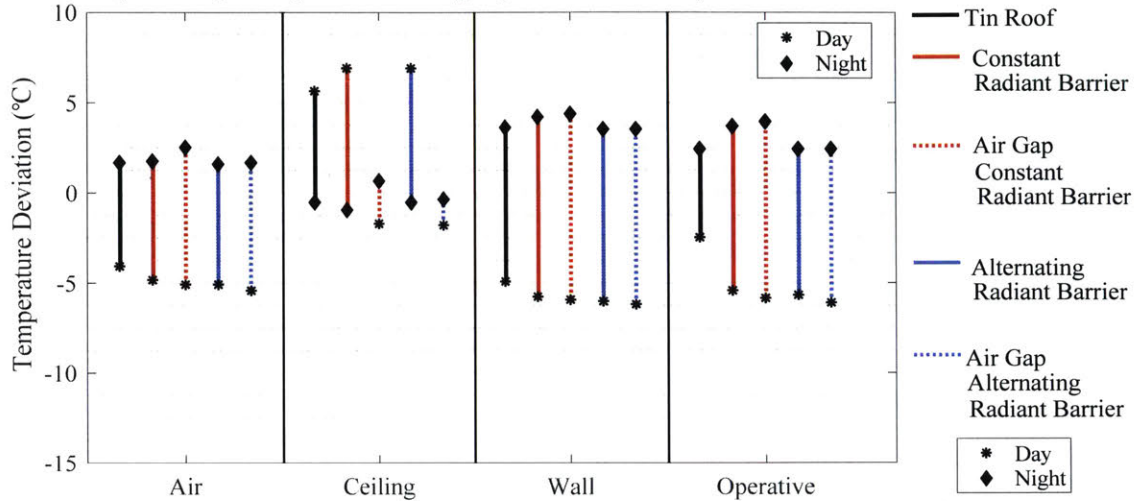


Figure 6-18: February Average Interior Temperature Deviations from Daily Peaks and Nightly Minimums for 5m by 5m by 2.4m Rooms with Various CGI Roof Types, Wall Insulation  $R = 0m^2K/W$ , Wall Absorptivity = 0.75

**5m Square Test Chamber, RCC Roof, Wall Insulation  $R = 0m^2K/W$ , Wall Absorptivity = 0.75**  
**February Average Daily Peak and Nightly Minimum Temperature Deviation**

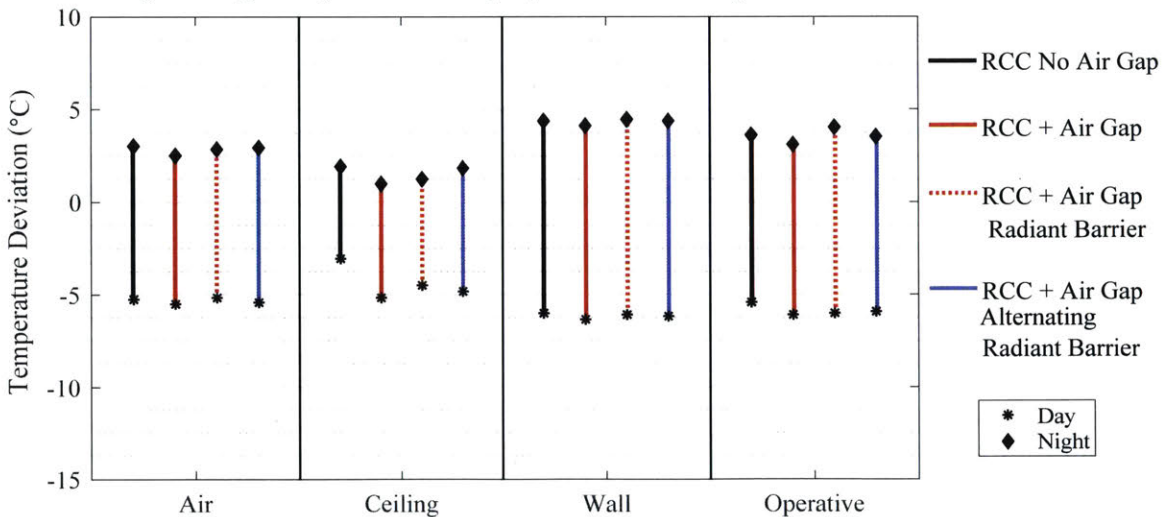


Figure 6-19: February Average Interior Temperature Deviations from Daily Peaks and Nightly Minimums for 5m by 5m by 2.4m Rooms with Various RCC Roof Types, Wall Insulation  $R = 0m^2K/W$ , Wall Absorptivity = 0.75

## 6.5 Recommendations

Based on results from simulations of varying roof types and wall protection techniques, the following conclusions regarding thermal passive design can be made.

- In order to achieve thermal autonomy in the hot arid climates of Bhuj, rooms with a 4:1 and 2:1 wall-to-roof ratio all require some level of wall protection regardless of roof type. By adding  $R = 0.25m^2K/W$  insulation or painting walls white, the peak indoor air and operative temperatures decrease by at least  $1^\circ\text{C}$ . Additionally, the effective performance of thermally passive roofs depends on minimizing heat stresses through the walls.
- The high conductivity of the CGI sheet causes the interior building environment to be vulnerable to solar heat gains. As a result, tin roofs require a low emissivity radiant barrier ceiling in order to reduce radiant heat transfer from the hot ceiling to interior building surfaces and the occupant. With this modification, operative temperatures decrease by at least  $5^\circ\text{C}$ . An alternating radiant air gap roof can further lower peak operative temperatures by  $2^\circ\text{C}$  if walls are well-insulated,  $R > 0.5m^2K/W$ .
- During the winter season, it is recommended to place a low emissivity surface on the CGI sheet roof at night to increase operative temperatures by  $>1^\circ\text{C}$ . For the RCC roof, a low emissivity surface should be installed 2.5 hours after the nightly minimum exterior temperatures and removed 2.5 hours after the daily maximum exterior temperatures in order to increase operative temperatures by  $1^\circ\text{C}$ .
- In rooms with an RCC roof, a constant air gap or some other form of insulation provides similar reductions in peak operative temperatures as an alternating radiant barrier system.

# Chapter 7

## Effects of Ceiling Fans on Thermal Comfort

### 7.1 Ceiling Fans

In hot climates, residents often use ceiling fans as a low energy means to improve thermal comfort and to mitigate risks that come with extreme heat. Previous studies conclude that air movement positively correlates with thermal comfort by enhancing the human body's natural heat releasing means of evaporative cooling and convective heat transfer. However, in the context of many developing world homes, this approach may be sub-optimal.

Many informal settlements found in resource-constrained communities use tin sheet roofs that easily become greater than 10°C warmer than the ambient outdoor temperatures. As the tin sheet ceiling transfers heat to the air directly underneath the ceiling, the ceiling fan circulates this hot air throughout the living space and increases the temperature at lower levels of the room surrounding the occupants. This chapter discusses the effects of ceiling fans on thermal comfort in low-income housing. Through field experiments, Computational Fluid Dynamics (CFD) simulations, and data analysis, the team examined the effects of ceiling fans in homes with various different roof types located in hot climates.

These recommendations on proper ceiling fan usage, applicable in Bhuj and world-

wide, were proposed based on experimental and analytic results.

## 7.2 Ceiling Fan Case Study in Bhuj

Site visits to the city of Bhuj, India, revealed that many residents often use tin sheets, cloth, or asbestos cement as a roofing material. Occupants frequently use a ceiling fan to provide some relief from the heat, as shown in Figure 7-1.



Figure 7-1: Informal Home with a Multilayer Tarpaulin, Cloth Roof and Ceiling Fan

Due to the ceiling's lack of protection from solar heat gains impacting the roof,



temperatures surrounding the ceiling can be significantly greater than the outside ambient temperature by as much as 22°C. This is further illustrated by the temperature map of the air surrounding the ceiling and the outside temperature in Figure 7-1.

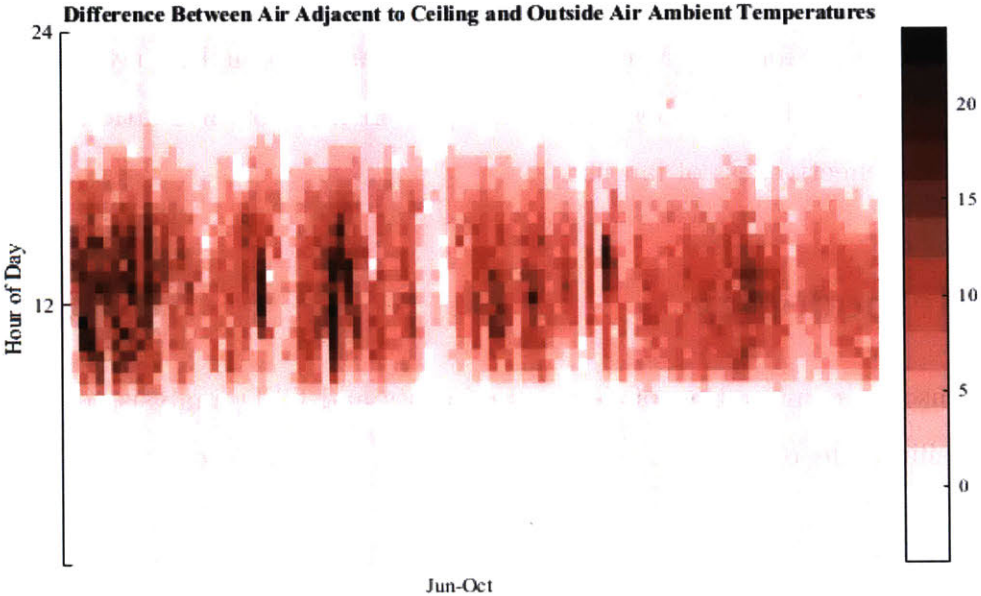


Figure 7-2: Temperature Map of the Temperature Difference Between the Outside and the Air Adjacent to the Ceiling

The majority of the families with the means to construct more substantial roofs choose to build a reinforced concrete cement (RCC) roof (Rupesh Hurmade and Tejas Kotak, 2016). These RCC roofs offer slightly more immediate protection from solar heat gains by delaying the effects of solar heat gains to later in the day with RCC’s high thermal mass properties. Additionally, thermally massive roofing also stays warmer at night. With sustained high-temperature weather, the RCC roof ceiling temperatures can still exceed the outside ambient temperatures due to the high thermal conductivity of the RCC.

The following research seeks to quantify the effects of ceiling fan use in rooms where ceiling temperatures exceed indoor air temperatures by more than 10°C. The team will assess the effects of ceiling fan usage during the dry season as well as during the monsoon season when high humidity levels reduce the thermal comfort benefits

of air movement. In addition, this research will look at the effects of ceiling fan use in two housing archetypes. The first archetype is a dwelling with sandstone walls and an RCC roof. The second archetype is a dwelling with sandstone walls and a 30°C peaked roof composed of tin sheets. Both homes are being constructed in Bhuj, India as part of a national government program to reduce the population of slum households, Housing for All (Ministry of Housing and Urban Poverty Alleviation, 2015). Using the results, roof design and fan placement recommendations are made to enhance the effectiveness of fan use.

## 7.3 Methodology

The team used a combination of field experiments and CFD analysis to study the effects of ceiling fans on thermal comfort and indoor temperatures.

### 7.3.1 Field Experiment Parameters

Two 2.4m by 2.4m by 2.4m test structures with 0.23m thick sandstone walls were used to study the temperature and thermal comfort effects of ceiling fans. Each test chamber was fitted with a different roof construction. One test chamber was constructed with a 0.5mm thick CGI sheet that is commonly found in informal settlements as shown in Figure 7-3 and Figure 7-4.

The temperatures of the single layer tin sheet can easily reach above 50°C. A ceiling fan was placed in the center of the ceiling and 0.20m below it. The fan diameter was 0.60m and the average air velocity immediately below the fan was 2.8-3.0m/s. Without the fan, the room's air will stratify with the hottest adjacent to the ceiling. At lower sections of the room, near the occupants, the air will be somewhat cooler. Air movement caused by the ceiling fan disrupts the stratification of the air, mixing the warmer air directly underneath the ceiling with the air at lower levels. In addition, the fan increases the convective heat transfer from the ceiling to the room.

Unrelated to the project, a barrier wall (Figure 7-4) for security was constructed around the test chamber with the single layer roof at most 60cm offset from the north

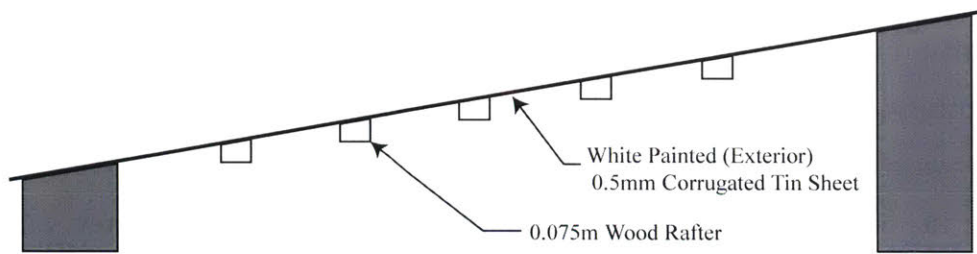


Figure 7-3: Single Layer Corrugated CGI Roof



Figure 7-4: Exterior View of Test Chamber with Single Layer Roof (Photo Courtesy of John Kongoletos)

and the west walls. While this may affect the absolute temperatures of the test chamber, relative differences between the fan-on and fan-off effects are still informative.

The other test chamber had a double layer CGI sheet roof that allows air circulation between the layers as shown in Figure 7-5 and Figure 7-6. A ceiling fan was placed in the center of the ceiling and 0.20m below it. The fan diameter was 0.60m and the average air velocity immediately below the fan was 2.8-3.0  $m/s$ . The ceiling temperatures of the double layer roof are more comparable to indoor temperatures.

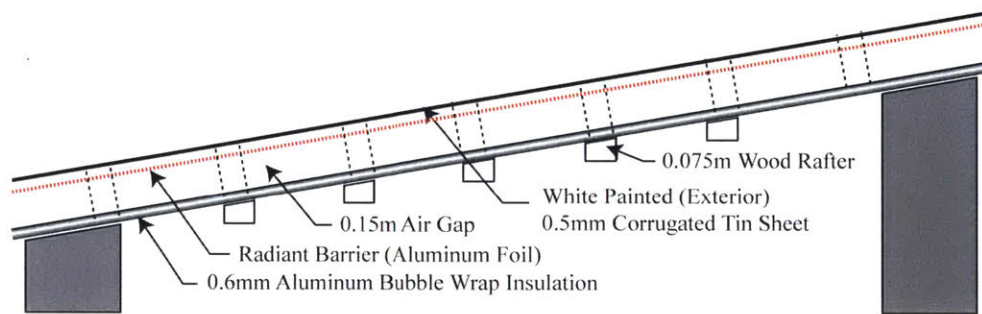


Figure 7-5: Double Layer Roof with Air Gap, Radiant Barrier, and Bubble Wrap Insulation



Figure 7-6: Exterior View of Test Chamber with Double Layer Roof (Photo Courtesy of John Kongoletos)

In both test chambers, onset HOBOTM Pro v2 sensors were placed to measure wall,

ceiling, roof air gap (if applicable), and stratified ambient temperatures at 1.75m and 0.75m from the floor in 30-minute increments as shown in Figure 7-7 and Figure 7-8. The mean radiant temperature was measured using a black painted 15.24cm (6inch) diameter copper sphere. A HOBO® Pro v2 sensor was then centrally placed inside the sphere.

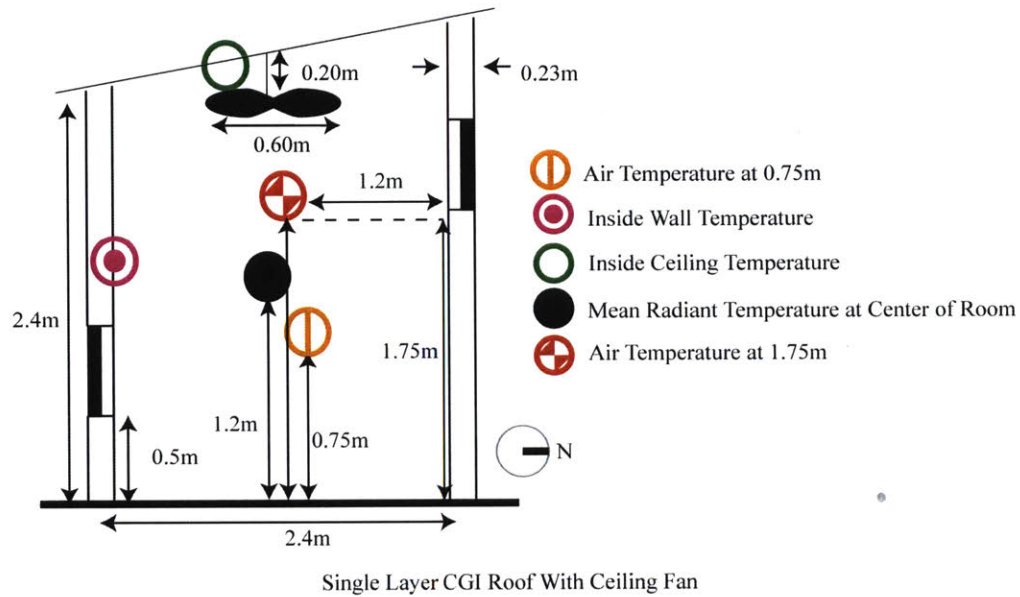


Figure 7-7: Sensor Placements for Test Chamber with a Single Layer Roof

Throughout the period of June 2016 to December 2016, the fans in each room operated on a two-day rotation (two days on/two days off). During the fan-on periods, fans operated continuously throughout the 48-hour time span. Periods with the same environmental conditions (outside ambient temperatures and solar heat flux) were compared to control for differences in external conditions across the fan off and fan on periods. The difference between the average outside peak temperatures for both the 65 days of fan-off and 65 days of fan-on periods was  $0.49^{\circ}\text{C}$ . The difference between the average solar heat flux for both the 65 days of fan on and 65 days of fan off periods was  $18\text{W}/\text{m}^2$ . During the data collection period, night flush ventilation was employed in both chambers. In a given 24-hour period, test chamber windows were closed from 7:00am to 7:00pm and opened 7:00pm to 7:00am. In addition to continually measuring

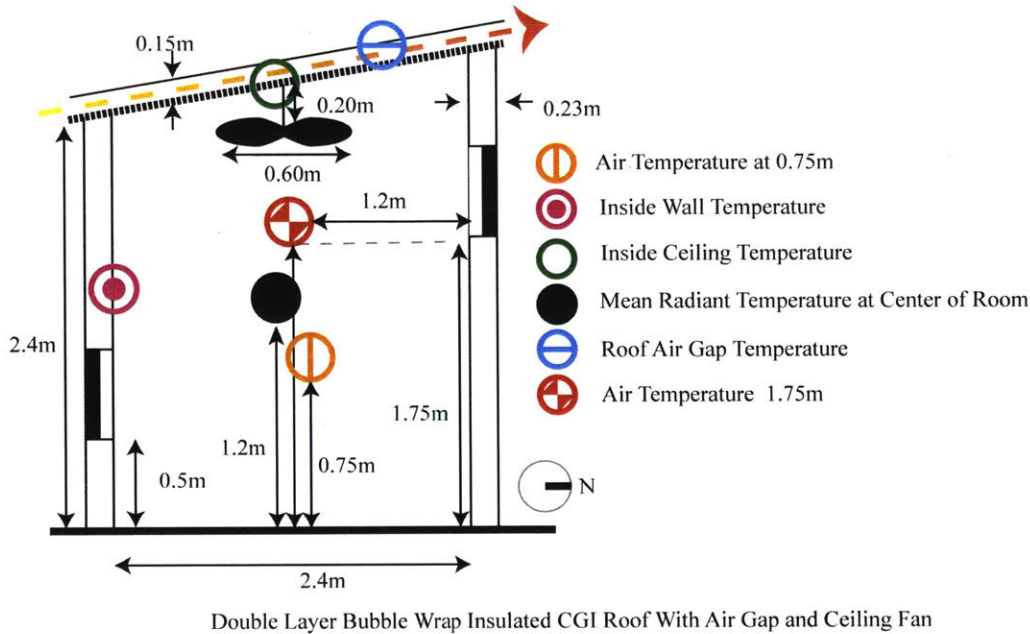


Figure 7-8: Sensor Placements for Test Chamber with a Double Layer Roof

test chamber temperatures, airspeeds under the fan were spot-measured with a using a Venier ANM-BTA Anemometer.

### 7.3.2 Simulation Parameters

ANSYS Fluent 17.2 was used to study the effects of ceiling fans on indoor air temperature distributions and velocity streamlines (Ansys Inc., 2016). The first set of simulations were used to calibrate and compare the simulation results with fieldwork results. Following calibration, simulations were used to investigate ways to mitigate the mixing of the hot air within the structure as well as to observe the effects of ceiling fans in a standard single story and double story home archetype found in Bhuj.

#### Simulation Boundary Conditions and Setup

A steady state analysis was used to study the indoor air within both the simulated test chamber and the simulated Housing for All home during the time of day when ceiling temperatures peak. In these simulations, the team assumed that windows remain closed during the day.

A pressure-based, upwind numerical scheme solver was applied and a turbulent viscous case was assumed using the RNG  $k-\epsilon$  model. The near-wall regions were meshed using very fine elements ( $y^+ \leq 5$ ), as required by the "enhanced wall treatment" used in this simulation. The surface-to-surface model was used to predict radiation. The maximum mesh size throughout the test chamber was  $8 \times 10^{-3}m$ . Three sets of boundary condition design parameters were used for the test chamber and Housing for All simulations. One set of input parameters represents the boundary conditions for a room with a single layer tin roof that is common among many low-income dwellings. The second set of input parameters represent the boundary conditions for a room with an RCC roof that is often constructed by families that can afford a more substantial roof. The third set of input parameters represents the boundary conditions for a room with a double layer insulated roof, a new roof design meant to protect against solar heat gains. The wall, ceiling, and floor boundary conditions were modeled as constant temperature surfaces. These boundary condition temperatures for the walls, floor, and ceiling for the rooms with a single layer tin roof are shown in Table 7.1. These temperatures were derived from collected test chamber temperature data during the hour in which ceiling temperatures peak as shown in Figure 7-9.

Table 7.1: Boundary Conditions for a Room with a Single Layer Roof

Element	Boundary Type	Condition
Test Chamber Walls	Wall	305K (31.85°C)
Test Chamber Ceiling	Wall	324K (50.85°C)
Test Chamber Floor	Wall	305K (31.85°C)

Table 7.2 shows the boundary conditions for the RCC roof. These temperatures were derived from collected temperature data during 15:00, the hour when ceiling temperatures peak as shown in Figure 7-10. For simulated rooms with an RCC roof, the wall temperature boundary conditions increase from 31.85°C to 34.85°C as a result of peak ceiling temperatures aligning more closely with peak temperatures of the thermally massive sandstone walls.

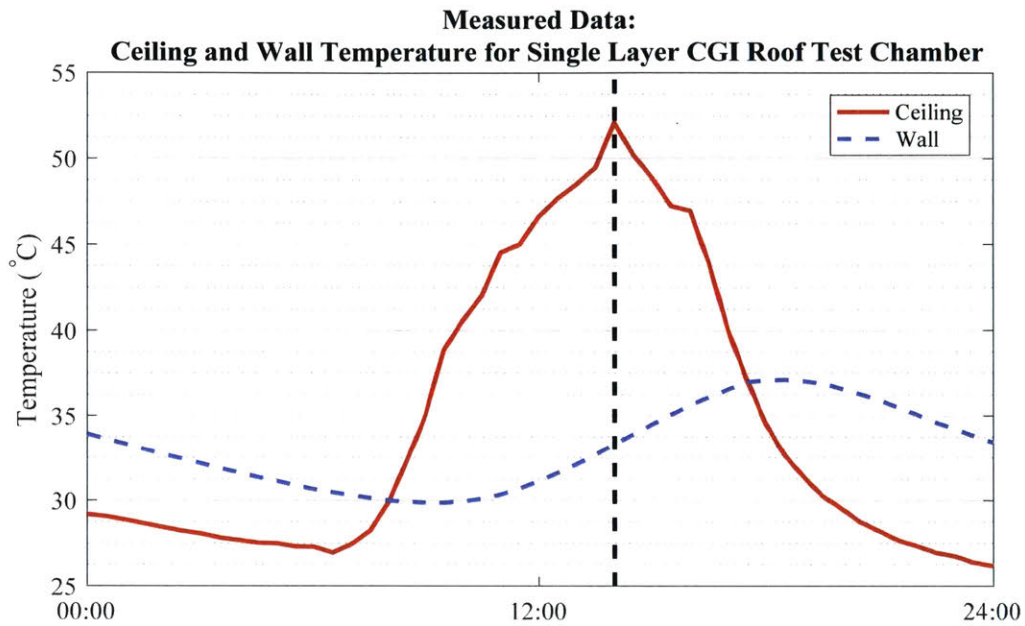


Figure 7-9: September 16, 2016 Transient Wall and Ceiling Temperatures for a Test Chamber with a Single Layer CGI Roof

Table 7.2: Boundary Conditions for a Room with an RCC Roof

Element	Boundary Type	Condition
Test Chamber Walls	Wall	308K (34.85°C)
Test Chamber Ceiling	Wall	314K (40.85°C)
Test Chamber Floor	Wall	308K (34.85°C)



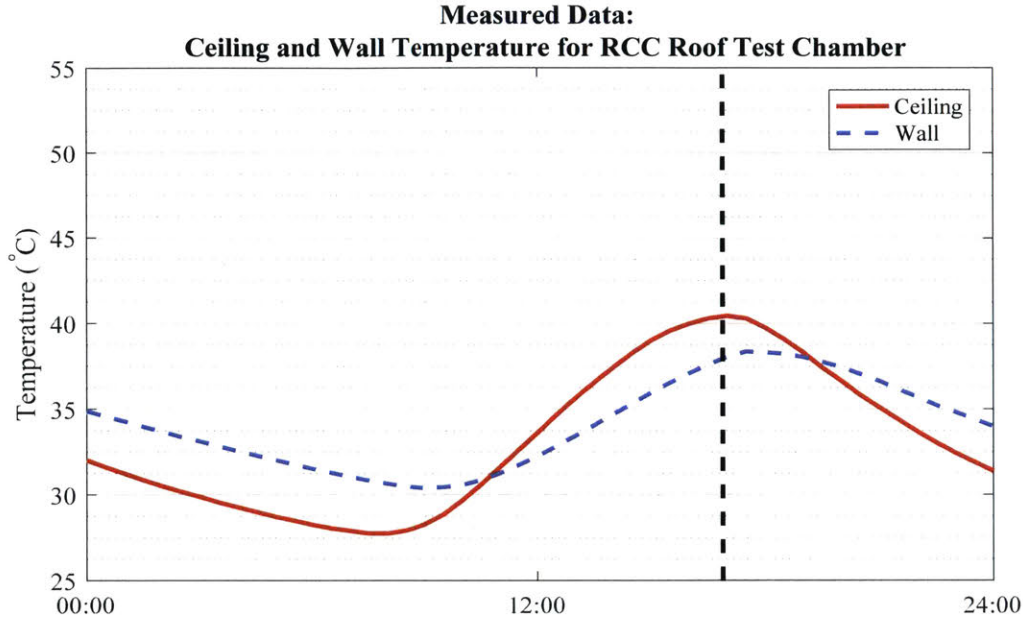


Figure 7-10: September 16, 2016 Transient Wall and Ceiling Temperatures for a Test Chamber with an RCC Roof

Table 7.3 shows boundary conditions for the double layer insulated roof. These temperatures are derived from collected test chamber temperature data during 13:00, the hour when ceiling temperatures peak (Figure 7-11).

Table 7.3: Boundary Conditions for a Room with a Double Layer Insulated Roof

Element	Boundary Type	Condition
Test Chamber Walls	Wall	305K (31.85°C)
Test Chamber Ceiling	Wall	311K (37.85°C)
Test Chamber Floor	Wall	305K (31.85°C)

The fan was modeled as an infinitely thin surface of 60cm diameter with a pressure difference of 10Pa. The pressure difference was selected to achieve air movements of approximately 2.8-3.0m/s 0.1m below the fan, the same air speeds measured in field tests using a Vernier ANM-BTA Anemometer.

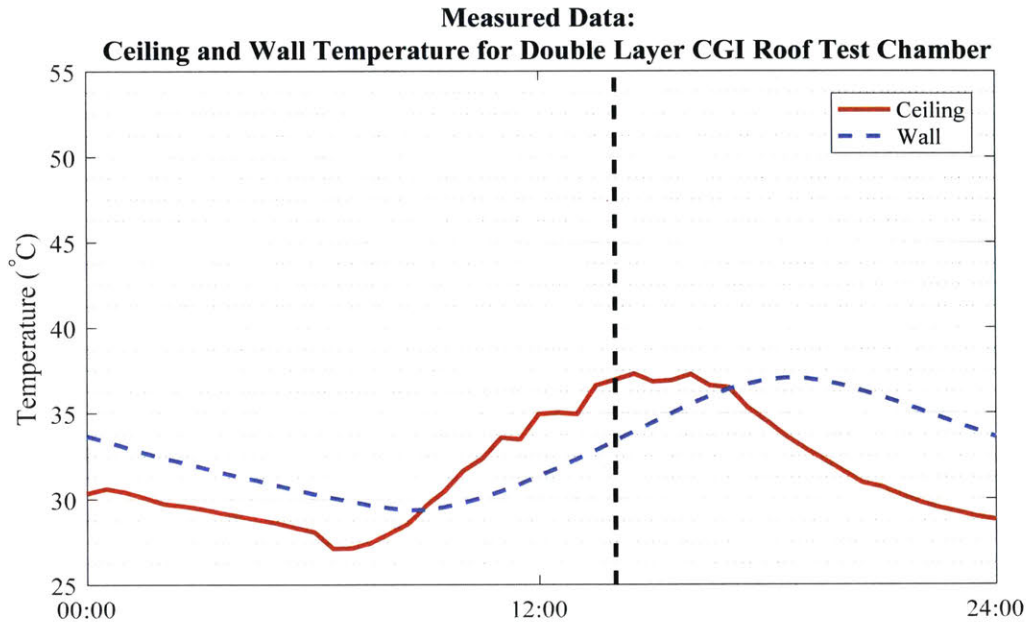


Figure 7-11: September 16, 2016 Transient Wall and Ceiling Temperatures for a Test Chamber with a Double Layer Insulated Roof

### Simulation Geometries

Simulations with several different geometries and fan locations were run to assess the effects of ceiling fans in both the test chambers and Housing for All homes. In addition, simulations were conducted to examine the effects of an upright fan moving air horizontally placed at two different heights, 1m and 1.6m above the floor, as a way to provide the thermal comfort benefits of air movement while minimizing the mixing of hot air directly underneath the ceiling. Test chamber configurations are shown in Figure 7-12. The test chambers were modeled as two-dimensional 2.4m square structures. Although some of the ceilings in the field experiment test chambers are slanted, the simulated test chambers are modeled with flat roofs. Windows were close for all simulation cases.

Simulation cases were run to see how ceiling fans would affect the inside temperature distributions in housing with geometries similar to that of two most common Housing for All archetypes. One archetype is a single story room with an RCC roof. Single story Housing for All simulations configurations are shown in Figure 7-13.

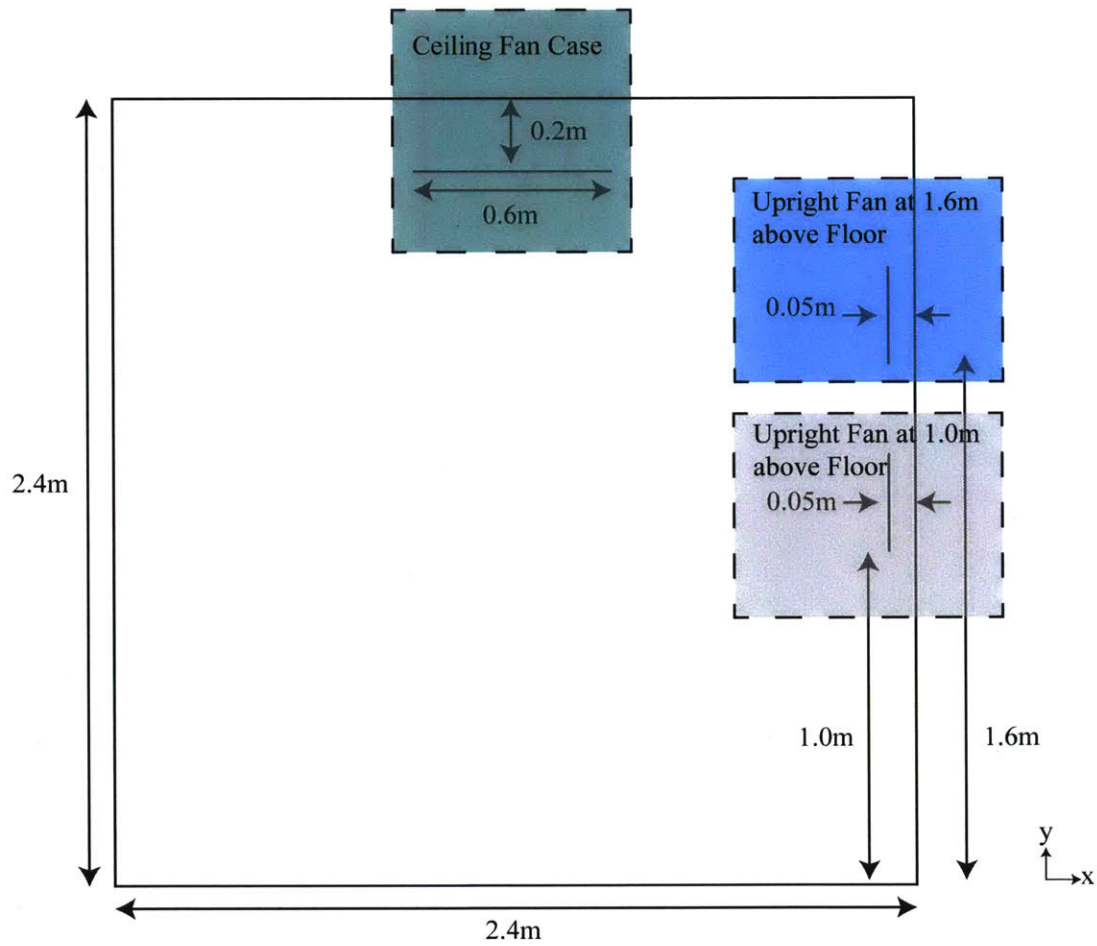


Figure 7-12: CFD Geometries for Test Chamber Simulations

Windows remain closed for all simulation cases. Both homes are modeled as two dimensional structures.

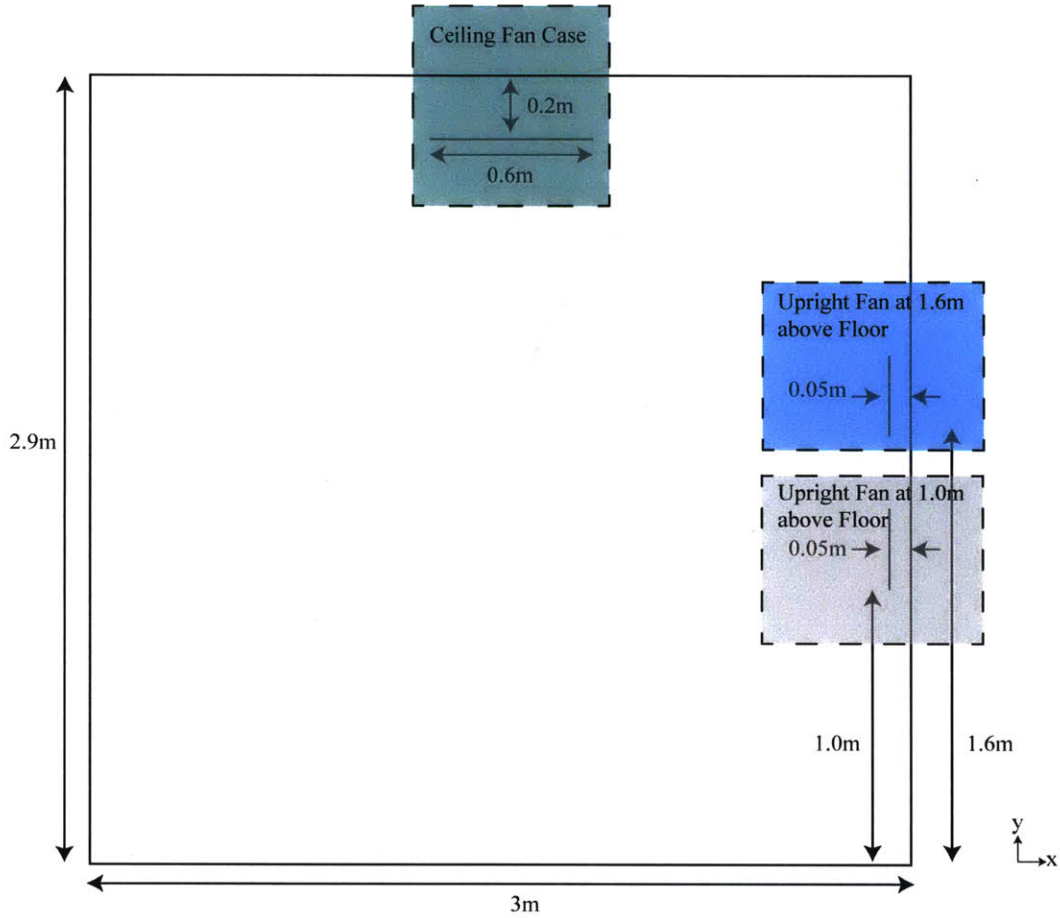


Figure 7-13: CFD Geometries for Single Story Housing for All Home with an RCC Roof

Another Housing for All archetype is composed of a room with a peaked roof. In these Housing for All simulation cases, the distance between the fan and ceiling peak was varied as shown in Figure 7-14. Windows were closed in all cases.

A summary of the various simulation runs is shown in Table 7.4. A total of 30 simulation cases were run.

Table 7.4: Summary of Simulation Cases

Test Chamber	Single Layer Roof	No Fan
		Ceiling Fan
		Upright Fan 1.0m Above the Floor
		Upright Fan 1.6m Above the Floor
	Double Layer Roof	No Fan
		Ceiling Fan
		Upright Fan 1.0m Above the Floor
		Upright Fan 1.6m Above the Floor
Single Story Housing for All Archetype	RCC Roof	No Fan
		Ceiling Fan
		Upright Fan 1.0m Above the Floor
		Upright Fan 1.6m Above the Floor
Peaked Roof Housing for All Archetype	Single Layer Roof	Fan Distance Below Peak Varies: 0.5-1.4m in 0.1m increments
	Double Layer Roof	Fan Distance Below Peak Varies: 0.5-1.4m in 0.1m increments

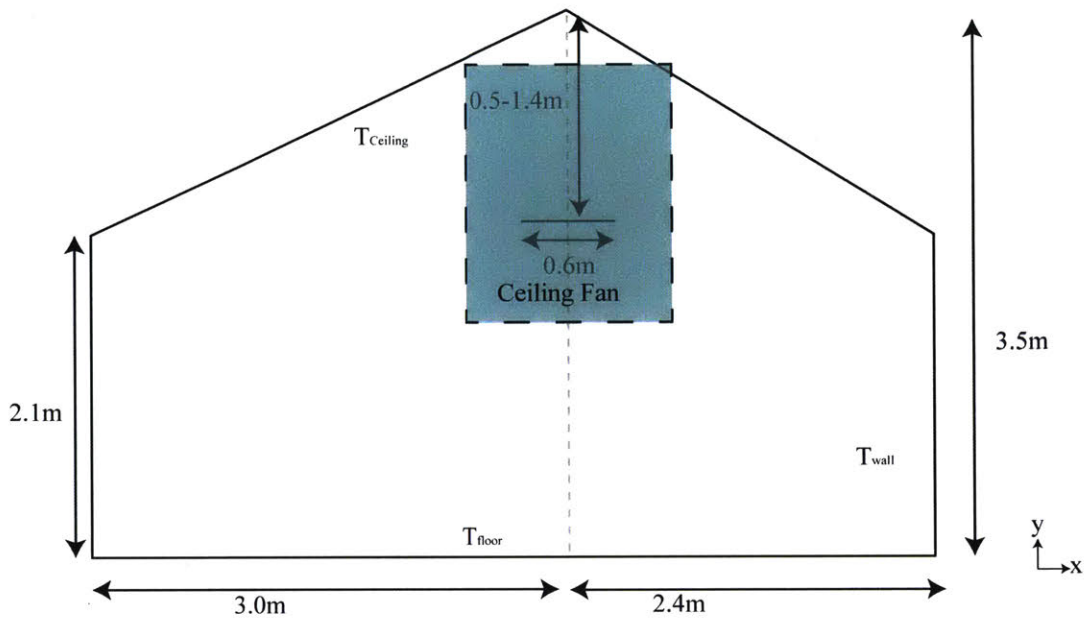


Figure 7-14: CFD Geometries for the Housing for All Archytype with a Peaked Roof

## 7.4 Performance Metric

Three metrics were used to quantitatively compare the performance of each test chamber and results from various simulations, average temperatures during the time when roof temperatures peak (average peak temperatures), ASHRAE-55 (ASHRAE, 2013), and the India Model for Adaptive Thermal Comfort (Manu et al., 2016). The average peak temperature is defined as

$$T_{peak}^- = \frac{\sum_{i=1}^n T_i(\text{time}(\max(T_{ceiling})))}{n} \quad (7.1)$$

Where  $n$  is the number of days in the data collection period and  $T_i$ , is the chosen temperature vector for a 24-hour period. This temperature vector can be ceiling, operative, radiant, air at 1.75m above the floor, or air at 0.75m above the floor. ASHRAE-55 Thermal Comfort Environment Conditions Standards were used to determine thermal comfort while considering air movement, humidity, and temperatures (ASHRAE, 2013). A tool that calculates comfort levels based on the ASHRAE-55 model developed by the Center for the Built Environment, University of California at

Berkeley was used to determine the comfort of inside conditions (Hoyt Tyler et al., 2013). The Predicted Mean Vote (PMV) model developed by Fanger, where -3 is too cold and +3 is too hot, was used to determine thermal comfort levels. The PMV can then be translated to the Predicted Percent of Dissatisfied (PPD), or the estimated percentage of people uncomfortable (P.O. Fanger, 1970). The ASHRAE and Fanger models, however, have limitations when defining comfort in the context of Indian buildings. Some residents in India may adapt differently to warmer ambient temperatures.

The IMAC adaptive model was developed to better assess the comfort of residents in India as compared to the ASHRAE-55 and European EN-15251 model. The IMAC model incorporates the results from several survey campaigns across India to determine the 80% acceptability limit, where "more than 80% of occupants find thermally acceptable".

Currently, the IMAC model does not consider air movement or humidity in their thermal comfort model. As a result, estimated observations on comfort will consider assessments using both the ASHRAE and IMAC comfort models.

## 7.5 Results

The results of field experiments and simulations revealed that the use of ceiling fans in rooms with poorly insulated roofs can lead to air and operative temperature increases.

### 7.5.1 Field Experiments

The perceived comfort gained from ceiling fan use is diminished due to the mixing of hot air directly beneath the ceiling. In both test chambers, temperature data shows the mixing of air surrounding the ceiling with the rest of the inside ambient air. Consequently, the temperature stratification in the test chamber disappears. Figure 7-15 and Figure 7-11 show the effects of fan use on temperature stratification. The not highlighted region (22-Dec to 23-Dec) marks the fan off period. The highlighted region (23-Dec to 24-Dec) marks the fan on period. The blue trace, representing air

temperatures at 1.75m above the floor, and the grey trace, representing air temperatures 0.75m above the floor, merge during periods of ceiling fan usage. In the days with no fan usage, the averaged difference between the temperature at 0.75m above the floor and 1.75m above the floor is  $0.9^{\circ}\text{C}$ . With fan usage, this average difference decreases to  $0.06^{\circ}\text{C}$ .

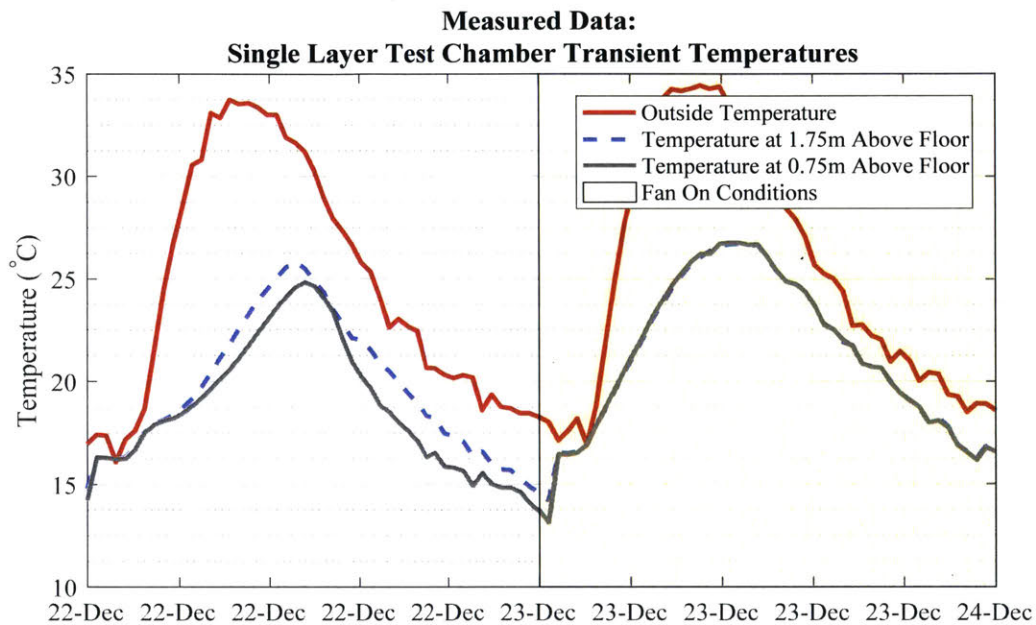


Figure 7-15: Changes in Temperature Stratification for the Test chamber with a Single Layer tin Sheet Roof

During the period with fan use, lower air and operative temperatures increase in the test chamber with a single layer tin roof. Due to the direct exposure to solar heat flux and the high thermal conductivity of the single layer roof, the average peak ceiling temperature during the fan off period is  $9.8^{\circ}\text{C}$  greater than the average outdoor ambient peak temperature. The ceiling fan draws the hot air from beneath the ceiling and mixes it throughout the room causing an increase in air and operative temperatures at lower levels where the occupant is residing. Figure 7-17 shows the average temperature during the time of day when the ceiling temperatures peak for both the fan on and fan off periods. The average operative temperature increases by  $1.7^{\circ}\text{C}$  with the use of a ceiling fan. The average air temperature at 0.75m above



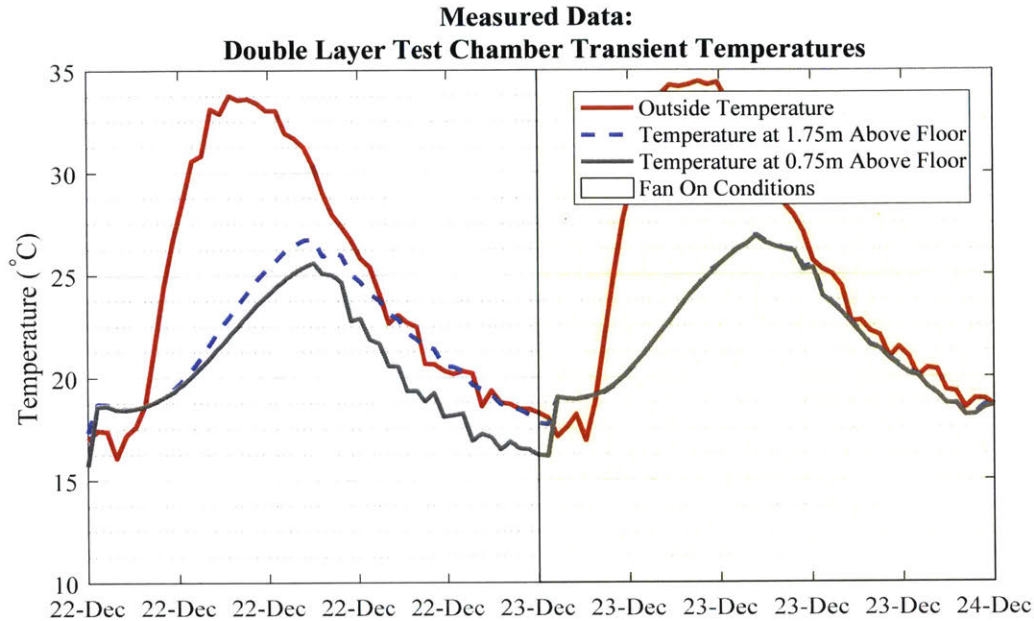


Figure 7-16: Changes in Temperature Stratification for the Test Chamber with a Double Layer Insulated Roof

the floor increases by  $2.4^{\circ}\text{C}$  while the average peak ceiling temperature decreases by  $4.1^{\circ}\text{C}$ . The change in ceiling temperatures corresponds to a higher total heat transfer from the ceiling with the interior. Despite the decrease in ceiling temperatures, the average radiant temperatures increase by  $1.4^{\circ}\text{C}$ . In the case of the test chamber with the single layer tin roof, radiant temperatures are dominated by wall temperature due to the low emissivity of the ceiling. The emissivity of the tin roof, measured by Surface Optics Corporation SOC 400T, is 0.09. The south wall temperatures between the fan on and fan off period increased by  $0.4^{\circ}\text{C}$ . Data was not collected for the north, east, or west wall temperatures.

Results from the double layer roof test chamber indicate that the increase in operative temperature due to ceiling fan usage can be mitigated with a properly insulated roof. By protecting the roof from solar heat gains and using night ventilation, the average peak ceiling temperature can be  $2.0^{\circ}\text{C}$  cooler than the outside ambient temperature or  $11.8^{\circ}\text{C}$  cooler than the single layer roof. In the double layer insulated roof test chamber, the average peak air, operative, and radiant temperatures vary by

**Measured Data Single Layer Test Chamber: Effects of Ceiling Fan Use on Temperatures**

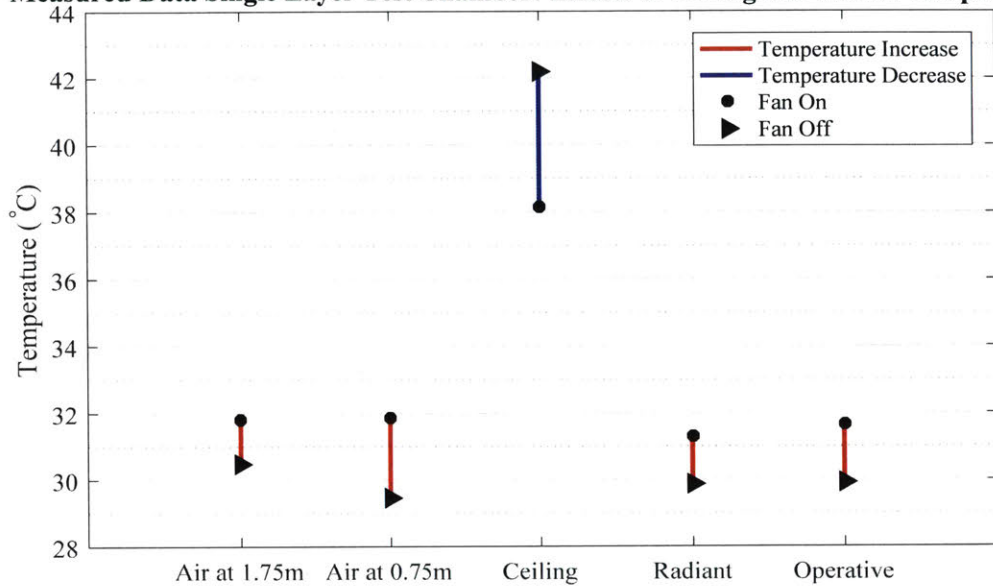


Figure 7-17: Changes in Average Peak Temperatures as a Result of Ceiling Fan Usage

less than 0.5°C between the fan on and fan off periods as shown in Figure 7-18.

**Measured Data Double Layer Test Chamber: Effects of Ceiling Fan Use on Temperatures**

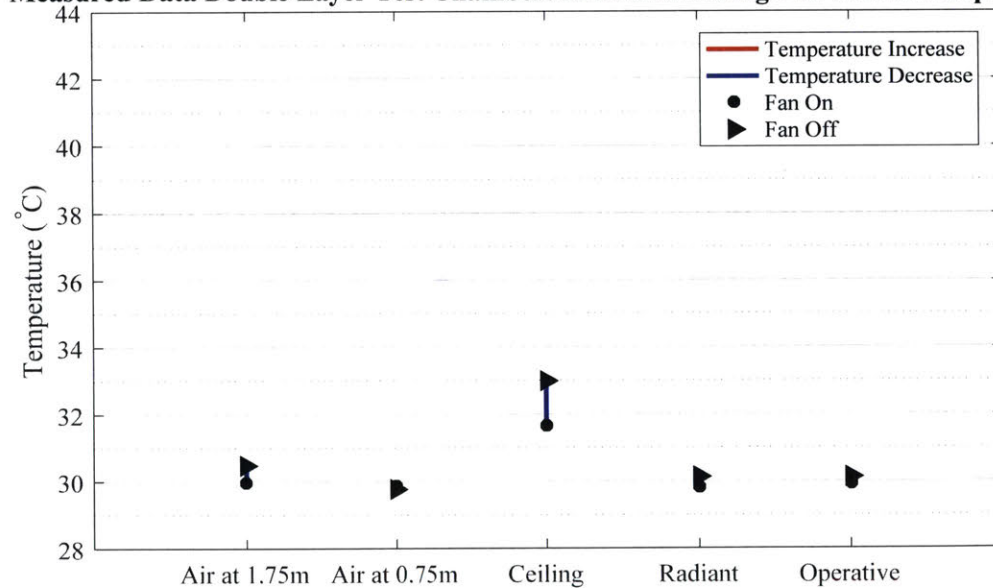


Figure 7-18: Changes in Average Peak Temperatures as a Result of Ceiling Fan Usage

The changes in operative temperatures lead to changes in the percentage of time in which operative temperatures exceed the upper IMAC 80% acceptability limit. For the test chamber with a single layer roof, ceiling fan usage causes a 6.8% increase in the amount of time where operative temperatures are deemed uncomfortable. This translates to an average of 1.6 more hours daily in which operative temperatures exceed the IMAC 80% acceptability limits. For the test chamber with a double layer insulated roof, ceiling fan usage has negligible impact on the percentage of time in which operative temperatures exceed the IMAC 80% acceptability limit.

The IMAC model, however, does not include influences from air velocity or humidity on thermal comfort. Consequently, the peak conditions of each day were also studied using the PMV model. It is important to note, though the PMV model considers the effects of air velocity and humidity, it does not accurately represent the adaptive comfort of Indian residents. Table A.1 and A.2 found in Appendix A show inputs for calculating the PMV for various test chamber experiments. With fan usage, the test chamber with the double layer roof is able to achieve a more acceptable comfort level of +0.04 as opposed to the test chamber with a single layer roof's comfort level of +0.61. This translates to a PPD of 5.0% for the double layer roof test chamber and 12.8% for the single layer roof test chamber. PPD values calculated for the single layer roof test chamber assuming a humidity level of 90%RH indicate thermal comfort gains from ceiling fans diminish as humidity increases. For the test chamber with the single layer roof, the improvement in PPD values decreases from 46.80% to 33.11% when the humidity increases from 50%RH to 90%RH. The temperatures during the fan off period are slightly warmer in the test chamber with the double layer roof than in the test chamber with the single layer roof. This can be attributed to the barrier wall which protects the north and west walls of the test chamber with the single layer roof.

The changes in operative temperatures lead to changes in the percentage of time in which operative temperatures exceed the upper IMATC 80% Acceptability Limit. For the test chamber with a single layer roof, ceiling fan usage causes a 6.8% increase in the amount of time where operative temperatures are deemed uncomfortable. This

translates to an average of 1.6 more hours daily in which operative temperatures exceed the IMATC 80% acceptability limits. For the test chamber with a double layer insulated roof, ceiling fan usage has negligible effects on the percentage of time in which operative temperatures exceed the IMATC 80% Acceptability Limit. The IMAC model, however, does not include the influence of air velocity or humidity on thermal comfort. Consequently, the peak conditions of each day were also studied using the PMV model. It is important to note, though the PMV model considers the effects of air velocity and humidity, it does not accurately represent the adaptive comfort of Indian residents. Table shows inputs for calculating the PMV for various test chamber experiments. With fan usage, the test chamber with the double layer roof is able to achieve a more acceptable comfort level of +0.04 PMV as opposed to the test chamber with a single layer roof's comfort level of +0.61 PMV. This translates to a PPD of 5.0% for the double layer roof test chamber and 12.8% for the single layer roof test chamber. PPD values calculated for the single layer roof test chamber assuming a humidity level of 90%RH indicate thermal comfort gains from ceiling fans diminish as humidity increases. For the test chamber with the single layer roof, the improvement in PPD values decreases from 46.80% to 33.11% when the humidity increases from 50%RH to 90%RH. The operative temperature distribution, PMV, and percentage of time in which operative temperatures exceed the upper IMAC 80% Acceptability Limit were calculated and graphed in Figure 7-19 and Figure 7-20 which show the results for the fan on and fan off period for the test chamber with the double layer roof with a relative humidity of 50%.

A properly insulated roof is necessary for maximum benefit of a ceiling fan.

## **7.5.2 CFD Simulations**

Simulation results confirmed the relative effects from ceiling fan usage as observed in field experiment. Temperature contours for both simulated test chambers and Housing for All homes show the phenomenon of the ceiling fan drawing hot air away from the ceiling and mixing it throughout the room.

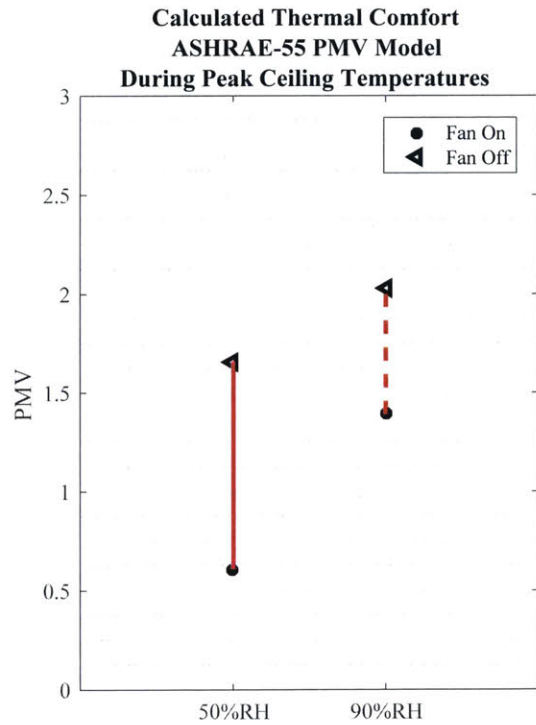
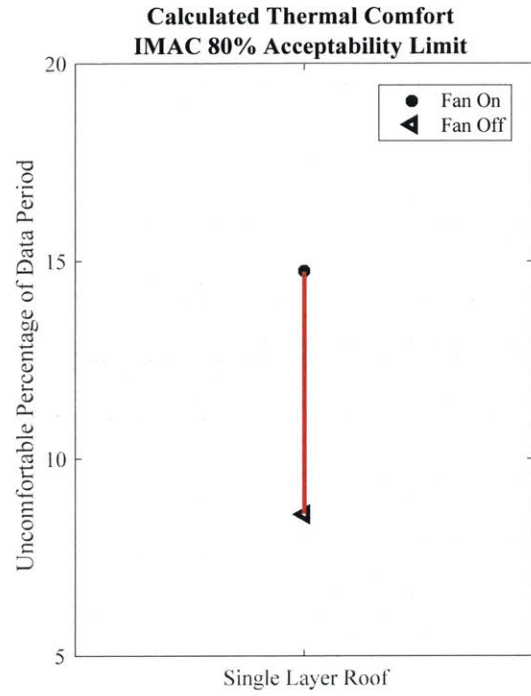
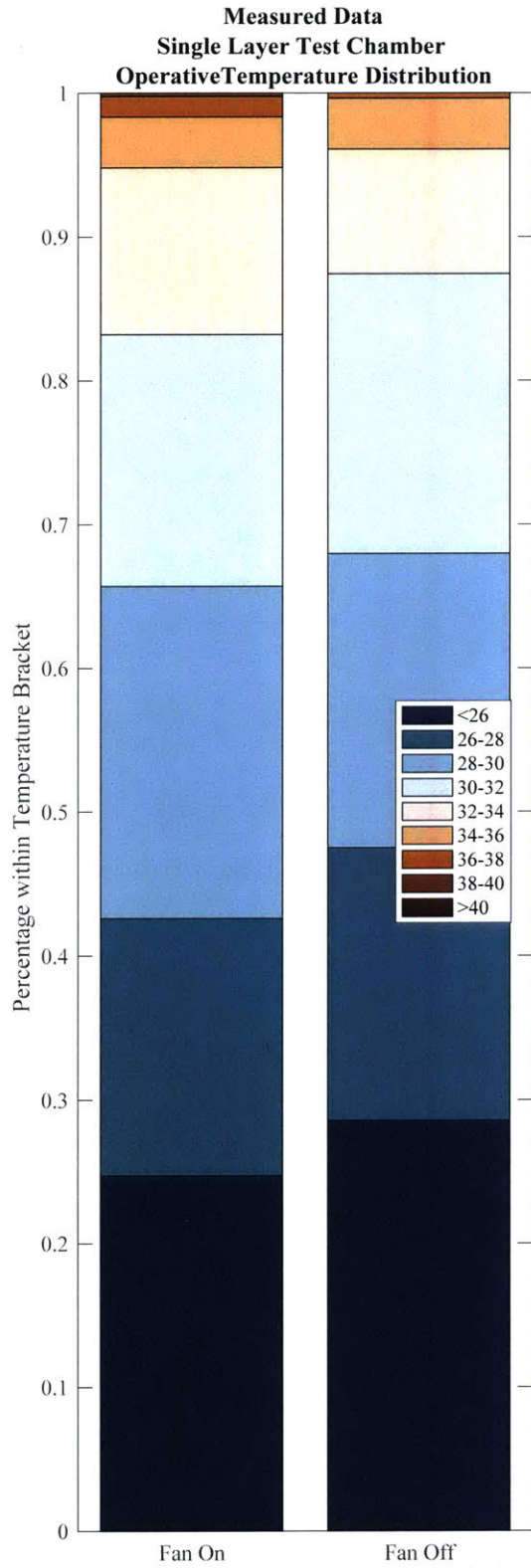


Figure 7-19: Effects on Thermal Comfort due to Ceiling Fan Use in the Test Chamber with a Single Layer Roof

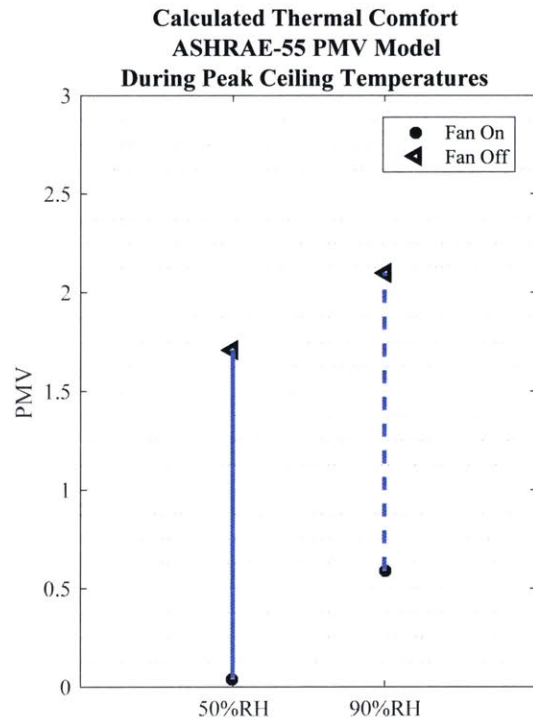
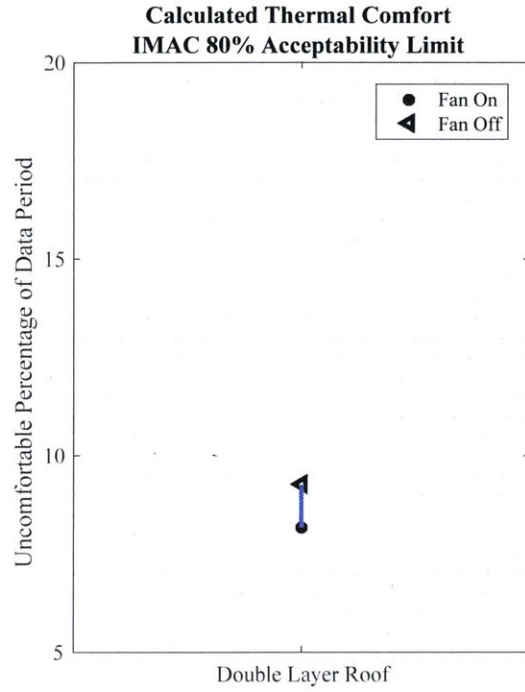
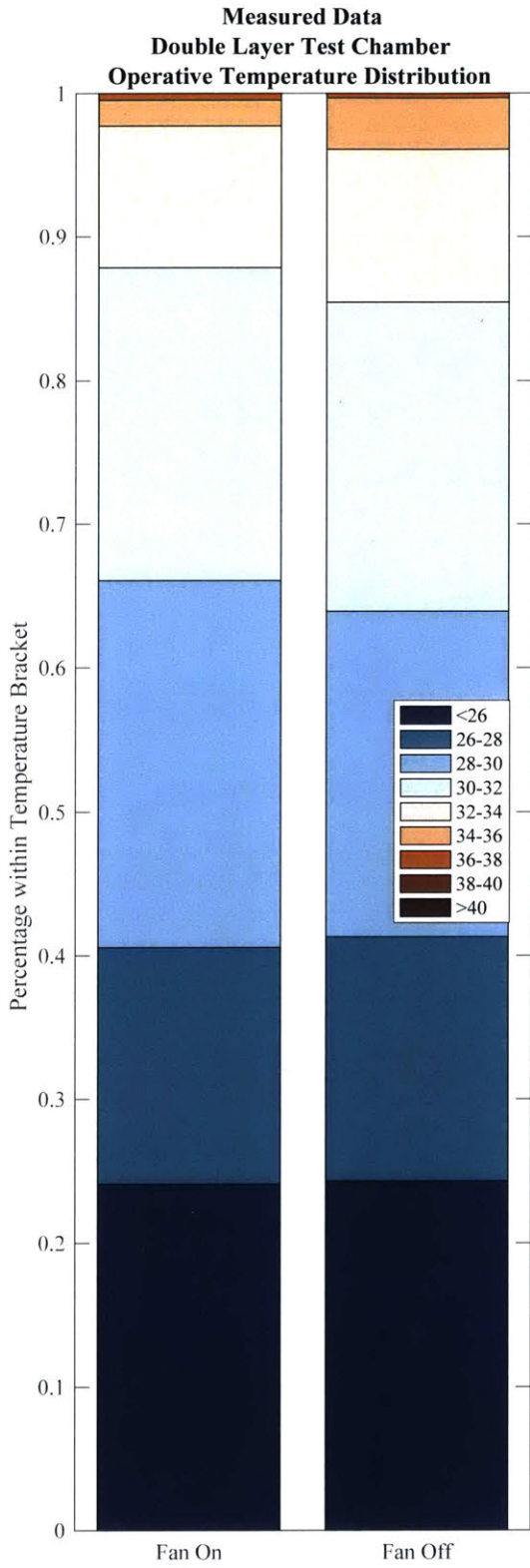


Figure 7-20: Effects on Thermal Comfort due to Ceiling Fan Use in the Test Chamber with a Double Layer Roof

### Test Chambers

CFD results for the single layer and double layer roof test chambers were compared to the measured data for both the fan on and fan off periods. Figure 7-21 and Figure 7-22 show the simulation and data comparisons for the single layer roof test chamber and the double layer roof test chamber. For the single layer test chamber, the CFD simulations prediction of the temperature changes between the fan on and fan off periods agree with the measured test data within 0.5°C. However the absolute temperatures predicted by the model disagree by 2°C. The CFD simulations tends to predict higher absolute temperatures for the single layer roof. This may be due to the fact that the CFD model for the test chamber with a single layer roof was modeled as flat rather than slightly sloped.

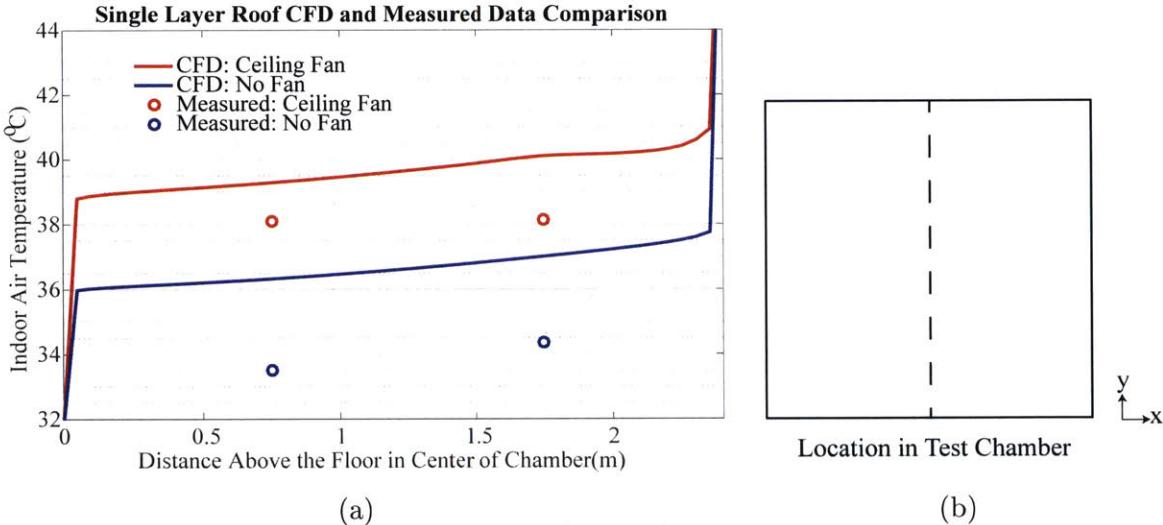


Figure 7-21: Comparison of Simulation and Field Experiment Results for the Test Chamber with a Single Layer Roof

For the double layer roof test chamber, the CFD simulations prediction of the temperature changes between the fan on and fan off periods agree with the measured test data within 0.5°C. The absolute temperatures predicted by the model disagree by less than 0.5°C.

Following the calibration of the CFD simulations, simulations were run for 30 different cases varying fan orientation, roof types, and room geometries. In the simulated test chambers, the inside ambient air temperatures increases due to the use

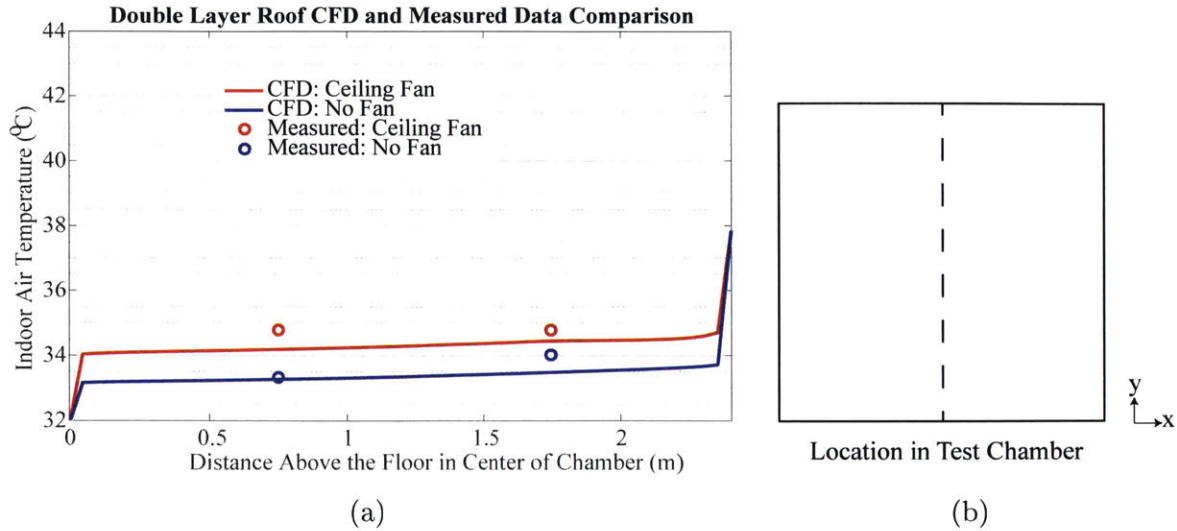


Figure 7-22: Comparison of Simulation and Field Experiment Results for the Test Chamber with a Double Layer Roof

of a 0.6m diameter ceiling fan are more pronounced in rooms where the ceiling temperatures reach 324K (50.85°C) as shown in Figure 7-23. The use of the ceiling fan eliminates the stratification of hot air directly adjacent to the ceiling and increases the temperature at lower levels.

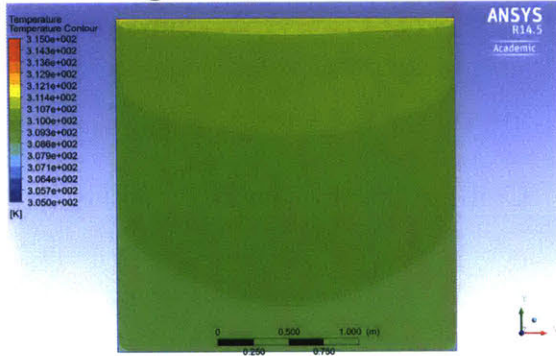
Results from simulation cases where a smaller upright horizontal air flow inducing fan of 0.3m diameter is placed 0.05m away from the wall, illustrate a method to mitigate the temperature increase due to the combination of ceiling fan usage and a poorly insulated roof. As shown in Figure 7-24, the upright fan, when compared to the ceiling fan, can provide air movement to enhance evaporative cooling and perceived thermal comfort while minimizing the mixing of hot air surrounding the ceiling.

The upright fan should be placed at 1.6m above the floor as more air moment will be felt by the occupant assuming the occupant is standing and the average height of an Indian man is 1.65m (Angus Deaton, 2008). Figure 7-25 shows the velocity along a horizontal line across the room placed 1.5m above the floor. In the test chamber simulations cases, velocity profiles do not vary with changes in roof types.

Though the 0.3m diameter upright fan mitigates the mixing of hot air surrounding the ceiling, much of the benefits of air movement disappear if the occupant is more than 1m away from the fan. An occupant located in the center of the test chamber

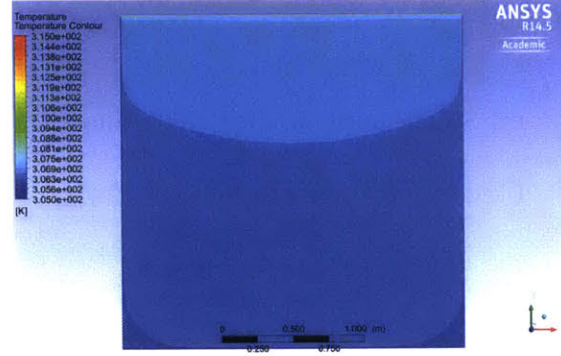


Ceiling Temperature = 324K



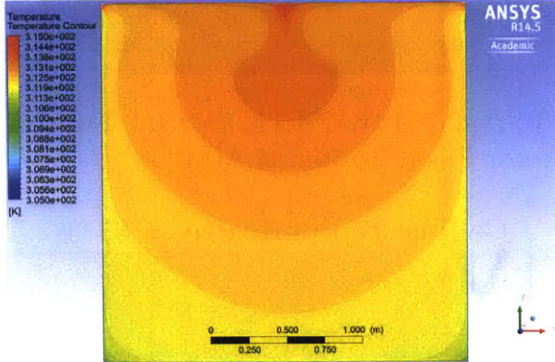
(a) Single Layer Roof, No Fan.

Ceiling Temperature = 311K



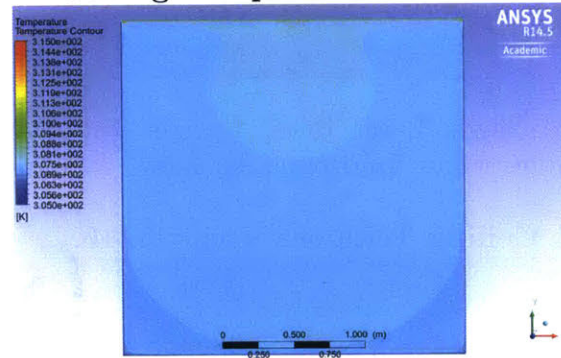
(b) Double Layer Roof, No Fan.

Ceiling Temperature = 324K



(c) Single Layer Roof, Ceiling Fan.

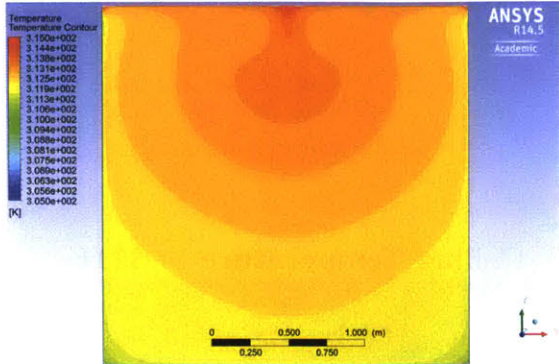
Ceiling Temperature = 311K



(d) Double Layer Roof, Ceiling Fan.

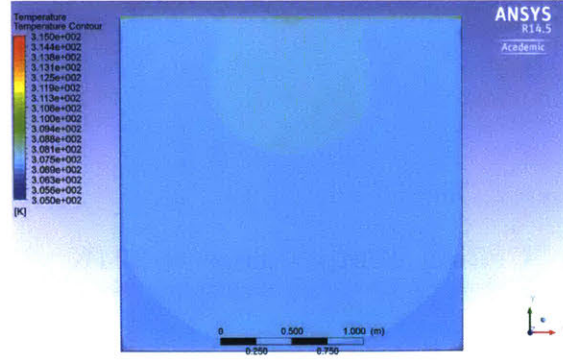
Figure 7-23: Temperature Contours of Simulated Test Chambers without and with a Ceiling Fan

Ceiling Temperature = 324K



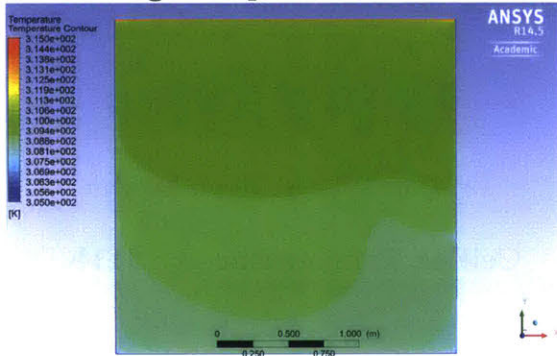
(a) Single Layer Roof, Ceiling Fan.

Ceiling Temperature = 311K



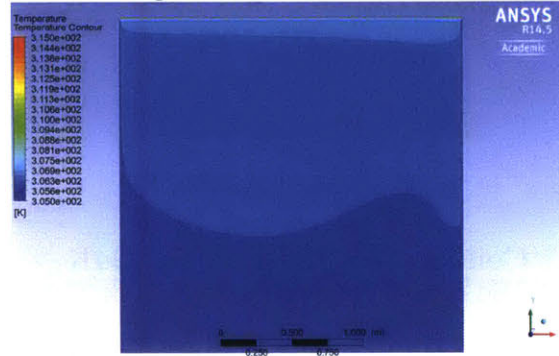
(b) Double Layer Roof, Ceiling Fan.

Ceiling Temperature = 324K



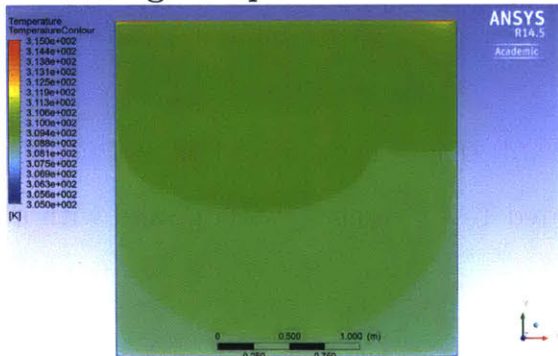
(c) Single Layer Roof, Upright Fan 1m Above Floor, Horizontal Air Flow

Ceiling Temperature = 311K



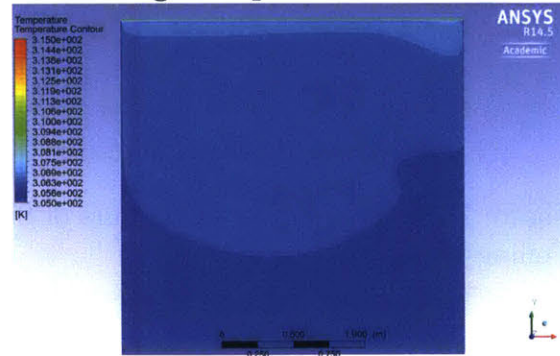
(d) Double Layer Roof, Upright Fan 1m Above Floor, Horizontal Air Flow

Ceiling Temperature = 324K



(e) Single Layer Roof, Upright Fan 1.6m Above Floor, Horizontal Air Flow

Ceiling Temperature = 311K



(f) Double Layer Roof, Upright Fan 1.6m Above Floor, Horizontal Air Floor

Figure 7-24: Temperature Contours of Simulated Test Chambers with Various Fan Configurations

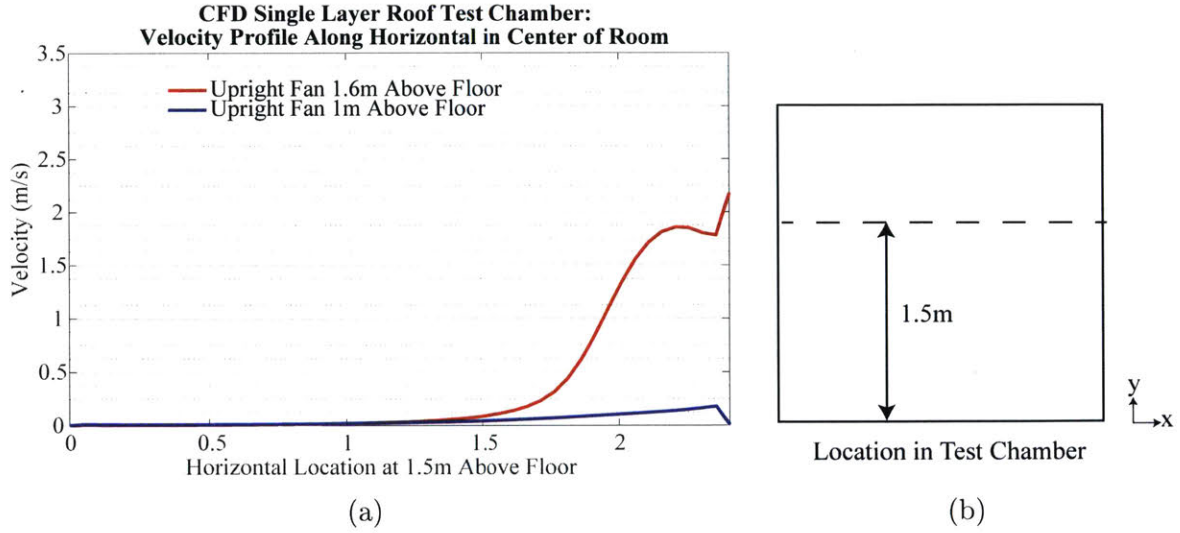


Figure 7-25: Velocity Along a Horizontal Line Placed 1.5 m Above the Floor in a Test Chamber with a Single Layer Tin Sheet

would not feel the same air movements with an upright near the wall fan as they would feel in a room with a ceiling fan as shown the velocity profile along a vertical line in the center of the room (Figure 7-26). However, an occupant located 0.5m from an upright fan near the wall would feel similar air movements as he/she would with a ceiling fan (Figure 7-27)

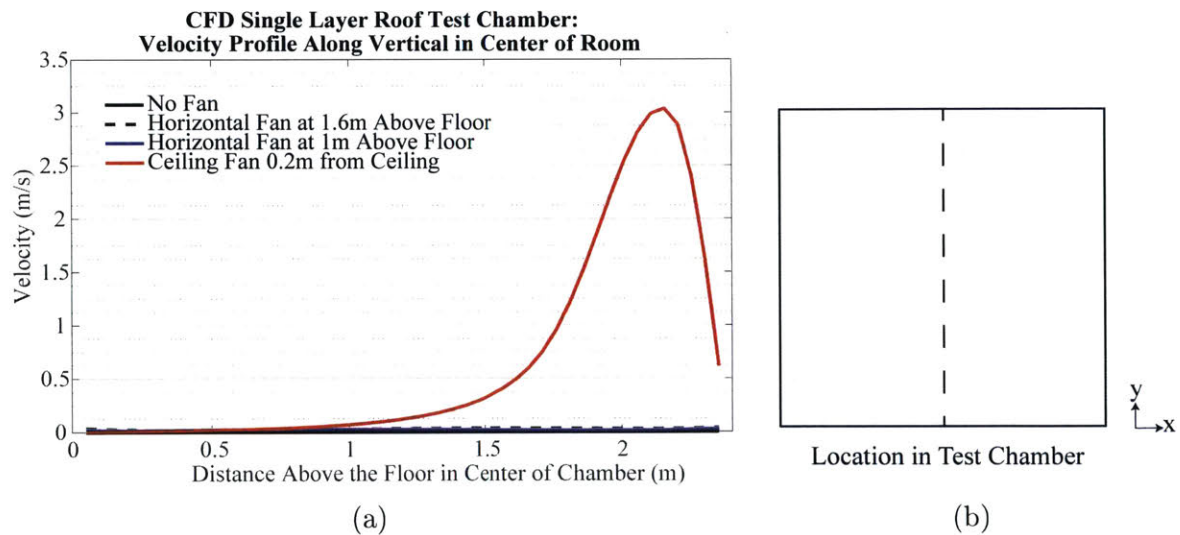


Figure 7-26: Comparison of the Velocity Profiles Along a Vertical Line in the Center of the Room for a Test Chamber with a Single Layer Tin Sheet

Figure 7-28 Comparison of the velocity profiles along a vertical line in the center

of the room for a test chamber with a single layer tin sheet and an upright fan near the wall. An occupant will not feel the horizontal air flow benefits of an upright fan near the wall if he/she is standing in the center of the 2.4m wide room.

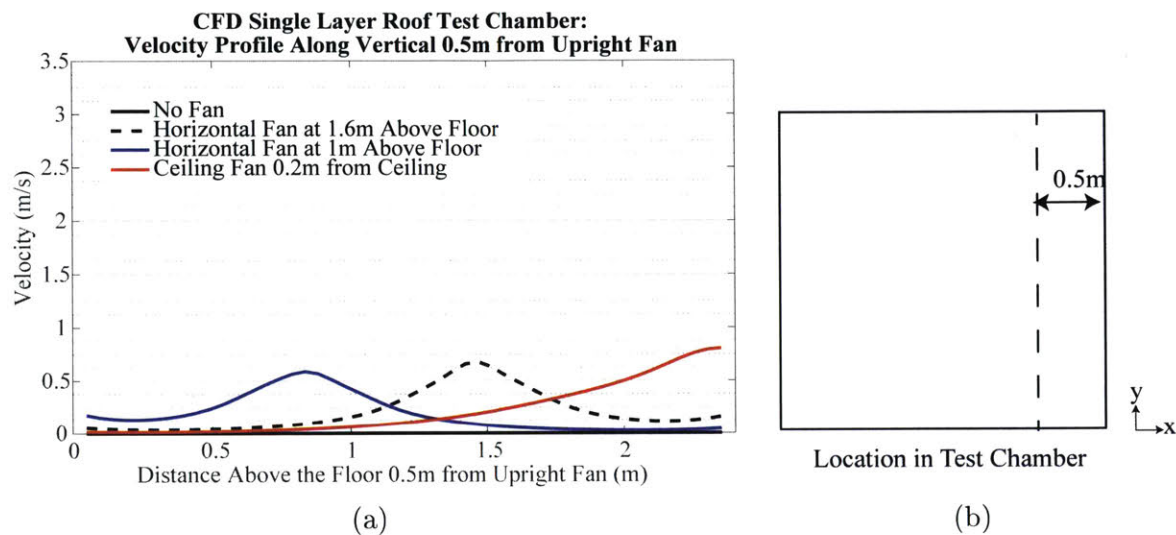


Figure 7-27: Comparison of the Velocity Profiles Along a Vertical line 0.5 m from the Upright Fan for a Test Chamber with a Single Layer Tin Sheet

Temperatures along a vertical line in the center of the test chamber were plotted for each test chamber simulation case. Figure 7-28 shows the temperature profiles for a simulated test chamber with a single layer roof. Figure 7-29 shows the temperature profiles for a simulated test chamber with a double layer roof. Similar to collected field data, the temperature profile plots show a 2°C increase in temperature for ceiling fan usage in the single layer tin roof test chamber and negligible temperature increases with a horizontal flow inducing upright fan. In contrast, there is a <1°C increase in temperature for ceiling fan usage in the double layer insulated roof test chamber.

### Single Story Housing for All Homes with RCC Roofs

The temperature increase effects caused by ceiling fan usage with a poorly insulated roof seen in the simulated test chambers can also be seen in the simulated Housing for All homes. Based on the simulation cases, studying the effects of ceiling fan usage in the single story RCC roof Housing for All archetype, recommendations can be made on fan placement. Temperature contours for the simulated RCC roof Housing for All

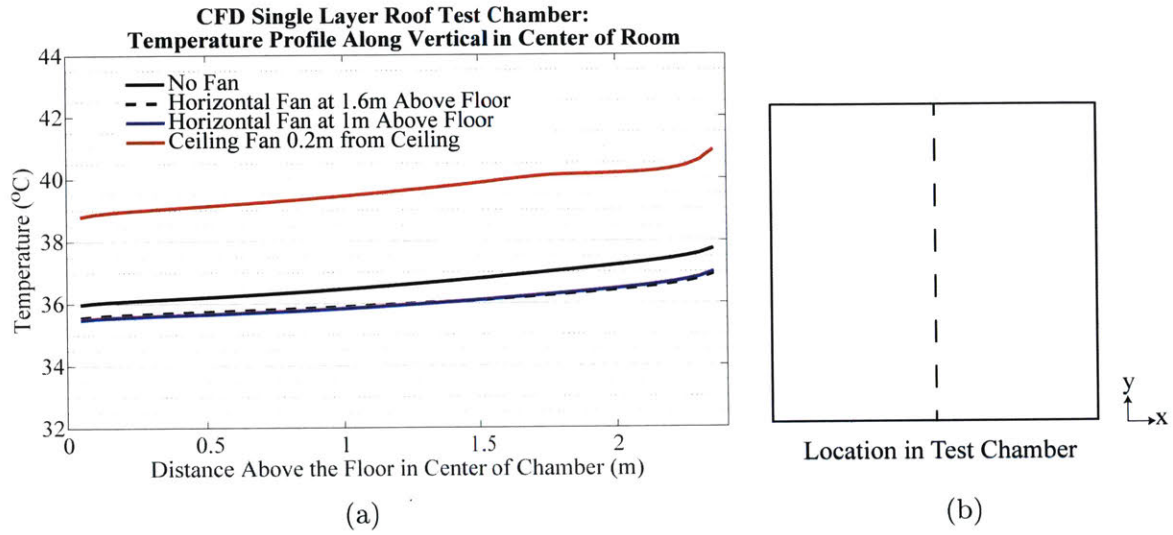


Figure 7-28: Temperatures Along a Vertical Line in the Center of the Simulated Test Chamber with a Single Layer Tin Roof

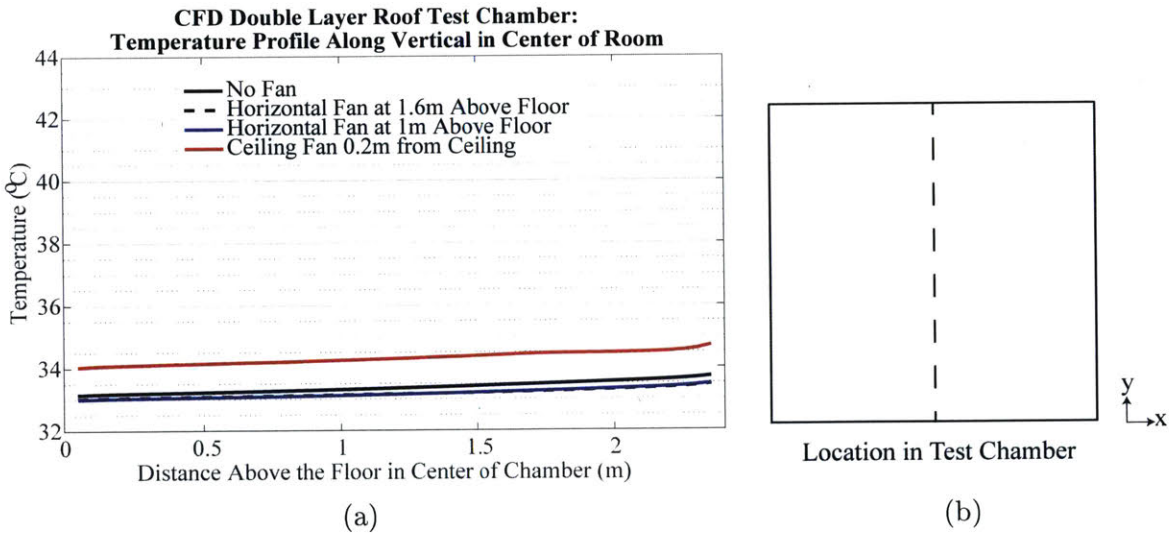


Figure 7-29: Temperatures Along a Vertical Line in the Center of the Simulated Test Chamber with a Double Layer Insulated Roof

archetypes are shown in Figure 7-30. Due to the hot air surrounding the RCC roof, it is suggested to place an upright fan at 1.6m above the floor to minimize temperature increase as shown in Figure 7-32, the temperature profile along a vertical line in the center of the room. Evaporative and convective cooling benefits for an occupant are maximized when the upright fan is placed close to the occupant. Figure 7-31 shows the horizontal velocity profiles along a horizontal line placed 1.5m above the floor. Much of the air movement caused by the upright fan cannot be felt in the center of the room suggesting the upright 0.3m diameter fan needs to be within 1m of the occupant.

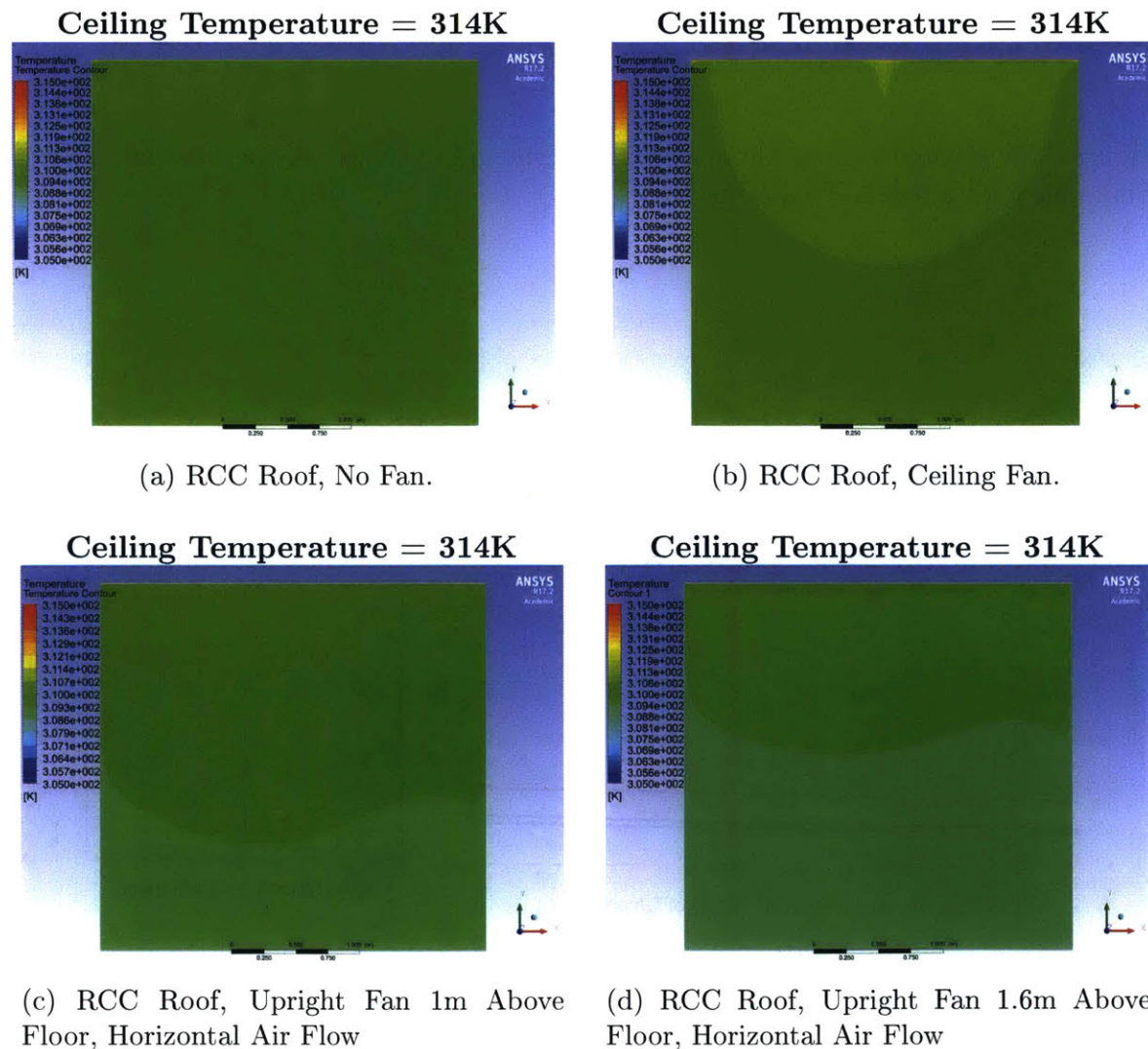


Figure 7-30: Temperature Contours of Simulated RCC Roof Housing for All Archetype with Different Fan Configurations

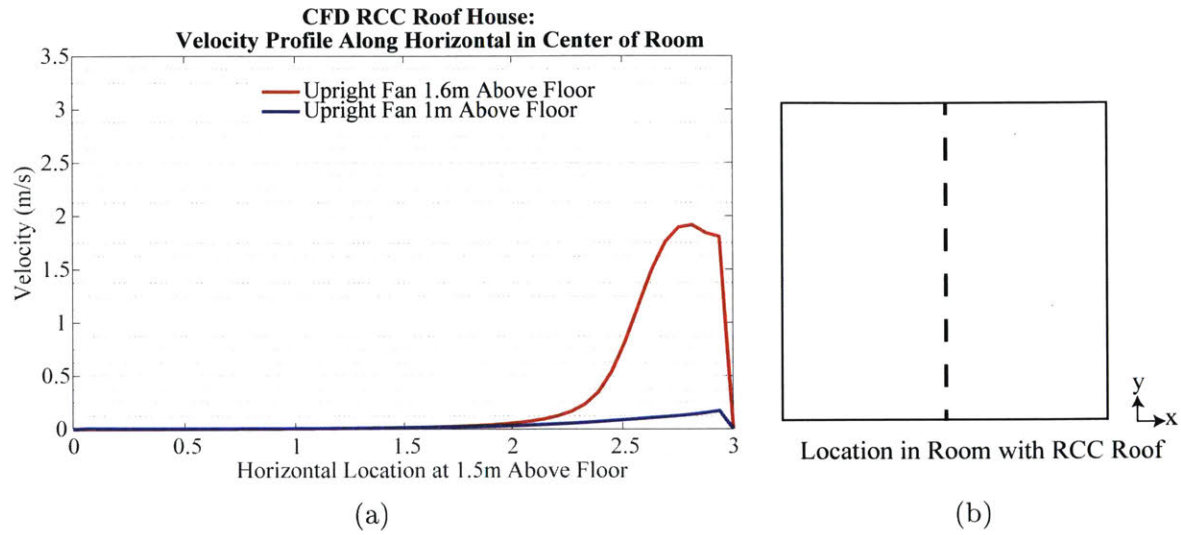


Figure 7-31: Velocity Along a Horizontal Line Placed 1.5 m Above the Floor in a Room with an RCC Roof

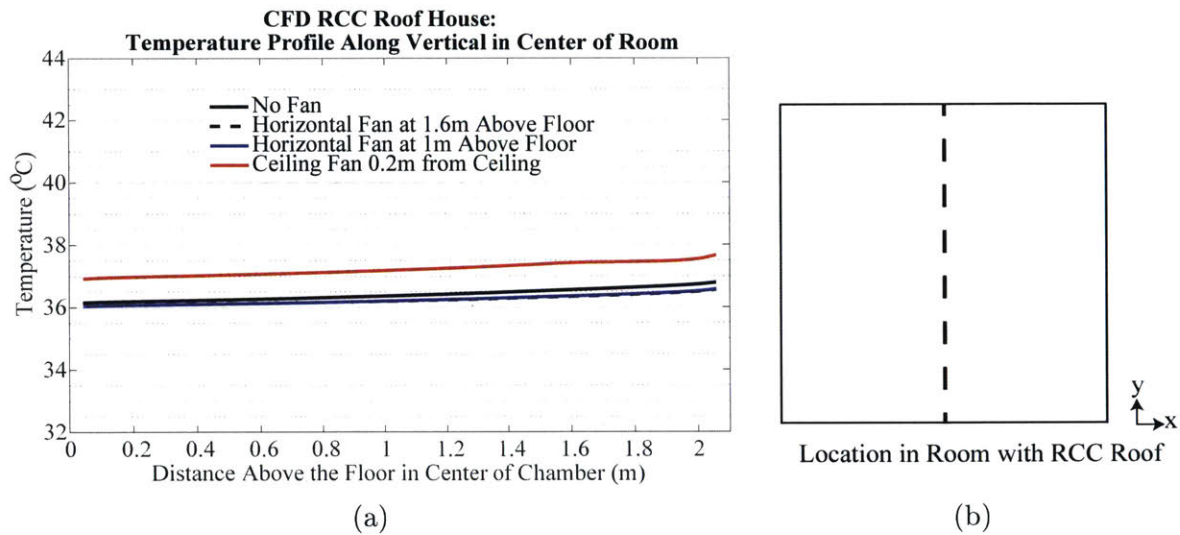


Figure 7-32: Temperatures Along a Vertical Line in the Center of the Simulated Housing for All home with an RCC Roof

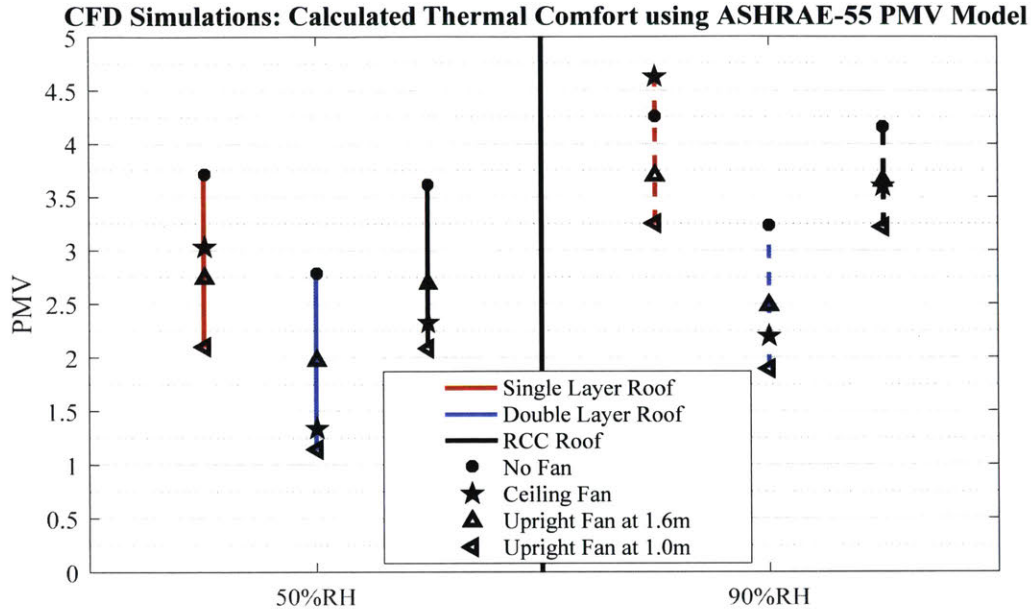


Figure 7-33: Calculated PMV Values for CFD Simulations of Test Chambers and Homes with RCC Roofs

To translate ambient temperatures and air velocities to comfort the PMV values were calculated and graphed in Figure 7-33 for each simulation the test chamber and the single story Housing for All room. Inputs for calculated the PMV are listed in Tables A.3, A.4, A.5, A.6, A.7, and A.8, found in Appendix A. For the PMV models, it is assumed that occupants are <1m away from the horizontal flow inducing fans. This translates to an assumed air flow of 2m/s for the upright horizontal air movement inducing fan at 1.6m above the floor. The assumed air flow for the upright horizontal flow inducing fan at 1m above the floor was 0.5m/s.

In conclusion, for rooms with a single layer tin sheet, it is best to place a 0.3m diameter horizontal flow inducing upright fan near the occupant (<1m) to maximize air flow while not raising operative and air temperatures. Rooms that have a properly insulated roof, such as a double layer roof with an air gap, are recommended to use ceiling fans for maximum thermal comfort. In more humid conditions of 90%RH where the positive comfort effects of air movement is diminished, using the ceiling fan in a room with a single layer tin sheet can be the least comfortable scenario.



## Housing for All Structures with Peaked Roofs

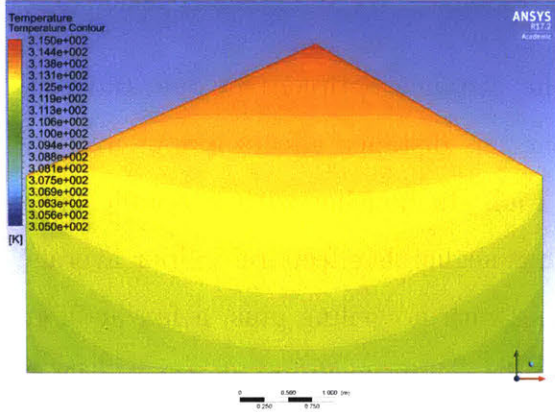
In housing archetypes with a peaked roof, the distance between the fan and roof peak was varied. Simulation results show that this distance affects indoor average temperatures in a house with a single layer roof. In housing with a double layer insulated roof, the distance between the roof has negligible effects on indoor average temperatures. Temperature contours of housing with no ceiling fans, a fan at 0.5m from the ceiling peak, and a fan at 1.4m from the ceiling peak are shown in Figure 7-34. Wall temperatures are 306K. Ceiling temperatures depend on the type of roof. Average room temperatures as a function of ceiling fan placement are shown in Figure 7-35. The average temperatures include the entire domain of the Housing for All home interior.

In housing similar to Housing for All homes, the increase of indoor temperatures due to a ceiling fan drawing hot air from the ceiling can be mitigating by placing the fan a sufficient distance from the ceiling. Given the Housing for All archetype, having a ceiling fan 1.4m away from the ceiling allows for the benefits of air moments while only raising average indoor temperatures by 0.5°C. In addition to mitigating temperature increases, placing the fan at 1.4m from the ceiling peak allows the residents to feel more air movement and evaporative cooling as shown in a plot of the velocity profile along a vertical line from the floor to the roof peak (Figure 7-36).

The thermal comfort levels for the Housing for All home with a peaked roof were calculated and graphed in Figure 7-37 using the PMV model. Inputs for calculated the PMV are listed in Tables A.9, A.10, A.11, and A.12 found in Appendix A.

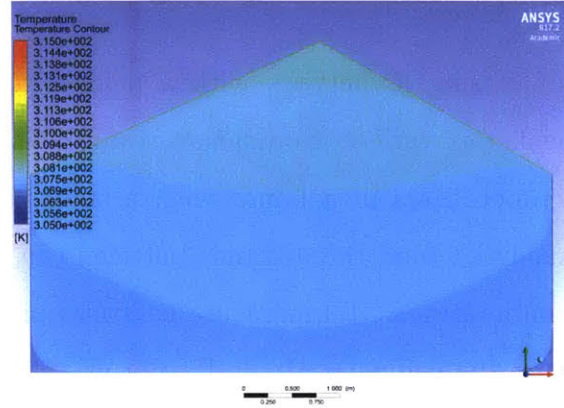
Regardless of whether the peaked roof in the Housing for All archetype is a single layer roof or a double layer roof, placing the fan 1.4m from the roof peak provides the most comfort due to reducing the mixing of hot air directly underneath the ceiling and increasing the air movement felt by the occupants. In climates with higher humidity levels, placing a ceiling fan 0.5m from a single layer peaked tin roof is not recommended as the lower level air temperature increases outweigh the thermal comfort benefits from air movements. With the proper combination of roof type and

Ceiling Temperature = 324K



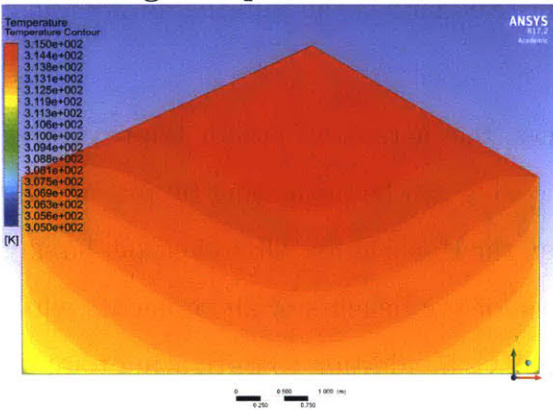
(a) Single Layer Roof, No Fan.

Ceiling Temperature = 311K



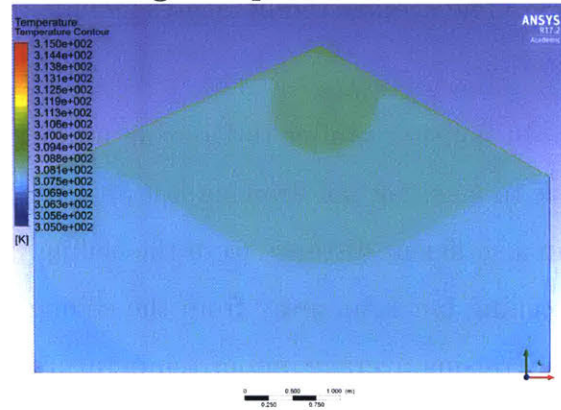
(b) Double Layer Roof, No Fan.

Ceiling Temperature = 324K



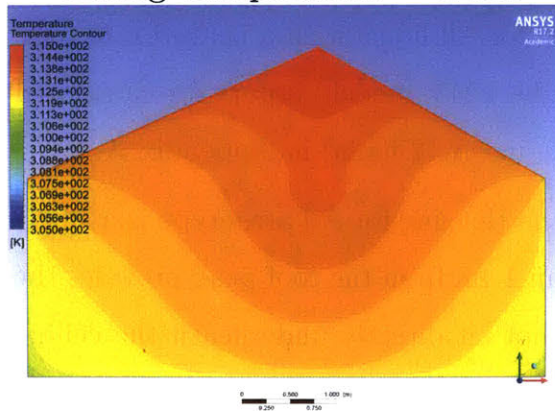
(c) Single Layer Roof, Ceiling Fan 0.5m From Ceiling Peak

Ceiling Temperature = 311K



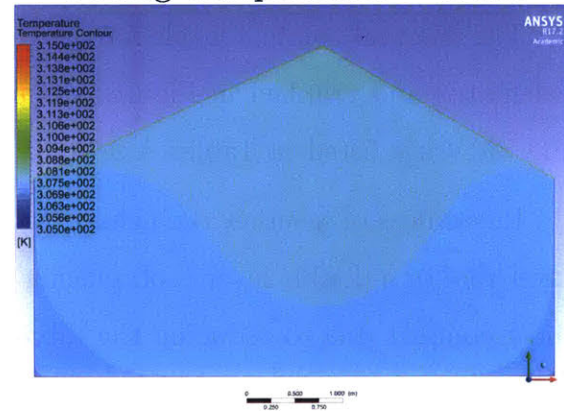
(d) Double Layer Roof, Ceiling Fan 0.5m From Ceiling Peak

Ceiling Temperature = 324K



(e) Single Layer Roof, Ceiling Fan 1.4m From Ceiling Peak

Ceiling Temperature = 311K



(f) Double Layer Roof, Ceiling Fan 1.4m From Ceiling Peak

Figure 7-34: Temperature Contours of Simulated Housing for All homes with Peaked Roofs with Various Fan Configurations

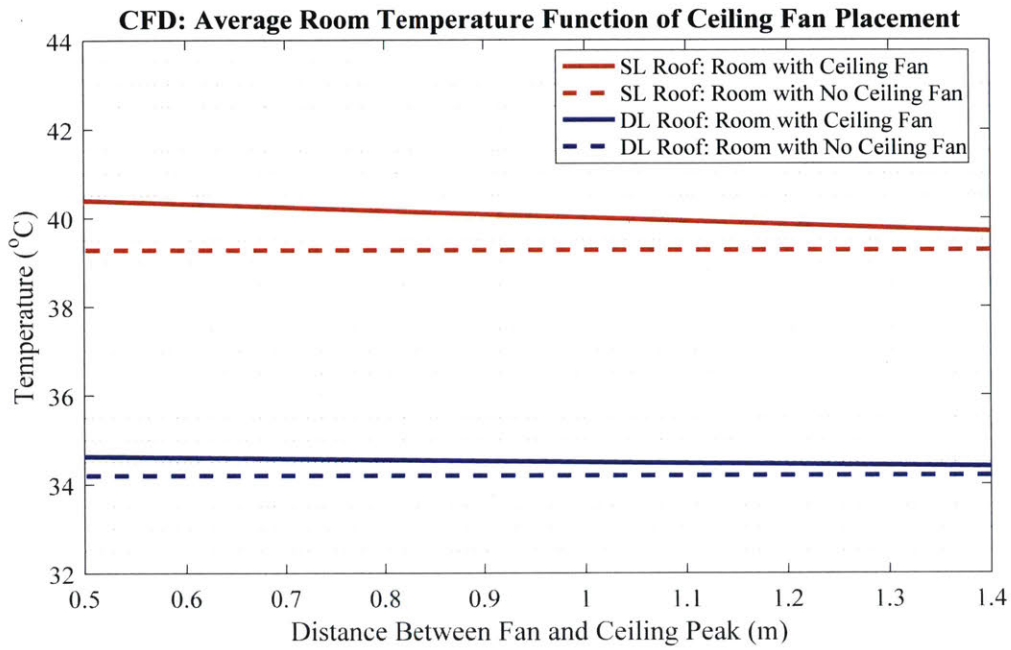


Figure 7-35: Average Room Temperatures as a Function of Ceiling Fan Placement

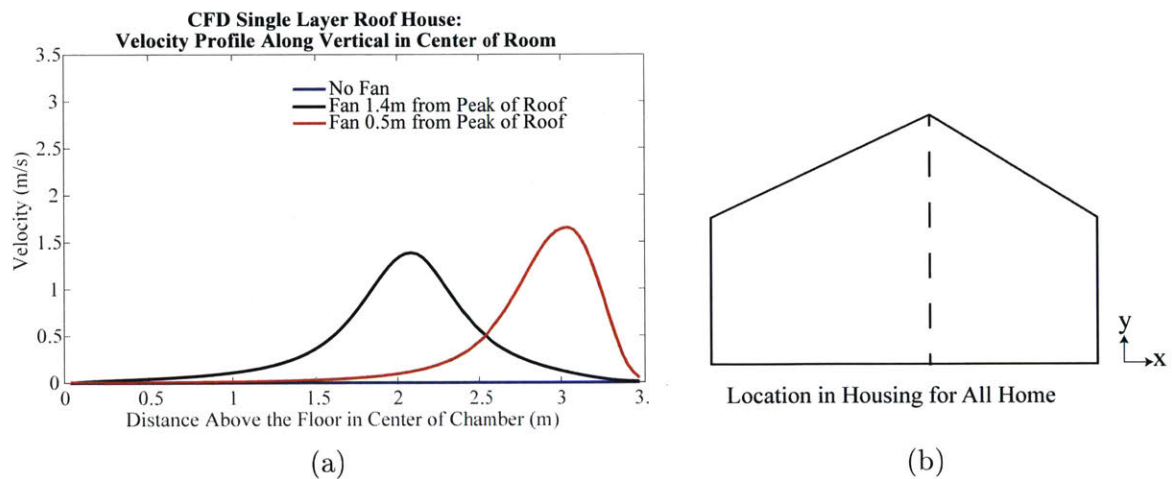


Figure 7-36: Velocity Profile Along a Vertical Line from the Floor to the Roof Peak

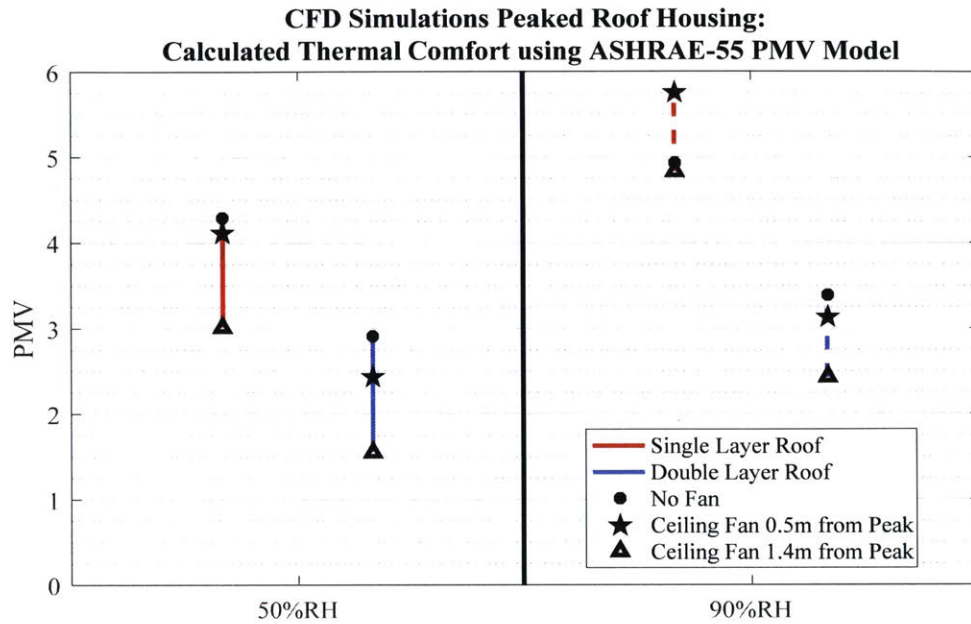


Figure 7-37: PMV Values for Simulated Housing for All Archetypes with Peaked Roofs

fan placement, PMV value can decrease from 4.6 (housing with a single layer tin roof and no ceiling fan) to 1.56 (housing with an insulated double layer roof and ceiling fan placed 1.4m from the roof peak). This translates to having a decrease in predicted percentage dissatisfied from 100% to 54%.

## 7.6 Recommendations

The results of field work and simulations show that even though air movement helps with thermal comfort in climates with moderate humidity, the benefits are diminished due to the ceiling fan’s mixing of hot air directly underneath the ceiling with the cooler air surrounding occupants at lower temperature stratifications.

In the test chamber field experiments, the use of a ceiling fan was shown to increase the percentage of time in which operative temperature exceed IMAC 80% Acceptability Standards by 6.8%. Average peak operative and air temperatures increased by more than 1°C. The simulations showed similar effects for structures with poorly in-

sulated roofs. With a moderate humidity level of 50%, ceiling fans improve thermal comfort. However, in climates with high humidity levels of 90%RH, the use of ceiling fans in homes with poorly insulated roofs can lead to more discomfort and a 0.55 increase in the Predicted Mean Vote (PMV). Lower level air temperature increases due to the mixing of hot air beneath the ceiling can outweigh the thermal comfort benefits of the air movement created by the fan. In humid conditions.

To mitigate the negative effects of the mixing of hot air beneath a poorly insulated ceiling, it is recommended to use an upright fan at a 1.6m height for single story rooms with poorly insulated roofs such as a single layer tin sheet roof and an RCC roof. The 0.3m diameter fan needs to be within 1m of the occupant. For single story homes with a double layer roof, ceiling fans provide the most thermal comfort. In homes with peaked roofs, regardless of roof type, it is recommended to place fans at least 1.4m from the ceiling peak to minimize the mixing of hot air surrounding the ceiling and to allow residents to feel the most air movement for perceived comfort.



# Chapter 8

## Conclusion

This chapter discusses recommendations on Design with Climate strategies (see Section 1.3 for details) in regions that experience extreme heat. Results from prototype field work, simulations, existing housing, and monitored pilot homes inform thermally passive housing design. Sections 8.1.1, 8.1.2, and 8.1.3 summarize and highlight guidelines for roof and wall design as well as fan placements. Following these recommendations, future work and next steps are discussed in Section 8.2.

### 8.1 Thermally Passive Design Recommendations

In order to maximize the hours of thermal autonomy in regions with extreme heat climates, roof and wall design must be integrated properly. Additionally occupants' methods of enhancing air flow via fan use must consider the housing design and geometry.

#### 8.1.1 Roof Design

Roofs often experience at least 25% of solar heat flux incident to a building. Consequently, roofs must properly insulate and protect the building interior from external heat stresses. Through test chamber experiments, pilot homes, and simulations, the following roof design modifications improve thermal comfort through passive means.

- **Low Heat Capacitance:** Ideally, roofing would be constructed from materials with a lower thermal mass than a 0.11m thick reinforced cement concrete (RCC) slab. Thermally massive roofs, such as an RCC slab, tend to decrease thermal comfort compared to a lightweight double layer insulated tin roof with a ventilated air gap during summer months where the roof surface experiences the most solar gains (Figure 8-1). According to the IMAC comfort standards, the percentage of time in which the thermally massive RCC roof exceeds the 80% acceptability standards is 13.34 percentage points greater than the amount of time in which the lightweight double layer roof exceeds comfort standards. The high heat capacitance of a thermally massive roof allows the roof to "store" the solar heat gains, making the interior environment warmer for a larger percentage of the day. The RCC roof, however, still does not reach the peak temperatures that the single layer tin roof does.
- **Insulation:** It is necessary to add insulation to the traditional RCC roof. During the summer, the insulation protects the interior from the effects of solar heat gains. In prototype test chambers, throughout the day, ceiling temperatures in the test chamber with an uninsulated RCC slab roof exceeded outdoor ambient air temperatures by more than 5°C. With the addition of insulation, ceiling temperatures remained within 5°C of outdoor ambient air temperatures. This modification decreased the percentage of time test chamber operative temperatures surpassed the IMAC 80% upper limit comfort threshold by 8.5 percentage points. During the winter, field experiments demonstrated that the insulation helps keep the ceiling warmer despite the RCC slab temperatures being more than 10°C cooler than outdoor ambient air temperatures during midday (Figure 4-2). The percentage of time in which the single layer RCC slab ceiling temperatures fell below outside temperatures in the winter month of December was 20 percentage points greater than that of the double layer insulated RCC slab. Simulations show that an air gap which provides some measure of insulation, can increase nighttime minimum operative temperatures by 1°C.



In summary, the results show that the addition of insulation to an RCC roof improves thermal comfort in both summer and winter conditions.

- **Emissivity:** A low emissivity ceiling surface effectively reduces operative temperatures in a room where ceiling temperatures exceed outdoor ambient air temperatures. During the test chamber data collection period, the operative temperatures of the low emissivity single layer corrugated galvanized iron (CGI) roof (R1) remained within the IMAC and ASHRAE comfort standards for a larger percentage of the time than that of the RCC slab despite average peak ceiling temperatures of R1 ceiling exceeding that of R2 ceiling as shown in Figure 8-1. Though ceiling temperatures for the CGI roof often exceeded 45°C, the radiant temperatures did not exceed 40°C as they often did in the test chamber with the RCC slab; showing that less radiation heat transfer from the low emissivity ceiling is reducing the operative temperatures.

Table 8.1 shows the performance rankings of the test chamber roofs based on operative temperature deviations from daily peak temperatures.

Table 8.1: Performance Rankings of Test Chamber Roof Types Based Operative Temperatures Peak Deviations

<i>Ranking</i>	<i>CGI Roof Type</i>
1 <sup>st</sup>	Double Layer CGI Roof with Ventilated Air Gap and Mud Roll Insulation
2 <sup>nd</sup>	Double Layer CGI Roof with Ventilated Air Gap and Bubble Wrap Insulation
3 <sup>rd</sup>	Double Layer RCC Roof with Ventilated Air Gap and Thermocol Insulation
4 <sup>th</sup>	Single Layer CGI Roof
5 <sup>th</sup>	RCC Slab Roof

Implementation of simulated and prototype test chamber roofs designs in four pilot homes demonstrated the effectiveness of a double layer ventilated roof on improving thermal comfort. All four pilot homes with the double layer roof geometry (see Section 3.3 for more details) remained within the ASHRAE 80% comfort standards for more than 60% of operating hours. The modification on the traditional CGI and

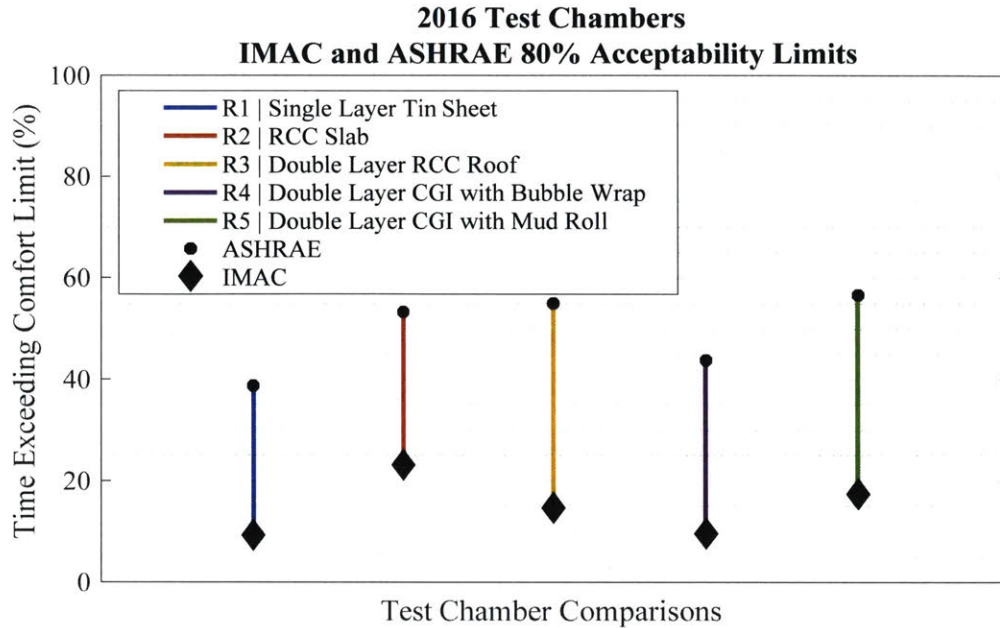


Figure 8-1: Percentage of the Data Collection Period (June 17, 2016 to December 30, 2016) in which 2016 Test Chamber Operative Temperatures Exceeded IMAC and ASHRAE 80% Acceptability Limits

Mangalore tile roof adds an air gap for insulation and allows hot air to ventilate through the air gap. In terms of the IMAC 80% acceptability criteria, the pilot homes' operative temperatures meet comfort standards more than 80% of the time, an improvement to the 65% of time meeting comfort standards in one of the monitored existing homes. Considering both the perception survey and the collected data, the ventilated Mangalore tile and mud roll roof design emerges as the best performing pilot roof type. Though all the pilot homes with double layer roofs provide more thermal comfort than existing homes, the ventilated Mangalore tile and mud roll roof best meets the aesthetic and social requirements of the residents. Additionally, this roof remained within the IMAC comfort range 88.5% of the time. On average, the interior air, south wall, ceiling and operative temperature were all at least 6°C cooler than exterior temperatures during the hottest part of the day. The rankings of the Housing for All homes based on the homes' operative temperature deviations from the daily maximum are listed in Table 8.2.

Table 8.2: Performance Rankings of Housing for All Homes Based Operative Temperatures Peak Deviations

<i>Ranking Housing for All Home</i>		
1 <sup>st</sup>	H1	Ventilated Double Layer Mangalore Tile and Mud Roll
2 <sup>nd</sup>	H3	Ventilated Double Layer Tin and Wood
3 <sup>rd</sup>	H2	Ventilated Double Layer Mangalore Tile and Wood
4 <sup>th</sup>	H4	Ventilated Double Layer Tin and Bubble Wrap

## Roof Implementation

The dissemination of the thermally passive roof designs conceived from prototype field work and simulations begins with the implementation of these passive techniques in four pilot homes Bhuj (see Section 3.3). Through this pilot homes case study, the implementation team can understand how housing can best meet the health, aesthetic, and social needs of those in resource-constrained regions. Given the successful implementation of thermally passive designs in Bhuj, these thermally passive methods can be introduced to other parts of India whether through new housing construction policies, product development and sales, or workforce and homeowner education.

An initial cost analysis was conducted on roofs to determine the affordability and the value of some proposed thermally passive designs for end users, policy makers, and possible entrepreneurs. In this report, affordability price points are set by EWS income group available resources (Section 1.2). Assuming housing is no more than four times the annual income (Deepak Parkh et al., 2008) and families spend up to 25% of the available housing budget on roofing (Rupesh Hurmade and Tejas Kotak, 2016), the roof prices should be approximately 100,000Rs ( \$1,500). Table 8.3 shows the material and labor costs of common roof types currently on the market as well as the size of roof given a 100,000Rs ( \$1500) budget. Given the budget of a homeowner from the EWS, the homeowner can afford to cover  $400\text{ ft}^2$  (  $37\text{ m}^2$ ) home with the following roof types:

- Single-layer 0.5 mm Metal Sheet Painted White

Table 8.3: Cost of Various Roof Types

Roof Type	Labor Cost (Rs/sqft)	Material Cost (Rs/sqft)	Total Cost (Rs/sqft)
Single-layer 0.5mm Metal Sheet Painted White	105	50	155
Mangalore Pattern Tiles	115	68	183
Country Tiles with 25mm Wood Plank Substructure	125	105	230
Mangalore Tiles with Mud Roll Insulation	165	68	233
400mm Thatch Panel, Alang Style (Braided Straw)	240	60	300
RCC, 120-150mm	225-300		225-300
Ferrocement Channels	170	50	220
Double-layer 0.5mm White Metal Sheet with Radiant Barrier	135	50	185
Double-layer 0.5mm White Metal Sheet with Bubble Wrap Insulation	155	50	205
Double-layer Clay Tile with Rigid Insulation Panels on Bottom	195	68	263
ModRoof (Turquoise Panel ReMaterial Roof)	350	140	490

- Mangalore Pattern Tiles
- Country Tiles with 25mm Wood Plank Substructure
- Mangalore Tiles with Mud Roll Insulation
- Ferrocement Channels
- Double-layer 0.5 mm White Metal Sheet with Radiant Barrier
- Double-layer 0.5 mm White Metal Sheet with Bubble Wrap Insulation

The proposed double layer roofs fit within the price points of lower income families. Should families desire a more aesthetically pleasing roof, the Mangalore Tile roof, though more expensive than the single layer sheet metal, still remains affordable. With subsidies from India's large-scale Housing for All program to provide housing for low-income residents throughout the country, these thermally passive methods could serve the needs of the approximate 1.25 million impoverished households residing in India's hot arid climates. The cost analysis also shows that the thermally passive roof design would also be economically advantageous for those in the Middle Income Group (MIG).

Assuming a roof area of  $1,500\text{ft}^2$  ( $140\text{m}^2$ ), residents could save up to 172,500Rs ( \$2,684), by opting for a Double-layer 0.5 mm White Metal Sheet with Radiant Barrier over a traditional RCC roof. The more expensive of the double layer roof structures, double-layer Mangalore clay tile with rigid insulation, would save a family 55,500Rs ( \$864) compared to the RCC roof. This cost analysis does not include the possible savings in energy costs associated with a thermally autonomous home.

### 8.1.2 Wall Design

Simulations, test chambers, and pilot homes experimental results indicate that regardless of roof type, wall protection is necessary for achieving thermal autonomy in Bhuj. The wall protection reduces the negative effects of solar heat gains and dampens external heat strains, allowing the thermally massive walls to retain coolness from

night conditions. Additionally, thermally passive roof designs work more effectively in homes with well-protected walls.

Wall protection and heat avoidance methods include

- **Insulation:** Simulation results showed that by adding insulation of  $R = 0.25m^2K/W$ , the peak indoor air and operative temperatures decrease by at least  $1^\circ C$ . When wall protection is coupled with a thermally passive roof such as a double layer roof with a ventilated air gap and radiant barrier, operative temperatures decrease by as much as  $5^\circ C$  compared to an uninsulated test room with a single layer tin sheet. Field work confirmed that the addition of 15cm thick straw as exterior wall insulation led to a  $1^\circ C$  decrease in maximum air temperatures and a  $3^\circ C$  decrease in maximum operative temperatures compared an uninsulated test chamber. In buildings with a well designed thermally passive roof, the average maximum air temperature decreased by as much as  $3^\circ C$  compared to a baseline single layer tin sheet. Maximum interior south wall, air, and operative temperatures decrease by  $5^\circ C$ . The aforementioned simulation and fieldwork results conclude that insulation is a viable wall protection technique.
- **Wall Color:** Depending on climate, different wall treatments are preferable. In places with a climate characterized as hot/arid or hot/humid, painting walls white lowers daytime south wall temperatures by more than  $4^\circ C$  when compared to a wall covered by a black tarp (Section 5.3). The decrease in wall temperature lead to a  $2^\circ C$  decrease in radiant and indoor temperatures. However, for colder regions, dark colored exterior walls are preferable to heat the building envelope. Similar to field experiment conclusions, simulations results for a 2.4m by 2.4m test chamber show, changing the wall absorptivity in the visible light spectrum from 0.75 to 0.2 reduces peak operative temperatures by  $2^\circ C$ .

The performance rankings of these wall protection methods are listed in Table 8.4.

This passive cooling technique of protected thermally massive wall works most effectively in regions where the climate is characterized by large diurnal temperature shifts, low humidity levels, and minimum cloud coverage. In the context of Bhuj,

a thermally massive wall will work best in the months of October to April where an average month has are less than ten cloudy days and diurnal temperatures shifts are greater than 15°C. Measured field data shows, though peak temperatures are greater in the pre-monsoon season (March-April) season and average temperatures are comparable throughout March-June, peak temperatures in test chambers during pre-monsoon season (March-April) were 3°C lower than in monsoon season (June-August, see Section 5.1). Consequently, the use of thermal mass as a passive cooling technique is recommended for dry regions with at least 10°C diurnal shift and humidity levels below 50%RH.

Table 8.4: Performance Rankings of Wall Treatments Based on Simulated Operative Temperature Deviations from Outdoor Ambient Temperature Peaks

<i>Ranking</i>	<i>Wall Insulation</i>
1 <sup>st</sup>	Exterior Wall Insulation, $R = 1m^2K/W$
2 <sup>nd</sup>	Exterior Wall Insulation, $R = 0.25m^2K/W$
3 <sup>rd</sup>	White Painted Exterior, $\alpha = 0.2$

### 8.1.3 Use of Ceiling Fan

In hot climates, residents often use ceiling fans as a low energy means to improve thermal comfort and to mitigate the risks that come with extreme heat. Though air movement helps with thermal comfort in climates with moderate humidity, the benefits are diminished when the ceiling fan is placed in a home with a poorly insulated roof. This is due to the mixing of hot air directly underneath the ceiling with the cooler air surrounding occupants. In the test chamber field experiments, the use of a ceiling fan was shown to increase the percentage of time in which operative temperature exceeded the IMAC 80% Acceptability Standards by 6.8 percentage points. Average peak operative and air temperatures increased by more than 1°C.

The simulations showed similar effects for structures with poorly insulated roofs. With a moderate humidity level of 50%, ceiling fans slightly improve thermal comforts.

However, in climates with high humidity levels of 90%RH, the use of ceiling fans in homes with poorly insulated roofs lead to more discomfort and a 0.55 increase in the Predicted Mean Vote (PMV). Lower level air temperature increases due to the mixing of hot air beneath the ceiling outweigh the thermal comfort benefits of the air movement created by the fan.

In humid conditions, to mitigate the negative effects of the mixing of hot air beneath a poorly insulated ceiling, occupants should use an upright fan at a 1.6m height for single story rooms with poorly insulated roofs such as a single layer tin sheet roof and an RCC roof. The 0.3m diameter fan needs to be within 1m of the occupant to improve thermal comfort. For single story homes with a double layer roof, ceiling fans provide the most thermal comfort. In homes with peaked roofs, regardless of roof type, it is recommended to place fans at least 1.4m from the ceiling peak to minimize the mixing of hot air surrounding the ceiling and to allow residents to feel the most air movement for perceived comfort. Table 8.5 and Table 8.6 list the rankings of fan usage in a home with a well-insulated roof and a poorly insulated roof.

Table 8.5: Home with a Well Insulated Roof: Performance Rankings of Fan Location and Usage Based on PMV Values

<i>Ranking</i>	<i>Fan Orientation</i>
1 <sup>st</sup>	Ceiling Fan, 0.6m Diameter
2 <sup>nd</sup>	Upright Fan, 0.3m Diameter less than 1m from the Occupant
3 <sup>rd</sup>	No Fan

\* This ranking holds true regardless of humidity levels.



Table 8.6: Home with a Single Layer Tin Sheet: Performance Rankings of Fan Location and Usage Based on PMV Values Assuming a 90%RH

<i>Ranking Fan Orientation</i>	
1 <sup>st</sup>	Upright Fan, 0.3m Diameter less than 1m from the Occupant
2 <sup>nd</sup>	No Fan
3 <sup>rd</sup>	Ceiling Fan, 0.6m Diameter

\* If humidity levels are moderate (<50%RH), the use of a ceiling fan is preferred to no fan usage.

## 8.2 Recommendations for Future Work

This section outlines possible future work in thermally passive housing designs in resource-constrained regions. Proposed projects and investigations include refining designs in extreme heat climates to adapting designs for application in cool climates.

### 8.2.1 Refining Thermal Autonomous Housing in Extreme Heat Climates.

#### Optimizing Night Time Radiant Cooling and Minimizing Daytime Solar heat Gains

In Chapter 6, simulations indicate that during the summer, tin roofs require a low emissivity radiant barrier during the day in order to reduce operative temperatures by at least 5°C. An alternating radiant air gap roof can further lower peak operative temperatures by 2°C if walls are well-insulated,  $R > 0.5m^2K/W$ . Table 8.7 outlines the rankings of the various simulated CGI roof Types discussed in Chapter 6.

For the RCC roof, simulation results show the alternating insulation and radiant barrier system did not significantly impact thermal comfort during the summer. The RCC ceiling temperatures do not experience the 25°C diurnal shifts that a CGI ceiling can experience. A constant radiant barrier system causes similar decreases in peak temperatures as an alternating radiant barrier/insulation system. Residents do not need to exert extra labor for an alternating system.

During the winter season or in colder climates, it is recommended to place a low emissivity surface on the interior of the CGI sheet roof at night to increase operative temperatures by  $>1^{\circ}\text{C}$  for winter heating. For the RCC roof, a low emissivity surface should be installed 2.5 hours after the nightly minimum exterior temperatures and removed 2.5 hours after the daily maximum exterior temperatures in order the increase operative temperatures by  $1^{\circ}\text{C}$ .

Table 8.7: Performance Rankings of Simulated CGI Roof Types Based Operative Temperatures Peak Deviations

<i>Ranking</i>	<i>CGI Roof Type</i>
1 <sup>st</sup>	CGI Roof with a Ventilated Air Gap and an Alternating Radiant Barrier
2 <sup>nd</sup>	CGI Roof Type with no Air Gap and an Alternating Radiant Barrier
3 <sup>rd</sup>	CGI Roof Type with a Ventilated Air Gap and a Constant Radiant Barrier
4 <sup>th</sup>	CGI Roof Type with no Air Gap and a Constant Radiant Barrier
5 <sup>th</sup>	CGI Roof Type with no Air Gap and no Radiant Barrier

Ideally, the results of these simulations would be confirmed by field experiments to determine if the concept of an alternating air gap radiant barrier system would be effective in practice. Should this method be effective, then researchers would need to develop a low-cost durable mechanism to easily change the emissivity and geometry of the roof daily.

### **Dissemination of Thermally Passive Designs in Resource-Constrained Regions**

Though many of the thermally passive cooling methods tested and implemented in Bhuj worked successfully by keeping operative temperatures withing IMAC comfort standards for more than 80% of operating hours, these methods might not easily translate to other parts of India or the world. The methods in Bhuj incorporated local artisan skills and recycled materials, such as wood from a nearby ship wrecking years and mud rolls with local straw. To successfully apply these thermally passive cooling techniques in other regions, there needs to be a dissemination model which

considers the locally available materials of a specified region. This model could be in the form of a modular roofing and housing designs or a set of housing construction guidelines that builders could follow. Though local resources vary by region, basic conclusions regarding thermal comfort in extreme heat regions still hold. Walls must be insulated or painted white, occupants should practice night flush ventilation, and a ventilated double layer roof with insulation improves comfort.

### **8.2.2 Housing Design Adaption for Thermal Control in Cold Climates**

Many of the Design with Climate techniques tested and implemented in Bhuj can be modified for resourced-constrained communities in regions with cooler temperatures. Due to limited access to clean energy, many residents in the developing world use open fires to cope with the cold weather. Thermally passive housing would reduce the need to use open fires, saving energy costs and improving health. Future work in this field could begin with a case study regions to start adapting thermally passive heating techniques. In this a preliminary performance assessment, the research goals include:

1. Assess design and performance of existing homes in the case study region to understand operational and material constraints, and analyze which structural surfaces are most in need of attention.
2. Develop preliminary designs using observed materials, based on passive comfort; on scalability, design, and construction,
3. Develop and test new insulation materials based on the use of indigenous low-cost materials.
4. Design an innovative roof system that simultaneously reduces earthquake-related injury in earthquake prone regions and provides improved thermal performance;
5. Apply the new materials and systems in the construction of full-scale homes based on proposed designs; and

6. Gather notes on occupant perception to refine (5) and work towards an accepted solution.

The future research in thermal passive heating needs to include issues of energy efficiency, sustainable materials, thermal comfort, air quality, and workforce training in the development of housing. Insulation concepts developed for India will in many instances also work well in cold climates. The addition of a 5cm layer of a low conductivity material ( $k=0.05W/mK$ ) on the interior of a 15cm stone wall will increase the insulation level of the wall by a factor of four or five. Within a short time period (usually one year or less) after a home is insulated, the savings in firewood used for heating will be equal to the volume of wood used for the insulated panels. Additionally, the innovative double layer ventilated air gap roof system developed in Bhuj, could be adapted to provide roof insulation for homes in regions that experience prolonged cold seasons. Beyond India, the approximate one billion people living in resource-constrained regions can adopt low-cost thermal passive techniques to build housing to shield against the harsh environmental conditions (United Nations, 2016).

# Appendix A

## Tables

Table A.1: Inputs for Calculating PMV of Field Experiment Test Chambers at 50%RH

Field Work Test Chambers	Single Layer Roof		Double Layer Roof	
	On	Off	On	Off
Fan State				
Air Temperature (°C)	32.34	31.39	31.49	31.51
Mean Radiant Temperature (°C)	32.12	31.20	31.10	31.58
Air Speed (m/s)	2.5	0	2.5	0
Metabolic Rate (met)	1.2	1.2	1.2	1.2
Clothing Level (clo)	0.5	0.5	0.5	0.5
Humidity (%RH)	50	50	50	50
PMV	0.61	1.66	0.04	1.71

Table A.2: Inputs for Calculating PMV of Field Experiment Test Chambers at 90%RH

Field Work Test Chambers	Single Layer Roof		Double Layer Roof	
	On	Off	On	Off
Fan State				
Air Temperature (°C)	32.34	31.39	31.49	31.51
Mean Radiant Temperature (°C)	32.12	31.20	31.10	31.58
Air Speed (m/s)	2.5	0	2.5	0
Metabolic Rate (met)	1.2	1.2	1.2	1.2
Clothing Level (clo)	0.5	0.5	0.5	0.5
Humidity (%RH)	90	90	90	90
PMV	1.39	2.03	0.59	2.1

Table A.3: Inputs for Calculating PMV of Simulated Single Layer Roof Test Chambers at 50%RH

Fan State	Horizontal fan at 1m	Horizontal fan at 1.6m	No Fan	Ceiling Fan
Air Temperature (°C)	35.99	36.01	36.38	39.33
Mean Radiant Temperature (°C)	37.08	37.08	37.16	37.75
Air Speed (m/s)	0.5	2	0	2.5
Humidity (%RH)	50	50	50	50
Metabolic Rate (met)	1.2	1.2	1.2	1.2
Clothing Level (clo)	0.5	0.5	0.5	0.5
PMV	2.74	2.1	3.71	3.03

Table A.4: Inputs for Calculating PMV of Simulated Single Layer Roof Test Chambers at 90%RH

Fan State	Horizontal fan at 1m	Horizontal fan at 1.6m	No Fan	Ceiling Fan
Air Temperature (°C)	35.99	36.01	36.38	39.33
Mean Radiant Temperature (°C)	37.08	37.08	37.16	37.75
Air Speed (m/s)	0.5	2	0	2.5
Humidity (%RH)	90	90	90	90
Metabolic Rate (met)	1.2	1.2	1.2	1.2
Clothing Level (clo)	0.5	0.5	0.5	0.5
PMV	3.1	3.25	4.25	4.62

Table A.5: Inputs for Calculating PMV of Simulated Double Layer Roof Test Chambers at 50%RH

Fan State	Horizontal fan at 1m	Horizontal fan at 1.6m	No Fan	Ceiling Fan
Air Temperature (°C)	33.16	33.17	33.35	34.21
Mean Radiant Temperature (°C)	33.91	33.91	33.95	34.12
Air Speed (m/s)	0.5	2	0	2.5
Humidity (%RH)	50	50	50	50
Metabolic Rate (met)	1.2	1.2	1.2	1.2
Clothing Level (clo)	0.5	0.5	0.5	0.5
PMV	1.97	1.14	2.78	1.34

Table A.6: Inputs for Calculating PMV of Simulated Double Layer Roof Test Chambers at 90%RH

Fan State	Horizontal fan at 1m	Horizontal fan at 1.6m	No Fan	Ceiling Fan
Air Temperature (°C)	33.16	33.17	33.35	34.21
Mean Radiant Temperature (°C)	33.91	33.91	33.95	34.12
Air Speed (m/s)	0.5	2	0	2.5
Humidity (%RH)	90	90	90	90
Metabolic Rate (met)	1.2	1.2	1.2	1.2
Clothing Level (clo)	0.5	0.5	0.5	0.5
PMV	2.48	1.9	3.24	2.2

Table A.7: Inputs for Calculating PMV of Simulated RCC Roof Room at 50%RH

Fan State	Horizontal fan at 1m	Horizontal fan at 1.6m	No Fan	Ceiling Fan
Air Temperature (°C)	36.17	36.18	36.59	37.21
Mean Radiant Temperature (°C)	36.31	36.32	36.40	36.52
Air Speed (m/s)	0.5	2	0	2.5
Humidity (%RH)	50	50	50	50
Metabolic Rate (met)	1.2	1.2	1.2	1.2
Clothing Level (clo)	0.5	0.5	0.5	0.5
PMV	3.01	2.09	3.62	2.32

Table A.8: Inputs for Calculating PMV of Simulated RCC Roof Room at 90%RH

Fan State	Horizontal fan at 1m	Horizontal fan at 1.6m	No Fan	Ceiling Fan
Air Temperature (°C)	36.17	36.18	36.59	37.21
Mean Radiant Temperature (°C)	36.31	36.32	36.40	36.52
Air Speed (m/s)	0.5	2	0	2.5
Humidity (%RH)	90	90	90	90
Metabolic Rate (met)	1.2	1.2	1.2	1.2
Clothing Level (clo)	0.5	0.5	0.5	0.5
PMV	3.65	3.22	4.16	3.61

Table A.9: Inputs for Calculating PMV of Simulated Housing for All Room with Single Layer Peaked Roof at 50%RH

Fan State	Fan 1.4m below ceiling peak	No Fan	Fan 0.5m below ceiling peak
Air Temperature (°C)	39.71	39.28	42.24
Mean Radiant Temperature (°C)	37.82	37.74	38.33
Air Speed (m/s)	1.5	0	0.3
Humidity (%RH)	50	50	50
Metabolic Rate (met)	1.2	1.2	1.2
Clothing Level (clo)	0.5	0.5	0.5
PMV	3.02	4.29	4.6



Table A.10: Inputs for Calculating PMV of Simulated Housing for All Room with Single Layer Peaked Roof at 90%RH

Fan State	Fan 1.4m below ceiling peak	No Fan	Fan 0.5m below ceiling peak
Air Temperature (°C)	39.71	39.28	42.24
Mean Radiant Temperature (°C)	37.82	37.74	38.33
Air Speed (m/s)	1.5	0	0.3
Humidity (%RH)	50	50	50
Metabolic Rate (met)	1.2	1.2	1.2
Clothing Level (clo)	0.5	0.5	0.5
PMV	4.83	4.93	5.75

Table A.11: Inputs for Calculating PMV of Simulated Housing for All Room with Double Layer Peaked Roof at 50%RH

Fan State	Fan 1.4m below ceiling peak	No Fan	Fan 0.5m below ceiling peak
Air Temperature (°C)	34.40	34.20	34.63
Mean Radiant Temperature (°C)	34.16	34.12	34.21
Air Speed (m/s)	1.5	0	0.3
Humidity (%RH)	50	50	50
Metabolic Rate (met)	1.2	1.2	1.2
Clothing Level (clo)	0.5	0.5	0.5
PMV	1.56	2.9	2.43

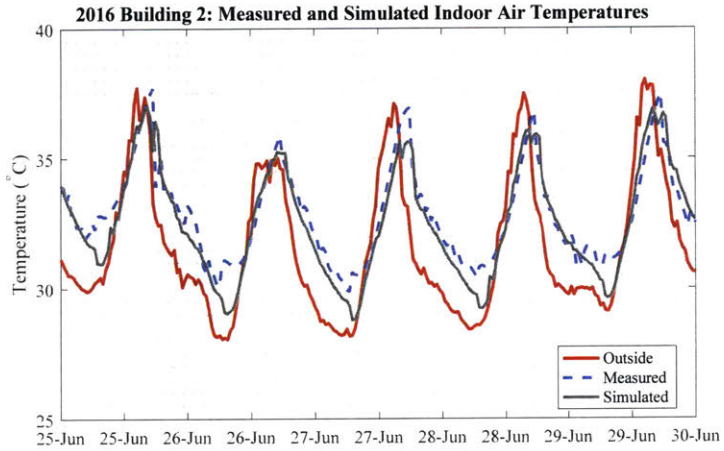
Table A.12: Inputs for Calculating PMV of Simulated Housing for All Room with Double Layer Peaked Roof at 90%RH

Fan State	Fan 1.4m below ceiling peak	No Fan	Fan 0.5m below ceiling peak
Air Temperature (°C)	34.40	34.20	34.63
Mean Radiant Temperature (°C)	34.16	34.12	34.21
Air Speed (m/s)	1.5	0	0.3
Humidity (%RH)	50	50	50
Metabolic Rate (met)	1.2	1.2	1.2
Clothing Level (clo)	0.5	0.5	0.5
PMV	2.43	3.38	3.13

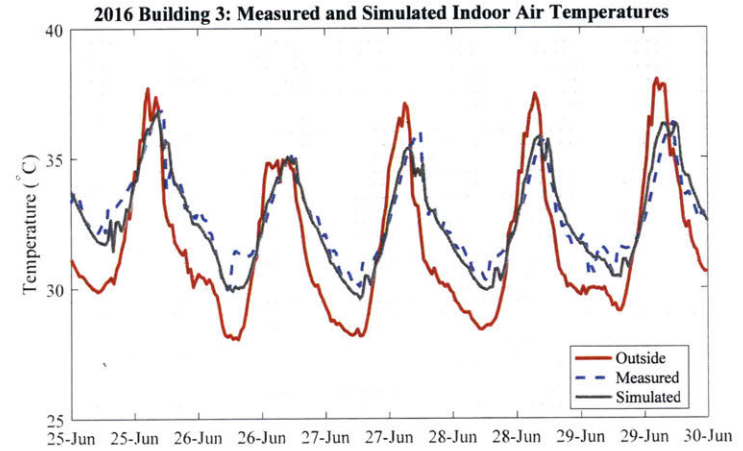


# Appendix B

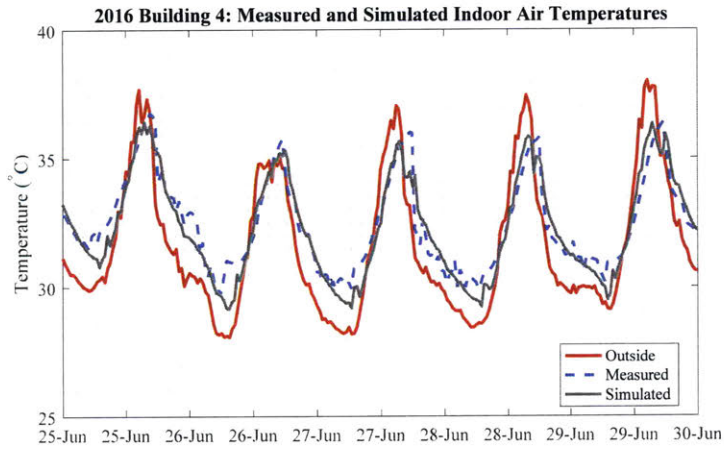
## Figures



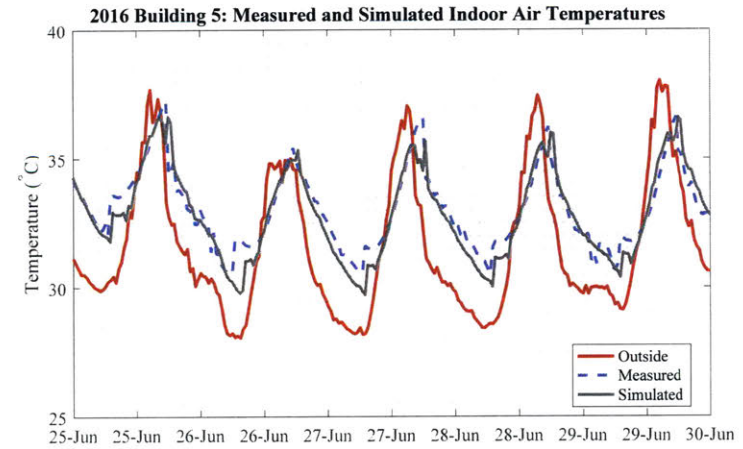
(a) Test Chamber with RCC Slab Roof



(b) Test Chamber with Insulated and Ventilated RCC Roof

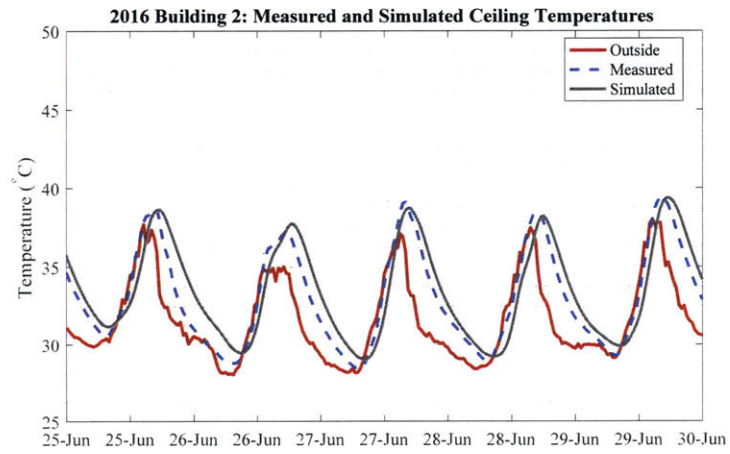


(c) Test Chamber with Ventilated Double Layer Tin Roof Insulated with Bubble Wrap

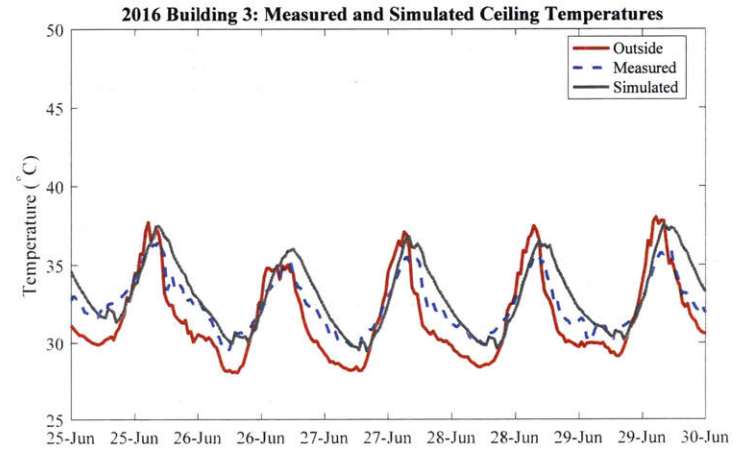


(d) Test Chamber with Ventilated Double Layer Tin Roof Insulated with Mud Rolls

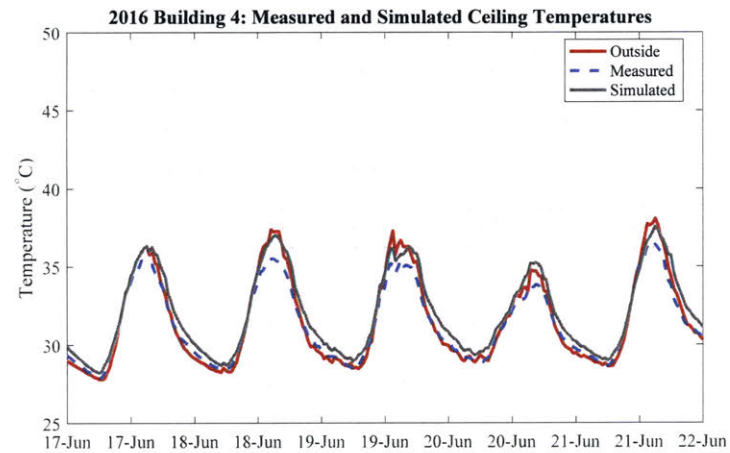
Figure B-1: Comparison Between Indoor Air Temperatures in Simulated Test Chambers with Full Scale Prototype Test Chambers with Roof Types R2-R5



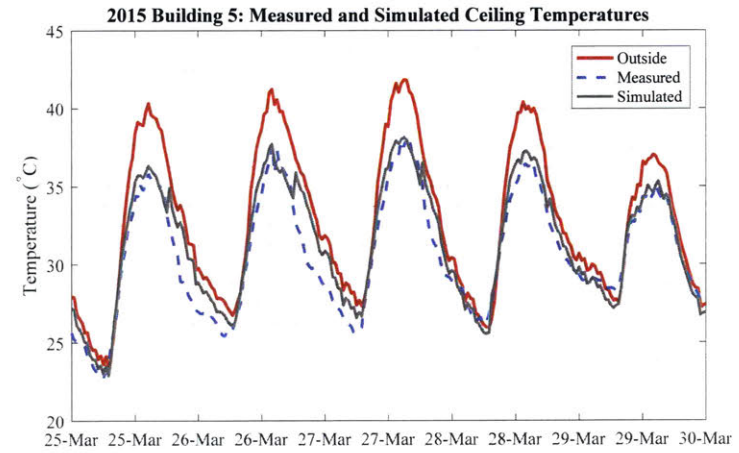
(a) Test Chamber with RCC Slab Roof



(b) Test Chamber with Insulated and Ventilated RCC Roof

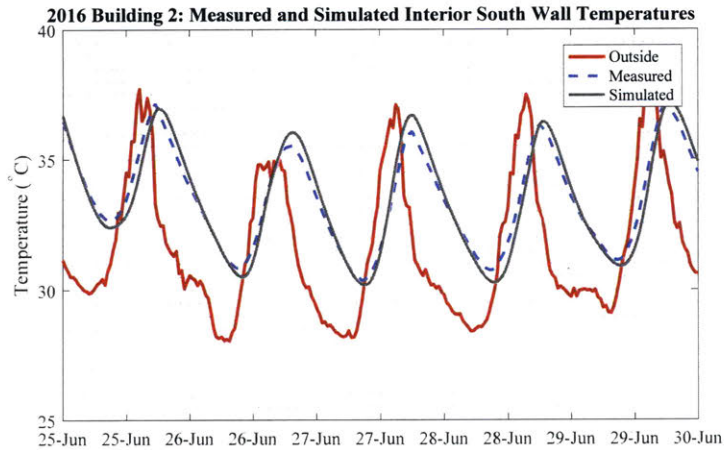


(c) Test Chamber with Ventilated Double Layer Tin Roof Insulated with Bubble Wrap

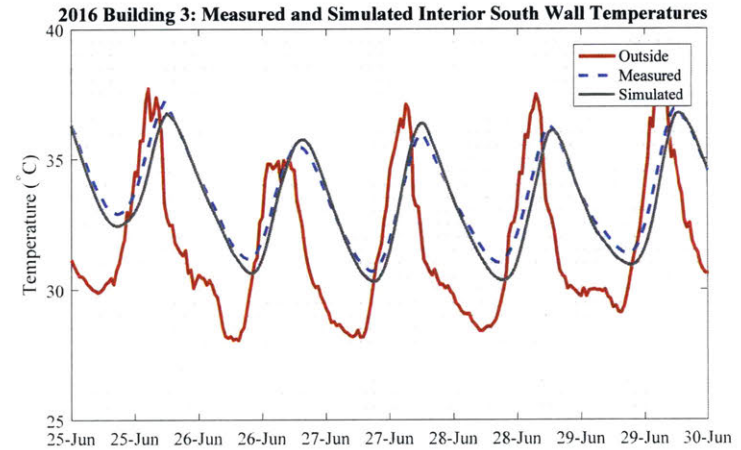


(d) Test Chamber with Ventilated Double Layer Tin Roof with Radiant Barrier

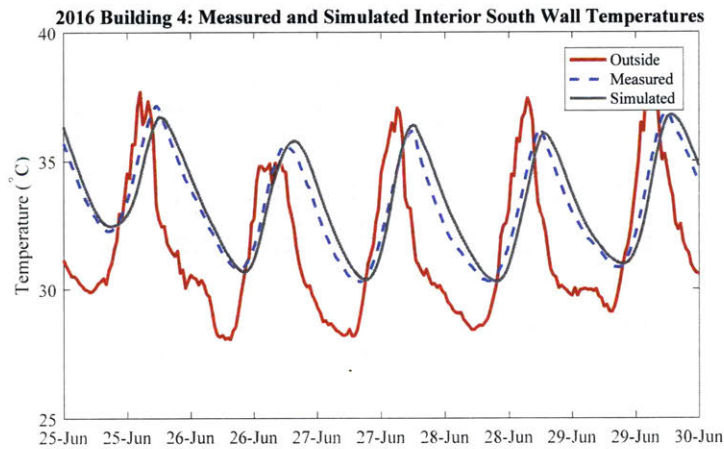
Figure B-2: Comparison Between Interior Ceiling Temperatures in Simulated Test Chambers with Full Scale Prototype Test Chambers with Roof Types R2-R5



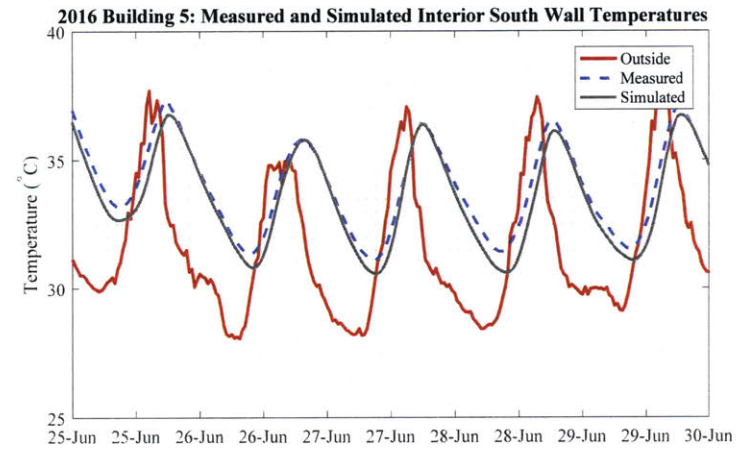
(a) Test Chamber with RCC Slab Roof



(b) Test Chamber with Insulated and Ventilated RCC Roof



(c) Test Chamber with Ventilated Double Layer Tin Roof Insulated with Bubble Wrap



(d) Test Chamber with Ventilated Double Layer Tin Roof Insulated with Mud Rolls

Figure B-3: Comparison Between Interior South Wall Temperatures in Simulated Test Chambers with Full Scale Prototype Test Chambers with Roof Types R2-R5

# Bibliography

- A. Rapoport (1969). *House Form and Culture. Englewood Cliffs.* Prentice-Hall, New Jersey.
- American Society of Heating, Refrigerating and Air-Conditioning Engineers (2005). *ASHRAE Handbook: Fundamentals.* American Society of Heating, Refrigerating, and Air-Conditioning Engineers, University of Virginia. Google-Books-ID: mmVFAAAAYAAJ.
- Angus Deaton (2008). Height, Health, and Inequality: The Distribution of Adult Heights in India. *The American Economic Review*, 98(2):468–474.
- Anshul Dhamija (2009). Big City Houses Out of Middle Income Group Reach - Times of India.
- Ansys Inc. (2016). ANSYS Fluent - CFD Software.
- Arens, Edward, Turner, Stephen, Paliaga, Gwelen, and Zhang, Hui (2009). Moving Air For Comfort. *ASHRAE Journal*, (51.5).
- ASHRAE (2013). ASHRAE Standard 55-2013, Thermal Environmental Conditions for Human Occupancy. American National Standards Institute American Society of Heating Refrigerating and Air Conditioning Engineers, Atlanta, GA.
- ASHRAE and Fanger (2017). Human Thermal Comfort | Sustainability Workshop.
- Azhar, G. S., Mavalankar, D., Nori-Sarma, A., Rajiva, A., Dutta, P., Jaiswal, A., Sheffield, P., Knowlton, K., and Hess, J. J. (2014). Heat-Related Mortality in India: Excess All-Cause Mortality Associated with the 2010 Ahmedabad Heat Wave. *PLOS ONE*, 9(3):e91831.
- B. Rudofsky (1964). *Architecture Without Architects, a Short Introduction to Non-Pedigreed Architecture.* Museum of Modern Art, New York.
- Balcomb, J. D. (1992). Longwave Radiation on the Outside of Buildings. In *Passive Solar Buildings*, page 160. MIT Press.
- Barry, E. and Davenport, C. (2016). Emerging Climate Accord Could Push A/C Out of Sweltering India's Reach. *The New York Times*.

- Binici, H., Eken, M., Dolaz, M., Aksogan, O., and Kara, M. (2014). An environmentally friendly thermal insulation material from sunflower stalk, textile waste and stubble fibres. *Construction and Building Materials*, 51:24–33.
- Bisoniya, T. S., Kumar, A., and Baredar, P. (2013). Experimental and analytical studies of earth-air heat exchanger (EAHE) systems in India: A review. *Renewable and Sustainable Energy Reviews*, 19:238–246.
- Blazejczyk, K., Epstein, Y., Jendritzky, G., Staiger, H., and Tinz, B. (2012). Comparison of UTCI to Selected Thermal Indices. *International Journal of Biometeorology*, 56(3):515–535.
- Bob Kopp (2015). The Deadly Combination of Heat and Humidity (a technical note).
- Brake, R. and Bates, G. (2002). A Valid Method for Comparing Rational and Empirical Heat Stress Indices. *The Annals of Occupational Hygiene*, 46(2):165–174.
- Brendon Levitt, M. Susan Ubbelohde, George Loisos, and Nathan Brown (2013). Thermal Autonomy as Metric and Design Process. In *Stream'5'Pushing'the'Boundaries:'Net'Positive'Buildings'(SB13*, Vancouver'BC, Canada.
- Briga-Sa, A., Nascimento, D., Teixeira, N., Pinto, J., Caldeira, F., Varum, H., and Paiva, A. (2013). Textile waste as an alternative thermal insulation building material solution. *Construction and Building Materials*, 38:155–160.
- Buzan, Jonathan, R. K. and Huber, M. (2015). The Deadly Combination of Heat and Humidity. *The New York Times*.
- C. Rangarajan, S. Mahendra Dev, K. Sundaram, Mahesh Vyas, and K.I. Datta (2015). Report of the Expert Group to Review the Methodology for Measurement of Poverty. Technical report, Government of India Planning Commission, India.
- Candido, C., de Dear, R. J., Lamberts, R., and Bittencourt, L. (2010). Air movement acceptability limits and thermal comfort in Brazil's hot humid climate zone. *Building and Environment*, 45(1):222–229.
- Census Population Data (2015). India Slums Population Census Data 2011.
- Christopher Porst (2015). *Confined Masonry for Seismically Resilient Low-Cost Housing in India : A Design and Analysis Method*. PhD thesis, Massachusetts Institute of Technology, Cambridge, MA.
- Clack, G. and Cook, J. (1989). Passive Cooling Systems. In *Passive Cooling*, pages 347–538. MIT Press.
- Deepak Parkh, Anand Bhatt, Renan Jhabvala, Amitabh Kundu, Om Prakash Mathur, Nasser Munjee, P.K. Pradhan, S.R. Rao, Anita Reddy, Utpal Sharma, Rajiv Singh, and S. Sridhar (2008). Report of the High Level Task Force on Affordable



- Housing for All. Technical report, India Ministry of Housing and Urban Poverty Alleviation, India.
- Department of Energy (2017). Cool Roofs | Department of Energy.
- Emily Buchanan and Bhasker (2011). Gujarat's astonishing rise from rubble of 2001 quake. *BBC News*.
- Epstein, Y. and Moran, D. S. (2006). Thermal comfort and the heat stress indices. *Industrial Health*, 44(3):388–398.
- Givoni, B. (1991). Performance and applicability of passive and low-energy cooling systems. *Energy and Buildings*, 17(3):177–199.
- Givoni, B. (2011). Indoor temperature reduction by passive cooling systems. *Solar Energy*, 85(8):1692–1726.
- Glicksman, L. R. and Lienhard, J. H. (2016). *Modeling and Approximation in Heat Transfer*. Cambridge University Press, New York, NY, 1 edition edition.
- Government of India Ministry of Housing and Urban Poverty Alleviation National Buildings Organization (2013). State of Housing in India, A statistical Compendium 2013. Technical report, Government of India Ministry of Housing and Urban Poverty Alleviation National Buildings Organization.
- Govindarajan, V., Trimble, C., and Dubois, P. (2013). The Future is Far From Home. In *Reverse Innovation: Create Far From Home, Win Everywhere*, page 5. Brilliance Audio, mp3 una edition edition.
- Gradillas, M. (2015). Analysis and Design for Thermally Autonomous Housing in Resource-Constrained Communities: A Case Study in Bhuj, India. Master's thesis, Massachusetts Institute of Technology, Cambridge, MA.
- Hay, H. (1978). A Passive Heating and Cooling System from Concept to Commercialization. In *Annual Meeting Am. Solar Energy Society*.
- Ho, S. H., Rosario, L., and Rahman, M. M. (2009). Thermal comfort enhancement by using a ceiling fan. *Applied Thermal Engineering*, 29(8):1648–1656.
- Hoyt Tyler, Schiavon Stefano, Piccioli Alberto, Moon Dustin, and Steinfeld Kyle (2013). CBE Thermal Comfort Tool for ASHRAE-55.
- Hunnarshala Foundation (2016). Urban Slum Redevelopment.
- Indian Agricultural Statistics Institute Research (2011). Report of the Committee on Slum Statistics/Census. Technical report, Government of India.
- International Energy Agency (2013). Transition to Sustainable Buildings. Technical report.

- Jackson, R. (2017). Global Climate Change: Effects.
- Khedari, J., Yamtraipat, N., Pratintong, N., and Hirunlabh, J. (2000). Thailand ventilation comfort chart. *Energy and Buildings*, 32(3):245–249.
- Koenigsberger, O. H. (1974). *Manual of Tropical Housing and Building*. London, Longman.
- Lawrence, M. G. (2005). The Relationship between Relative Humidity and the Dew-point Temperature in Moist Air: A Simple Conversion and Applications. *Bulletin of the American Meteorological Society*, 86(2):225–233.
- Lori Perkins (2014). Five-Year Global Temperature Anomalies from 1880 to 2013.
- M. Fishenden and O. A. Saunders (1950). *An Introduction to Heat Transfer*. Oxford University Press, London.
- M. Wilson and Nicol J. F. (2010). An overview of the European Standard EN 15251. page 34, Cumberland Lodge, Windsor, UK. London: Network for Comfort and Energy Use in Buildings.
- Mallick, F. H. (1996). Thermal comfort and building design in the tropical climates. *Energy and Buildings*, 23(3):161–167.
- Manu, S., Shukla, Y., Rawal, R., Thomas, L. E., and de Dear, R. (2016). Field studies of thermal comfort across multiple climate zones for the subcontinent: India Model for Adaptive Comfort (IMAC). *Building and Environment*, 98:55–70.
- Maps of India (2012). India Poverty Map.
- Mastouri, H., Benhamou, B., Hamdi, H., and Mouyal, E. (2017). Thermal performance assessment of passive techniques integrated into a residential building in semi-arid climate. *Energy and Buildings*, 143:1–16.
- MathWorks (2017). Partial Differential Equations - MATLAB & Simulink.
- Mendoza, H. R. (2014). Instead of Corrugated Metal a Company is Looking to Produce 3d Printed Roofing in Developing World.
- Meteoblue (2014). Climate Bhuj Airport.
- Ministry of Housing and Urban Poverty Alleviation (2007). National Urban Housing & Habitat Policy (NUHHP). Technical report, Government of India.
- Ministry of Housing and Urban Poverty Alleviation (2015). "Housing for All by 2022" Mission - National Mission for Urban Housing.
- Nahar, N. M., Sharma, P., and Purohit, M. M. (2003). Performance of different passive techniques for cooling of buildings in arid regions. *Building and Environment*, 38(1):109–116.

- National Geographic Society (2017). Deserts – National Geographic.
- Nicol, F. (2004). Adaptive thermal comfort standards in the hot&#x2013;humid tropics. *Energy and Buildings*, 36(7):628–637.
- NIOSH (2017). Criteria for a Recommended Standard: Occupational Exposure to Heat and Hot Environments. Atlanta, GA. National Institute of Occupational Safety and Health.
- Nolan, L. B. (2015). Slum Definitions in Urban India: Implications for the Measurement of Health Inequalities. *Population and development review*, 41(1):59–84.
- Occupational Safety and Health Administration (2017). OSHA’s Campaign to Prevent Heat Illness in Outdoor Workers | Using the Heat Index - Estimating Work Rates or Loads | Occupational Safety and Health Administration.
- Palyvos, J. A. (2008). A survey of wind convection coefficient correlations for building envelope energy systems&#x2013; modeling. *Applied Thermal Engineering*, 28(8-9):801–808.
- Pearlmutter, D. and Meir, I. A. (1995). Assessing the climatic implications of lightweight housing in a peripheral arid region. *Building and Environment*, 30(3):441–451.
- P.O. Fanger (1970). *Thermal comfort : analysis and applications in environmental engineering*. Danish Technical Press, Copenhagen.
- ReMaterials (2017). ModRoof.
- Rogers, E. M. (2003). Elements of Diffusion. In *Diffusion of Innovations, 5th Edition*, page 5. Free Press, New York, 5th edition edition.
- Rupesh Hurmade and Tejas Kotak (2016). Hunnarshala Housing Costs and Beneficiary Characterization.
- S. W. Churchill and H. H. S. Chu (1975). Correlating Equations for Laminar and Turbulent Free Convection from a Vertical Plate. *Int. J. Heat Mass Transfer*, 18:1323.
- Santamouris, M. and Kolokotsa, D. (2013). Passive cooling dissipation techniques for buildings and other structures: The state of the art. *Energy and Buildings*, 57:74–94.
- Schiavon, S. and Melikov, A. K. (2008). Energy saving and improved comfort by increased air movement. *Energy and Buildings*, 40(10):1954–1960.
- Seth H. Holmes (2016). Energy Model Validation for Indoor Occupant Heat Stress Analysis. In *ASHRAE and IBPSA-USA SimBuild 2016*, Salt Lake City, UT.

- Soebarto, V. and Bennetts, H. (2014). Thermal comfort and occupant responses during summer in a low to middle income housing development in South Australia. *Building and Environment*, 75:19–29.
- Tav Commins and Jeff Christian (1998). R-Value of Straw Bales Lower Than Previously Reported.
- Tetra Pak, Sidel, and DeLaval (2014). Green Roof Project.
- the Centre for Research on the Epidemiology of Disasters (CRED) (2015). Emergency Events Database EM-DAT.
- The Hindu Business Line (2012). Those Earning up to Rs 1 Lakh a Year are Economically Weak.
- The National Institute for Occupational Safety and Health (NIOSH) (2016). CDC - Heat Stress - NIOSH Workplace Safety and Health Topic.
- Tom Di Liberto (2015). India Heat Wave Kills Thousands.
- United Nations (2010). 2010-2020: UN Decade for Deserts and the Fight against Desertification.
- United Nations (2016). UN-HABITAT: Slum data 2015 | UN System Data Catalog.
- US Department of Commerce and NOAA (2017). Wet Bulb Globe Temperature.
- Vejelienė, J. (2012). Processed Straw as Effective Thermal Insulation for Building Envelope Constructions. *Engineering Structures and Technologies*, 4(3):96–103.
- Vijesh Vasanth Joshi (2015). *Thermal Performance of Various Roof Elements under Different Weather Conditions*. Doctor of Philosophy, Indian Institute of Science, Bangalore.
- WE DESIGNS LLC (2014). Resilient Modular Systems [RMS].
- World Climate Maps (2007). World Climate Maps.
- World Health Organization (2009). WHO | Slums, Climate Change and Human Health in Sub-Saharan Africa.
- World Health Organization (2010). International Workshop on Housing, Health and Climate Change: Technical report, Geneva.
- Zhai, Y., Ma, Y., David, S. N., Zhao, D., Lou, R., Tan, G., Yang, R., and Yin, X. (2017). Scalable-manufactured randomized glass-polymer hybrid metamaterial for daytime radiative cooling. *Science*, page eaai7899.